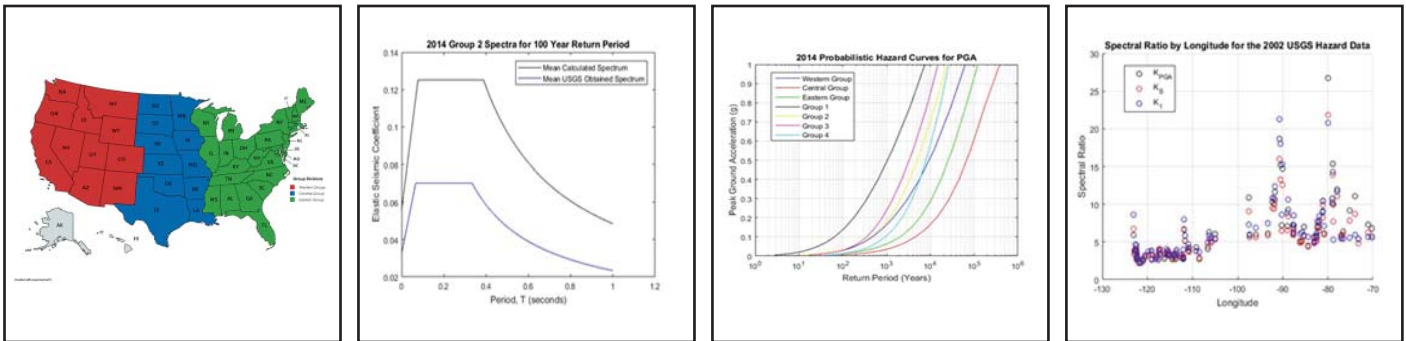


Reduction of Seismic Acceleration Parameters for Temporary Bridge Design

by
Conor Stucki and Michel Bruneau



Technical Report MCEER-18-0001

March 22, 2018

NOTICE

This report was prepared by the University at Buffalo, State University of New York, as a result of research sponsored by MCEER. Neither MCEER, associates of MCEER, its sponsors, University at Buffalo, State University of New York, nor any person acting on their behalf:

- a. makes any warranty, express or implied, with respect to the use of any information, apparatus, method, or process disclosed in this report or that such use may not infringe upon privately owned rights; or
- b. assumes any liabilities of whatsoever kind with respect to the use of, or the damage resulting from the use of, any information, apparatus, method, or process disclosed in this report.

Any opinions, findings, and conclusions or recommendations expressed in this publication are those of the author(s) and do not necessarily reflect the views of MCEER, the National Science Foundation or other sponsors.

Reduction of Seismic Acceleration Parameters for Temporary Bridge Design

by

Conor Stucki¹ and Michel Bruneau²

Publication Date: March 22, 2018

Submittal Date: June 7, 2017

Technical Report MCEER-18-0001

- 1 Structural Engineer, CHA Consulting, Inc.; former Graduate Student, Department of Civil, Structural and Environmental Engineering, University at Buffalo, State University of New York
- 2 Professor, Department of Civil, Structural and Environmental Engineering, University at Buffalo, State University of New York

MCEER

University at Buffalo, State University of New York

212 Ketter Hall, Buffalo, NY 14260

E-mail: mceer@buffalo.edu; Website: <http://buffalo.edu/mceer>

Preface

MCEER is a national center of excellence dedicated to the discovery and development of new knowledge, tools and technologies that equip communities to become more disaster resilient in the face of earthquakes and other extreme events. MCEER accomplishes this through a system of multidisciplinary, multi-hazard research, in tandem with complimentary education and outreach initiatives.

Headquartered at the University at Buffalo, The State University of New York, MCEER was originally established by the National Science Foundation in 1986, as the first National Center for Earthquake Engineering Research (NCEER). In 1998, it became known as the Multidisciplinary Center for Earthquake Engineering Research (MCEER), from which the current name, MCEER, evolved.

Comprising a consortium of researchers and industry partners from numerous disciplines and institutions throughout the United States, MCEER's mission has expanded from its original focus on earthquake engineering to one which addresses the technical and socio-economic impacts of a variety of hazards, both natural and man-made, on critical infrastructure, facilities, and society.

The Center derives support from several Federal agencies, including the National Science Foundation, Federal Highway Administration, Department of Energy, Nuclear Regulatory Commission, and the State of New York, foreign governments and private industry.

This report presents a simple and conservative method for developing seismic response acceleration spectra to be used in the design of temporary bridges. A method for modifying the response spectra used in the design of permanent bridges with spectral reduction factors is defined. The spectral reduction factors are used to reduce the response spectra corresponding to a 1000 year return period to one having an approximated 100 year return period. This result was obtained by first grouping seismic data by geographic location and, alternatively, by magnitude of response spectra to develop spectral reduction factors. The seismic data analyzed in this report was collected from the United States Geological Survey's (USGS) website. The report provides two spectral reduction factors proposed for consideration by design specifications, and a design example to illustrate the procedure.

ABSTRACT

There is presently no prevailing method for reducing the seismic response acceleration parameters PGA , S_S , and S_1 from probabilistic seismic hazard values used for permanent bridge design to levels suitable for temporary bridge design. The American Association of State Highway and Transportation Officials (AASHTO) does not explicitly specify a return period to be used for temporary bridge design, rather, it limits the magnitude of reduction for the seismic response spectrum used in permanent bridge design when designing a temporary bridge. The AASHTO *LRFD Bridge Design Specifications (2016)* specifies a spectral reduction of no greater than 2, while the AASHTO *Guide Specifications for LRFD Seismic Bridge Design (2015)* restricts the magnitude of spectral reduction to no greater than 2.5.

In this study, proposed spectral reduction factors are defined and used to reduce the spectral response acceleration parameters, PGA , S_S , and S_1 , from the 1000 year return period used for permanent bridge design, to a return period suitable for temporary bridge design. The return period used in this study for determining seismic demands in temporary bridge design, 100 years, corresponds with the 10 percent probability of exceedance in 10 years currently employed by the California Department of Transportation for temporary bridge design (Caltrans 2011).

The spectral reduction factors proposed in this report will operate as the ratio between the return period used for the seismic design of a permanent bridge and the return period used for the seismic design of a temporary bridge. Initially, separate spectral reduction factors are examined for each of the three aforementioned spectral response coefficients. To arrive at suitable values for the spectral reduction factors, seismic hazard data was obtained from the United States Geological Survey's website (USGS 2002; USGS 2014) for 100 different sites across the conterminous United States, with site selection criteria defined in this report. The 100 site locations are categorized into common Seismic Groups, with the defining criteria for the Seismic Groups initially chosen based on geographic location, and, alternatively, based on AASHTO defined Seismic Performance Zone. The Seismic Groups are used with the goal of finding a set of defining criteria which can be applied to any arbitrary location designating it to a specific Seismic Group, with the goal that within each Seismic Group, sites will share similar valued spectral ratios. For this study, the spectral ratios is

defined as the ratio between the seismic response coefficients corresponding to a 1000 year return period, and the response coefficients corresponding to a 100 year return period.

A spectral ratio is obtained for each of the three seismic response acceleration coefficients. The mean values of spectral ratios within each Seismic Group is used to determine the spectral reduction factors. As a result, two spectral reduction factors for seismic design of temporary bridges are proposed: One spectral reduction factor of 2.5 to reduce each of PGA, S_s , and S_1 for the western United States, and one spectral reduction factor of 3.75 to reduce PGA, S_s , and S_1 for the central and eastern United States.

ACKNOWLEDGEMENTS

The authors would like to express their appreciation to Nicolas Luco, Research Structural Engineer, of the United States Geological Survey for providing us with assistance that was vital in the completion of this report. The USGS data used in this report was previously accessed through a Java Application which was discontinued before this study's completion. Mr. Luco provided two MATLAB interpolation functions which were used to complete the data analysis.

TABLE OF CONTENTS

SECTION 1 INTRODUCTION.....	1
1.1 General.....	1
1.2 Objectives	4
1.3 Report Outline.....	6
SECTION 2 LITERATURE REVIEW	9
2.1 General.....	9
2.2 Regional Differences in Seismic Acceleration Response Spectra and Hazard Curves for the Continental United States.....	9
2.3 Notable Changes from the 2002 and the 2014 USGS Seismic Hazard Data	10
2.4 Current State Practices of Seismic Design of Temporary Bridges	11
SECTION 3 SEISMIC SPECTRAL REDUCTION FACTORS.....	19
3.1 General.....	19
3.2 Site Locations Obtained for Analysis	19
3.3 Method of Interpolation	21
3.4 The Spectral Reduction Factors	24
3.5 Method of Calculating K_{PGA} , K_{DS} , and K_{D1}	26
SECTION 4 DESIGN REDUCTION FACTORS BY GEOGRAPHIC LOCATION.....	29
4.1 General Procedure for Each Group.....	31
4.2 Group 1	34
4.3 Group 2	37
4.4 Group 3	40
4.5 Group 4	43
4.6 Western Group	46
4.7 Central Group.....	49
4.8 Eastern Group	52

TABLE OF CONTENTS (CONT'D)

4.9	Observations	54
SECTION 5 DESIGN REDUCTION FACTORS BY AASHTO SEISMIC PERFORMANCE ZONE.....63		
5.1	General Procedure for Each Group.....	64
5.2	Group A	65
5.3	Group B.....	68
5.4	Group C.....	71
5.5	Group D	74
5.6	Observations	77
SECTION 6 SPECTRAL REDUCTION EXAMPLE.....81		
6.1	Introduction.....	81
6.2	Spectral Reduction and the Temporary Bridge Design Response Spectrum.....	82
6.3	Example Temporary Bridge.....	85
6.4	Transverse Period of the Temporary Bridge.....	86
6.5	Longitudinal Period of the Temporary Bridge.....	90
6.6	Design Earthquake Load.....	92
SECTION 7 CONCLUSION		
SECTION 8 REFERENCES.....97		
APPENDIX A		
APPENDIX A103		
A.1	MATLAB Function for Spatial Interpolation	103
A.2	MATLAB Function for Hazard Curve Interpolation.....	104
A.3	2002 USGS Seismic Hazard Data.....	105
A.4	2014 USGS Seismic Hazard Data.....	108
A.5	Weight of Example Temporary Bridge.....	112

LIST OF FIGURES

Figure 3-1: Map of the continental United States with the 100 site locations. Graphic created with <http://batchgeo.com> and map data from Google. 20

Figure 3-2: Example illustration of two-dimensional interpolation. 22

Figure 4-1: Visual illustration of Seismic Groups 1 through 4. Graphic created with <http://batchgeo.com> and map data from Google. 29

Figure 4-2: Division of Seismic Groups by state. Graphic created with <http://mapchart.net>..... 31

Figure 4-3: Mean spectral ratios for Group 1: (A) spectral ratio for mean peak ground acceleration, K_{PGA} ; (B) spectral ratio for mean short-period response acceleration, K_S ; (C) spectral ratio for mean long-period response acceleration, K_L 34

Figure 4-4 : Comparison of calculated response spectra coefficient values versus obtained values for Group 1: (A) coefficient for peak ground acceleration calculated using $K_{PGA} - \sigma_{PGA}$; (B) coefficient for short-period response acceleration calculated using $K_{S\mu} - \sigma_S$; (C) coefficient for long-period response acceleration calculated using values $K_{L\mu} - \sigma_L$ 35

Figure 4-5: Comparison of mean response spectra produced using calculated spectral reduction factors, and of mean response spectra produced using USGS obtained values for Group 1: (Left) 2002 USGS seismic hazard data; (Right) 2014 USGS seismic hazard data. 36

Figure 4-6: Mean spectral ratios for Group 2: (A) spectral ratio for mean peak ground acceleration, K_{PGA} ; (B) spectral ratio for mean short-period response acceleration, K_S ; (C) spectral ratio for mean long-period response acceleration, K_L 37

Figure 4-7: Comparison of calculated response spectra coefficient values versus obtained values for Group 2: (A) coefficient for peak ground acceleration calculated using $K_{PGA} - \sigma_{PGA}$; (B) coefficient for short-period response acceleration calculated using $K_{S\mu} - \sigma_S$; (C) coefficient for long-period response acceleration calculated using values $K_{L\mu} - \sigma_L$ 38

LIST OF FIGURES (CONT'D)

Figure 4-8: Comparison of mean response spectra produced using calculated spectral reduction factors, and of mean response spectra produced using USGS obtained values for Group 2: (Left) 2002 USGS seismic hazard data; (Right) 2014 USGS seismic hazard data.....	39
Figure 4-9: Mean spectral ratios for Group 3: (A) spectral ratio for mean peak ground acceleration, K_{PGA} ; (B) spectral ratio for mean short-period response acceleration, K_S ; (C) spectral ratio for mean long-period response acceleration, K_1	40
Figure 4-10: Comparison of calculated response spectra coefficient values versus obtained values for Group 3: (A) coefficient for peak ground acceleration calculated using $K_{PGA} - \sigma_{PGA}$; (B) coefficient for short-period response acceleration calculated using $K_{S\mu} - \sigma_S$; (C) coefficient for long-period response acceleration calculated using values $K_{1\mu} - \sigma_1$	41
Figure 4-11: Comparison of mean response spectra produced using calculated spectral reduction factors, and of mean response spectra produced using USGS obtained values for Group 3: (Left) 2002 USGS seismic hazard data; (Right) 2014 USGS seismic hazard data.....	42
Figure 4-12: Mean spectral ratios for Group 4: (A) spectral ratio for mean peak ground acceleration, K_{PGA} ; (B) spectral ratio for mean short-period response acceleration, K_S ; (C) spectral ratio for mean long-period response acceleration, K_1	43
Figure 4-13: Comparison of calculated response spectra coefficient values versus obtained values for Group 4: (A) coefficient for peak ground acceleration calculated using $K_{PGA} - \sigma_{PGA}$; (B) coefficient for short-period response acceleration calculated using $K_{S\mu} - \sigma_S$; (C) coefficient for long-period response acceleration calculated using values $K_{1\mu} - \sigma_1$	44
Figure 4-14: Comparison of mean response spectra produced using calculated spectral reduction factors, and of mean response spectra produced using USGS obtained values for Group 4: (Left) 2002 USGS seismic hazard data; (Right) 2014 USGS seismic hazard data.....	45

LIST OF FIGURES (CONT'D)

Figure 4-15: Mean spectral ratios for the Western Group: (A) spectral ratio for mean peak ground acceleration, K_{PGA} ; (B) spectral ratio for mean short-period response acceleration, K_S ; (C) spectral ratio for mean long-period response acceleration, K_L 46

Figure 4-16: Comparison of calculated response spectra coefficient values versus obtained values for the Western Group: (A) coefficient for peak ground acceleration calculated using $K_{PGA} - \sigma_{PGA}$; (B) coefficient for short-period response acceleration calculated using 47

Figure 4-17: Comparison of mean response spectra produced using calculated spectral reduction factors, and of mean response spectra produced using USGS obtained values for the Western Group: (Left) 2002 USGS seismic hazard data; (Right) 2014 USGS seismic hazard data. 48

Figure 4-18: Mean spectral ratios for the Central Group: (A) spectral ratio for mean peak ground acceleration, K_{PGA} ; (B) spectral ratio for mean short-period response acceleration, K_S ; (C) spectral ratio for mean long-period response acceleration, K_L 49

Figure 4-19: Comparison of calculated response spectra coefficient values versus obtained values for the Central Group: (A) coefficient for peak ground acceleration calculated using $K_{PGA} - \sigma_{PGA}$; (B) coefficient for short-period response acceleration calculated using $K_{SM} - \sigma_S$; (C) coefficient for long-period response acceleration calculated using values $K_{L\mu} - \sigma_L$ 50

Figure 4-20: Comparison of mean response spectra produced using calculated spectral reduction factors, and of mean response spectra produced using USGS obtained values for the Central Group: (Left) 2002 USGS seismic hazard data; (Right) 2014 USGS seismic hazard data. 51

Figure 4-21: Mean spectral ratios for the Eastern Group: (A) spectral ratio for mean peak ground acceleration, K_{PGA} ; (B) spectral ratio for mean short-period response acceleration, K_S ; (C) spectral ratio for mean long-period response acceleration, K_L 52

LIST OF FIGURES (CONT'D)

Figure 4-22: Comparison of calculated response spectra coefficient values versus obtained values for the Eastern Group: (A) coefficient for peak ground acceleration calculated using $K_{PGA} - \sigma_{PGA}$; (B) coefficient for short-period response acceleration calculated using $K_{S\mu} - \sigma_S$; (C) coefficient for long-period response acceleration calculated using values $K_{1\mu} - \sigma_1$	53
Figure 4-23: Comparison of mean response spectra produced using calculated spectral reduction factors, and of mean response spectra produced using USGS obtained values for the Eastern Group: (Left) 2002 USGS seismic hazard data; (Right) 2014 USGS seismic hazard data.	54
Figure 4-24: Seismic Group hazard curves for peak ground acceleration: (Left) 2002 USGS Seismic Hazard Set; (Right) 2014 USGS Seismic Hazard Set.	56
Figure 4-25: Spectral ratio as a function of longitude for the 100 site locations: (Left) corresponding to the 2002 USGS seismic hazard data; (Right) corresponding to the 2014 USGS seismic hazard data.	58
Figure 4-26: For the 2002 USGS seismic hazard data, a comparison of calculated response spectra coefficient values versus obtained values using a spectral reduction factor of 2.5 for the western United states and 3.75 for the central and eastern United States: (A) coefficient for peak ground acceleration; (B) coefficient for short-period response acceleration; (C) coefficient for long-period response acceleration.	60
Figure 4-27: For the 2014 USGS seismic hazard data, a comparison of calculated response spectra coefficient values versus obtained values using a spectral reduction factor of 2.5 for the western United states and 3.75 for the central and eastern United States: (A) coefficient for peak ground acceleration; (B) coefficient for short-period response acceleration; (C) coefficient for long-period response acceleration. 61	61
Figure 5-1: Mean spectral ratios for Group A: (A) spectral ratio for mean peak ground acceleration, K_{PGA} ; (B) spectral ratio for mean short-period response acceleration, K_S ; (C) spectral ratio for mean long-period response acceleration, K_1	65

LIST OF FIGURES (CONT'D)

Figure 5-2: Comparison of calculated response spectra coefficient values versus obtained values for Group A: (A) coefficient for peak ground acceleration calculated using $K_{PGA} - \sigma_{PGA}$; (B) coefficient for short-period response acceleration calculated using $K_{s\mu} - \sigma_S$; (C) coefficient for long-period response acceleration calculated using values $K_{l\mu} - \sigma_1$ 66

Figure 5-3: Comparison of mean response spectra produced using calculated spectral reduction factors, and of mean response spectra produced using USGS obtained values for Group A: (Left) 2002 USGS seismic hazard data; (Right) 2014 USGS seismic hazard data. 67

Figure 5-4: Mean spectral ratios for Group B: (A) spectral ratio for mean peak ground acceleration, K_{PGA} ; (B) spectral ratio for mean short-period response acceleration, K_S ; (C) spectral ratio for mean long-period response acceleration, K_1 68

Figure 5-5: Comparison of calculated response spectra coefficient values versus obtained values for Group B: (A) coefficient for peak ground acceleration calculated using $K_{PGA} - \sigma_{PGA}$; (B) coefficient for short-period response acceleration calculated using $K_{s\mu} - \sigma_S$; (C) coefficient for long-period response acceleration calculated using values $K_{l\mu} - \sigma_1$ 69

Figure 5-6: Comparison of mean response spectra produced using calculated spectral reduction factors, and of mean response spectra produced using USGS obtained values for Group B: (Left) 2002 USGS seismic hazard data; (Right) 2014 USGS seismic hazard data. 70

Figure 5-7: Mean spectral ratios for Group C: (A) spectral ratio for mean peak ground acceleration, K_{PGA} ; (B) spectral ratio for mean short-period response acceleration, K_S ; (C) spectral ratio for mean long-period response acceleration, K_1 71

Figure 5-8: Comparison of calculated response spectra coefficient values versus obtained values for Group C: (A) coefficient for peak ground acceleration calculated using $K_{PGA} - \sigma_{PGA}$; (B) coefficient for short-period response acceleration calculated using $K_{s\mu} - \sigma_S$; (C) coefficient for long-period response acceleration calculated using values $K_{l\mu} - \sigma_1$ 72

LIST OF FIGURES (CONT'D)

Figure 5-9: Comparison of mean response spectra produced using calculated spectral reduction factors, and of mean response spectra produced using USGS obtained values for Group C: (Left) 2002 USGS seismic hazard data; (Right) 2014 USGS seismic hazard data..... 73

Figure 5-10: Mean spectral ratios for Group D: (A) spectral ratio for mean peak ground acceleration, K_{PGA} ; (B) spectral ratio for mean short-period response acceleration, K_S ; (C) spectral ratio for mean long-period response acceleration, K_L 74

Figure 5-11: Comparison of calculated response spectra coefficient values versus obtained values for Group D: (A) coefficient for peak ground acceleration calculated using $K_{PGA} - \sigma_{PGA}$; (B) coefficient for short-period response acceleration calculated using $K_{S\mu} - \sigma_S$; (C) coefficient for long-period response acceleration calculated using values $K_{L\mu} - \sigma_L$ 75

Figure 5-12: Comparison of mean response spectra produced using calculated spectral reduction factors, and of mean response spectra produced using USGS obtained values from the 2002 hazard data set for Group D. 76

Figure 5-13: Spectral ratio as a function of long-period response acceleration coefficient corresponding to a 7 percent probability of exceedance in 75 years for the 100 site locations: (Left) corresponding to the 2002 USGS seismic hazard data; (Right) corresponding to the 2014 USGS seismic hazard data. 78

Figure 6-1: The site location for the design example shown on a map of the short-period response acceleration coefficient for Region 4 corresponding to the 1000 year return period. The map was borrowed from AASHTO LRFD-BDS Figure 3.10.2.1-14. 82

Figure 6-2: Design response spectrum for the example temporary bridge 85

Figure 6-3: Elevation view of the temporary bridge..... 85

Figure 6-4: Cross section view of typical: (Left) intermediate bent; (Right) end bent..... 86

Figure 6-5: Composite section properties of the hollow core slab and barrier rail..... 86

Figure 6-6: (Left) Model temporary bridge with an applied unit load of 1 kip/in; (Right) the deformed shape of the bridge under loading..... 89

LIST OF TABLES

Table 4-1: Bounds for Seismic Groups 1 through 4 using latitude and longitude.....	30
Table 4-2: Mean spectral ratios for Group 1.....	35
Table 4-3: Spectral reduction factors for Group 1	36
Table 4-4: Mean spectral ratios for Group 2.....	38
Table 4-5: Spectral reduction factors for Group 2	39
Table 4-6: Mean spectral ratios for Group 3.....	41
Table 4-7: Spectral reduction factors for Group 3	42
Table 4-8: Mean spectral ratios for Group 4.....	44
Table 4-9: Spectral reduction factors for Group 4	45
Table 4-10: Mean spectral ratios for the Western Group	47
Table 4-11: Spectral reduction factors for the Western Group.....	48
Table 4-12: Mean spectral ratios for the Central Group	50
Table 4-13: Spectral reduction factors for the Central Group	51
Table 4-14: Mean spectral ratios for the Eastern Group.....	53
Table 4-15: Spectral reduction factors for the Eastern Group	54
Table 4-16: West coast Seismic Groups mean value of the three spectral reduction factors	55
Table 5-1: Group by Seismic Performance Zone (from LRFD-BDS Table 3.10.6-1)	63
Table 5-2: Mean spectral ratios for Group A.....	66
Table 5-3: Spectral reduction factors for Group A	67
Table 5-4: Mean spectral ratios for Group B	69
Table 5-5: Spectral reduction factors for Group B	70
Table 5-6: Mean spectral ratios for Group C	72
Table 5-7: Spectral reduction factors for Group C	73
Table 5-8: Mean spectral ratios for Group D.....	75
Table 5-9: Spectral reduction factors for Group D.....	76
Table 5-10: Mean spectral ratios for Group C using the 2002 USGS hazard data set, without the site location in Salt Lake City, Utah.....	77

LIST OF TABLES (CONT'D)

Table 6-1: The coordinates and spectral coefficients corresponding to the 1000 year return period used in the example.....	83
Table 6-2: Transverse section properties for the temporary bridge	88
Table 6-3: Transverse deflections of the temporary bridge	89
Table A-1: The 100 site locations and the corresponding seismic hazard data from the 2002 USGS data set	105
Table A-2: The 100 site locations and the corresponding seismic hazard data from the 2014 USGS data set	108
Table A-3: Weight of each span for temporary bridge example	112
Table A-4: Weight of each intermediate bent for temporary bridge example	112
Table A-5: Weight of each end bent for temporary bridge example	113

SECTION 1

INTRODUCTION

1.1 General

The first step in seismic design is defining the design hazard with a corresponding level of acceptable risk (Newmark and Hall 1982). Considering the short history of reliable seismic data (Blume 1965), and given the number of uncertainties in earthquake design including event frequency and magnitude, seismic risk can be suitably expressed as a function of return period (Cornell 1968). The American Association of State Highway and Transportation Officials' (AASHTO) LRFD Bridge Design Specifications (LRFD-BDS) specifies a probabilistic approach for the seismic design of bridges in Article 3.10.1 (2016); in this approach, bridge acceleration response spectra, based on a uniform risk of a 7 percent probability of exceedance in 75 years, are used to define the acceptable seismic hazard level in which the bridge “may suffer significant damage” but “have a low probability of collapse.” The 7 percent probability of exceedance in 75 years corresponds to what is roughly a 1000 year return period. The relationship between the return period and the probability of exceedance is given below by Equation 1-1 (NHI 2014):

$$P = 1 - e^{-\gamma t} \quad (1-1)$$

where P is the probability of exceedance for a period of time, t, and γ is the inverse of the return period.

The AASHTO LRFD-BDS does not explicitly define incremental levels of risk for seismic design, in that it only explicitly defines a single return period for the design of the structure. The advantages of varying increments of risk and potential damage in the design process have long been advocated (Blume 1965), but the current design approach embodies the long-standing philosophy that “some economic loss” is admissible “under these moderate, not unexpected earthquake effects” (Cornell 1968).

In AASHTO's General Procedure specified in Article 3.10.2.1 of the LRFD-BDS, response spectra are used to relate the return period to seismic hazard demands. The response spectra defined in

Article 3.10.4.1 of the AASHTO LRFD-BDS, are calculated from the peak ground acceleration and the five percent damped maximum response accelerations which correspond to AASHTO's aforementioned specified probability of exceedance, or return period. Response spectra, a widely used method for earthquake analysis of structures, were first conceptualized in 1932 by M.A. Biot (Chopra 2012; Trifunac 2003). The response spectrum specified by AASHTO is the pseudo-acceleration response spectrum. The pseudo-acceleration response spectrum relates the pseudo-acceleration response of the structure to the natural vibration period of the structure. The term pseudo is used to differentiate the design maximum response and the true maximum response of the structure (Chopra 2012) A plot of the seismic acceleration response spectrum used by AASHTO serves as a visual representation of the expected maximum response acceleration a bridge may be subject to during its design lifespan. The acceleration response spectra are used in the AASHTO LRFD-BDS to calculate the design earthquake load, a horizontal load to be applied to the structure during analysis. The design earthquake load is an idealization of inertia effects caused by earthquake ground excitation (Bruneau et al. 2011).

There is no national consensus on what method should be used in design practice to reduce the seismic design criteria used for permanent bridges to levels suitable for the design of temporary bridges. While spectral response coefficients given by the maps for the same return period as new bridges can be used in the design of temporary bridges, some engineers may find these values too conservative as they do not reflect the reduced design lifespan of a temporary bridge, and are thus not as cost effective as using spectral response coefficients that incorporate the reduced time of exposure (Mohammadi and Heydari 2008). Presently, AASHTO does not provide an alternate return period to be used for temporary bridge design that reflects the reduced design lifespan of a temporary bridge; it does however provide restrictions governing the use of alternate response spectra for temporary bridges. In the AASHTO LRFD-BDS, Article 3.10.10 restricts the reduction of response spectra for temporary bridges by a factor no greater than 2. The *AASHTO Guide Specifications for LRFD Seismic Bridge Design* (LRFD-SBD), however, restricts the reduction of response spectra for temporary bridges by a factor of no greater than 2.5, as specified in Article 3.6 (2015).

There are two primary methods for calculating the design spectra contained within the LRFD-BDS, the general procedure and the site specific procedure. The site specific procedure is a more comprehensive approach for calculating the response spectra; its use is specified for design sites close to an active fault, sites designated Site Class F, for anticipated long-duration earthquakes, and for bridges of high importance. Further details regarding when to use the site specific procedure can be found in Article 3.10.2 of the LRFD-BDS. The content in this report will focus on the general procedure. Note that per Article 3.10.2.2 of the LRFD-BDS, deterministic response spectra can be used within specified limits near known active faults.

Using AASHTO's general procedure, the seismic response spectra are defined using the corresponding mapped spectral acceleration coefficients given by the maps in Article 3.10.4.1 of the LRFD-BDS, namely, the peak ground acceleration coefficient, PGA, the short-period response acceleration coefficient, S_s , and the long-period response acceleration coefficient, S_1 . The design maps from which the response coefficients are given, are produced using the aforementioned 7 percent probability of exceedance in 75 years, and with an assumed damping ratio of 5 percent. In addition to PGA, S_s , and S_1 , the Site Factors must be obtained. Each of the three mapped coefficients has a corresponding Site Factor defined in Article 3.10.3.2: F_{pga} is the Site Factor for the peak ground acceleration coefficient given in Table 3.10.3.2-1, F_a is the Site Factor for the short-period response acceleration coefficient given in Table 3.10.3.2-2, and F_v is the Site Factor for the long-period response coefficient given in Table 3.10.3.2-3. The values of the Site Factors are dependent upon the Site Class, defined in Article 3.10.3 and determined from the soil properties specific to the location. Once the Site Factors have been obtained, design values for the response spectra can be calculated from the mapped response coefficients.

One practice currently employed by some state transportation departments, is to specify a return period that is reduced from the 1000 year return period given by AASHTO, to be used for temporary bridge design (Caltrans 2011; IDOT 2012; SCDOT 2008). In May 2011, the California Department of Transportation (Caltrans) issued a memo to state bridge engineers setting a standard for the response spectra to be used in temporary bridge design. They specified that temporary bridges "that carry or cross over public vehicular traffic" should be designed per a response spectra corresponding to a 10 percent probability of exceedance in 10 years, corresponding to a return

period of roughly 100 years (Caltrans 2011). Recognizing that Caltrans' *Seismic Design Criteria* over the years has helped shape AASHTO's LRFD-SBD (NHI 2014), the method proposed in this report is based on the assumption that the probabilistic approach utilized by Caltrans for temporary bridges would be nationally acceptable to state bridge engineers as far as return period is concerned, and as far as the definition of a temporary bridge is concerned. Caltrans defines temporary bridges as bridges with a design lifespan of five years or less, and the aforementioned 10 percent probability of exceedance in 10 years is recommended as the design standard for temporary bridges herein, and was used as the target return period for the research presented in this report.

Currently, for temporary bridge design with a reduced return period, the engineer must search the USGS website for the set of response parameters corresponding to that return period. In other words, given that there is only one set of design maps in AASHTO, based on a 1000 year return period, the use of the USGS website is necessary when designing with a reduced return period. This report outlines a method using proposed reduction factors to reduce the spectral acceleration coefficients used for the design of permanent bridges and given in the maps in Article 3.10.4.2, to obtain the new values to be used for the design of a temporary bridge to the lower target return period, with the understanding that some states favor using a simpler procedure that does not require the use of the USGS website for obtaining a new set of spectral acceleration coefficients. Using the method proposed in this report, an engineer designing a temporary bridge would be able to obtain values for the response parameters, PGA, S_s , and S_1 , from the AASHTO maps corresponding to a 1000 year return period employing the same procedure used for permanent bridge design, and reduce these values using a spectral reduction factor, without the need to use the USGS website.

1.2 Objectives

The primary goal of this report is to propose a simple and conservative method for reducing the seismic demands considered in the design of temporary bridges, based on the current set of AASHTO mapped spectral response coefficients and without requiring use of the USGS website. This simplified method of producing seismic response spectra is aimed at temporary bridges that

correspond with AASHTO's definition of a "regular" bridge given in Article 4.7.4.3 of the LRFD-BDS, and for areas that typically do not require intensive seismic analysis.

The temporary bridge seismic response spectra proposed in this report will be constructed by reducing the values of the peak ground acceleration, PGA, as well as the short-period and long-period response spectral acceleration parameters, S_s and S_1 respectively, given by the maps in Article 3.10.4.2 of the LRFD-BDS with a proposed spectral reduction factor, defined in Section 3.4. The spectral response coefficients would be reduced from the requirements outlined for permanent bridges, to magnitudes corresponding to a comparable probabilistic earthquake hazard employed by Caltrans for temporary bridges, thus effectively reducing the design spectra from a seven percent probability of exceedance in 75 years to a ten percent probability of exceedance in ten years. The method proposed in this report would allow state engineers to use a reduced seismic design spectra without having to follow a more complex procedure to use the United States Geological Survey's website to determine the hazard parameters corresponding to a 10 percent probability of exceedance in 10 years. The resulting designs will be considered conservative if the spectral response accelerations calculated by the method outlined in this report are greater in magnitude than the spectral response accelerations obtained from the USGS website.

For this proposed method, the value of the spectral reduction factor an engineer would use to create the temporary bridge design spectrum would depend upon the "Seismic Group" corresponding to the location of the bridge. Seismic Groups will be used in this report in a similar manner as the Seismic Performance Zones used by AASHTO and defined in Article 3.10.6 of the LRFD-BDS. Each Seismic Group has distinct defining criteria and within each group there are distinct spectral reduction factors. Two separate sets of defining criteria for Seismic Groups will be examined in this report: one defined by geographic location and one using the previously mentioned AASHTO defined Seismic Performance Zones. The purpose of using Seismic Groups is to establish a limited set of fixed-values for the reduction factors applicable to a wide range of locations where one spectral reduction factor for reducing the peak ground acceleration, one spectral reduction factor for the short-period response spectral acceleration coefficient, and one for the long-period response spectral acceleration coefficient can be used to conservatively create a temporary bridge design spectrum. These reduction factors would be the same for all locations within each Seismic Group

and would reduce the design spectra from probabilistic response values for permanent bridge design to those for temporary bridge design. Three spectral reduction factors will be examined for each Seismic Group for the sake of comparison, with the goal of proposing a single spectral reduction factor for each Seismic Group for simplicity.

1.3 Report Outline

Section 2 provides a brief overview of some of the literature relevant to this report. This overview begins with literature pertaining to regional variations in seismic response spectra and seismic hazard curves, then highlights notable differences between the 2002 and 2014 USGS seismic hazard data, and concludes with an overview of state department of transportation policies for the seismic design of temporary bridges.

In Section 3, the process of seismic hazard data selection and seismic hazard data processing are outlined. The seismic hazard data used in this study corresponds to 100 site locations chosen around the conterminous United States, the process of selecting these site locations is given in Section 3.2. In Section 3.3, the interpolation method used to process the seismic hazard data is defined. The method of calculating the spectral reduction factors, which will be used to reduce the seismic response spectrum from a 7 percent probability of exceedance in 75 years to a 10 percent probability of exceedance in 10 years, is defined in Sections 3.4 and 3.5.

In Section 4, the site locations examined in this report are categorized into Seismic Groups by geographic location and spectral reduction factors are calculated unique to each Seismic Group. The procedure for each Seismic Group is defined in Section 4.1, and the results for each group are presented in Section 4.2 through 4.8. The observations of the authors for the results of Section 4 are given in Section 4.9.

Section 5 categorizes the site locations into Seismic Groups by AASHTO defined Seismic Performance Zone; this method is independent of the results of Section 4. The general procedure for each group is given in Section 5.1 with the results presented in Section 5.2 through Section 5.5. The observations of the authors for the results of Section 5 are given in Section 5.6.

Section 6 provides a design example illustrating the implementation of the spectral reduction factor in obtaining design earthquake loads for temporary bridge design. The AASHTO defined Uniform Load Method is used in this example.

Section 7 summarizes the key research findings.

SECTION 2

LITERATURE REVIEW

2.1 General

This section provides a brief overview of some of the literature and documents relevant to this report. In Section 2.2, a discussion of findings regarding temporal differences in seismic response spectra and seismic hazard curves from previously published literature is presented. In Section 2.3, some of the notable differences between the 2002 USGS seismic hazard data and the 2014 USGS seismic hazard data are discussed. Current state policies regarding seismic design of temporary bridges are presented in Section 2.4.

2.2 Regional Differences in Seismic Acceleration Response Spectra and Hazard Curves for the Continental United States

Response spectra in the eastern and central United States can be characterized as having a higher frequency content on average than characteristic response spectra in the western United States (Chung and Bernreuter 1981; Judd and Charney 2014). This can in part be explained by observed areas of higher attenuation in the western United States, and areas with a lower relative attenuation in the central and eastern United States (Benz et al. 1997; Chung and Bernreuter 1981; Solomon and Toksöz 1970). An idealized demarcation line between the two contrasting attenuation behaviors can be taken at the border of the Great Plains province and the North American Cordillera (Mitchell 1975). Attenuation is the decrease in amplitude as the wave propagates due to energy losses (Burland et al. 2012). For near-field seismic events, attenuation is generally comparable between the eastern and western United States, but for the far-field a pattern of higher attenuation in the western United States is observed (Chung and Bernreuter 1981). One attribute typical of the central and eastern United States is a greater felt area than an earthquake of similar magnitude in the western United States (NHI 2014). Regional variations in attenuation have been attributed to differences in volume of water in pore spaces (Mitchell 1975), differences in ground absorption (Chung and Bernreuter 1981), high heat flow regions and higher rates attenuation (Mikami and Hirahara 1981), and variations in crustal structure (Gregersen 1984).

Attenuation is a factor in both probabilistic and deterministic seismic design, and attenuation rates are used to estimate ground motions for earthquake design parameters (Campbell 1997). In the

central and eastern United States, greater uncertainty in attenuation and response exists due to a lower frequency of earthquakes (Judd and Charney 2014). The lower attenuation exhibited in the central and eastern United States combined with a greater average distance from event generating faults leads to seismic hazard curves that are dominated by far-field events, particularly as spectral period increases (Judd and Charney 2014). In 2014, Judd observed temporal differences in seismic hazard curves and that the average ratio of spectral acceleration for a 72 year return period to the maximum considered event (MCE) was 20 percent in the western United States compared to 10 percent found in the eastern United States. Such a factor of 2 is significant for designing structures at a low-return period when using values derived from a long-return period spectra.

2.3 Notable Changes from the 2002 and the 2014 USGS Seismic Hazard Data

The 2002 USGS seismic hazard data was produced with an earthquake catalog extending through December 2001 (Frankel et al. 2002), and the 2014 USGS seismic hazard data contains a moment magnitude based earthquake catalog extending through 2012 (Petersen et al. 2014). In addition to the updated earthquake catalog, the data available twelve years later accounted for numerous revisions to fault geometries, fault modeling methodology, recurrence rates, magnitude uncertainty models, and updated ground-motion and attenuation relations (Frankel et al. 2002; Petersen et al. 2008; Petersen et al. 2014).

Beginning in 2003, the Pacific Earthquake Engineering Research Center (PEER) formed five teams of researchers tasked to formulate what became known as the Next Generation Attenuation (NGA) ground-motion models. Minimum requirements were set forth for the NGA models, to provide coverage over a spectral period range of 10 seconds, and validity at distances of up to 200 km and up to moment magnitudes of 8.5 (Campbell and Bozorgnia 2006). In 2008, the five ground-motion prediction equations previously used in the 2002 USGS model for crustal faults were replaced with newly formulated NGA equations for attenuation. For the USGS 2008 hazard data, the new NGA models for attenuation resulted in lower ground motions at the 1 second period in the western United States (Petersen et al. 2008). In 2014, the previously used 200 km radius for maximum distance of ground motions stemming from crustal sources was increased to 300 km. Also new to the USGS 2014 hazard data was an adaptive smoothing model which can cause ground

motions to increase in areas of frequent earthquakes, but in general, ground motions decrease more rapidly with distance than in previous hazard maps.

In the central and eastern United States, updated equations developed from the NGA ground motion database resulted in spectral ground motions that decay more rapidly with increasing distance in the 2014 USGS maps than in years previous (particularly for greater magnitude earthquakes), correspondingly reducing ground motions across all spectral periods (Petersen et al. 2014). Furthermore, since the 2002 hazard data, there have been some notable changes in earthquake occurrence rates in parts of the country. The central and eastern United States saw an unusual spike in occurrence of magnitude 3 earthquakes between 2010 and 2012 (Petersen et al. 2014). Between 1967 and 2000 the Central United States had an average of around 21 earthquakes a year of magnitude 3 or greater, this increased to around 100 a year between 2010 and 2012 (Petersen et al. 2015), and even more in recent years. The increase in occurrence frequency is often attributed to fluid injection (Ellsworth 2013; McGarr 2014). Note that the USGS seismic hazard maps prior to 2014 were produced with a methodology used to remove nontectonic earthquake events (Mueller 2010; Petersen et al. 2008; Petersen et al. 2014).

2.4 Current State Practices of Seismic Design of Temporary Bridges

This section provides a summary of current state bridge policies regarding seismic demand criteria for temporary bridge design. This section is not necessarily comprehensive in that some policies, supporting documents, or other relevant criteria may exist but were not found by the authors of this report. Due to the number of state DOT policies regarding seismic design, and temporary bridge design, only seismic demand criteria specific to temporary bridge design and applicable to the entire structure are included here. Therefore, temporary bridge policies pertaining only to temporary supports, or other specific structural components, are not included. Seismic response spectra specifications differing from either the AASHTO LRFD-BDS or the AASHTO LRFD-SBD are included.

California, Illinois, and South Carolina were the only states found to specify alternate return periods for seismic demand criteria corresponding to temporary bridge design. As mentioned in Section 1.1 of this report, California specifies a 10 percent probability of exceedance in 10 years

for temporary bridges (Caltrans 2011). In 2008, the Illinois DOT switched from using a 500 year return period for the seismic design of new bridges to the current AASHTO standard 1000 year return period, but still uses the 500 year return period for “retrofitting of existing bridges, temporary bridge construction, and local bridges” (IDOT 2012). Similar to California, the South Carolina Department of Transportation uses a 5 year service limit to define temporary bridges in Article 3.11 of the *Seismic Design Specifications for Highway Bridges* (SCDOT 2008). In South Carolina the “Functional Evaluation Earthquake (FEE)” is used for temporary bridge design, as specified in Articles 3.3 and 3.11. In Article 2.1, the FEE is defined as a “seismic event with a 15 percent probability of exceedance in 75 years.”

Information found specific to a number of other states follows (presented in alphabetical order of state name):

The Florida Department of Transportation’s *Structures Design Guidelines* in Article 2.3.1 specifies that “only the connections between the superstructure and substructure need to be designed for the seismic forces” (FDOT 2017). No policy specific to seismic design of temporary bridges was found.

The Idaho Transportation Department’s *Load Resistance Factor Design (LRFD) Bridge Manual* in Article 3.4.1 specifies an earthquake load factor of zero for Extreme Event I loading of bridges (IDT 2002).

The Iowa Department of Transportation’s *LRFD Bridge Design Manual* specifies that seismic loading is only to be done for “unusual projects such as bridge sites determined to be Site Class F and for Missouri River and Mississippi River bridges.” The seismic analysis is to conform to the AASHTO LRFD-BDS (IOWA DOT 2016).

Seismic demand criteria specific to temporary bridges was not found in the Louisiana Department of Transportation and Development’s *Bridge Design and Evaluation Manual*; however, under Article 3.3 Performance Criteria pertaining to moveable bridge design, the manual specified that designers must “establish seismic performance goals, consistent with the importance of the

bridge,” and referred to AASHTO LRFD-BDS and the section pertaining to seismic design of bridges in the Louisiana manual for further guidelines (LaDOTD 2014).

The Massachusetts Department of Transportation’s *LRFD Bridge Manual* specifies that all temporary bridges are to be designed using the loads applicable to permanent structures. However, it does allow for the State Bridge Engineer to waive the seismic design requirement (MassDOT 2013).

The Missouri Department of Transportation’s *751 LRFD Bridge Design Guidelines* in Article 751.9.1.1 Applicability of Guidelines, specifies that “seismic design of bridges shall conform to AASHTO Division I-A, 1996 and Interims thru 1998.” It does additionally state that “special considerations” can be made for temporary bridges (MoDOT 2010).

The New Hampshire Department of Transportation’s *Bridge Design Manual* specifies that, for seismic design of bridges in New Hampshire, all bridges must conform to Article 3.10 of the LRFD-BDS and to the LRFD-SBD. It is not clear whether the limiting factor of 2 from the LRFD-BDS or 2.5 from the LRFD-SBD is applicable for temporary bridge design in New Hampshire. The *Bridge Design Manual* does however state that for nonconventional bridges the Bridge Design Chief can approve of “project-specific design requirements” (NHDOT 2015). Note at the time of this report, Chapter 9 Miscellaneous Structures was listed as “not completed” on the department’s website.

The New Mexico Department of Transportation’s *Bridge Procedures and Design Guide* specifies the use of either the AASHTO LRFD-BDS or LRFD-SBD for the seismic design of bridges (NMDOT 2013).

The North Dakota Department of Transportation’s *Design Manual* refers to the AASHTO LRFD-BDS for seismic design, but additionally has a load modifying factor of 0.90 given in Article IV-04.03.02 for temporary bridges (NDDOT 2017).

The Ohio Department of Transportation's Office of Structural Engineer's *Bridge Design Manual* in Section 503 Detail Design specifies that temporary bridges are to be designed as permanent bridges conforming to the procedures of the AASHTO LRFD-BDS, with the exception of a live load reduction (ODOT 2007).

The Oregon Department of Transportation's *Bridge Design and Drafting Manual* in Article 1.17.2.1 specifies for temporary bridges that have a design lifespan greater than one year to conform to Article 3.10.10 of the AASHTO LRFD-BDS. For bridges with a design lifespan less than one year, only the minimum support length is to be provided conforming to Article 4.7.4.4 of the AASHTO LRFD-BDS. The *Bridge Design and Drafting Manual* in Article 1.38.2 defines temporary detour bridges as having a maximum design lifespan of five years (Oregon DOT 2016).

The Pennsylvania Department of Transportation's *Design Manual* in Article 5.5.3.4.3 states that normally temporary bridges are to be in service for two years or less. For temporary bridges to be in service for longer than three years, the Bureau of Project Delivery must approve the design. In Article 5.5.3.4.3-c-2 it specifies, "No seismic loads," for temporary bridge design (PennDOT 2015).

The State of Rhode Island Department of Transportation's *Rhode Island LRFD Bridge Design Manual* uses two separate return periods for bridge design. In Article 3.6.2 it specifies that "essential" bridges will remain open after a 475-year earthquake and that "critical" bridges will remain open only for emergency vehicles after a 2500-year earthquake. No separate criteria for temporary bridges was found (RIDOT 2007).

The Texas Department of Transportation's *Bridge Design Manual – LRFD* in Section 2 specifies that seismic loading is not required for bridge design in the state of Texas. Several counties are listed as exceptions and are directed to Article 3.10 of the AASHTO LRFD-BDS (TxDOT 2015).

The Utah Department of Transportation's *Structures Design and Detailing Manual* in Article 13.4.2 specifies using the permanent bridge acceleration response spectra divided by 2.

Additionally, the Seismic Design Category will be based on the long-period response acceleration divided by 2 (UDOT 2015).

The Vermont Agency of Transportation's *VTrans Structures Design Manual* specifies in Article 3.8.1 that AASHTO LRFD-BDS is to be used for the seismic design of bridges. Additionally, specified in Article 3.2.2 is a load modifying factor of 0.90 for temporary bridges (VTrans 2010).

The Washington State Department of Transportation's *Bridge Design Manual (LRFD)* in Article 10.13.1 defines a maximum service life of 5 years for temporary bridges. In Article 10.13.2 it specifies that temporary bridges be designed according to the AASHTO LRFD-SBD, and that the Seismic Design Category be based on the reduced spectra used. A temporary bridge that would have been classified as in Seismic Design Category B, C, or D can't be reclassified as Seismic Design Category A (WSDOT 2016).

The West Virginia Department of Transportation's *Bridge Design Manual* specifies in Article 3.1.4.1.5 that "critical" bridges are to be designed for a 2500-year earthquake, "essential" bridges are to be designed for a 475-year earthquake, and all other bridges are to be designed for a 50-year earthquake. It cannot be inferred that other bridges includes temporary bridges. Additionally, in Article 3.21, it states, "All temporary structures shall be designed in accordance with the Governing Specifications" (WVDOH 2004).

The following manuals state they are either supplementary to the AASHTO LRFD-BDS, or refer to the AASHTO LRFD-BDS for loading specific to temporary bridges, general loading requirements without specifying separate criteria for temporary bridges, or changes to other non-seismic loading procedures but reference the LRFD-BDS for seismic criteria:

- Alaska Department of Transportation & Public Facilities' *Alaska Highway Preconstruction Manual* (DOT&PF 2013)
- Arizona Department of Transportation's *Bridge Design Guidelines* (draft not fully completed, Preface section on ADOT website refers to AASHTO LRFD-BDS) (ADOT 2001)
- Colorado Department of Transportation's *Bridge Design Manual* (CDOT 2012)

- Connecticut Department of Transportation *Bridge Design Manual (ConnDOT 2003)*
- Delaware Department of Transportation's *Bridge Design Manual (DelDOT 2016)*
- Georgia Department of Transportation's *Bridge and Structures Design Manual (GDOT 2016)*
- Kansas Department of Transportation's *Design Manual (KDOT 2016)*
- Maine Department of Transportation's *Bridge Design Guide (MaineDOT 2003)*
- Michigan Department of Transportation's *Michigan Design Manual (MDOT 2009)*
- Minnesota Department of Transportation's *LRFD Bridge Design Manual (MnDOT 2016)*
- Mississippi Department of Transportation's *Bridge Design Manual (Mississippi DOT 2010)*
- Montana Department of Transportation's *Structures Manual (MDT 2002)*
- Nebraska Department of Roads' *Bridge Office Policies and Procedures (NDOR 2016)*
- Nevada Department of Transportation's *Structures Manual (NDOT 2008)*
- New York State *Bridge Manual (NYSDOT 2006)*
- State of North Carolina Department of Transportation's *Structures Management Unit Manual (NCDOT 2016)*
- Virginia Department of Transportation's *VDOT Modifications to the AASHTO LRFD Bridge Design Specifications, 7th Edition, 2014 (VDOT 2015)*
- Wisconsin Department of Transportation's *WisDOT Bridge Manual (WisDOT 2017)*

The following manuals refer to the AASHTO LRFD-SBD for seismic analysis:

- Alabama Department of Transportation's *Structural Design Manual (ALDOT 2016)*
- Indiana Department of Transportation's *2013 Design Manual (INDOT 2013)*
- New Jersey Department of Transportation's *Design Manual for Bridges & Structures (NJDOT 2016)*
- Wyoming Department of Transportation's *Bridge Design Manual (WYDOT 2013)*

No bridge design manual, or similar comprehensive document with design guidelines for bridges could be found from the website of:

- The Arkansas State Highway and Transportation Department

- Hawaii Department of Transportation
- Kentucky Transportation Cabinet (Structural Design manual listed as “Draft Status”)
- Maryland Department of Transportation
- Oklahoma Department of Transportation
- South Dakota Department of Transportation
- Tennessee Department of Transportation

SECTION 3

SEISMIC SPECTRAL REDUCTION FACTORS

3.1 General

The method proposed here for the reduction of the seismic design spectra is based on the idea that any location on the map of the United States can be identified to belong to a pre-identified Seismic Group, and that such Seismic Groups can be defined such that all locations within that group can share identical values for the three separate spectral reduction factors that must be used to reduce the design spectra defined in Article 3.10.4.1 from a 7 percent probability of exceedance in 75 years to a 10 percent probability of exceedance in 10 years. Therefore, for each group, three spectral reduction factors are calculated, namely one for each of the spectral acceleration coefficients used in creating the design spectra defined in Article 3.10.4.1 of the LRFD-BDS. In other words, one spectral reduction factor is for reducing the peak ground acceleration coefficient, one for the short-period spectral response coefficient, and one for the long-period spectral response coefficient. These three spectral reduction factors are referred to here as the “peak ground acceleration spectral reduction factor”, K_{PGA} , the “short-period spectral reduction factor”, K_{DS} , and the “long-period spectral reduction factor”, K_{D1} .

3.2 Site Locations Obtained for Analysis

One hundred locations were selected to provide adequate geographic coverage of the continental United States. Preference was given to areas of the country perceived as seismically active and large population centers. Additionally, locations were selected to ensure that each of the Seismic Groups given in Section 4 had at least 10 locations. The GPS coordinates for each location were retrieved using Google Earth. The locations selected can be seen below in Figure 3-1.

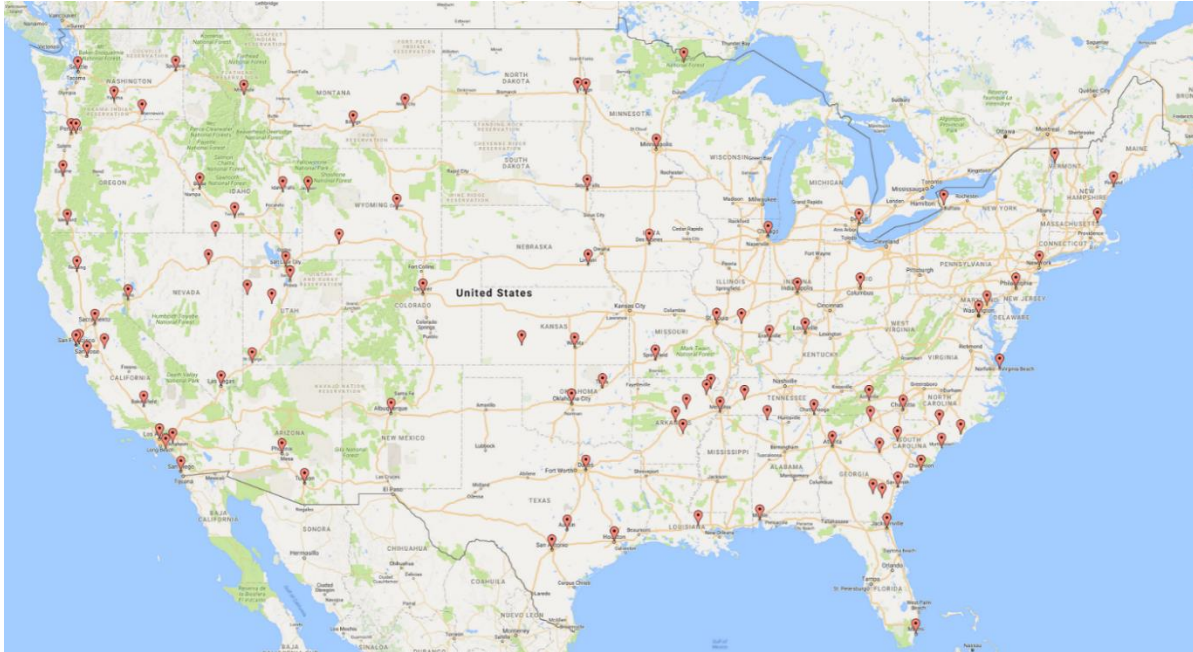


Figure 3-1: Map of the continental United States with the 100 site locations. Graphic created with <http://batchgeo.com> and map data from Google.

For each location, the peak ground acceleration, as well as the short-period and long-period spectral response acceleration coefficients corresponding to a 10 percent probability of exceedance in 10 years and a 7 percent probability of exceedance in 75 years were obtained from the seismic hazard data available on the USGS website. The values were obtained for the 2002 USGS seismic hazard data that was used in the development of the 2009 AASHTO seismic maps. In addition to the 2002 seismic hazard data, the same three spectral response coefficients were also obtained using the 2014 seismic hazard data, assuming that future editions of AASHTO could refer to the most recent seismic maps; selected obtained values were also used for direct comparisons of how seismic demands have changed over time at the locations considered, and how the coefficients calculated by the present methodology are affected by recent changes in the seismic hazard data maps.

Two separate methods are used to regroup the 100 site locations into Seismic Groups. One method, presented in Section 4, divides the 100 site locations into 7 Seismic Groups that are defined as a function of geographic location. The other method, outlined in Section 5, divides the

100 site locations into 4 separate Seismic Groups that correspond to the AASHTO's Seismic Performance Zones (such zones are defined in Article 3.10.6 of the LRFD-BDS).

3.3 Method of Interpolation

The seismic data for the peak ground acceleration coefficient, the short-period acceleration coefficient, and the long-period acceleration coefficient were downloaded from the USGS website in .txt file format. Each coefficient had a corresponding .txt file, thus six files were obtained, three for the 2002 set and three for the 2014 set, all of which are publically available on the USGS website. The data is provided in a gridded format with incremental values of latitude and longitude dividing the United States. Each file contains 19 to 20 spectral acceleration values depending on the spectral response coefficient. For each point of intersection between latitude and longitude, a mean annual frequency of exceedance (MAFE) value is provided for each of the corresponding spectral acceleration values. The MAFE is equivalent to the inverse of return period. Every point of intersection within a given file uses the same set of spectral acceleration values, each point of intersection has its own set of MAFE values that correspond to the spectral acceleration values.

The USGS, courtesy of Nicolas Luco, Research Structural Engineer, provided the authors of this report with two MATLAB functions that allow the user to specify a location with coordinates of latitude and longitude, and specify a return period for which MATLAB will output a corresponding value of spectral acceleration for the location to that specified return period. The two functions were combined into a MATLAB script and altered slightly to the preferences of the authors of this report. The core processes of the functions remain intact, and were written by Nicolas Luco. The two functions provided by Nicolas Luco can be found in Appendix Sections A.1 and A.2. The values used in this report do not contain the deterministic values that are used in the USGS applications near known active faults. Spectral acceleration values obtained using the seismic design maps in the AASHTO LRFD-BDS, or found through a USGS hazard application, have capped maximum values near known active faults, which will in some cases result in discrepancies between values obtained using the available seismic hazard data and those from the design maps found in AASHTO LRFD-BDS, or from the USGS applications. The deterministic capped ground motions are used in the seismic design maps when the value is smaller than the probabilistic value, thus using the probabilistic ground motions without the deterministic capping is more conservative

(Luco et al. 2007). The seismic hazard data was used in this report so spectral acceleration values could be determined for any desired return period and because of its availability on the USGS website.

The MATLAB script functions were used as follows. Each of the 100 locations outlined in Section 3.2 have corresponding latitude and longitude coordinates. A given location has coordinates that place it on a grid between 4 points of intersection provided by the USGS file as seen in Figure 3-2. A method known as bilinear interpolation is then performed between the 4 gridded points and the input location. The result is an array of MAFE values corresponding to the spectral acceleration values for a specified location. The equation for bilinear interpolation is given below (Steer 2010):

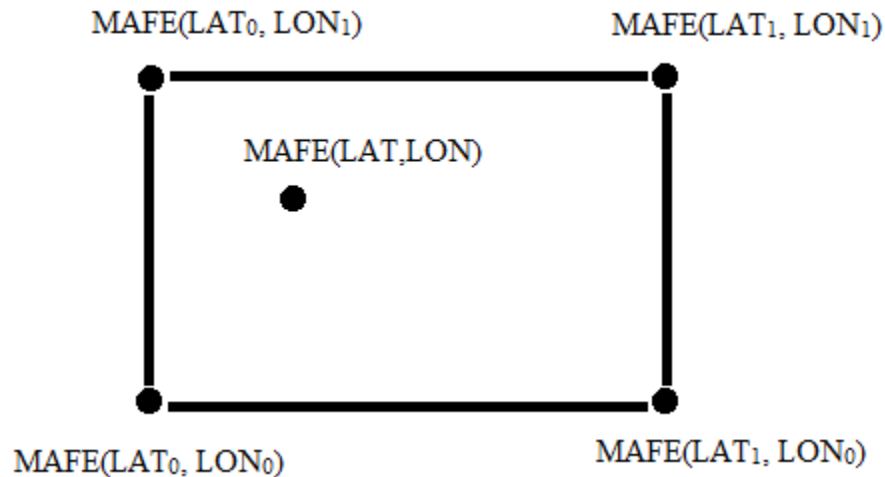


Figure 3-2: Example illustration of two-dimensional interpolation.

$$\begin{aligned}
 MAFE_j(LAT, LON) = & \frac{1}{(LAT_1 - LAT_0) * (LON_1 - LON_0)} * [MAFE(LAT_0, LON_0) * (LAT_1 - LAT) * (LON_1 - LON) \\
 & + MAFE(LAT_1, LON_0) * (LAT - LAT_0) * (LON_1 - LON) + MAFE(LAT_0, LON_1) * (LAT_1 - LAT) \\
 & * (LON - LON_0) + MAFE(LAT_1, LON_1) * (LAT - LAT_0) * (LON - LON_0)]
 \end{aligned}$$

where $MAFE_j(LAT, LON)$ is a MAFE value corresponding to one of the 19 to 20 given spectral accelerations. Thus, the above equation must be used 19 to 20 times, depending on the number of spectral accelerations used in the interpolation, to form an array of values. The points $LAT_1, LAT_0,$

LON₁, and LON₀ are the latitude and longitude values for the 4 points of intersection. The coordinates LAT and LON are the latitude and longitude values for the input location. The values of MAFE(LAT₀, LON₀), MAFE(LAT₁, LON₀), MAFE(LAT₀, LON₁), and MAFE(LAT₁, LON₁) are the MAFE values for a given spectral acceleration of the 4 points of intersection. Once this has been completed for each spectral acceleration value (19 to 20 times depending on the file), linear interpolation is used between the inverse of the input return period (MAFEI), the MAFE_j array of values for the location, and the given 19 to 20 spectral acceleration values. Due to the data being stored in a logarithmic scale, the natural logarithm of each component must be used in the final step of interpolation. The equation for linear interpolation is given below: (Walker 2016):

$$\ln(SA) = \ln(SA_j) + \frac{\ln(MAFEI) - \ln(MAFE_j)}{\ln(MAFE_{j+1}) - \ln(MAFE_j)} (\ln(SA_{j+1}) - \ln(SA_j))$$

$$SA = e^{\ln(SA)}$$

where SA is the output spectral response acceleration value for the location, MAFEI is the inverse of the input return period, MAFE_j and MAFE_{j+1} are the upper and lower bound MAFE values from the bilinear interpolation above, and SA_j and SA_{j+1} are the spectral response accelerations corresponding with MAFE_j and MAFE_{j+1}.

Note that for the response coefficients corresponding to permanent bridge design, a return period corresponding to a 5 percent probability of exceedance in 50 years was used instead of a 7 percent probability of exceedance in 75 years (which are equivalent for all practical purposes). During the preliminary stages of the report, a USGS java application was used to obtain directly spectral coefficients; this application did not have an option to obtain values corresponding to a 7 percent probability of exceedance in 75 years, but it could provide values corresponding to a 5 percent probability of exceedance in 50 years, which was used as an alternative. Unfortunately, this java application became “disabled” by USGS during the conduct of this project and the more complex procedure outline above had to be used. Note that the complexity of this procedure would be deemed by most structural engineers to exceed what is practical for the design of temporary bridge, which is why this study is investigating the possibility of developing constant reduction factors.

The spectral response coefficients given by interpolation of the seismic hazard data may subsequently be referred to as “obtained values,” as opposed to the spectral response coefficients calculated by the proposed method outlined in the next section, which may be referred to as “calculated values.”

Note that both the 2002 and the 2014 USGS seismic hazard data sets truncated the data at a minimum peak ground acceleration of 0.05 g, a minimum short-period response acceleration of 0.05 g, and a minimum long-period response acceleration of 0.025 g when generating hazard curves. A response acceleration below the truncated values cannot be obtained by interpolation. In this report for a given location that contains a spectral response coefficient that fails to meet the minimum acceleration value corresponding to that coefficient, the spectral response acceleration coefficient that fails to meet the minimum will not be considered in the analysis in Sections 4 and 5. This does not mean that all spectral response coefficients at that location will be ignored, only the coefficients that do not meet the minimum acceleration values.

3.4 The Spectral Reduction Factors

The methodology used for calculating the three spectral reduction factors proceeds per the following steps, using the various parameters defined as follows. First, to reduce the peak ground acceleration from the value for a 7 percent probability of exceedance in 75 years (for permanent bridges) to that for the 10 percent probability of exceedance in 10 years (for temporary bridges), a peak ground acceleration spectral reduction factor is defined as follows:

$$A_S = \frac{PGA_{75}}{K_{PGAD}} \quad (3-1)$$

where A_S is the design ground acceleration coefficient for temporary bridges, PGA_{75} is the peak ground acceleration coefficient corresponding to a 7 percent probability of exceedance in 75 years, and K_{PGAD} is the corresponding peak ground acceleration spectral reduction Factor.

Second, a short-period spectral reduction factor is used to reduce the response spectral acceleration coefficient pertaining to the short-period as follows:

$$S_{DS} = \frac{S_{S-75}}{K_{DS}} \quad (3-2)$$

where S_{DS} is the design short-period response spectral acceleration coefficient for temporary bridges, S_{S-75} is the short-period response acceleration coefficient corresponding to a 7 percent exceedance in 75 years, and K_{DS} is the short-period spectral reduction factor.

A long-period spectral reduction factor is used to reduce the response spectral acceleration coefficient pertaining to long-period as follows:

$$S_{D1} = \frac{S_{1-75}}{K_{D1}} \quad (3-3)$$

where S_{D1} is the design long-period response spectral acceleration for temporary bridges, S_{1-75} is the long-period response acceleration coefficient corresponding to a 7 percent exceedance in 75 years, and K_{D1} is the long-period spectral reduction factor.

Note that when using a reduced spectrum, it will be assumed that the specification given in Article 3.6 of the LRFD-SBD still applies, namely that the Seismic Design Category of the bridge will be determined from the reduced spectrum used for the temporary bridge design, with the one exception that, “a temporary bridge classified in SDC B, C, or D based on the unreduced spectrum cannot be reclassified to SDC A based on the reduced/modified response spectrum.” It will be assumed that this provision similarly applies to the Seismic Performance Zones, defined in Article 3.10.6 of the AASHTO LRFD-BDS, given that Seismic Performance Zones have almost identical defining criteria to the Seismic Design Categories defined in Article 3.5 of the AASHTO LRFD-SBD. Thus, it will be assumed that a temporary bridge meeting the criteria for Seismic Performance Zone 2, 3, or 4 using the 1000 year return period, cannot be reclassified as Seismic Performance Zone 1 using the reduced response spectrum. This is not explicitly specified in Article 3.10.10 of the AASHTO LRFD-BDS, the article governing seismic requirements for temporary bridges, but will be assumed for the proposed method in this report to provide continuity between AASHTO’s LRFD-SBD and LRFD-BDS.

Soil Site Class B, defined in Article 3.10.3.2 of the LRFD-BDS, was assumed for every location considered in this report, such as to ensure that the site factor at zero-period on acceleration spectrum, F_{pga} , the site factor for the short-period range, F_a , and the site factor for the long-period range, F_v , will all have a value of 1.0. This assumption has been made to eliminate the use of Equations 3.10.4.2-2, 3.10.4.2-3, and 3.10.4.2-6 given in Article 3.10.4.2 of the LRFD-BDS.

3.5 Method of Calculating K_{PGA} , K_{DS} , and K_{D1}

Using the response spectral acceleration parameters retrieved from the USGS website, three separate spectral reduction ratios are calculated for each location. The spectral reduction ratios correspond to the coefficients PGA , S_S , and S_1 , and will be used to derive the spectral reduction factors for the Seismic Groups. The first of these is the peak ground acceleration spectral reduction ratio, given by:

$$K_{PGA} = \frac{PGA_{75}}{PGA_{10}} \quad (3-4)$$

where PGA_{75} is the peak ground acceleration coefficient corresponding to a 7 percent probability of exceedance in 75 years obtained from interpolation, and PGA_{10} is the peak ground acceleration coefficient corresponding to a 10 percent probability of exceedance in 10 years:

The second is the short-period spectral reduction ratio, K_S , calculated as follows:

$$K_S = \frac{S_{S-75}}{S_{S-10}} \quad (3-5)$$

where S_{S-75} is the short-period acceleration coefficient corresponding to a 7 percent probability of exceedance in 75 years,, and S_{S-10} is the short-period acceleration coefficient corresponding to a 10 percent probability of exceedance in 10 years:

The third ratio is the long-period spectral reduction ratio, K_1 , given by:

$$K_1 = \frac{S_{1-75}}{S_{1-10}} \quad (3-6)$$

where S_{1-75} is the long-period acceleration coefficient corresponding to a 7 percent probability of exceedance in 75 years, and S_{1-10} is the long-period acceleration coefficient corresponding to a 10 percent probability of exceedance in 10 years-

For each Seismic Group, the mean value of the peak ground acceleration spectral reduction ratio, $K_{PGA\mu}$, the mean value of the short-period spectral reduction ratio, $K_{S\mu}$, and the mean value of the long-period spectral reduction ratio, $K_{1\mu}$, are used here to establish a preliminary value for respective reduction factors corresponding to each group. To ensure conservatism, one standard deviation is subtracted from the mean value to obtain a design value for the group. One standard deviation is expected to be appropriate, and will be discussed in Section 4.9. For the Design Peak Ground Acceleration Reduction Factor:

$$K_{PGAD} = K_{PGA\mu} - \sigma_{PGA} \quad (3-7)$$

where K_{PGAD} is the design peak ground acceleration reduction factor and σ_{PGA} is the sample standard deviation from $K_{PGA\mu}$. The design peak ground acceleration reduction factor will be used in Equation 3-1 to reduce the peak ground acceleration to values corresponding to a 10 percent probability of exceedance in 10 years. For the design short-period spectral reduction factor:

$$K_{DS} = K_{S\mu} - \sigma_S \quad (3-8)$$

where K_{DS} is the design short-period spectral reduction factor and σ_S is the standard deviation from $K_{S\mu}$. This value of K_{DS} will be used in Equation 3-2 to reduce the short-period response spectral acceleration coefficient. Likewise, the Long-Period Reduction Factor is calculated such that:

$$K_{D1} = K_{1\mu} - \sigma_1 \quad (3-9)$$

where K_{D1} is the design long-period spectral reduction factor and σ_1 is the sample standard deviation from $K_{1\mu}$. The value of K_{D1} will be used in Equation 3-3 to reduce the long-period spectral response acceleration coefficient to values corresponding to a 10 percent probability of exceedance in 10 years.

SECTION 4

DESIGN REDUCTION FACTORS BY GEOGRAPHIC LOCATION

Given the regional differences in seismic hazard curves outlined in Section 2.2, the following describes the method used here for defining Seismic Groups as a function of geographic location.

The 100 locations considered (shown in Chapter 3) were divided into seven Seismic Groups. The boundaries for Group 1, Group 2, Group 3, and Group 4 were taken from Seismic Region 1, Region 2, Region 3, and Region 4 defined in Article 3.10.2.1 of the LRFD-BDS. The GPS coordinates of these bounds were taken from the seismic design maps found in Article 3.10.2.1 of that document, with a minor alteration made to remove the area of overlap between Region 1 and Region 2, and are listed in Table 4-1. These geographic regions were given special consideration here as they are seismically active regions relative to the rest of the country.

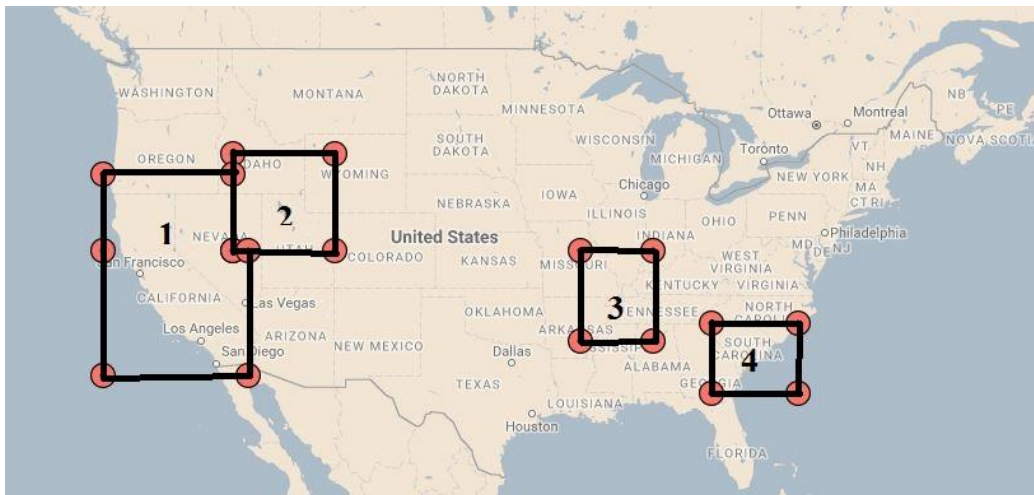


Figure 4-1: Visual illustration of Seismic Groups 1 through 4. Graphic created with <http://batchgeo.com> and map data from Google.

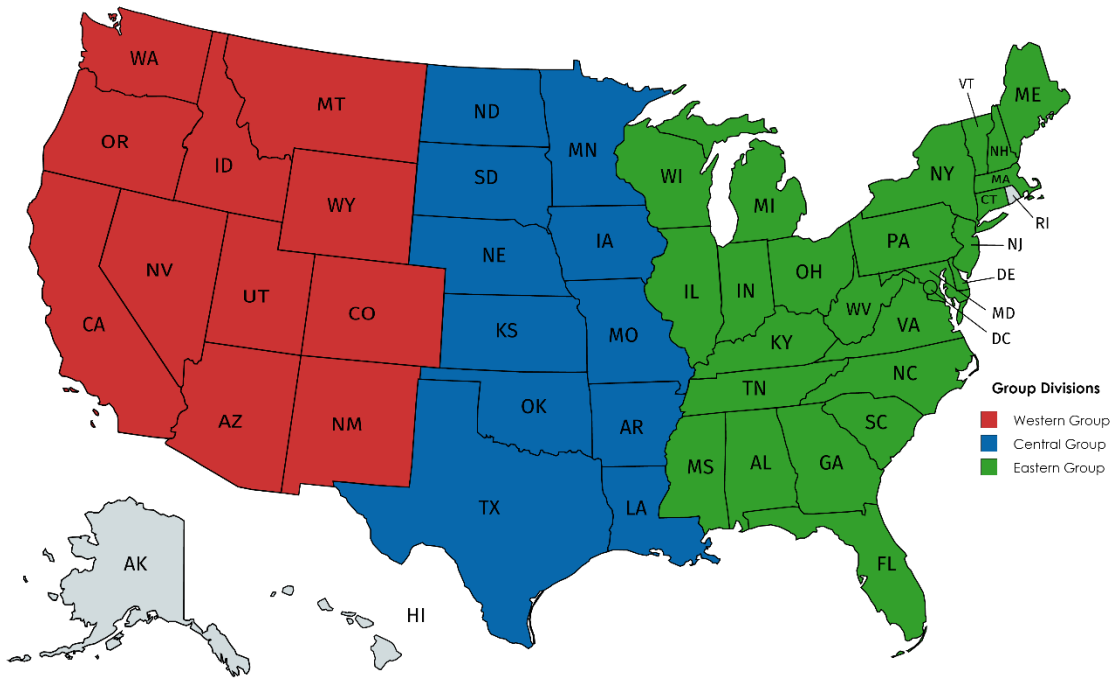
Table 4-1: Bounds for Seismic Groups 1 through 4 using latitude and longitude

Group	Latitude	Longitude
1	32°N to 39°N 39°N to 43°N	115°W to 125°W 116°W to 125°W
2	39°N to 44°N	109°W to 116°W
3	34°N to 39°N	87°W to 92°W
4	31°N to 35°N	77°W to 83°W

As many of the 100 locations considered did not fall into Seismic Groups 1 through 4, the rest of the continental United States was divided into three additional Groups:

- The Western Group, consisting of New Mexico, Colorado, Wyoming, Montana, Idaho, Utah, Arizona, Nevada, California, Oregon, and Washington
- The Central Group, consisting of North Dakota, South Dakota, Nebraska, Minnesota, Iowa, Kansas, Missouri, Oklahoma, Arkansas, Texas, and Louisiana.
- The Eastern Group, consisting of Wisconsin, Illinois, Mississippi, Michigan, Indiana, Kentucky, Tennessee, Alabama, Ohio, Georgia, Florida, Maine, New Hampshire, Vermont, Massachusetts, Rhode Island, Connecticut, New Jersey, Delaware, Maryland, West Virginia, New York, Pennsylvania, Virginia, North Carolina, South Carolina, and Washington, D.C.

The division by state for these three additional Seismic Groups is illustrated below in Figure 4-2. The seismic hazard data obtained for each location from the 2002 USGS seismic hazard data set can be found in Section 6.3, and the data obtained from the 2014 USGS seismic hazard data set can be found in Section 6.4.



Created with mapchart.net ©

Figure 4-2: Division of Seismic Groups by state. Graphic created with <http://mapchart.net>

4.1 General Procedure for Each Group

The results for each Seismic Group were determined using the same general procedure and are presented in sections 4.2 through 4.8 with the same general format. The results are presented for both the 2002 and 2014 USGS seismic hazard data sets. For comparison, the data sets are presented graphically in a side-by-side format.

For each Seismic Group, the values of K_{PGA} , K_S , and K_I were calculated for each location, respectively using equations 3-4, 3-5, and 3-6. The first figure presented for each group, contains plots with trendlines corresponding to the group's mean values for K_{pga} , K_S , and K_I . The first plot within the first figure gives each location's peak ground acceleration corresponding to a 7 percent probability of exceedance in 75 years on the y-axis, and a location's peak ground acceleration corresponding to a 10 percent probability of exceedance in 10 years on the x-axis. Similarly, the two additional plots within the first figure give each location's short-period response acceleration value corresponding to a 7 percent probability of exceedance in 75 years on the y-axis and the

short-period response acceleration value corresponding to a 10 percent probability of exceedance in 10 years on the x-axis, and each location’s long-period response acceleration value corresponding to a 7 percent probability of exceedance in 75 years on the y-axis and the long-period response acceleration value corresponding to a 10 percent probability of exceedance in 10 years on the x-axis. A subsequent table gives each Seismic Groups mean value and standard deviation for K_{pga} , K_S , and K_1 . As defined in equations 3-7, 3-8, and 3-9, a subtraction of one standard deviation from the mean gives the spectral reduction factors for each Seismic Group, A_{SD} , S_{SD} , and S_{1D} . The three spectral reduction factors are the proposed alternative to using the USGS website for spectral response coefficient values corresponding to temporary bridge design.

For each location, AASHTO’s three spectral response coefficients have been calculated using the proposed spectral reduction factors. In order to compare the values of the spectral response coefficients calculated using the proposed spectral reduction factors with the values obtained directly from the USGS seismic hazard data, the following ratios are used:

$$\frac{A_{SD}}{PGA_{10}} \quad (4-1)$$

$$\frac{S_{SD}}{S_{S-10}} \quad (4-2)$$

$$\frac{S_{1D}}{S_{1-10}} \quad (4-3)$$

The spectral response coefficients given in the numerator of each ratio have been calculated using the proposed spectral reduction factors, the denominators contain the obtained values from the USGS seismic hazard data. Thus, a value greater than 1 given by either of 4-1, 4-2, or 4-3, is a conservative response spectra relative to the spectra obtained directly from the USGS website. Plots of the three ratios are shown in the second figure for each Seismic Group. A horizontal bold line in each plot is shown at the value of 1; points below the line indicate non-conservative calculated values relative to obtained values, in that the result is a calculated response spectrum smaller in magnitude than the obtained spectral response acceleration, and points above the line are conservative relative to obtained values in that the calculated gives a spectral response coefficient greater than the obtained value. The second table for each Seismic Group provides the design spectral reduction ratio for each coefficient.

Finally, a third figure is provided for each Seismic Group with the seismic design spectra comparing the average calculated seismic design spectrum and the average USGS obtained seismic design spectrum. The spectra were produced using the new seismic response coefficients following the procedure given in AASHTO LRFD-BDS Article 3.10.4.1, with an assumed designation of Site Class B.

It should be noted that within each Seismic Group, only the spectral reduction factors remain the same for any two locations within the same Seismic Group. The acceleration parameters that are being reduced are identical to the ones that would be used at a location for permanent bridge design. Thus, being in the same Seismic Group does not mean an equivalent or similar probabilistic earthquake hazard.

4.2 Group 1

Group 1 contains 14 of the 100 site locations considered. Results for those sites, obtained per the procedure outlined above, are presented below.

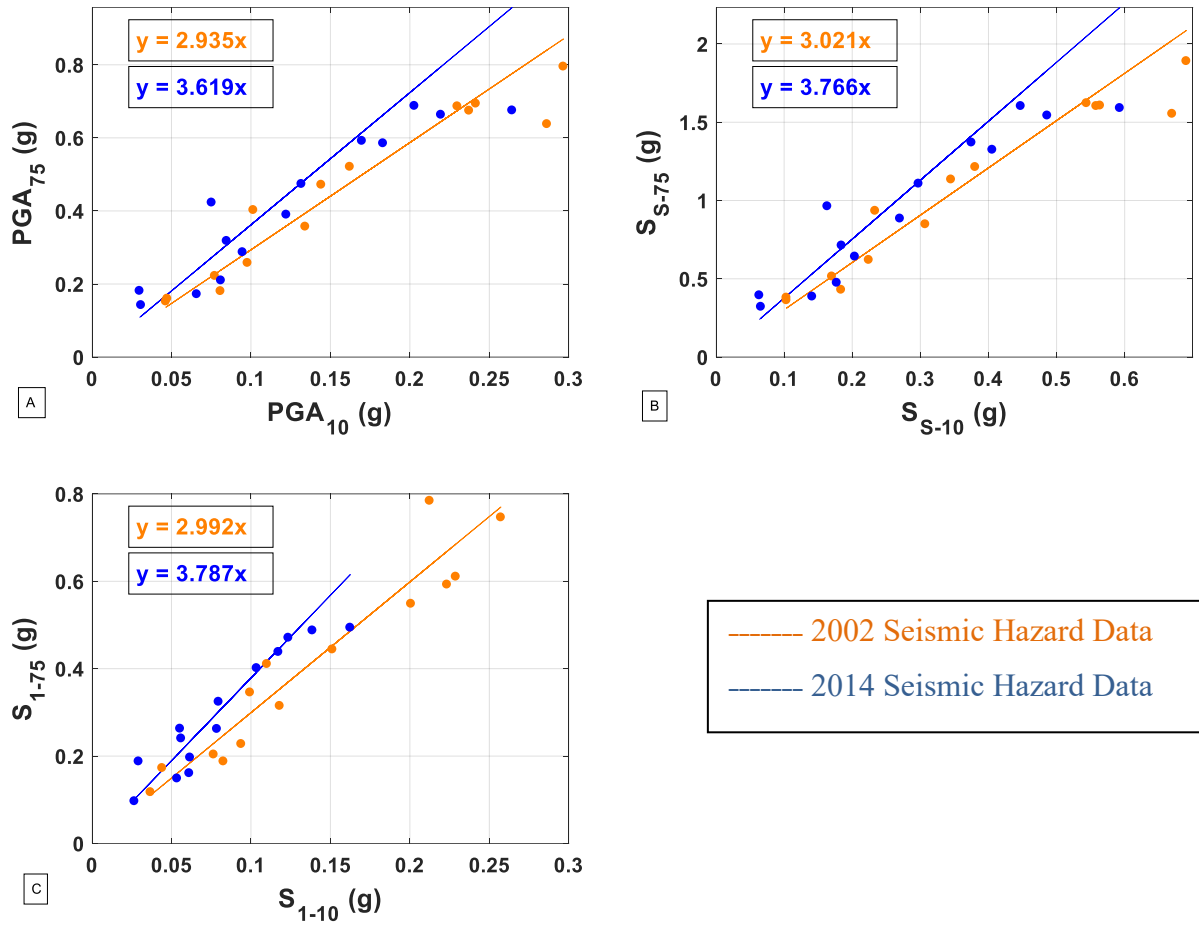


Figure 4-3: Mean spectral ratios for Group 1: (A) spectral ratio for mean peak ground acceleration, K_{PGA} ; (B) spectral ratio for mean short-period response acceleration, K_S ; (C) spectral ratio for mean long-period response acceleration, K_L .

Table 4-2: Mean spectral ratios for Group 1

Parameter	2002 Value	2014 Value
$K_{PGA\mu}$	2.935	3.619
σ_{PGA}	0.464	1.083
$K_{S\mu}$	3.021	3.766
σ_S	0.475	1.121
$K_{1\mu}$	2.992	3.787
σ_1	0.519	0.948

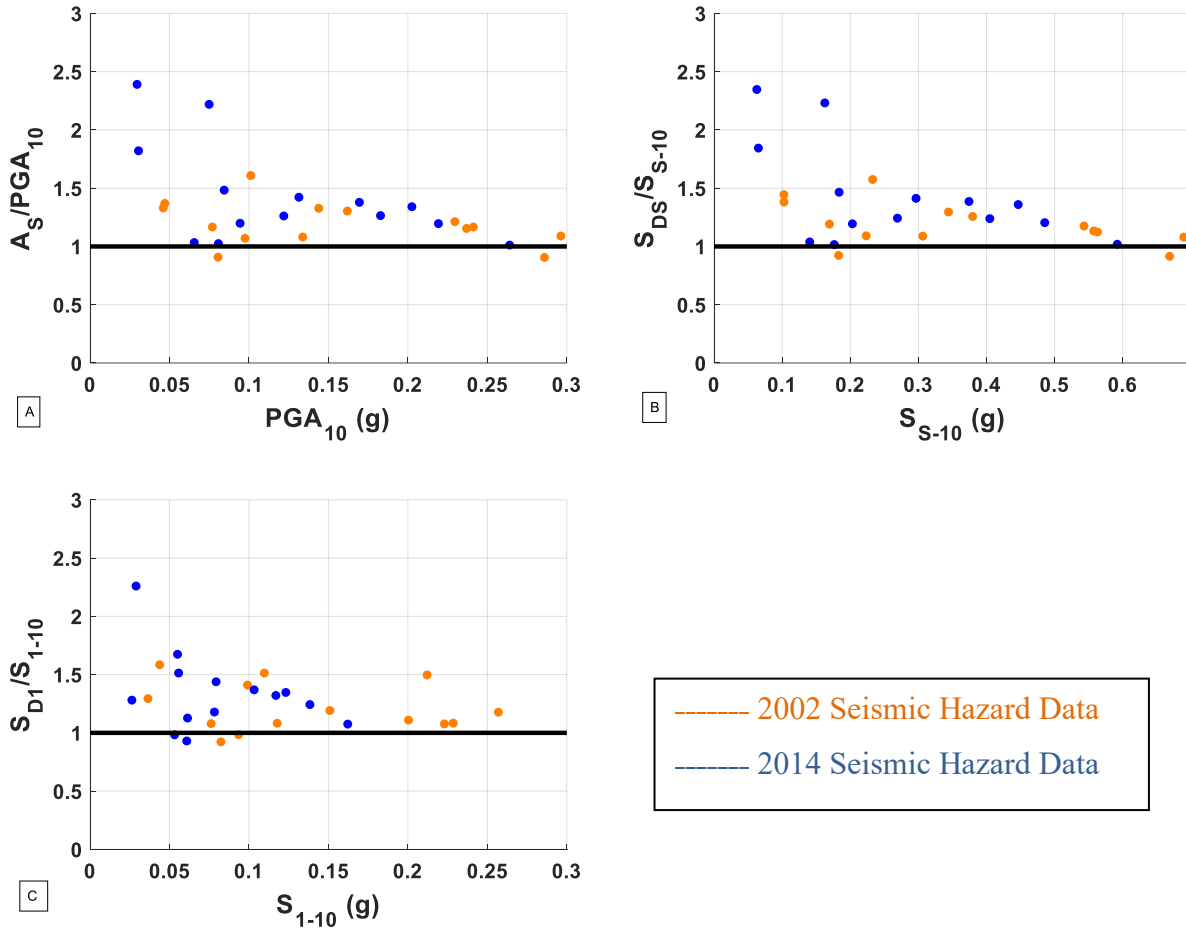


Figure 4-4 : Comparison of calculated response spectra coefficient values versus obtained values for Group 1: (A) coefficient for peak ground acceleration calculated using $K_{PGA} - \sigma_{PGA}$; (B) coefficient for short-period response acceleration calculated using $K_{S\mu} - \sigma_S$; (C) coefficient for long-period response acceleration calculated using values $K_{1\mu} - \sigma_1$.

Table 4-3: Spectral reduction factors for Group 1

Parameter	2002	2014
K_{PGAD}	2.471	2.536
K_{SD}	2.546	2.645
K_{1D}	2.473	2.839

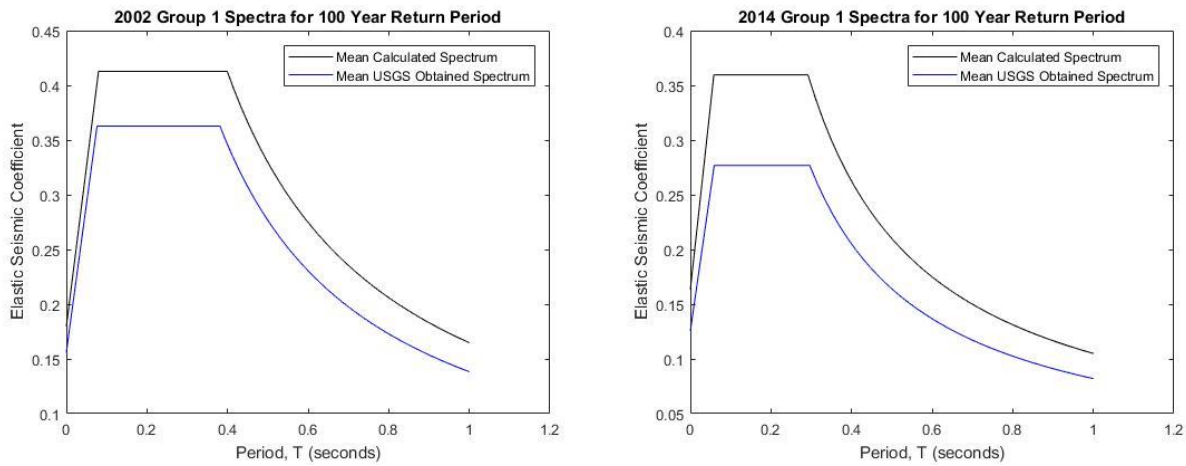


Figure 4-5: Comparison of mean response spectra produced using calculated spectral reduction factors, and of mean response spectra produced using USGS obtained values for Group 1: (Left) 2002 USGS seismic hazard data; (Right) 2014 USGS seismic hazard data.

4.3 Group 2

Group 2 contains 10 of the 100 site locations considered. Results for those sites, obtained per the procedure outlined above, are presented below.

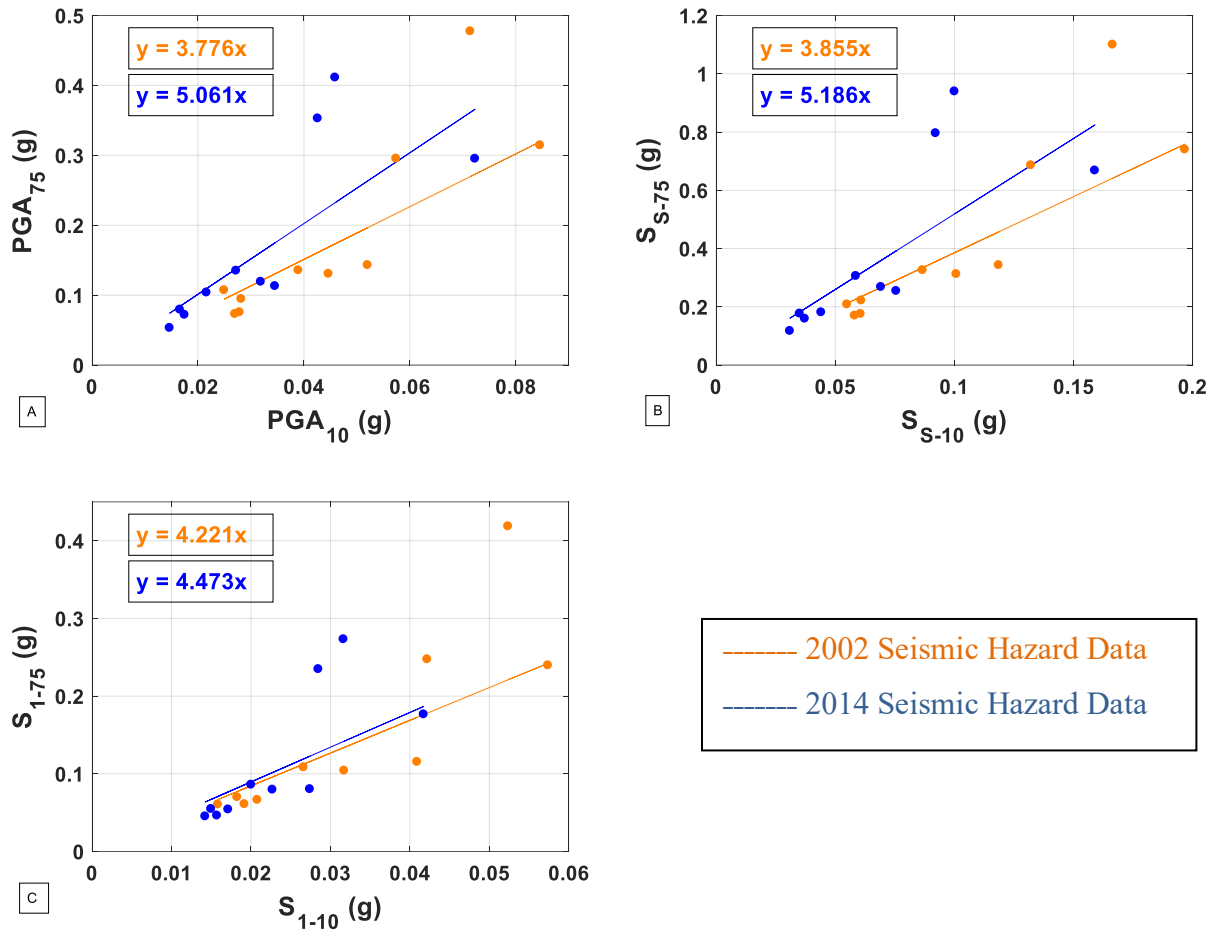


Figure 4-6: Mean spectral ratios for Group 2: (A) spectral ratio for mean peak ground acceleration, K_{PGA} ; (B) spectral ratio for mean short-period response acceleration, K_S ; (C) spectral ratio for mean long-period response acceleration, K_L .

Table 4-4: Mean spectral ratios for Group 2

Parameter	2002	2014
$K_{PGA\mu}$	3.776	5.061
σ_{PGA}	1.288	1.960
$K_{S\mu}$	3.855	5.186
σ_S	1.190	2.097
$K_{1\mu}$	4.221	4.473
σ_1	1.573	2.144

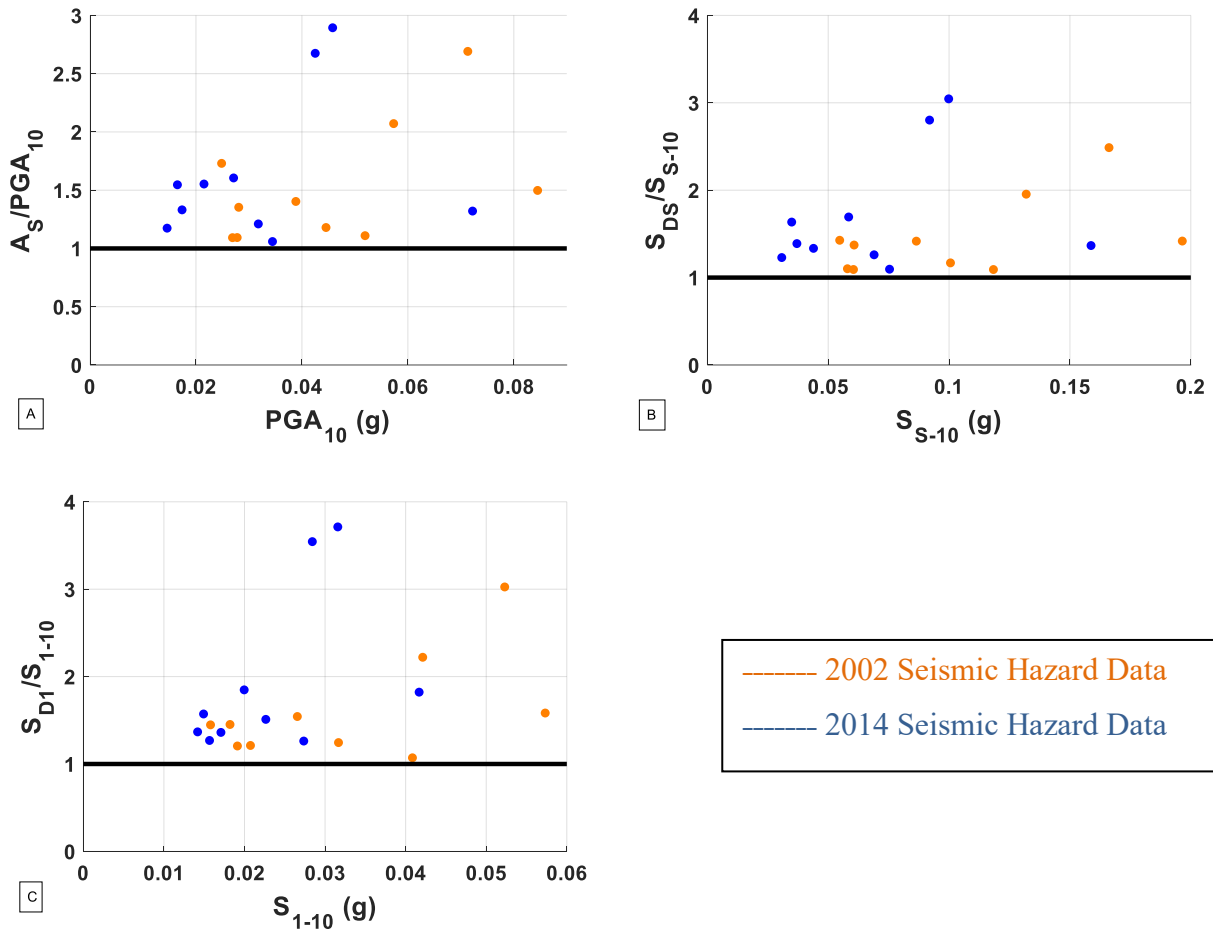


Figure 4-7: Comparison of calculated response spectra coefficient values versus obtained values for Group 2: (A) coefficient for peak ground acceleration calculated using $K_{PGA} - \sigma_{PGA}$; (B) coefficient for short-period response acceleration calculated using $K_{S\mu} - \sigma_S$; (C) coefficient for long-period response acceleration calculated using values $K_{1\mu} - \sigma_1$.

Table 4-5: Spectral reduction factors for Group 2

Parameter	2002	2014
K_{PGAD}	2.488	3.101
K_{SD}	2.665	3.089
K_{1D}	2.648	2.329

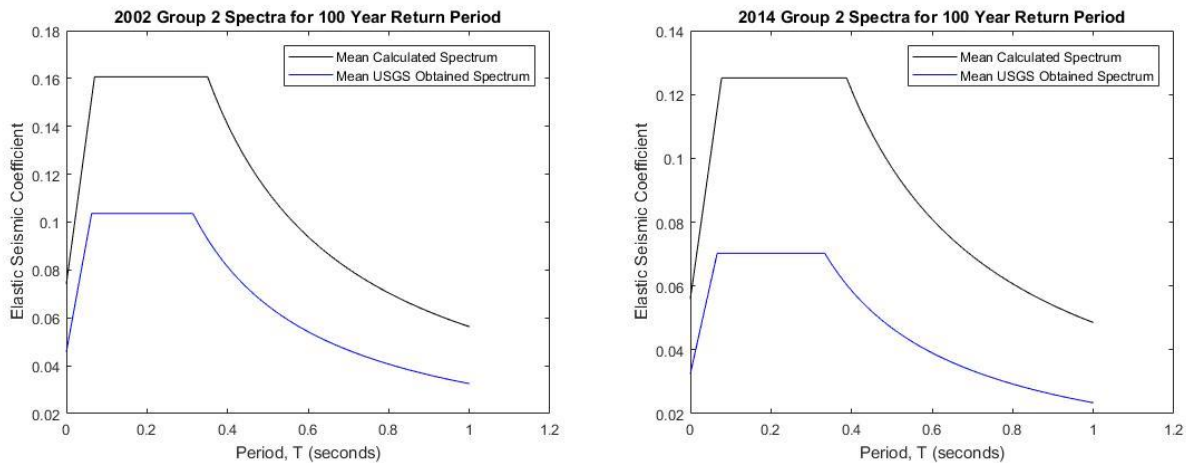


Figure 4-8: Comparison of mean response spectra produced using calculated spectral reduction factors, and of mean response spectra produced using USGS obtained values for Group 2: (Left) 2002 USGS seismic hazard data; (Right) 2014 USGS seismic hazard data.

4.4 Group 3

Group 3 contains 10 of the 100 site locations considered. Results for those sites, obtained per the procedure outlined above, are presented below.

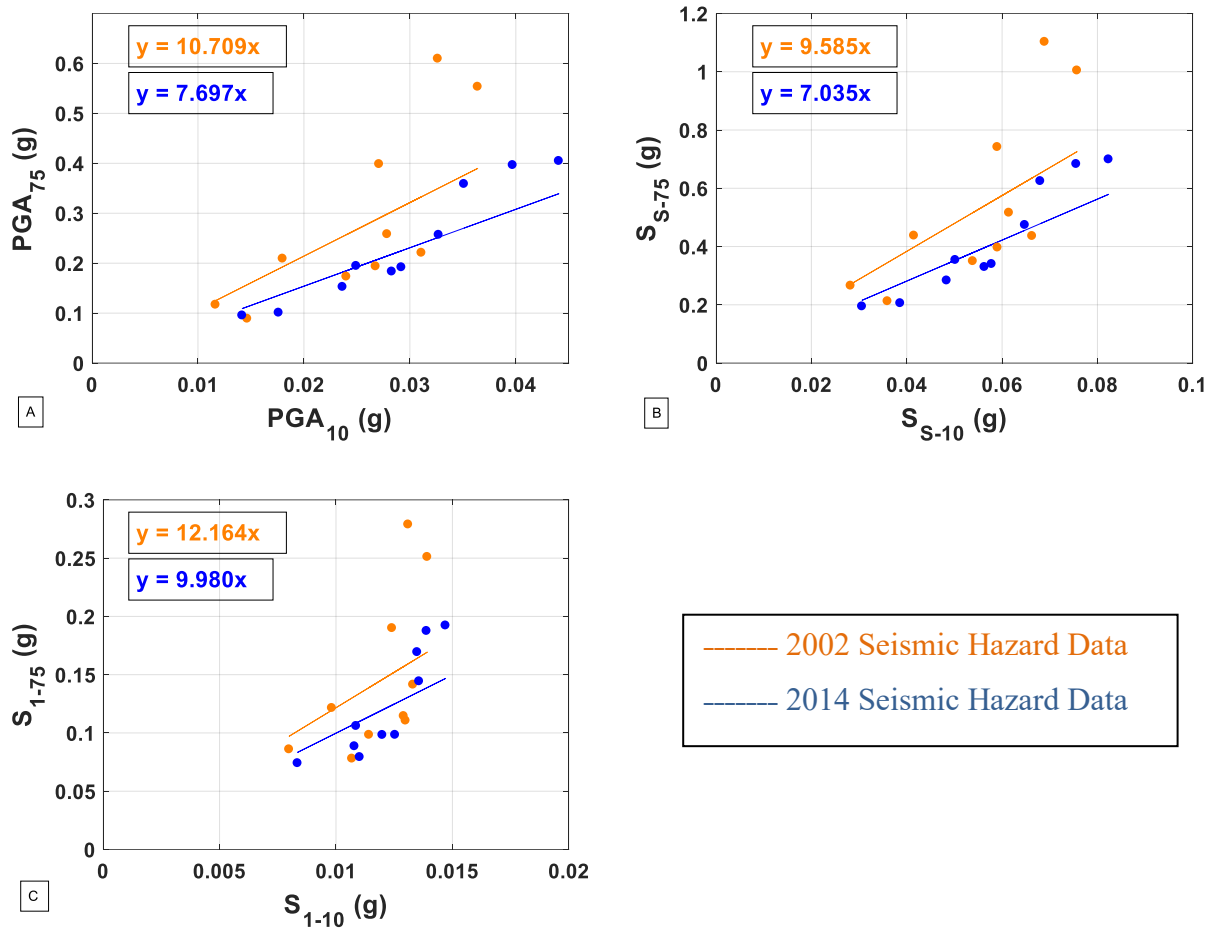


Figure 4-9: Mean spectral ratios for Group 3: (A) spectral ratio for mean peak ground acceleration, K_{PGA} ; (B) spectral ratio for mean short-period response acceleration, K_S ; (C) spectral ratio for mean long-period response acceleration, K_L .

Table 4-6: Mean spectral ratios for Group 3

Parameter	2002	2014
$K_{PGA\mu}$	10.709	7.697
σ_{PGA}	4.241	1.598
$K_{S\mu}$	9.585	7.035
σ_S	3.436	1.429
$K_{l\mu}$	12.164	9.980
σ_l	4.624	2.332

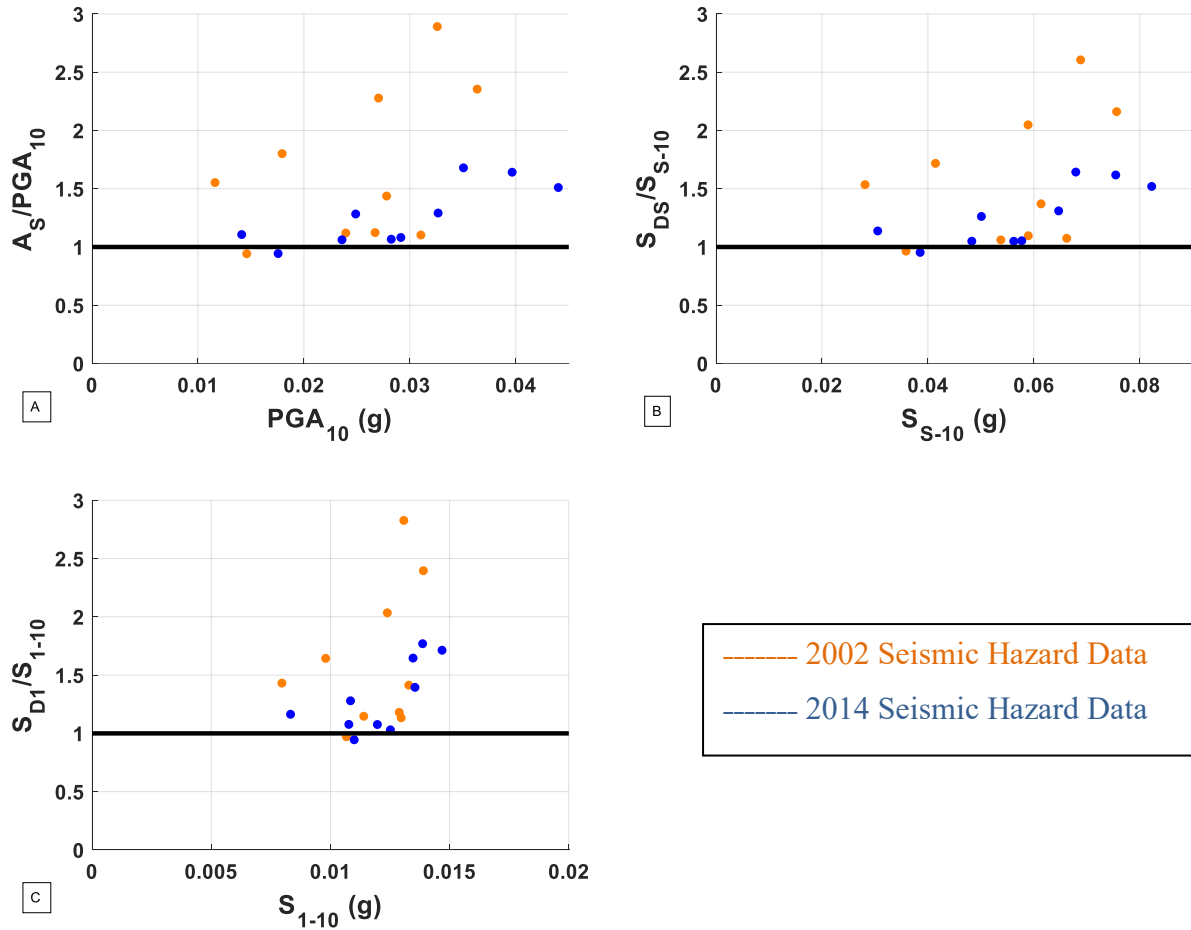


Figure 4-10: Comparison of calculated response spectra coefficient values versus obtained values for Group 3: (A) coefficient for peak ground acceleration calculated using $K_{PGA} - \sigma_{PGA}$; (B) coefficient for short-period response acceleration calculated using $K_{S\mu} - \sigma_S$; (C) coefficient for long-period response acceleration calculated using values $K_{l\mu} - \sigma_l$.

Table 4-7: Spectral reduction factors for Group 3

Parameter	2002	2014
K_{PGAD}	6.468	6.100
K_{SD}	6.149	5.606
K_{1D}	7.540	7.648

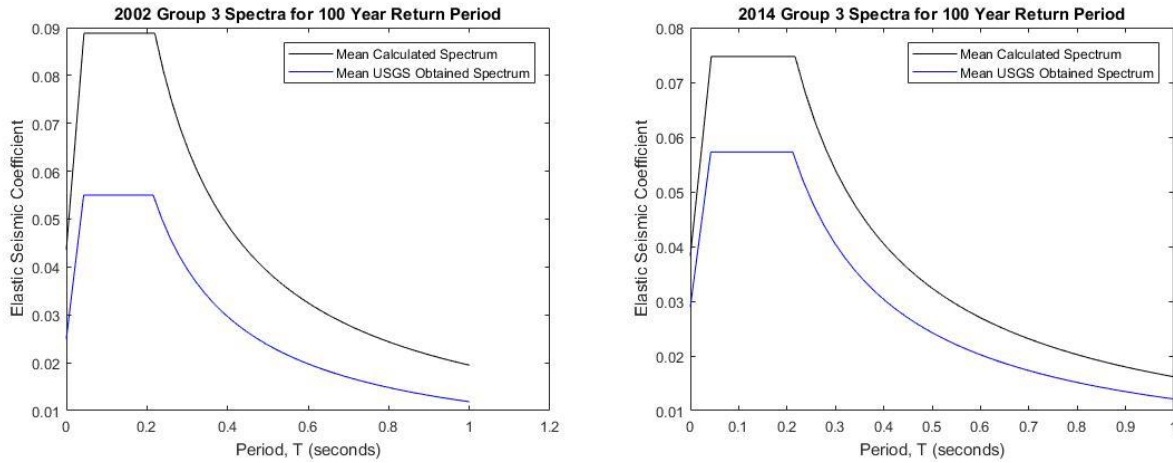


Figure 4-11: Comparison of mean response spectra produced using calculated spectral reduction factors, and of mean response spectra produced using USGS obtained values for Group 3: (Left) 2002 USGS seismic hazard data; (Right) 2014 USGS seismic hazard data.

4.5 Group 4

Group 4 contains 10 of the 100 site locations considered. Results for those sites, obtained per the procedure outlined above, are presented below.

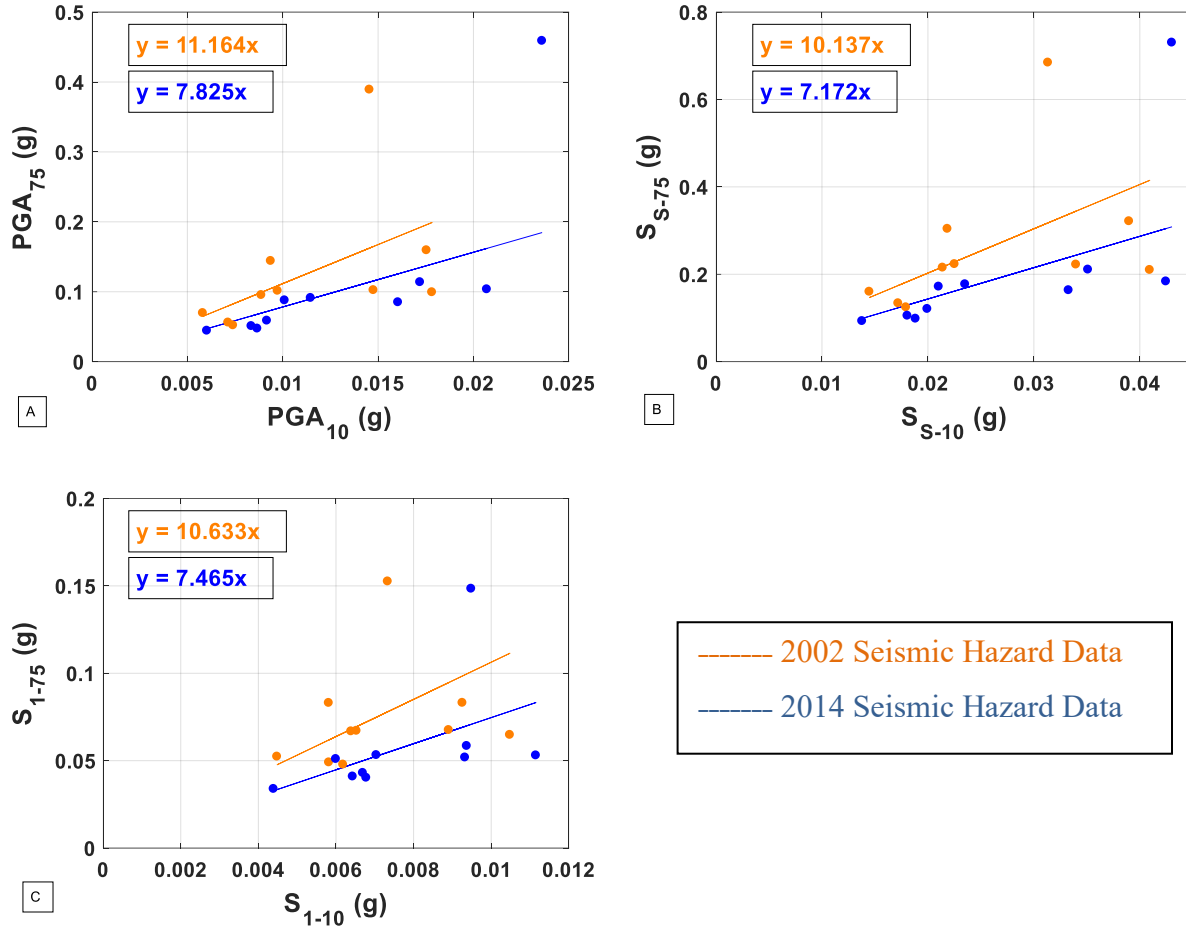


Figure 4-12: Mean spectral ratios for Group 4: (A) spectral ratio for mean peak ground acceleration, K_{PGA} ; (B) spectral ratio for mean short-period response acceleration, K_S ; (C) spectral ratio for mean long-period response acceleration, K_L .

Table 4-8: Mean spectral ratios for Group 4

Parameter	2002	2014
$K_{PGA\mu}$	11.164	7.825
σ_{PGA}	6.176	4.249
$K_{S\mu}$	10.137	7.172
σ_S	4.825	3.632
$K_{l\mu}$	10.633	7.465
σ_l	4.257	3.075

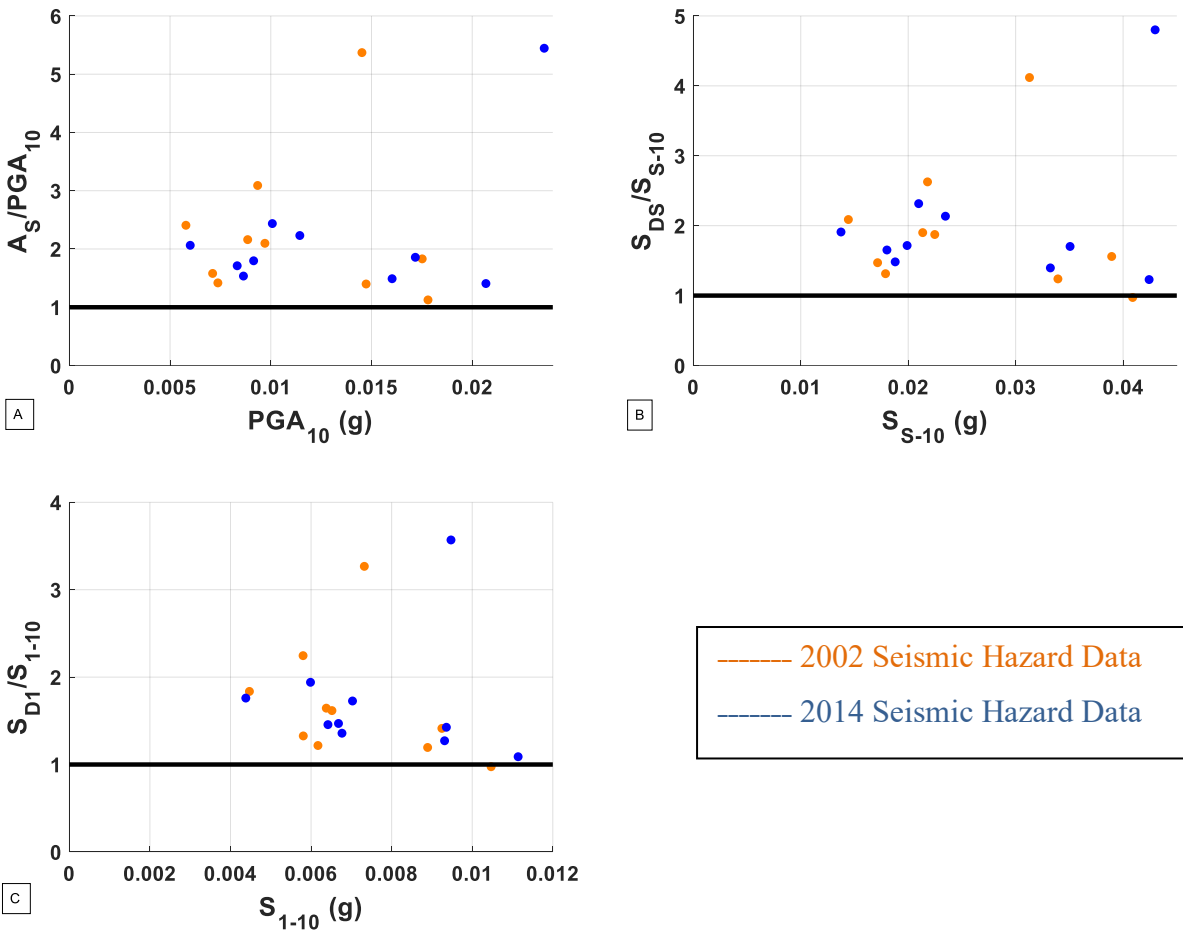


Figure 4-13: Comparison of calculated response spectra coefficient values versus obtained values for Group 4: (A) coefficient for peak ground acceleration calculated using $K_{PGA} - \sigma_{PGA}$; (B) coefficient for short-period response acceleration calculated using $K_{S\mu} - \sigma_S$; (C) coefficient for long-period response acceleration calculated using values $K_{l\mu} - \sigma_l$.

Table 4-9: Spectral reduction factors for Group 4

Parameter	2002	2014
K_{PGAD}	4.987	3.576
K_{SD}	5.312	3.540
K_{ID}	6.376	4.389

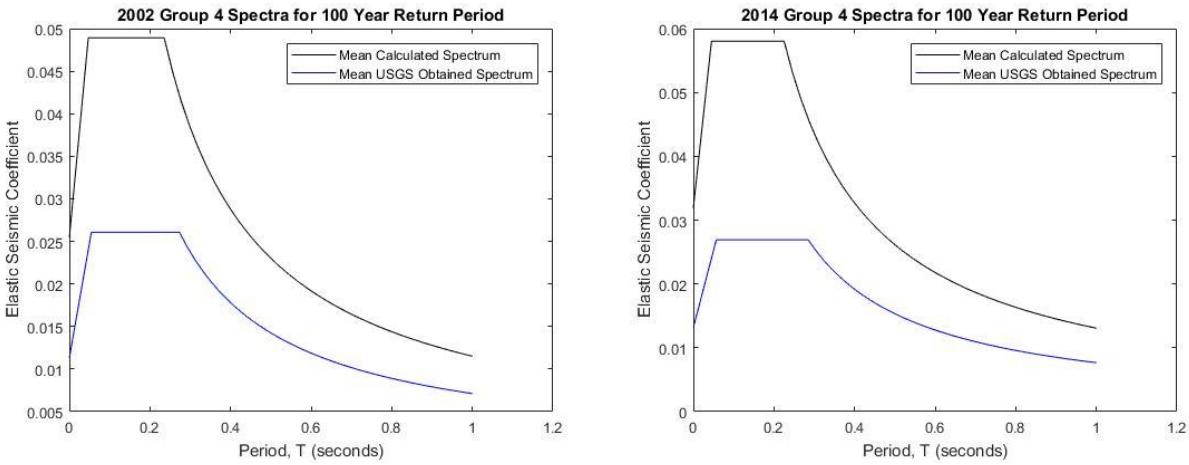


Figure 4-14: Comparison of mean response spectra produced using calculated spectral reduction factors, and of mean response spectra produced using USGS obtained values for Group 4: (Left) 2002 USGS seismic hazard data; (Right) 2014 USGS seismic hazard data.

4.6 Western Group

The Western Group contains 17 of the 100 site locations considered. Results for those sites, obtained per the procedure outlined above, are presented below.

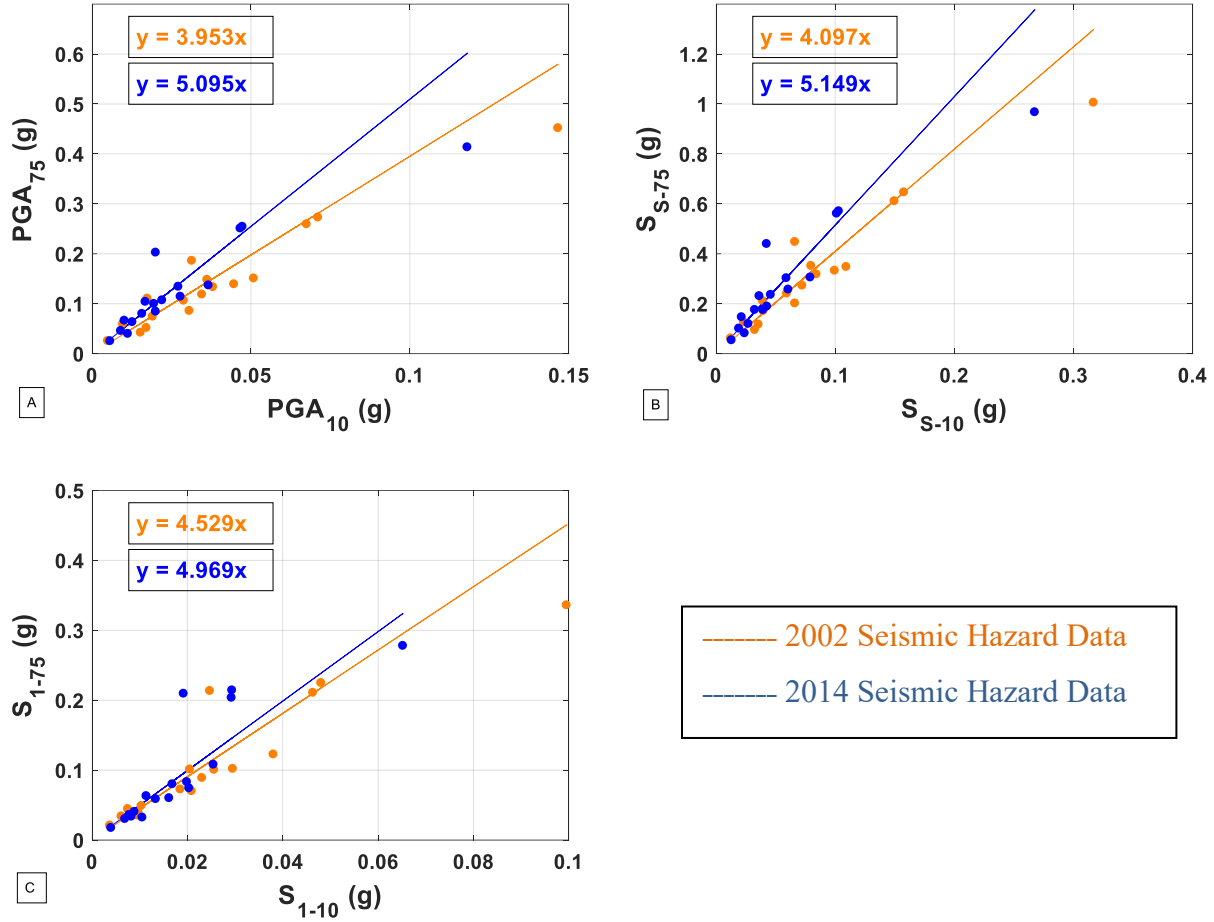


Figure 4-15: Mean spectral ratios for the Western Group: (A) spectral ratio for mean peak ground acceleration, K_{PGA} ; (B) spectral ratio for mean short-period response acceleration, K_S ; (C) spectral ratio for mean long-period response acceleration, K_L .

Table 4-10: Mean spectral ratios for the Western Group

Parameter	2002	2014
$K_{PGA\mu}$	3.953	5.095
σ_{PGA}	1.168	1.528
$K_{S\mu}$	4.097	5.149
σ_S	1.025	1.616
$K_{I\mu}$	4.529	4.969
σ_I	1.332	1.869

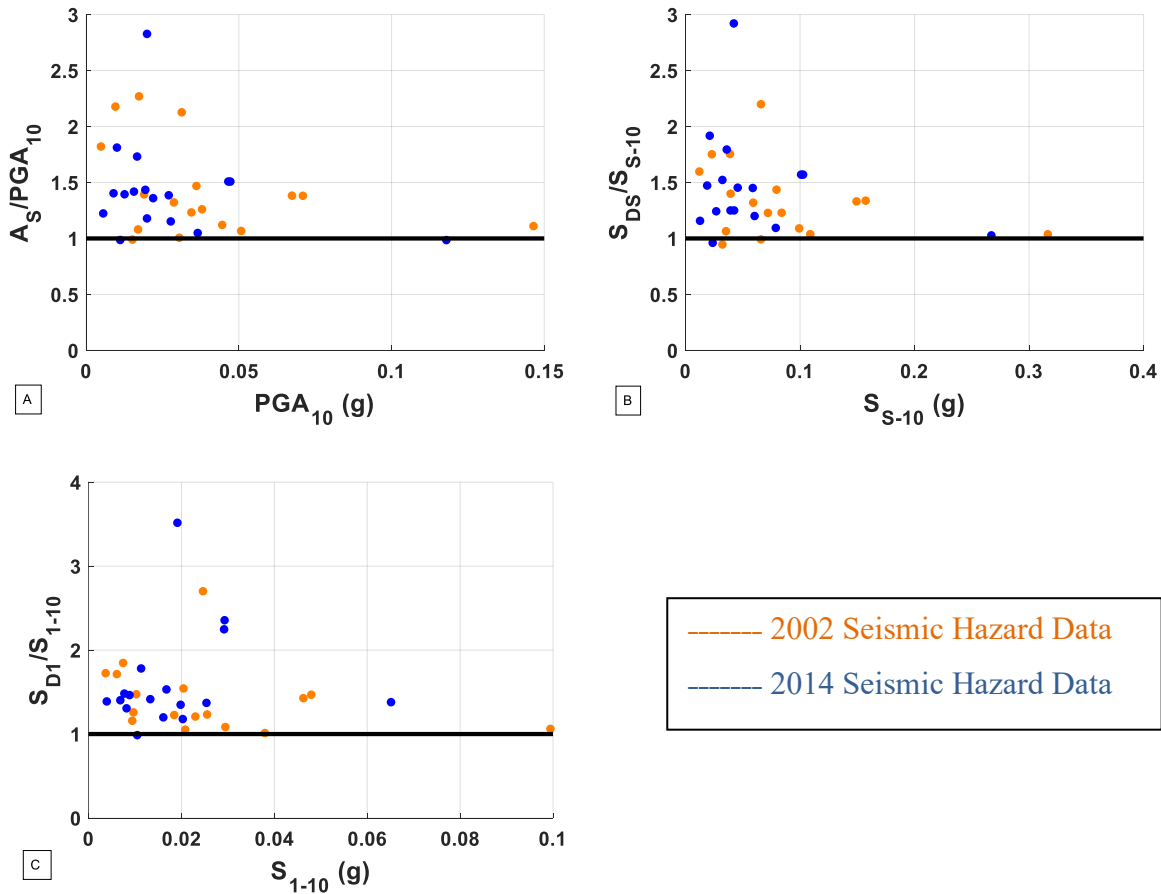


Figure 4-16: Comparison of calculated response spectra coefficient values versus obtained values for the Western Group: (A) coefficient for peak ground acceleration calculated using $K_{PGA} - \sigma_{PGA}$; (B) coefficient for short-period response acceleration calculated using

Table 4-11: Spectral reduction factors for the Western Group

Parameter	2002	2014
K_{PGAD}	2.785	3.568
K_{SD}	3.072	3.533
K_{ID}	3.197	3.100

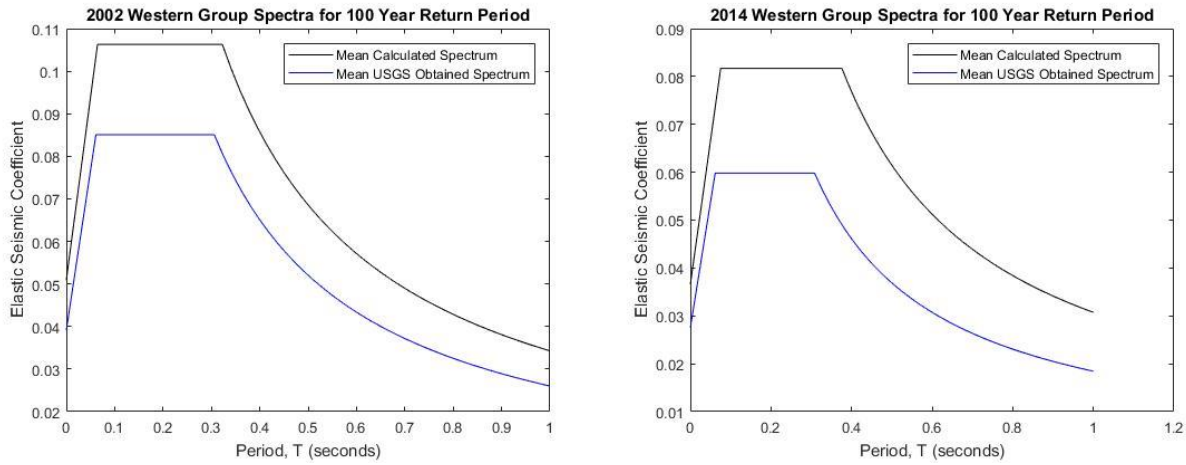


Figure 4-17: Comparison of mean response spectra produced using calculated spectral reduction factors, and of mean response spectra produced using USGS obtained values for the Western Group: (Left) 2002 USGS seismic hazard data; (Right) 2014 USGS seismic hazard data.

4.7 Central Group

The Central Group contains 18 of the 100 site locations considered. Results for those sites, obtained per the procedure outlined above, are presented below. For the 2002 seismic hazard data, a total of 13 site locations are below the minimum peak ground acceleration, 4 site locations are below the minimum short-period response acceleration, and 6 site locations are below the minimum long-period response acceleration. For the 2014 seismic hazard data, 11 site locations are below the minimum peak ground acceleration, 3 site locations are below the minimum short-period response acceleration, and 4 site locations are below the minimum long-period response acceleration. As previously stated, values below the minimum were not considered in analysis.

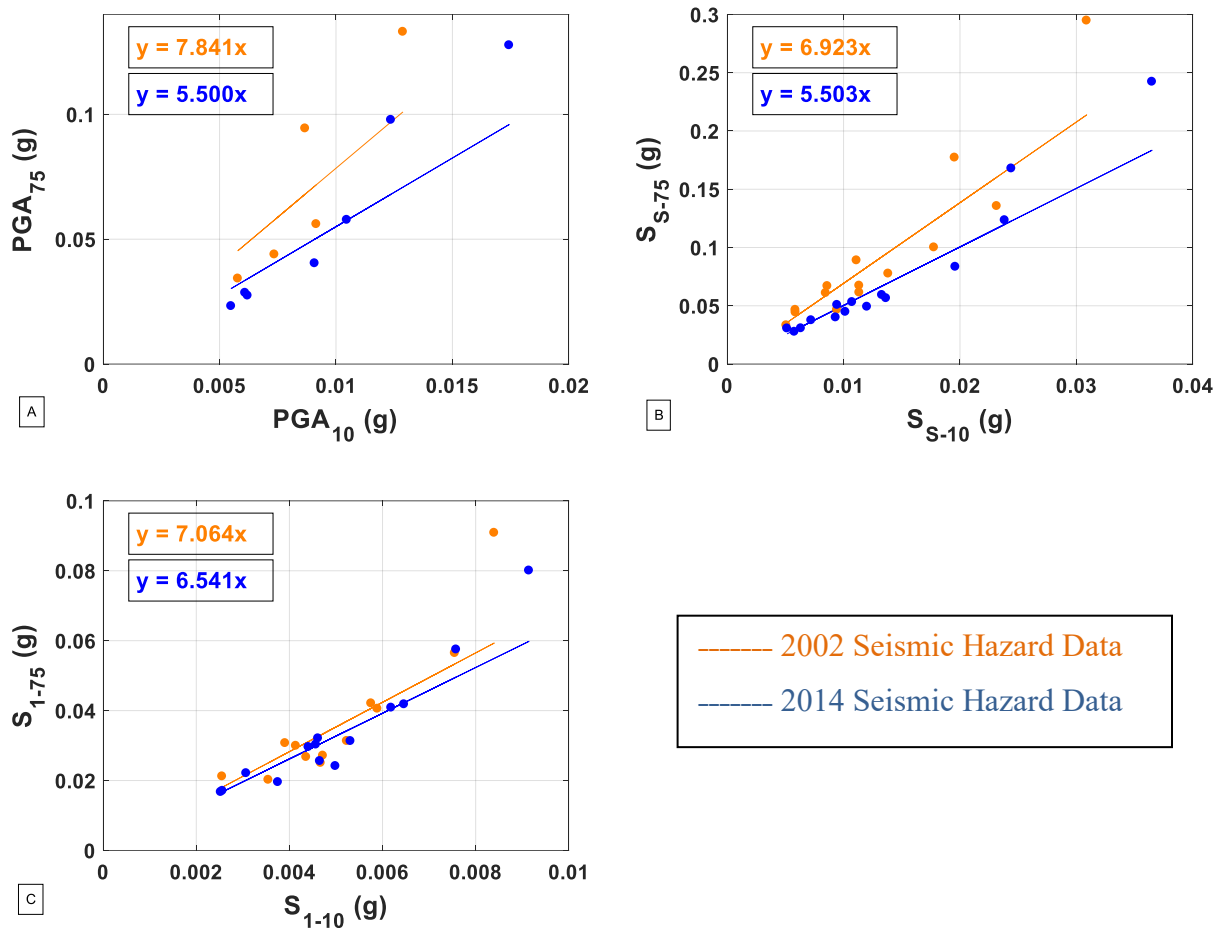


Figure 4-18: Mean spectral ratios for the Central Group: (A) spectral ratio for mean peak ground acceleration, K_{PGA} ; (B) spectral ratio for mean short-period response acceleration, K_S ; (C) spectral ratio for mean long-period response acceleration, K_L .

Table 4-12: Mean spectral ratios for the Central Group

Parameter	2002	2014
$K_{PGA\mu}$	7.841	5.500
σ_{PGA}	2.530	1.512
$K_{S\mu}$	6.923	5.026
σ_S	1.434	0.870
$K_{l\mu}$	7.064	6.541
σ_l	1.510	0.994

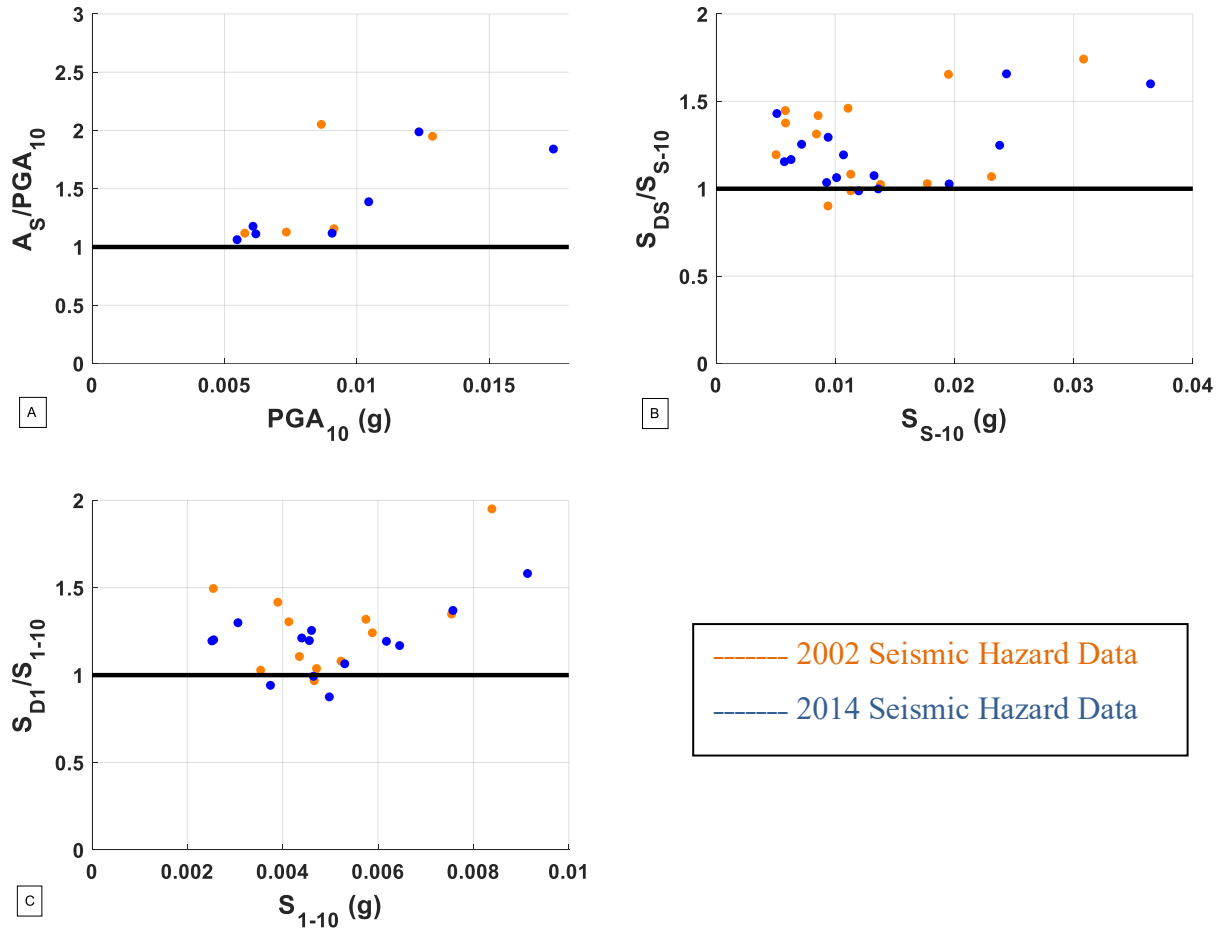


Figure 4-19: Comparison of calculated response spectra coefficient values versus obtained values for the Central Group: (A) coefficient for peak ground acceleration calculated using $K_{PGA} - \sigma_{PGA}$; (B) coefficient for short-period response acceleration calculated using $K_{S\mu} - \sigma_S$; (C) coefficient for long-period response acceleration calculated using values $K_{l\mu} - \sigma_l$.

Table 4-13: Spectral reduction factors for the Central Group

Parameter	2002	2014
K_{PGAD}	5.312	3.988
K_{SD}	5.489	4.156
K_{ID}	5.553	5.547

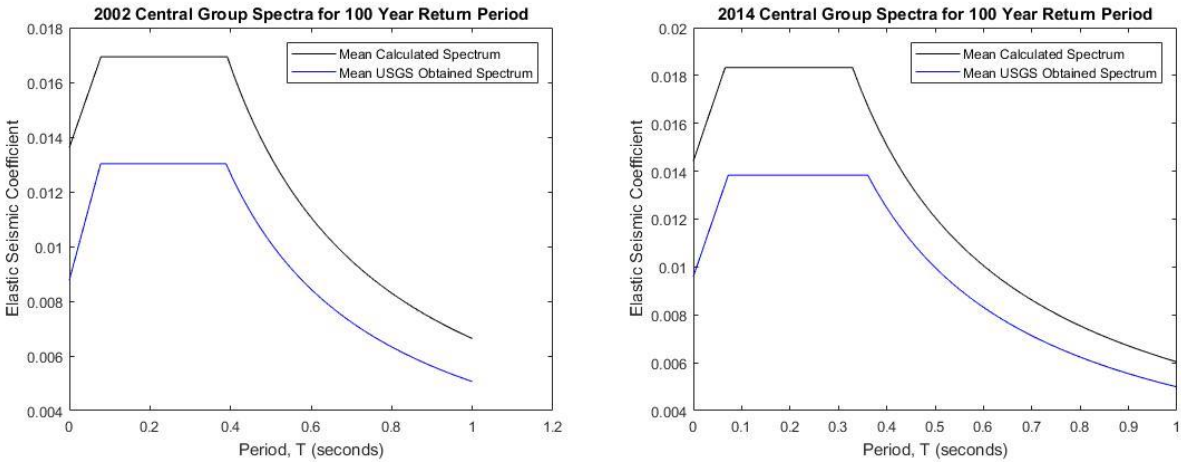


Figure 4-20: Comparison of mean response spectra produced using calculated spectral reduction factors, and of mean response spectra produced using USGS obtained values for the Central Group: (Left) 2002 USGS seismic hazard data; (Right) 2014 USGS seismic hazard data.

4.8 Eastern Group

The Eastern Group contains 21 of the 100 site locations considered. Results for those sites, obtained per the procedure outlined above, are presented below. For the 2002 USGS seismic hazard data, a total of 4 site locations are below the minimum peak ground acceleration, 1 site location is below the minimum short-period response acceleration, and 1 location is below the minimum long-period response acceleration. For the 2014 USGS seismic hazard data, 2 site locations are below the minimum peak ground acceleration, 1 site location is below the minimum short-period response acceleration, and 1 site location is below the minimum long period response acceleration. As previously stated, values below the minimum will not be considered for analysis.

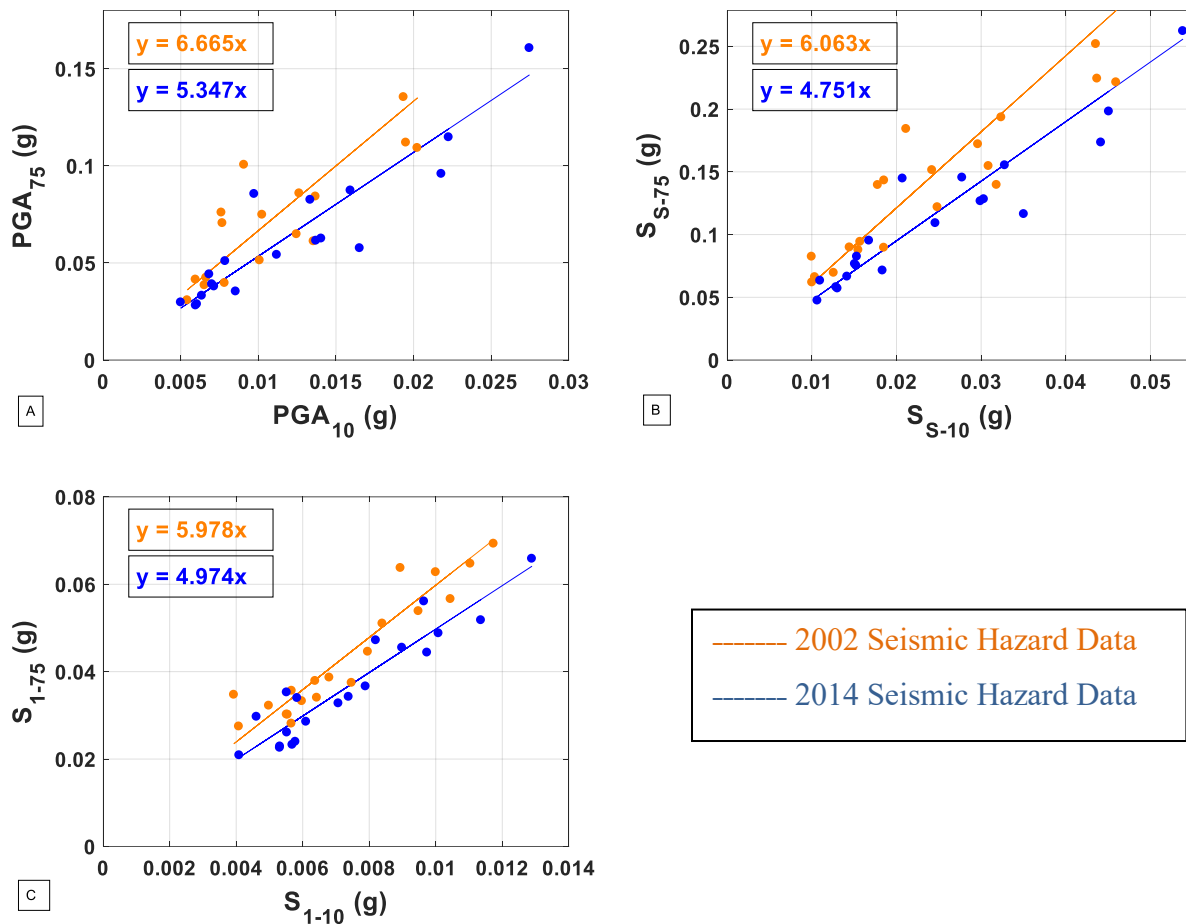


Figure 4-21: Mean spectral ratios for the Eastern Group: (A) spectral ratio for mean peak ground acceleration, K_{PGA} ; (B) spectral ratio for mean short-period response acceleration, K_S ; (C) spectral ratio for mean long-period response acceleration, K_L .

Table 4-14: Mean spectral ratios for the Eastern Group

Parameter	2002	2014
$K_{PGA\mu}$	6.665	5.347
σ_{PGA}	1.827	1.157
$K_{S\mu}$	6.063	4.751
σ_S	1.205	0.800
$K_{l\mu}$	5.978	4.974
σ_l	0.865	0.707

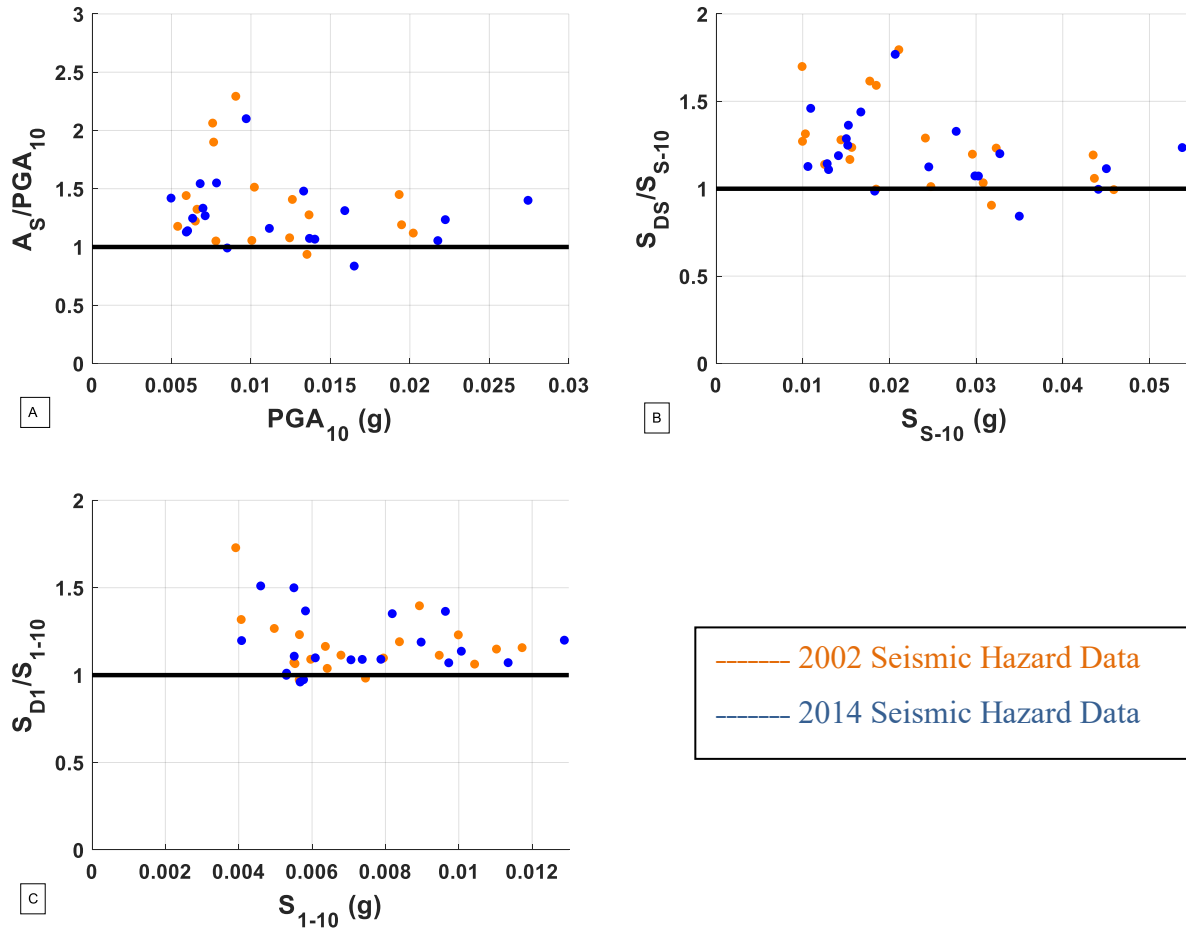


Figure 4-22: Comparison of calculated response spectra coefficient values versus obtained values for the Eastern Group: (A) coefficient for peak ground acceleration calculated using $K_{PGA} - \sigma_{PGA}$; (B) coefficient for short-period response acceleration calculated using $K_{S\mu} - \sigma_S$; (C) coefficient for long-period response acceleration calculated using values $K_{l\mu} - \sigma_l$.

Table 4-15: Spectral reduction factors for the Eastern Group

Parameter	2002	2014
K_{PGAD}	4.838	4.189
K_{SD}	4.858	3.951
K_{ID}	5.113	4.267

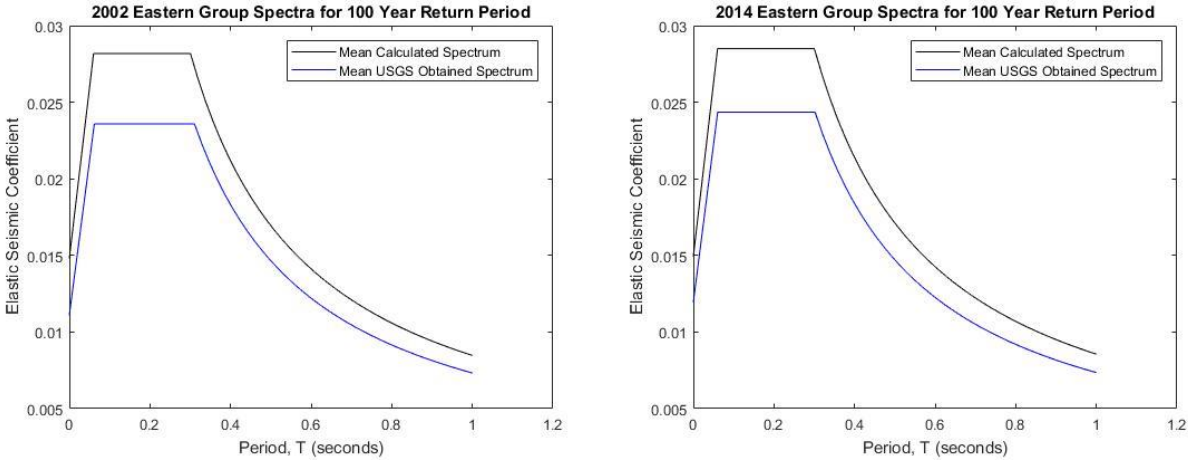


Figure 4-23: Comparison of mean response spectra produced using calculated spectral reduction factors, and of mean response spectra produced using USGS obtained values for the Eastern Group: (Left) 2002 USGS seismic hazard data; (Right) 2014 USGS seismic hazard data.

4.9 Observations

The spectral reduction factors for Group 1 derived from the 2002 USGS hazard data, given in Table 4-3, align closely with the spectral reduction limit of 2.5 for temporary bridge design specified in Article 3.6 of the LRFD-SBD. Intuitively, this makes sense considering that the vast majority of California resides within the confines of Group 1, the role that Caltrans has played in the development of the LRFD-SBD, and the fact that considering the 100 year return period for temporary bridge design as done in this report was borrowed from Caltrans Memo to Designers 20-2 (Caltrans 2011). The spectral reduction factors derived from the 2014 USGS hazard data for Group 1, also provided in Table 4-3, are slightly higher at 2.67, but suggest that conservative results still be obtained with the limit of 2.5.

The spectral reduction factors of 2.6 and 2.84 for the 2002 and 2014 USGS hazard data for Group 2, which borders Group 1, also roughly correspond with the limit of 2.5. Shown below in Table 4-16 are the average spectral reduction factor values of the three Seismic Groups in the western half of the United States. Values are somewhat higher when considering the other western states, at 3.02 and 3.4 respectively for the 2002 and 2014 USGS data. This seems to suggest that the current reduction limit of 2.5 employed by the LRFD-SBD is appropriate for the western United States.

Table 4-16: West coast Seismic Groups mean value of the three spectral reduction factors

Seismic Group	2002	2014
Group 1	2.50	2.67
Group 2	2.60	2.84
Western Group	3.02	3.40

Unlike the seismically active regions found on the west coast, the spectral ratios observed in Seismic Groups 3 and 4 indicate a considerably larger variation in maximum probable ground motion between return periods for seismically active areas on the east coast in comparison with those on the west coast. This is a consequence of the fact that strong ground motion has occurred on the east coast (e.g., the 1886 Charleston, South Carolina, earthquake (Obermeier et al. 1985)) and can be felt over a great area in comparison to the western United States (Bollinger 1973; NHI 2014), but the frequency of such large magnitude earthquake occurrence is lower in the eastern United States in comparison with the west (Algermissen 1969).

One interesting observation is the slightly smaller standard deviation from the mean spectral ratio of the Eastern Group for the 2014 USGS hazard data in comparison with Group 1. This is somewhat unexpected given the greater geographic area covered by the Eastern Group, the lower seismicity on the east coast earthquake, and the close proximity to known active faults of the site locations in Group 1. While there has been an increase in variation for spectral ratios between the 2002 and 2014 hazard data for Group 1, it is not clear why this has led to a decrease in variation in the results obtained for the Eastern Group. Spectral ratios between return periods generally increased for Seismic Groups in the western United States between the 2002 and 2014 data set, and decreased for the Seismic Groups in the central and eastern United States. One possible

explanation for the decrease in spectral ratios found in eastern and central Seismic Groups, in addition to the updated probabilistic modeling methodology used by the USGS, is the recent increase in earthquakes of magnitude 3 or greater in the eastern United States (Petersen et al. 2014). Additionally, ground motion equations for spectral periods decay more quickly in the central and eastern United States with the updated methodology (Petersen et al. 2014).

The results indicate that spectral reduction factors should be obtained specific to the seismic hazard data set used for design. For each group, discrepancies between mean spectral reduction ratios between the 2002 and 2014 seismic hazard data set are evident but none more prominent than in Seismic Group 4, given in Table 4-9. These discrepancies are the result of different seismic hazard curves which differ between editions of seismic hazard data sets due to a longer catalogued seismic history being used for more recent hazard data sets, as well as the use of updated methods for modeling ground motion and event probability (Petersen et al. 2014). Additionally, the previously mentioned variations in regional earthquake rates occur over periods of time. A visual illustration of the hazard curves for peak ground acceleration are given below in Figure 4-24 for both the 2002 and 2014 USGS seismic hazard data.

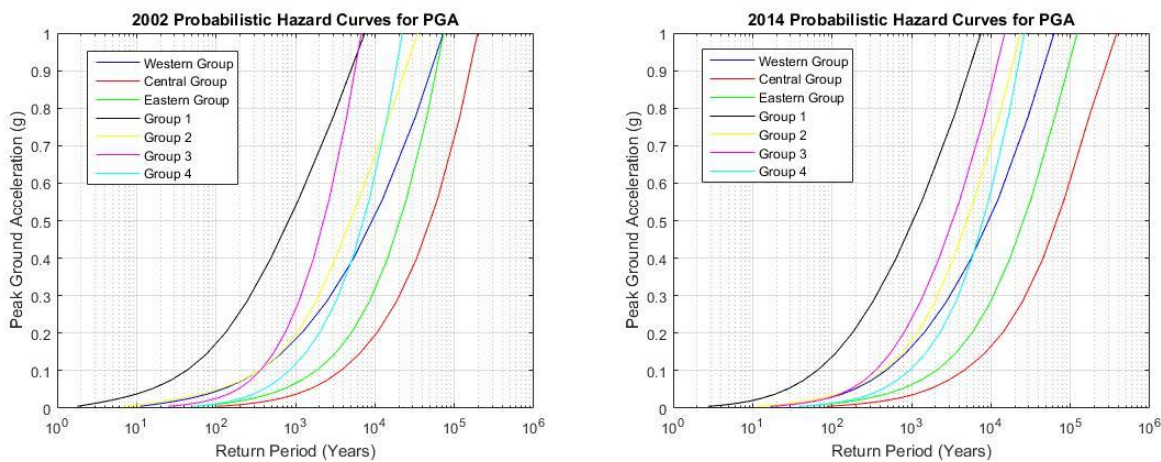


Figure 4-24: Seismic Group hazard curves for peak ground acceleration: (Left) 2002 USGS Seismic Hazard Set; (Right) 2014 USGS Seismic Hazard Set.

The results using values reduced by one standard deviation from each Seismic Group’s mean spectral ratio appear appropriate when examining Figures 4-4, 4-7, 4-10, 4-13, 4-16, 4-19, and 4-

22, with spectral reduction factors achieving a conservative reduction in most instances. While Seismic Groups with lower variations from mean spectral ratio values corresponded more closely with the spectral reduction factors and thus achieved a more accurate spectral reduction, Seismic Groups with larger variations from mean spectral values had large standard deviations which were subtracted from the mean to ensure conservative spectral reduction. The largest standard deviations were observed in Seismic Groups 3 and 4, with a mean standard deviation of 4.10 for Seismic Group 3 and a mean standard deviation of 5.09 for Seismic Group 4 using the 2002 hazard data. Despite the relatively large standard deviations, conservative spectral reduction is apparent when examining Figure 4-10 and Figure 4-13. The relatively large variations found in Seismic Groups 3 and 4 result in greater subtractions from mean spectral ratio values when using equations 3-7, 3-8, and 3-9 to obtain Seismic Group spectral reduction factors. This effect can be observed in Figure 4-10, where the calculated response spectra coefficients are greater than USGS obtained response spectra coefficients in 9 of the 10 site locations for both the 2002 and 2014 hazard sets for Seismic Group 3. A similar effect is observed in Figure 4-13, where comparing calculated versus obtained spectral response coefficients, all 10 site locations have greater calculated spectral response coefficients for peak ground acceleration, short-period response, and long-period response with the 2014 hazard data for Seismic Group 4. With the 2002 hazard data, all 10 site locations in Seismic Group 4 have greater calculated peak ground accelerations, and 9 of 10 have greater short-period and long-period response coefficients.

The spectral ratio between the 1000 year return period and the 100 year return period is observed to increase from west to east across the continental United States reflecting the greater variation between return periods exhibited in site locations for the Seismic Groups in the central and eastern United States. This is not unexpected given previous seismic hazard curve observations (Judd and Charney 2014). The trend of increasing spectral ratio from west to east correlates more closely with the 2002 USGS hazard data set. Shown below in Figure 4-25 is a plot of the average of the three spectral ratios K_{PGA} , K_S , and K_I as a function of longitude.

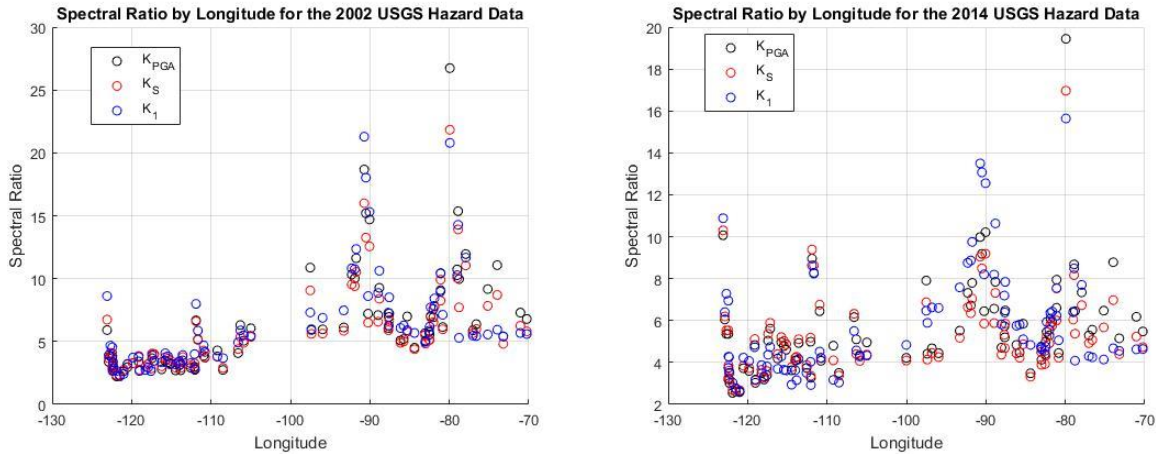


Figure 4-25: Spectral ratio as a function of longitude for the 100 site locations: (Left) corresponding to the 2002 USGS seismic hazard data; (Right) corresponding to the 2014 USGS seismic hazard data.

Considering the lateral variation in spectral ratios with longitude across the continental United States, the corresponding spectral reduction factor values between the Eastern Seismic Group, Central Seismic Group, Seismic Group 3, and Seismic Group 4, as well as the corresponding spectral reduction factor values exhibited between the three west coast Seismic Groups, the results seem to suggest that one different spectral reduction factor can be used for the western United States and one for the central and eastern United States. With the understanding that simplicity is likely desired from engineers who chose not to obtain a spectrum from the USGS website, it is proposed here to use one spectral reduction factor for the western United States, and one for the central and eastern United States. The western United States is in this case the Seismic Groups 1 and 2 as well as the Western Group, with Seismic Groups 3 and 4 along with the Central and Eastern Groups being considered as the central and eastern United States. As a further simplification, it is proposed to use a single factor to reduce all three of the design parameters, PGA, S_S , and S_1 .

As previously mentioned in this section, a single spectral reduction factor of 2.5 seems appropriate for the western United States irrespective of whether it is applied to seismic maps derived from the 2002 or the 2014 hazard data set. For the 2014 seismic hazard data, a conservative spectral reduction is obtained for every examined point in the western United States

using a reduction value of 2.5. Using the spectral reduction factor of 2.5 for the western United States with the 2002 seismic hazard data, results in a conservatively reduced spectra with the following exceptions:

- An unconservative reduction of the peak ground acceleration by 10.93% (San Jose) and 10.72% (Sacramento)
- An unconservative reduction of the short-period response acceleration coefficient by 7.2% (San Jose) and 6.42% (Sacramento)
- An unconservative reduction of the long-period response acceleration coefficient by 9.2% (Sacramento) and 3.09% (Modesto)

For the central and eastern United States, a single spectral reduction factor of 3.75 would conservatively reduce the peak ground acceleration, the short-period response acceleration coefficient, and the long-period response acceleration coefficient for every site location with both the 2002 and 2014 USGS hazard data set, with the exception of one site (Atlanta, Georgia) when using 2014 hazard data for which the value would be 7.11% and 11.51% unconservative respectively for the peak ground acceleration and the short-period response coefficient.

Figures 4-26 and 4-27 illustrate the comparison of spectral response coefficients calculated using the proposed spectral reduction factors of 2.5 for the western United States and 3.75 for the central and eastern United States, with the alternative USGS obtained spectral response coefficients. The vertical axis of these figures shows the calculated peak ground acceleration, A_s , short-period response acceleration coefficient, S_{DS} , and long-period response acceleration coefficient, S_{D1} , divided by the respective obtained peak ground acceleration, PGA_{10} , short-period response acceleration coefficient, S_{S-10} , and long-period response acceleration coefficient, S_{1-10} . A bold line is shown at the value of 1, with points above the line representing a conservative reduction of the response spectra using the spectral reduction factors, and points below the line representing an unconservative reduction. The Figure 4-26 was generated with the 2002 USGS seismic hazard data, and Figure 4-27 with the 2014 USGS seismic hazard data.

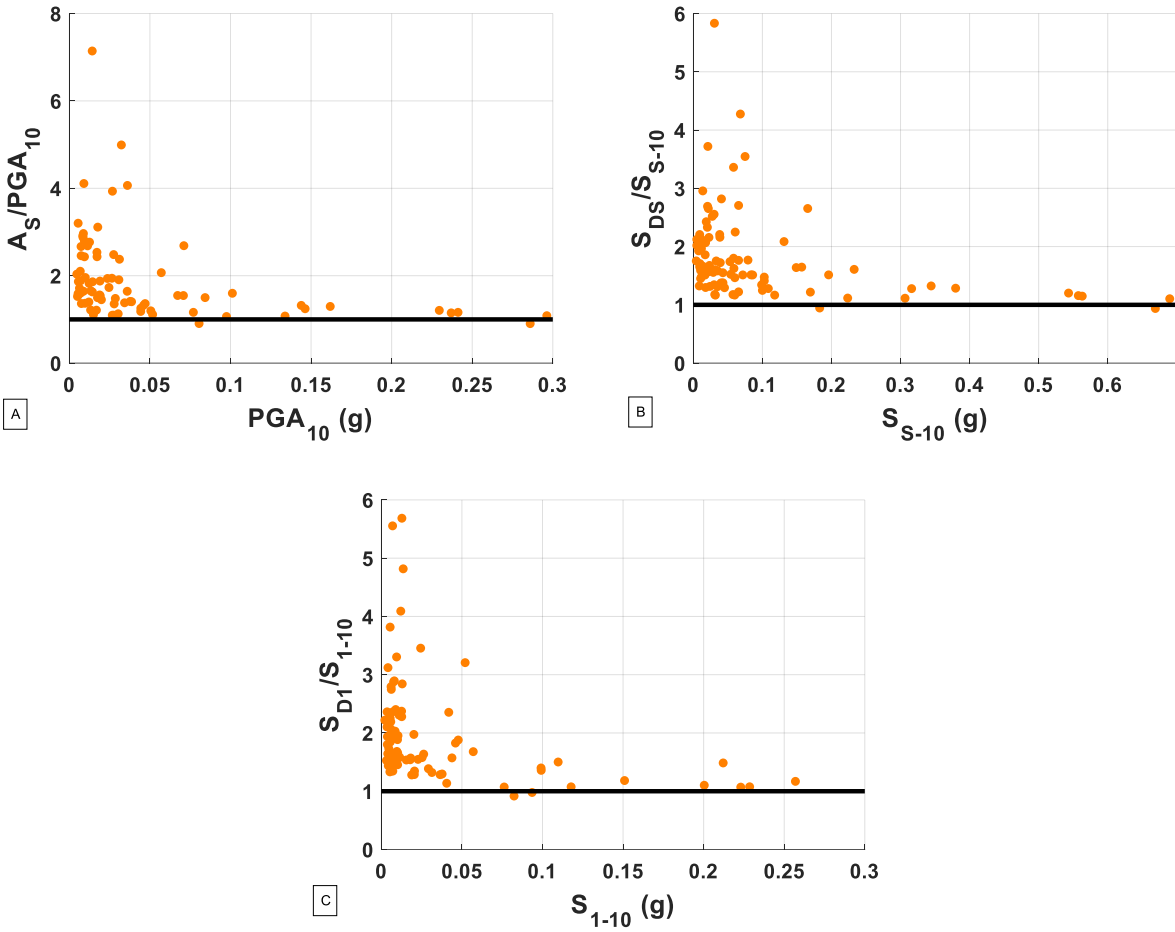


Figure 4-26: For the 2002 USGS seismic hazard data, a comparison of calculated response spectra coefficient values versus obtained values using a spectral reduction factor of 2.5 for the western United states and 3.75 for the central and eastern United States: (A) coefficient for peak ground acceleration; (B) coefficient for short-period response acceleration; (C) coefficient for long-period response acceleration.

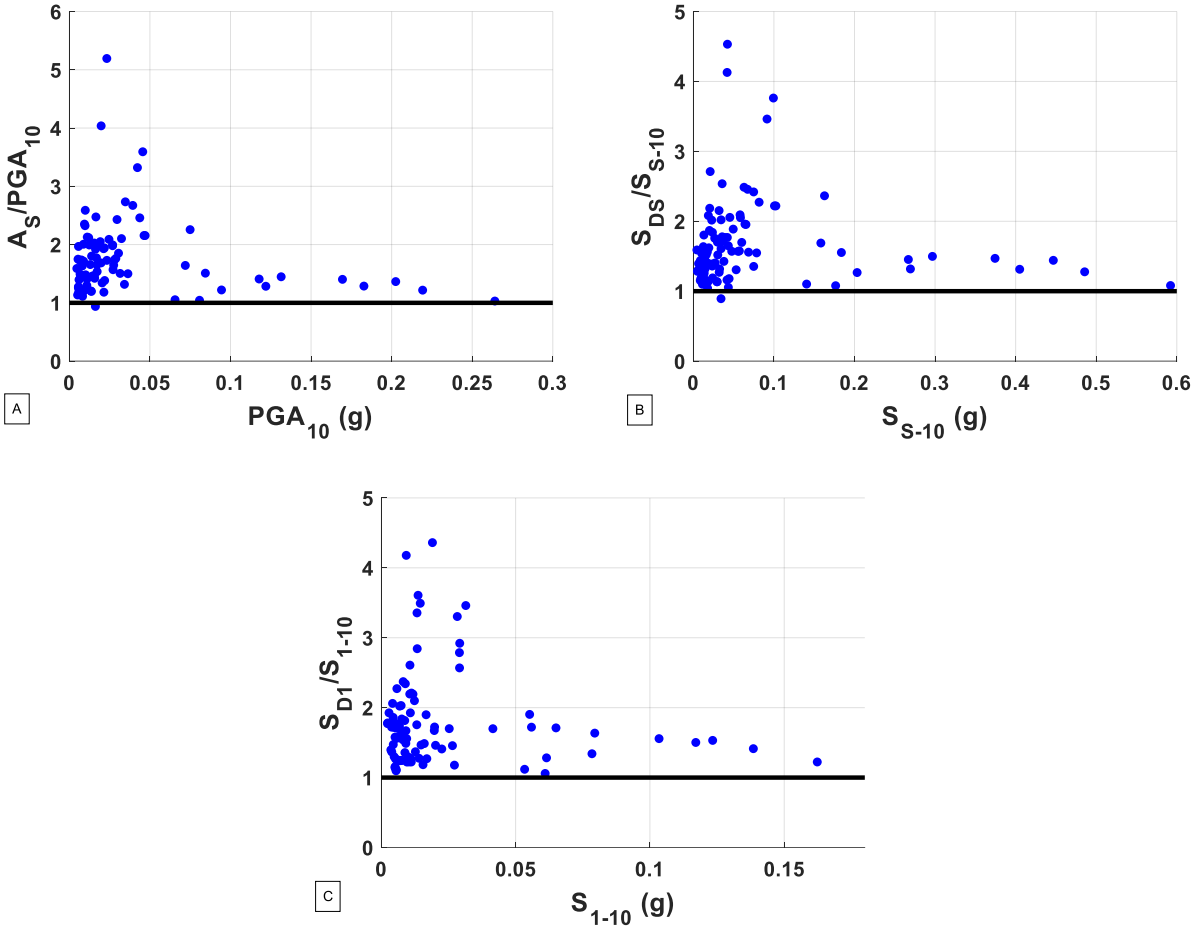


Figure 4-27: For the 2014 USGS seismic hazard data, a comparison of calculated response spectra coefficient values versus obtained values using a spectral reduction factor of 2.5 for the western United states and 3.75 for the central and eastern United States: (A) coefficient for peak ground acceleration; (B) coefficient for short-period response acceleration; (C) coefficient for long-period response acceleration.

SECTION 5

**DESIGN REDUCTION FACTORS BY AASHTO SEISMIC
PERFORMANCE ZONE**

The second method of categorization considered here is based upon AASHTO’s Seismic Performance Zones defined in Article 3.10.6 of the LRFD-BDS. In the approach followed below, the same 100 locations determined previously are again divided into four separate groups, but different ones. Here, the defining criteria for Seismic Performance Zones 1 to 4 are used for Groups A to B, respectively. While AASHTO’s Seismic Performance Zones are determined by the design value of the long-period response acceleration parameter, a Site Class of B is assumed within this report so the value of S_{1-75} for each location is used for classification.

This section explores the relationship between site locations grouped by magnitude of the long-period response acceleration parameter, and the Seismic Group’s mean spectral reduction ratios for each of the three parameters. In this section, due to variations in long-period response acceleration coefficient values between USGS data sets, the number of locations that are in each group are not necessarily equal for the 2002 seismic hazard data and the 2014 seismic hazard data. This method of categorization is separate and distinct from the method used in Section 4. The bounds for Groups A through D are given below in Table 4-1.

Table 5-1: Group by Seismic Performance Zone (from LRFD-BDS Table 3.10.6-1)

Group	Long-Period Acceleration (g)
A	$S_1 \leq 0.15$
B	$0.15 < S_1 \leq 0.30$
C	$0.30 < S_1 \leq 0.50$
D	$0.50 < S_1$

5.1 General Procedure for Each Group

The same procedure and presentation of data outlined in Section 4.1 is followed in Section 5.2 through Section 5.5. While the criteria defining each Seismic Group has changed from Section 4 to Section 5, all other operations remain the same. The spectral ratios and seismic reduction factors are obtained using the same procedure.

5.2 Group A

Group A contains 76 of the 100 site locations considered for the 2002 USGS seismic hazard data, and 78 of the 100 site locations considered for the 2014 USGS seismic hazard data. Results for those sites, obtained per the procedure outlined above, are presented below. For the 2002 seismic hazard data, a total of 17 site locations are below the minimum peak ground acceleration, 5 site locations are below the minimum short-period response acceleration, and 7 site locations are below the minimum long-period response acceleration. For the 2014 seismic hazard data, 13 site locations are below the minimum peak ground acceleration, 4 site locations are below the minimum short-period response acceleration, and 5 site locations are below the minimum long-period response acceleration. As previously stated, values below the minimum were not considered in analysis.

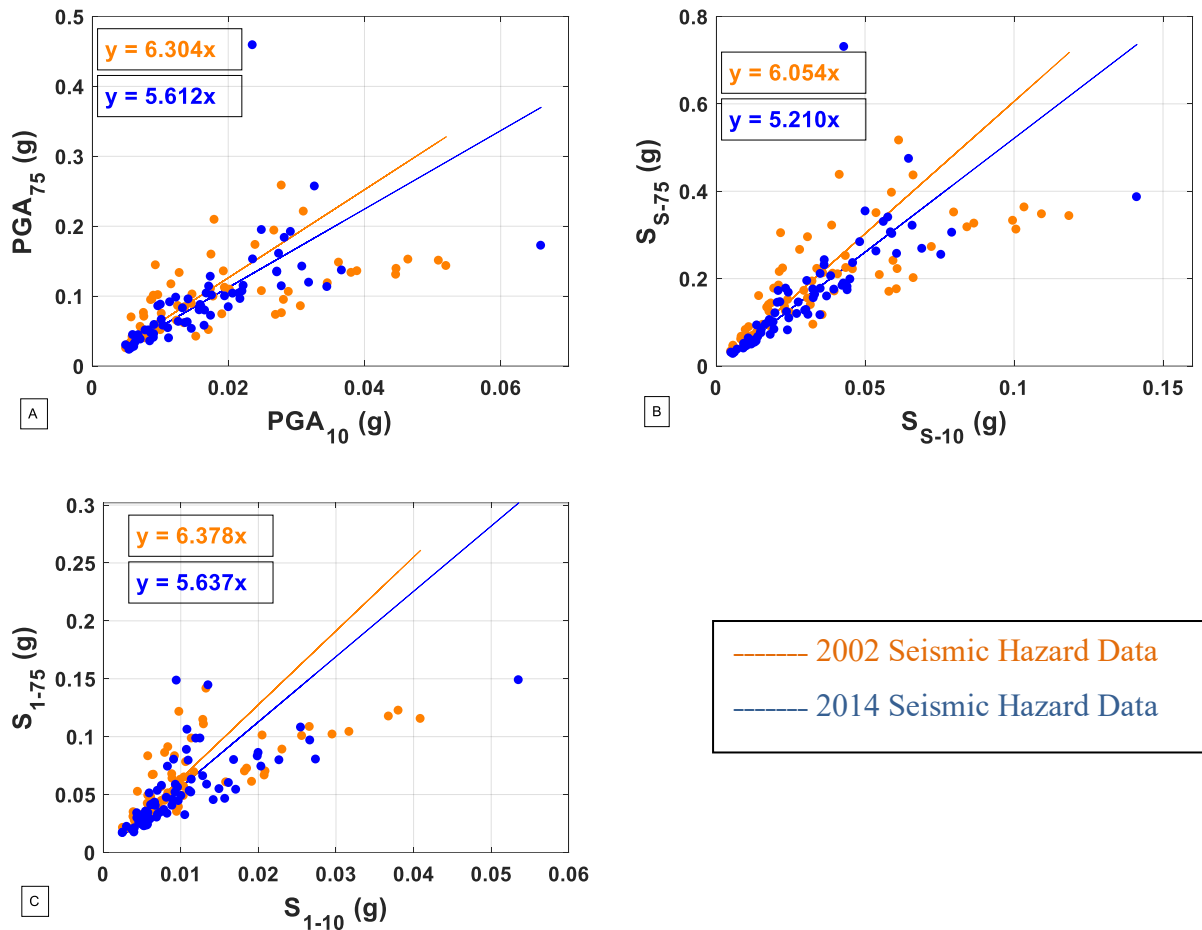


Figure 5-1: Mean spectral ratios for Group A: (A) spectral ratio for mean peak ground acceleration, K_{PGA} ; (B) spectral ratio for mean short-period response acceleration, K_S ; (C) spectral ratio for mean long-period response acceleration, K_L .

Table 5-2: Mean spectral ratios for Group A

Parameter	2002 Value	2014 Value
$K_{PGA\mu}$	6.304	5.612
σ_{PGA}	2.880	2.195
$K_{S\mu}$	6.054	5.210
σ_S	2.257	1.751
$K_{l\mu}$	6.378	5.637
σ_l	2.460	2.085

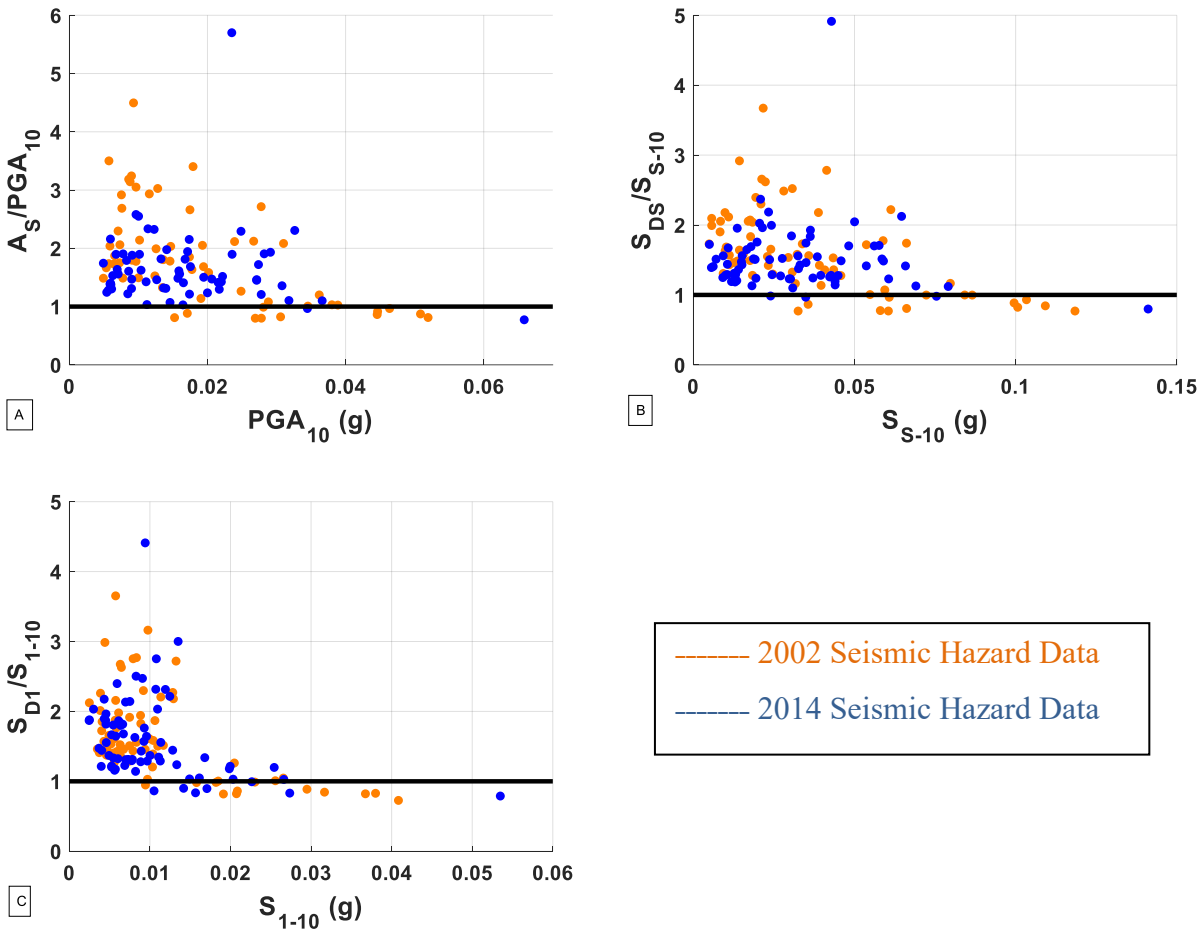


Figure 5-2: Comparison of calculated response spectra coefficient values versus obtained values for Group A: (A) coefficient for peak ground acceleration calculated using $K_{PGA} - \sigma_{PGA}$; (B) coefficient for short-period response acceleration calculated using $K_{S\mu} - \sigma_S$; (C) coefficient for long-period response acceleration calculated using values $K_{l\mu} - \sigma_l$.

Table 5-3: Spectral reduction factors for Group A

Parameter	2002 Value	2014 Value
K_{PGAD}	3.424	3.416
K_{SD}	3.797	3.459
K_{ID}	3.918	3.553

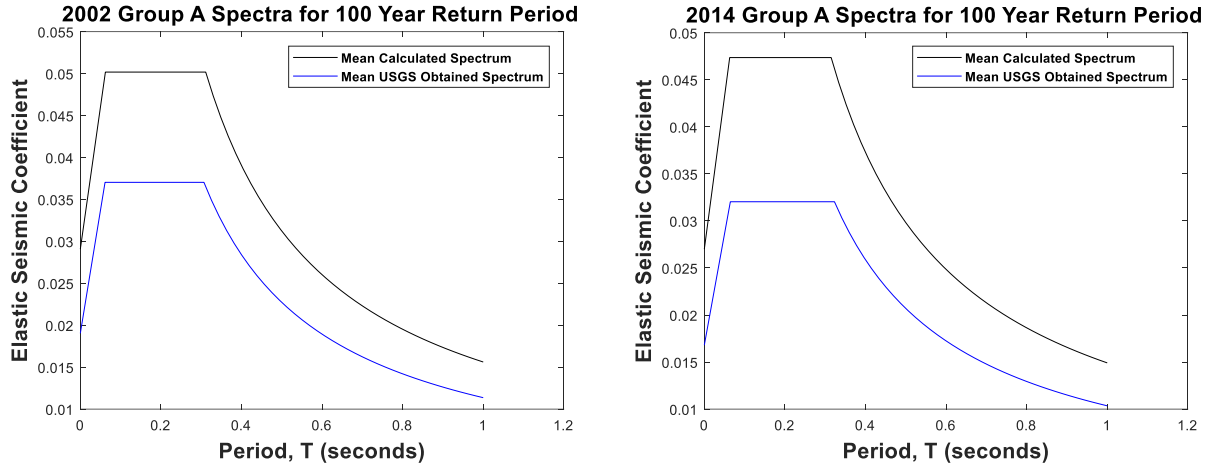


Figure 5-3: Comparison of mean response spectra produced using calculated spectral reduction factors, and of mean response spectra produced using USGS obtained values for Group A: (Left) 2002 USGS seismic hazard data; (Right) 2014 USGS seismic hazard data.

5.3 Group B

Group B contains 13 of the 100 site locations considered for the 2002 USGS seismic hazard data, and 16 of the 100 site locations considered for the 2014 USGS seismic hazard data. Results for those sites, obtained per the procedure outlined above, are presented below.

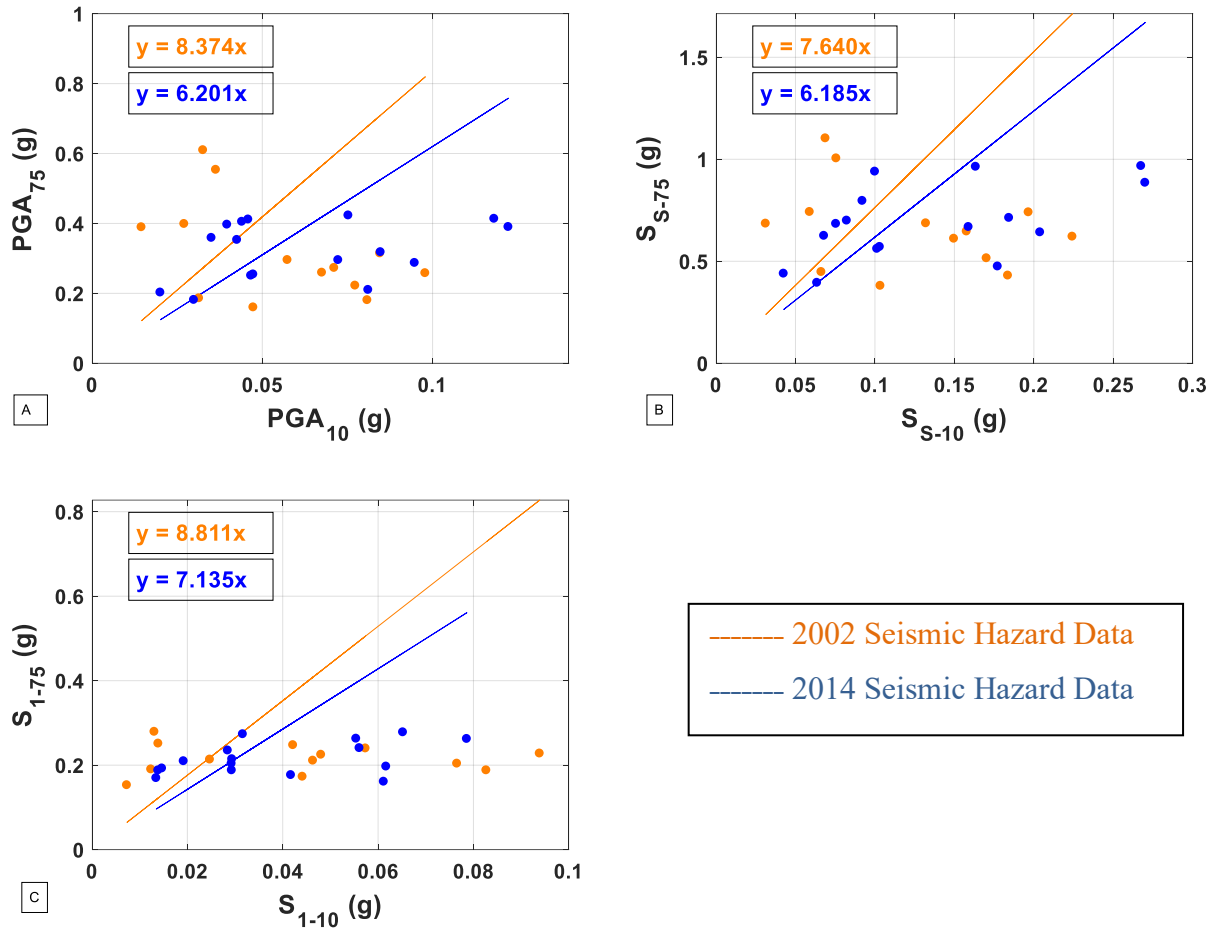


Figure 5-4: Mean spectral ratios for Group B: (A) spectral ratio for mean peak ground acceleration, K_{PGA} ; (B) spectral ratio for mean short-period response acceleration, K_S ; (C) spectral ratio for mean long-period response acceleration, K_L .

Table 5-4: Mean spectral ratios for Group B

Parameter	2002 Value	2014 Value
$K_{PGA\mu}$	8.374	6.201
σ_{PGA}	7.828	2.805
$K_{S\mu}$	7.640	6.185
σ_S	6.214	2.615
$K_{l\mu}$	8.811	7.135
σ_l	7.288	3.689

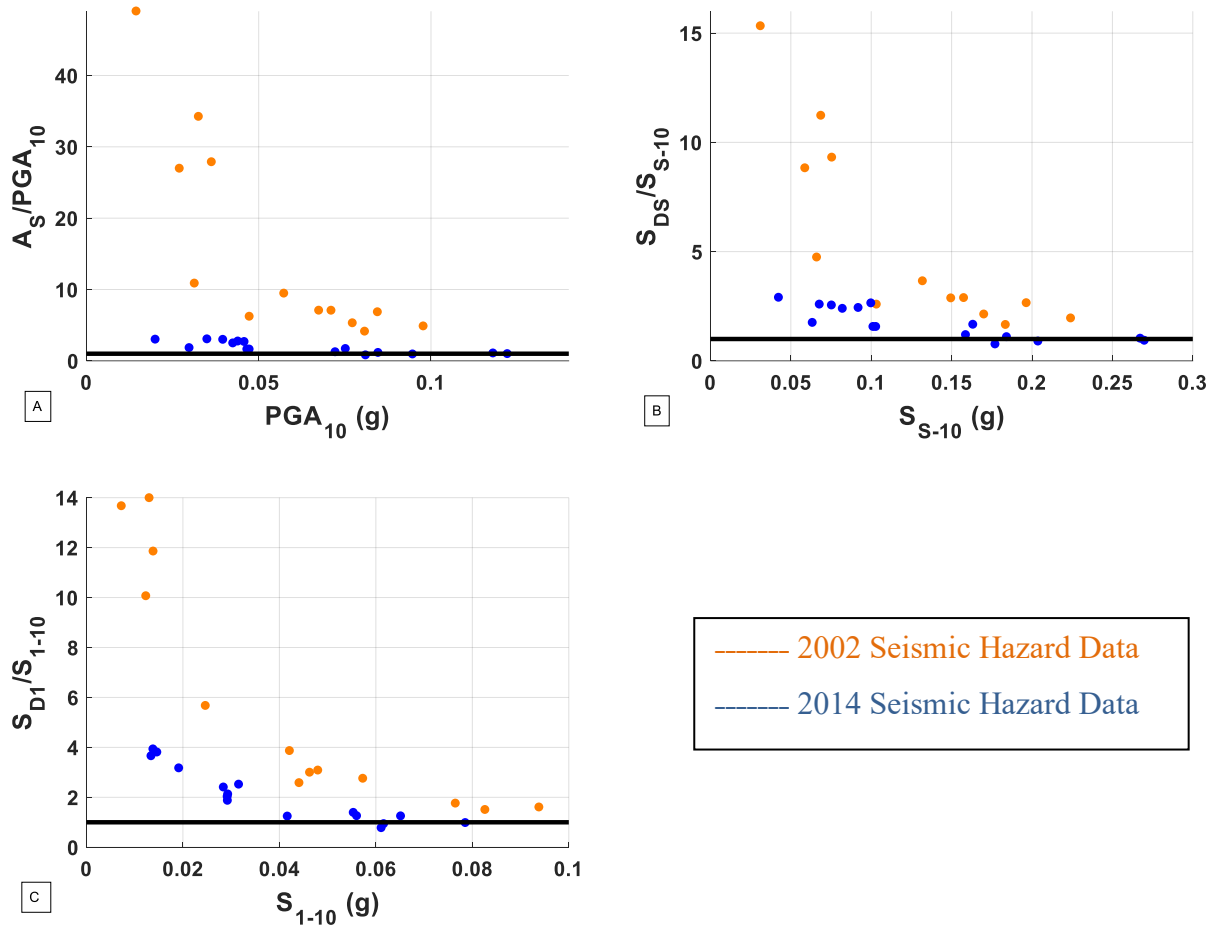


Figure 5-5: Comparison of calculated response spectra coefficient values versus obtained values for Group B: (A) coefficient for peak ground acceleration calculated using $K_{PGA\mu} - \sigma_{PGA}$; (B) coefficient for short-period response acceleration calculated using $K_{S\mu} - \sigma_S$; (C) coefficient for long-period response acceleration calculated using values $K_{l\mu} - \sigma_l$.

Table 5-5: Spectral reduction factors for Group B

Parameter	2002 Value	2014 Value
K_{PGAD}	0.546	3.396
K_{SD}	1.426	3.570
K_{1D}	1.523	3.446

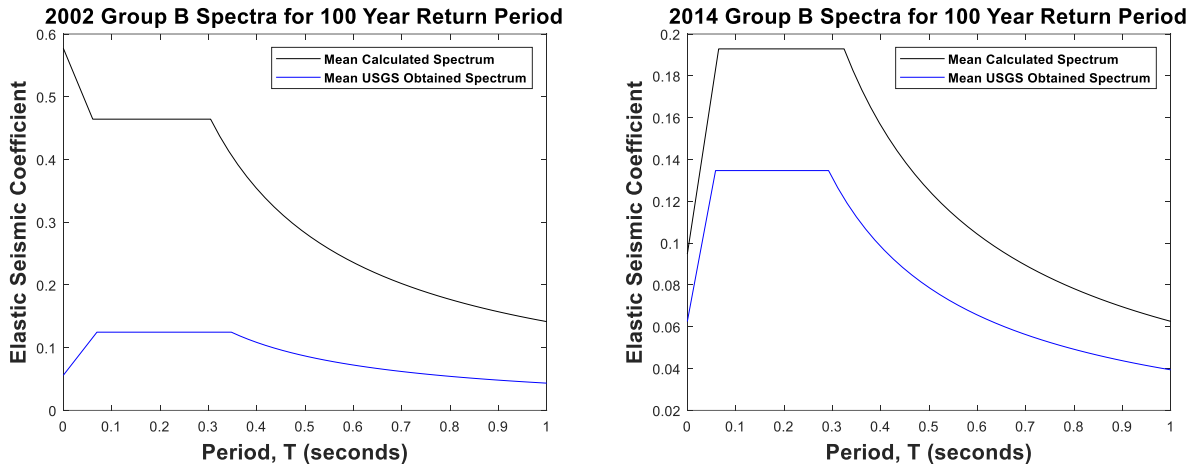


Figure 5-6: Comparison of mean response spectra produced using calculated spectral reduction factors, and of mean response spectra produced using USGS obtained values for Group B: (Left) 2002 USGS seismic hazard data; (Right) 2014 USGS seismic hazard data.

5.4 Group C

Group C contains 6 of the 100 site locations considered for the 2002 USGS seismic hazard data, and 6 of the 100 site locations considered for the 2014 USGS seismic hazard data. Results for those sites, obtained per the procedure outlined above, are presented below.

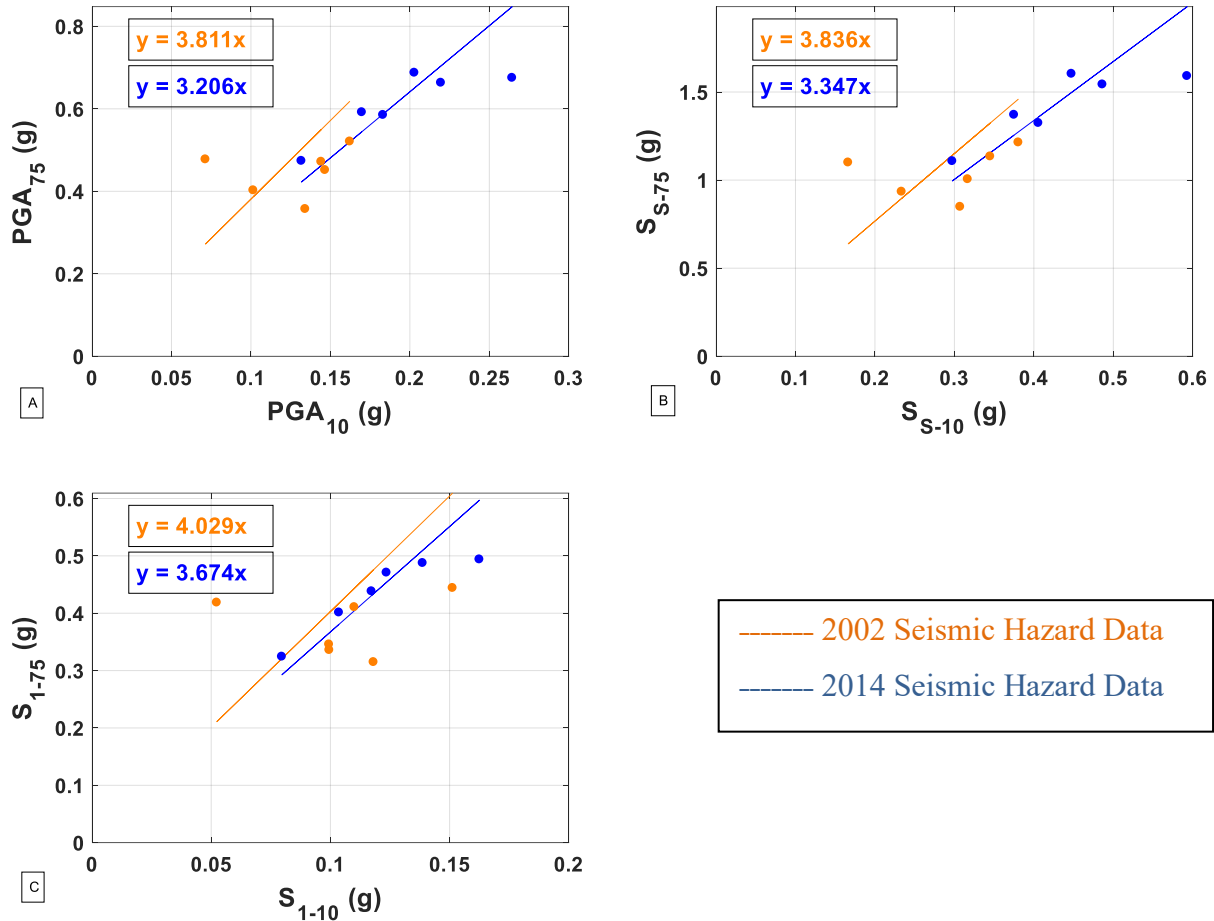


Figure 5-7: Mean spectral ratios for Group C: (A) spectral ratio for mean peak ground acceleration, K_{PGA} ; (B) spectral ratio for mean short-period response acceleration, K_S ; (C) spectral ratio for mean long-period response acceleration, K_L .

Table 5-6: Mean spectral ratios for Group C

Parameter	2002 Value	2014 Value
$K_{PGA\mu}$	3.811	3.206
σ_{PGA}	1.470	0.380
$K_{S\mu}$	3.836	3.347
σ_S	1.417	0.393
$K_{l\mu}$	4.029	3.674
σ_l	1.980	0.360

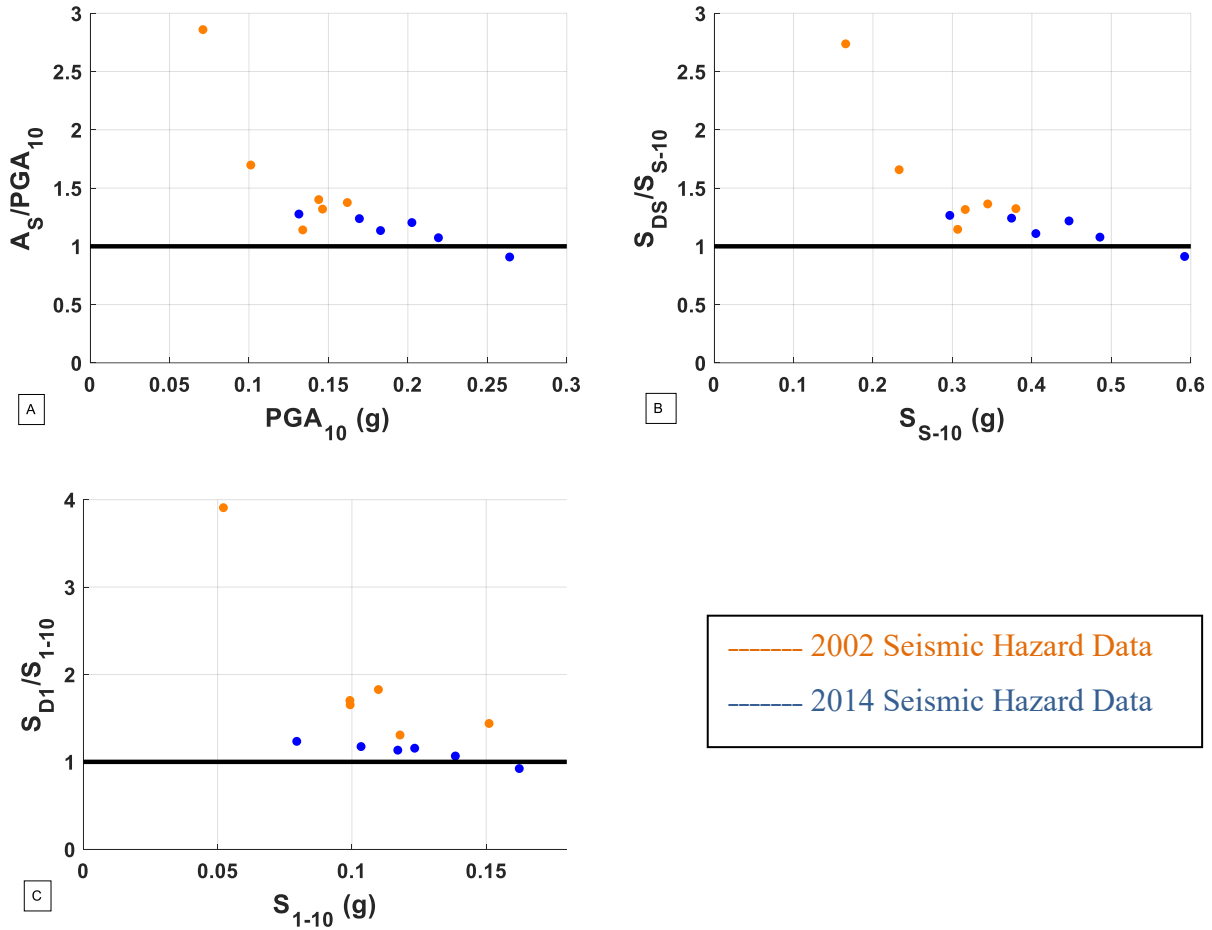


Figure 5-8: Comparison of calculated response spectra coefficient values versus obtained values for Group C: (A) coefficient for peak ground acceleration calculated using $K_{PGA} - \sigma_{PGA}$; (B) coefficient for short-period response acceleration calculated using $K_{S\mu} - \sigma_S$; (C) coefficient for long-period response acceleration calculated using values $K_{l\mu} - \sigma_l$.

Table 5-7: Spectral reduction factors for Group C

Parameter	2002 Value	2014 Value
K_{PGAD}	2.342	2.826
K_{SD}	2.419	2.954
K_{1D}	2.049	3.314

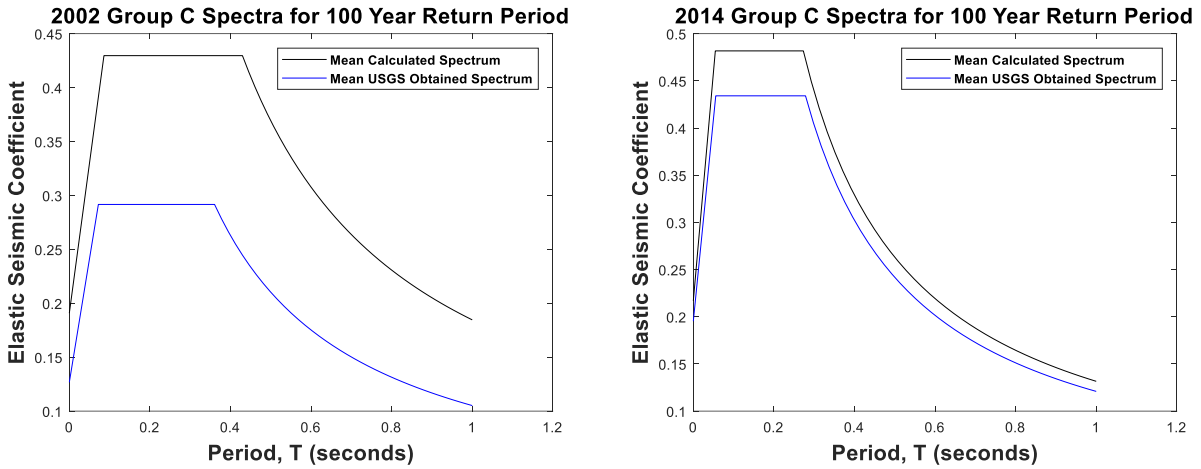


Figure 5-9: Comparison of mean response spectra produced using calculated spectral reduction factors, and of mean response spectra produced using USGS obtained values for Group C: (Left) 2002 USGS seismic hazard data; (Right) 2014 USGS seismic hazard data.

5.5 Group D

Group D contains 5 of the 100 site locations considered for the 2002 USGS seismic hazard data, and none of the site locations considered for the 2014 USGS seismic hazard data. Results for those sites, obtained per the procedure outlined above, are presented below.

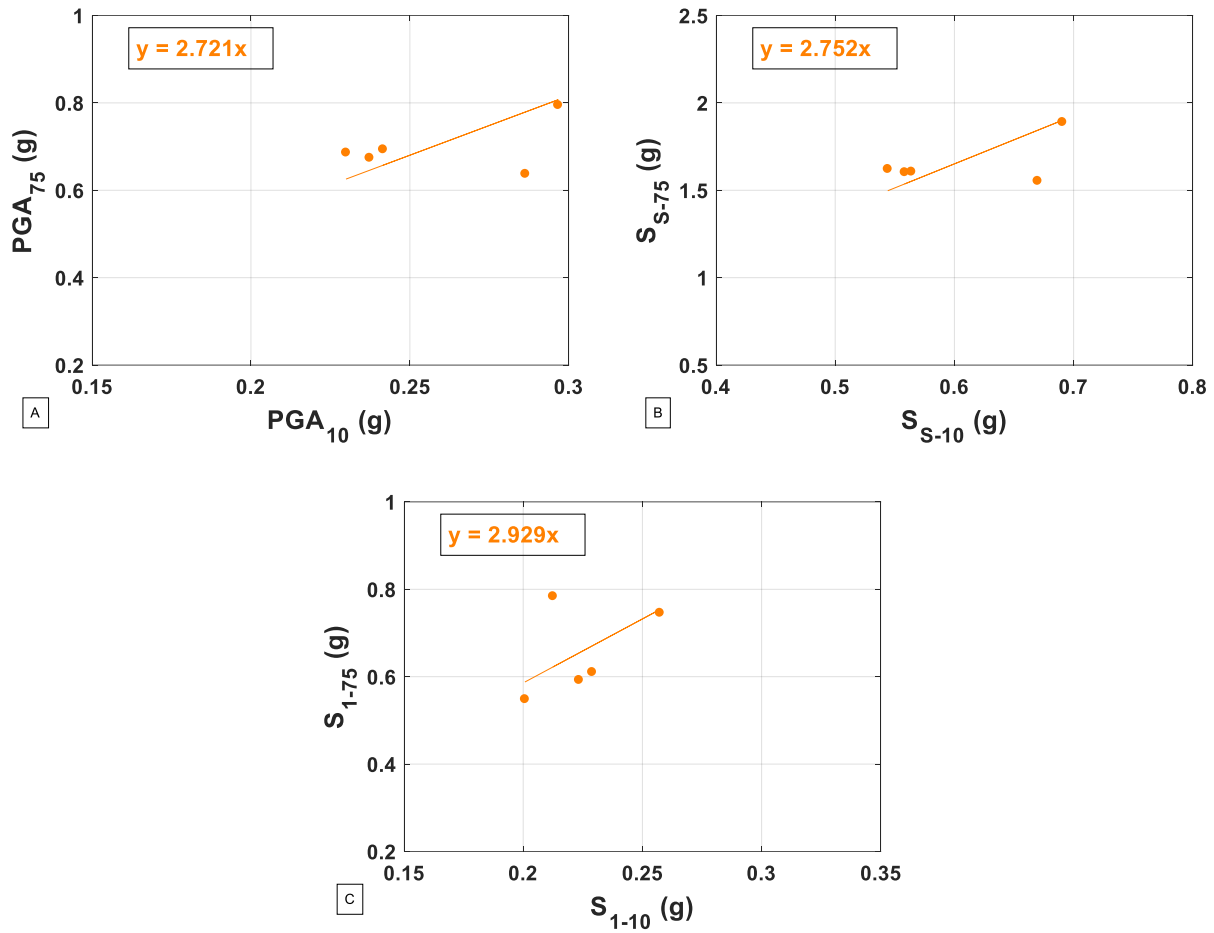


Figure 5-10: Mean spectral ratios for Group D: (A) spectral ratio for mean peak ground acceleration, K_{PGA} ; (B) spectral ratio for mean short-period response acceleration, K_S ; (C) spectral ratio for mean long-period response acceleration, K_L .

Table 5-8: Mean spectral ratios for Group D

Parameter	2002 Value
$K_{PGA\mu}$	2.721
σ_{PGA}	0.297
$K_{S\mu}$	2.752
σ_S	0.256
$K_{I\mu}$	2.929
σ_I	0.437

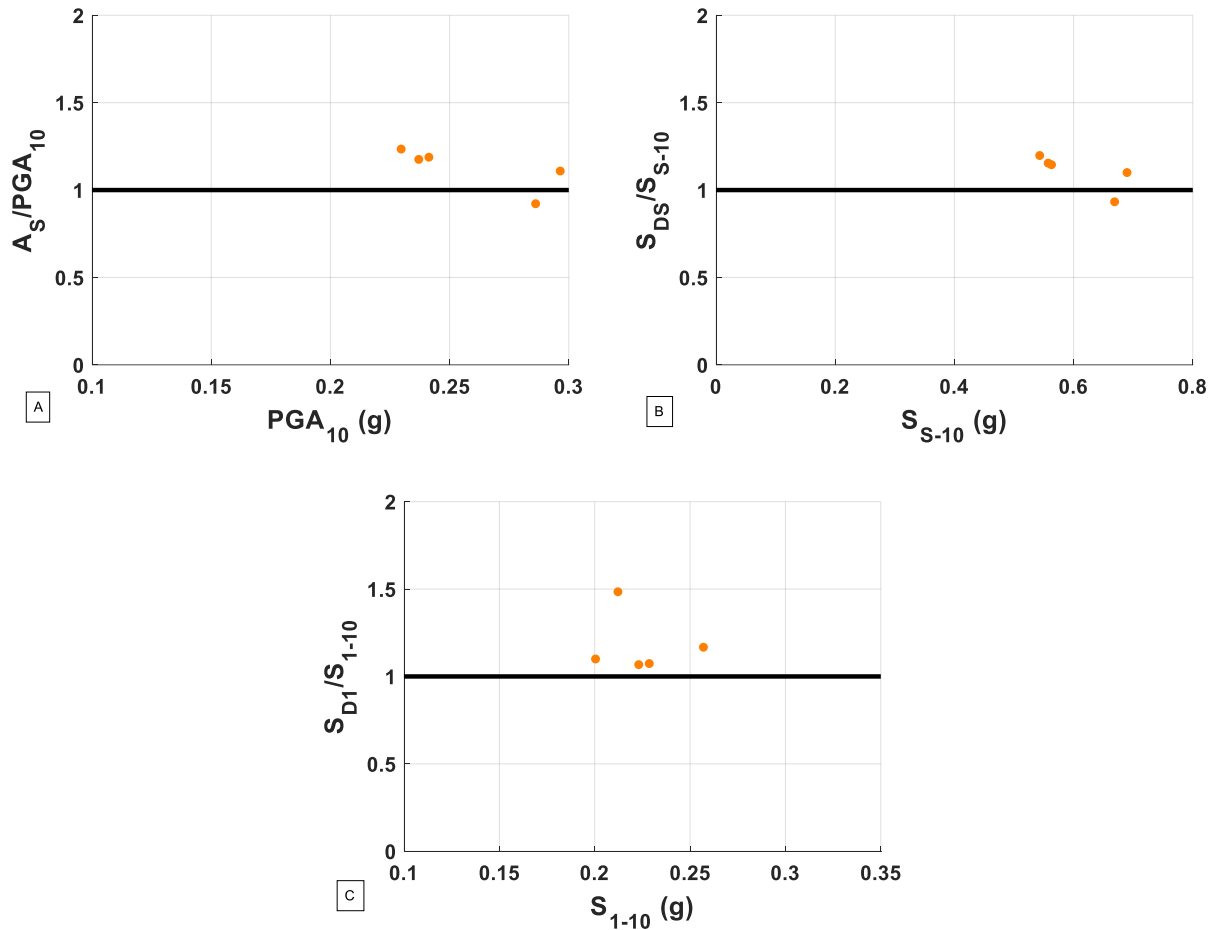


Figure 5-11: Comparison of calculated response spectra coefficient values versus obtained values for Group D: (A) coefficient for peak ground acceleration calculated using $K_{PGA\mu} - \sigma_{PGA}$; (B) coefficient for short-period response acceleration calculated using $K_{S\mu} - \sigma_S$; (C) coefficient for long-period response acceleration calculated using values $K_{I\mu} - \sigma_I$.

Table 5-9: Spectral reduction factors for Group D

Parameter	2002 Value
K_{PGAD}	2.424
K_{SD}	2.495
K_{ID}	2.491

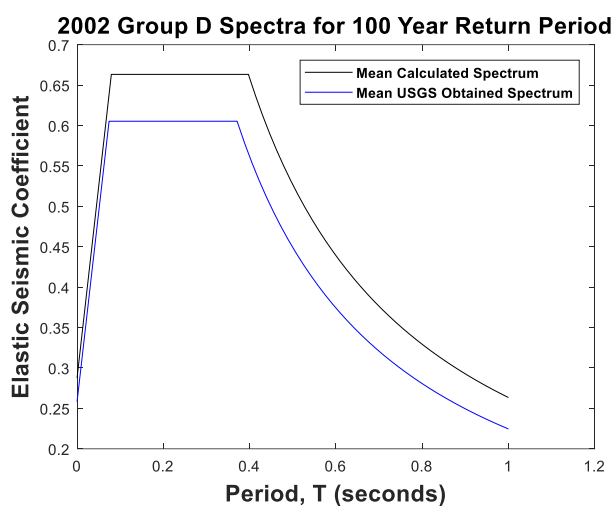


Figure 5-12: Comparison of mean response spectra produced using calculated spectral reduction factors, and of mean response spectra produced using USGS obtained values from the 2002 hazard data set for Group D.

5.6 Observations

Spectral ratios correspond closely with one another within Group C for the 2014 USGS seismic hazard data and within Group D for the 2002 USGS seismic hazard data, evident by the relatively small standard deviations given in Tables 5-7 and 5-8. The observed convergence of spectral ratios might lead one to conclude that spectral ratios between site locations converge at higher magnitudes of long-period acceleration parameters, but it should be noted that five of the six site locations corresponding with Group C for 2014 hazard data set are located in California (the exception being Reno, Nevada) and site locations corresponding with Group D for the 2002 hazard data set are all located in California. Thus, the convergence of spectral ratios in Groups C and D may be related to the site locations geographical proximity instead of similar magnitude long-period response acceleration values. For the site locations corresponding with Group C for 2002 hazard data set, four of the six locations are in California (Reno, Nevada and Salt Lake City, Utah are the exceptions). If the furthest geographical outlier, Salt Lake City, is removed from the group the result is notably smaller standard deviations of mean spectral values given below in Table 5-10.

Table 5-10: Mean spectral ratios for Group C using the 2002 USGS hazard data set, without the site location in Salt Lake City, Utah

Parameter	2002 Value
$K_{PGA\mu}$	3.236
σ_{PGA}	0.471
$K_{S\mu}$	3.281
σ_S	0.449
$K_{I\mu}$	3.236
σ_I	0.429

In Figure 5-6, the plot of the mean calculated seismic response spectrum using the 2002 USGS seismic hazard data begins with a declining slope from the peak ground acceleration, meaning the peak ground acceleration is greater than the short-period response acceleration coefficient. This observation is unusual for response spectra and is the result of spectral reduction factor of 0.546 being less than one. A spectral reduction factor less than one results in a response spectrum for

temporary bridge design greater in magnitude than the response spectrum used for permanent bridge design. This increase in response spectrum despite a smaller return period suggests that a one standard deviation reduction from the group mean spectral ratio is too conservative for Group B when using the 2002 USGS seismic hazard data set. All three spectral reduction factors calculated for Group B using the 2002 USGS seismic hazard data are well below the spectral reduction limit of 2, specified by the LFRD-BDS, and 2.5, specified by the LFRD-SBD. The conservative spectral reduction factors are the result of large standard deviations of spectral ratios exhibited in Group B. The effect of the conservative spectral reduction factors is evident when looking at Figure's 5-5-A, 5-5-B, and 5-5-C, with calculated spectral response coefficients all significantly above obtained values represented by the bold line at one.

Given below in Figure 5-13 is spectral ratio as a function of long-period response acceleration.

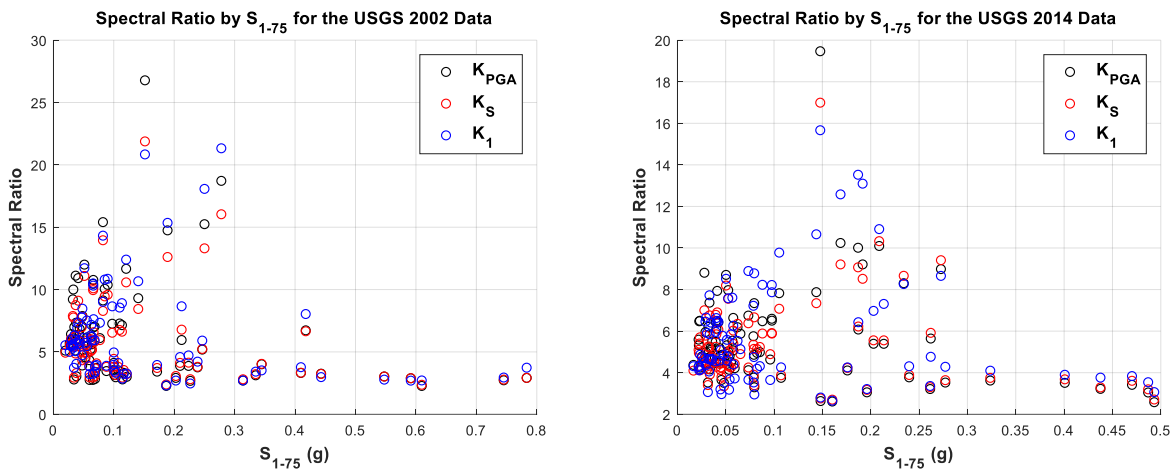


Figure 5-13: Spectral ratio as a function of long-period response acceleration coefficient corresponding to a 7 percent probability of exceedance in 75 years for the 100 site locations: (Left) corresponding to the 2002 USGS seismic hazard data; (Right) corresponding to the 2014 USGS seismic hazard data.

In Section 4.9 a trend of increasing spectral ratio as one moves from west to east across the United States was observed, seen in Figure 4-25. Looking closely at Figure 5-13 no clear trend between spectral ratio and long-period response acceleration exists up until long-period response accelerations greater than about 0.3 g. For long-period response accelerations greater than 0.3 g,

spectral ratios converge at values of 2.5 to 3 for the 2002 USGS seismic hazard data, and spectral ratio values of 3 to 4 for the 2014 USGS seismic hazard data. In comparing Figure 4-25 and Figure 5-13, a linear trend is more apparent when spectral ratio is a function of longitude than when it is a function of long-period response acceleration. Given a more distinct trend between spectral ratio and geographic location, it is not recommended that spectral reduction factors be determined based upon magnitude of long-period response acceleration.

SECTION 6

SPECTRAL REDUCTION EXAMPLE

6.1 Introduction

The purpose of this example is to demonstrate the application of the seismic spectral reduction factor in the design of a temporary bridge by calculating the period and corresponding design earthquake load for an example temporary bridge, not to provide a comprehensive design example for temporary bridge design. In light of that, a number of assumptions will be made to simplify the example. The method used in this example will be the Uniform Load Method outlined in AASHTO LRFD-BDS Article 4.7.4.3.2c. The temporary bridge used in this example has member dimensions, dead load calculations, and other features loosely based on the Pea Island Interim Bridge (NCDOT 2015), with modifications made to simplify the example. The Pea Island Interim Bridge will be used in this example due to the availability of its plans as well as the bridge's interim designation. Design examples provided by the Illinois Department of Transportation (IDOT 2008), and from the joint MCEER and ATC venture *Design Examples, Recommended LRFD Guidelines for the Seismic Design of Highway Bridges* (ATC/MCEER 2003).

The spectral reduction factor suggested for the central and eastern United States in Section 4.9, denoted K_D , will be used to calculate the applicable response spectrum for the temporary bridge. For the design spectrum values, A_S , S_{DS} , and S_{D1} denote the design values for the temporary bridge response spectrum corresponding to the peak ground acceleration, short-period response spectral acceleration, and long-period response spectral acceleration defined in Article 3.10.4.2 of the AASHTO LRFD-BDS.

$$K_D = 3.75$$

The modifications made to the design of the bridge for the purposes of this example include, but are not limited to, reducing the number of spans from 47 to 3, eliminating the skew in the bridge, eliminating the slope of the cross section, and the depth of the piles. These modifications are all considered appropriate as this example's purpose is to illustrate the process of spectral reduction, not to replicate the design of the Pea Island Interim Bridge. In order to have a determinate structure,

it will be assumed the superstructure is discontinuous which simplifies the distribution of shear force to the cap beams.

6.2 Spectral Reduction and the Temporary Bridge Design Response Spectrum

The location of the site for the bridge in this example is Charleston, South Carolina. As was done in previous sections, Site Class B will be assumed for this example, Site Class is defined in Article 3.10.3.1 of the AASHTO LRFD-BDS. The latitude and longitude for the site in decimal degrees, as well as the peak ground acceleration, short-period response acceleration, and long-period response acceleration corresponding to a 7% probability of exceedance in 75 years are provided in the Table 6-1. Note that the 2002 USGS seismic data is used in this example. The approximate location of the site is shown on a map of the short period response acceleration for Region 4 taken from Figure 3.10.2.1-14 of the AASHTO LRFD-BDS in Figure 6-1.

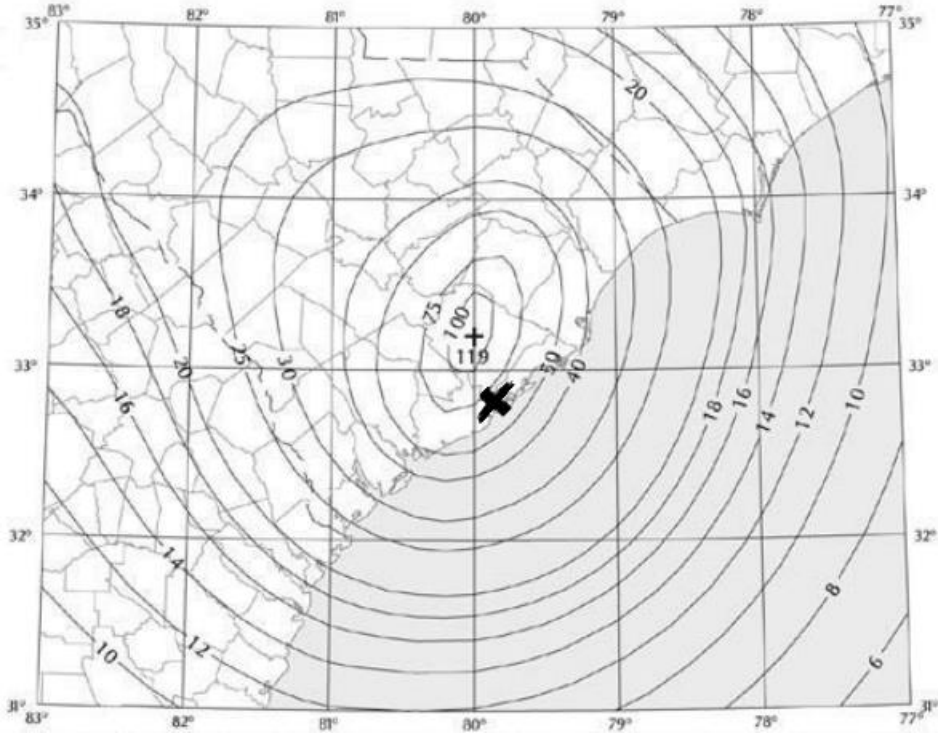


Figure 6-1: The site location for the design example shown on a map of the short-period response acceleration coefficient for Region 4 corresponding to the 1000 year return period. The map was borrowed from AASHTO LRFD-BDS Figure 3.10.2.1-14.

Table 6-1: The coordinates and spectral coefficients corresponding to the 1000 year return period used in the example

Latitude	Longitude	PGA ₇₅	S _{S-75}	S _{I-75}
32.78°N	79.93°W	0.39 g	0.69 g	0.153 g

The long-period response spectral acceleration of 0.153 g for the 1000 year return period corresponds to Seismic Performance Zone 2 defined in Article 3.10.6 of the AASHTO LRFD-BDS, and as previously stated in Section 3.4, it will be assumed that the site cannot be redefined as Seismic Performance Zone 1 based on the reduced response spectrum.

The design response spectrum corresponding to the bridge's temporary designation can now be determined. The single spectral reduction factor suggested for the central and eastern United States in Section 4.9, will be used in Equations 3-1, 3-2, and 3-3, to calculate the design acceleration coefficient A_S , the design short-period response acceleration coefficient, S_{DS} , and the design long-period response acceleration coefficient, S_{D1} . First, the Site Factors, given in Tables 3.10.3.2-1, 3.10.3.2-2, and 3.10.3.2-3 of the AASHTO LRFD-BDS, must be applied. Given the previously stated assumption of Site Class B, the three Site Factors are all equal to unity as shown below.

$$F_{pga} = 1 \text{ and } F_a = 1 \text{ and } F_v = 1$$

AASHTO LRFD-BDS Equations 3.10.4.2-2, 3.10.4.2-3, and 3.10.4.2-6 will now be used, note the number 75 contained within each subscript identifying the corresponding 7% probability of exceedance in 75 years.

$$A_{S-75} = F_{pga}PGA_{75} = 0.39g \quad (\text{AASHTO Eqn. 3.10.4.2-2})$$

$$S_{DS-75} = F_a S_{S-75} = 0.69g \quad (\text{AASHTO Eqn. 3.10.4.2-3})$$

$$S_{D1-75} = F_v S_{I-75} = 0.15g \quad (\text{AASHTO Eqn. 3.10.4.2-6})$$

Now, the spectral reduction factor will be used to calculate the design response coefficients corresponding to the bridge's temporary designation.

$$A_S = \frac{A_{S-75}}{K_D} = 0.104 g$$

$$S_{DS} = \frac{S_{DS-75}}{K_D} = 0.184 g$$

$$S_{D1} = \frac{S_{D1-75}}{K_D} = 0.041 g$$

From here, the design response spectrum will be determined in the same manner that is done for a permanent bridge. Note that while in this example the site's classification of Seismic Performance Zone 2 (Seismic Design Category B if using the LRFD-SBD) cannot be redefined, if the site had been classified as Seismic Performance Zone 3 or 4 (Seismic Design Categories C and D if using the LRFD-SBD) based on the 1000 year return period, reclassification can be performed as long as the site is not redefined as Seismic Performance Zone 1 (Seismic Design Category A using the LRFD-SBD).

The reference periods for the response spectrum will now be calculated using the equations shown in Figure 3.10.3.1-1 of the LRFD-BDS.

$$T_S = \frac{S_{D1}}{S_{DS}} = 0.222 \text{ sec}$$

$$T_0 = 0.2T_S = 0.044 \text{ sec}$$

Finally, a plot of the design response spectrum can be determined using LRFD-BDS Equation 3.10.4.2-1, 3.10.4.2-4, and 3.10.4.2-5 to define the elastic seismic coefficient, C_{sm} , for the applicable period.

$$C_{sm} = A_S + (S_{DS} - A_S) * \left(\frac{T_m}{T_0}\right) \quad \text{for} \quad T_m \leq T_0 \quad (\text{AASHTO Eqn. 3.10.4.2-1})$$

$$C_{sm} = S_{DS} \quad \text{for} \quad T_0 \leq T_m \leq T_S \quad (\text{AASHTO Eqn. 3.10.4.2-4})$$

$$C_{sm} = S_{D1} \div T_m \quad \text{for} \quad T_S < T_m \quad (\text{AASHTO Eqn. 3.10.4.2-5})$$

Shown below in Figure 6-2, is the design response spectrum for the temporary bridge.

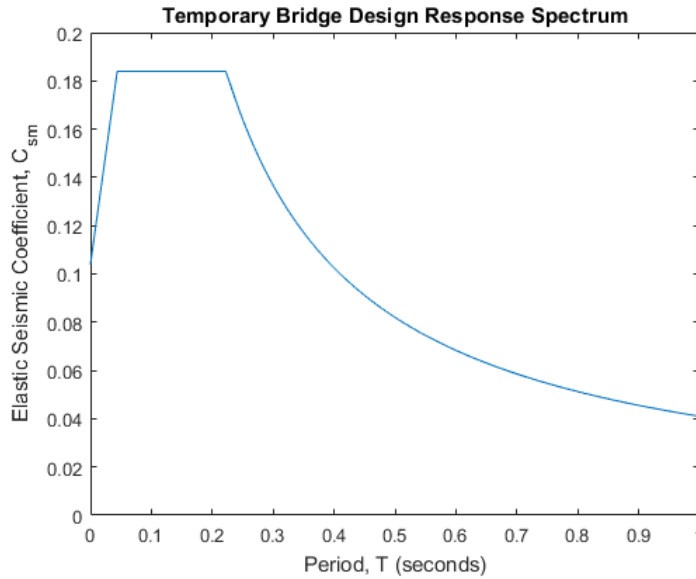


Figure 6-2: Design response spectrum for the example temporary bridge

6.3 Example Temporary Bridge

The temporary bridge in this example consists of three simply supported 50 ft. spans. The three spans are assumed to have identical mass, as are the two intermediate bents, and the two end bents. The Section Designer in SAP2000 was used to calculate the composite properties of the hollow core slab and the barrier rail. Shown below is an elevation view of the temporary bridge in Figure 6-3, a typical cross section view of the end bents and intermediate bents in Figure 6-4, and the hollow core slab and barrier rail with uncracked section properties in Figure 6-5.

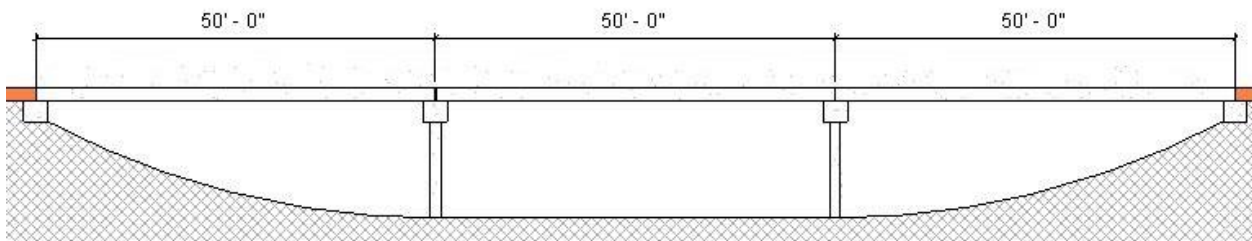


Figure 6-3: Elevation view of the temporary bridge.

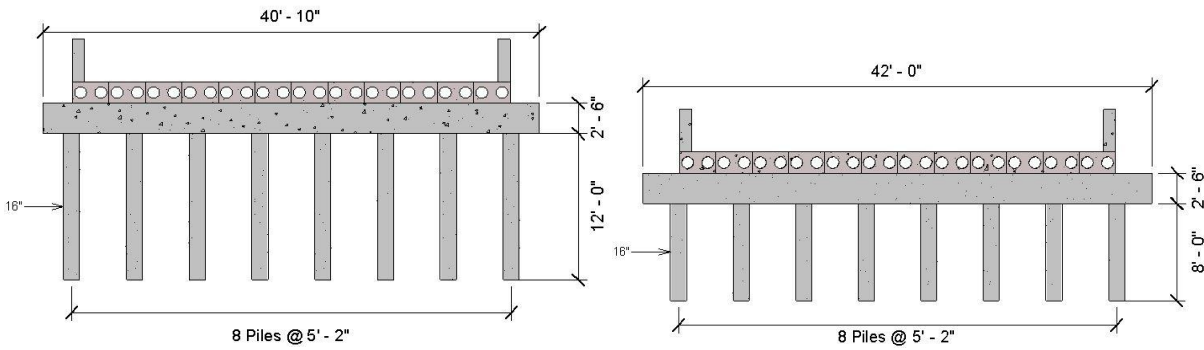


Figure 6-4: Cross section view of typical: (Left) intermediate bent; (Right) end bent.

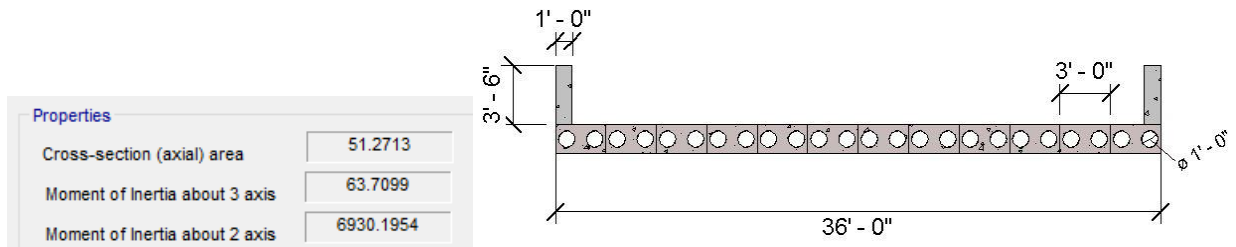


Figure 6-5: Composite section properties of the hollow core slab and barrier rail.

The weights of each component used in this example are given in Appendix Section A.5. The uniform weight for the temporary bridge is calculated below.

$$w_{span} = 398 \text{ kip}$$

The weight of each span.

$$w_{bent} = 74.83 \text{ kip}$$

The weight of each intermediate bent.

$$w_{EndBent} = 70.5 \text{ kip}$$

The weight of each end bent.

$$W_{bridge} = 3 * w_{span} + 2 * w_{bent} + 2 * w_{EndBent} = 1485 \text{ kip}$$

$$w_{bridge} = \frac{W_{bridge}}{150 \text{ ft}} = 0.825 \text{ kip/in}$$

6.4 Transverse Period of the Temporary Bridge

The transverse period of the bridge will be calculated using the assumed uniform weight of the bridge given in Section 6.4 and a SAP2000 model of the bridge with the superstructure modeled

as frame elements and the piles modeled as springs fixed at their base. Thus, the pile heights used will be from the bottom of the cap to the depth of fixity. Each span will be discretized using five individual frame elements, each 10 ft. in length. A unit load of 1 kip/in will be applied to the SAP2000 model in the transverse direction to obtain the maximum deflection. The stiffness will be equivalent in either direction of transverse loading for this example. The maximum deflection will be used to obtain an effective stiffness value for the temporary bridge using the following relationship (Chopra 2012):

$$k_{effective} = \frac{f_{applied}}{\Delta_{max}}$$

where $f_{applied}$ is the applied load and Δ_{max} is the maximum deflection.

The stiffness at each intermediate bent and end bent are calculated as follows:

$$h_{BentPile} = 12 \text{ ft}$$

The pile Height at each intermediate bent.

$$h_{EndBentPile} = 8 \text{ ft}$$

The pile height at each end bent.

$$\Phi_{pile} = 16 \text{ in}$$

The diameter of each pile.

$$f'_c = 10 \text{ ksi}$$

The compressive strength of the piles.

$$w_c = 0.14 \frac{\text{kip}}{\text{ft}^3} + 0.001 * f'_c = 0.15 \text{ kip/ft}^3$$

(AASHTO Table 3.5.1-1)

$$K_1 = 1$$

The assumed aggregate factor.
(AASHTO Article 5.4.2.4)

$$E_{pile} = 33000K_1w_c^{1.5}\sqrt{f'_c} = 6062 \text{ ksi}$$

(AASHTO Eqn. 5.4.2.4-1)

$$I_{uncracked} = \frac{\pi}{4} \left(\frac{\Phi_{pile}}{2} \right)^4 = 3217 \text{ in}^4$$

The stiffness of each pile before cracking.

$$I_{effective} = 0.6I_{uncracked} = 1930 \text{ in}^4$$

(AASHTO Guide Article 5.6.2)

The stiffness at each intermediate bent will be determined by calculating the stiffness for each pile and then multiplying by the number of piles at each bent. The lateral stiffness of each pile will be obtained with a basic static relationship (Chopra 2012), where the columns behave as clamped-clamped columns.

$$n = 8$$

The number of piles at each bent.

$$k_{BentUncracked} = \frac{12E_{pile}I_{uncracked}}{h_{BentPile}^3} * n = 627 \frac{kip}{in}$$

The stiffness of each intermediate bent before cracking.

$$k_{BentEffective} = \frac{12E_{pile}I_{effective}}{h_{BentPile}^3} * n = 376 \frac{kip}{in}$$

The effective stiffness of each intermediate bent

Now the stiffness at each end bent will be calculated using the same procedure.

$$k_{EndBentUncracked} = \frac{12E_{pile}I_{uncracked}}{h_{EndBentPile}^3} * n = 2116 \frac{kip}{in}$$

The stiffness of each end bent before cracking.

$$k_{EndBentEffective} = \frac{12E_{pile}I_{effective}}{h_{EndBentPile}^3} * n = 1270 \frac{kip}{in}$$

The effective stiffness of each end bent.

The moment of inertia of the hollow core slab and barrier rail for both the transverse and longitudinal direction are given in Figure 6-5 from the SAP2000 Section Designer. For the effective stiffness of the hollow core slab and barrier rail, an assumed effective stiffness of 1/10 the un-cracked stiffness of the section will be made. This is to reduce the effect of the superstructure behaving as a rigid element, but as so far as to assume the deck is a collection of independent beams (IDOT 2008). A summary of the section properties for each component that will be used in a SAP2000 model of the temporary bridge is given below in Table 6-2 for both the un-cracked and effective values.

Table 6-2: Transverse section properties for the temporary bridge

	Uncracked	Effective
Superstructure Moment of Inertia	143704532 in ⁴	14370453 in ⁴
Intermediate Bent Stiffness	627 kip/in	376 kip/in
End Bent Stiffness	2116 kip/in	1270 kip/in

Applying unit load of 1 kip/in is applied to the temporary bridge in SAP2000 shown below in Figure 6-6 along with the deflected shape, allows us to obtain the maximum deflection necessary to calculate the period of the bridge.

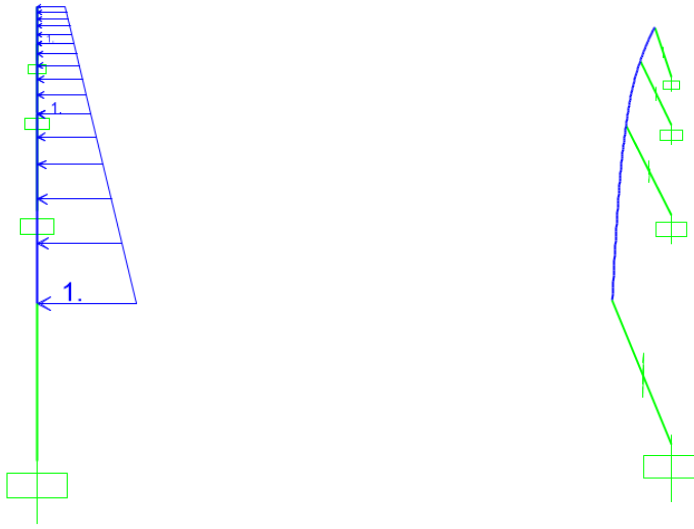


Figure 6-6: (Left) Model temporary bridge with an applied unit load of 1 kip/in; (Right) the deformed shape of the bridge under loading.

Given below in Table 6-3 are the transverse deflections for the temporary bridge subject to the applied unit load for uncracked and effective section properties.

Table 6-3: Transverse deflections of the temporary bridge

	Uncracked Deflection (in)	Effective Deflection (in)
Intermediate Bent	0.424	1.078
End Bent	0.2997	0.390
Maximum	0.443	1.18

Now using the maximum deflection to calculate the effective stiffness for the transverse direction.

$$L = 150 \text{ ft}$$

The total length of the bridge.

$$\Delta_{max} = 1.18 \text{ in}$$

The maximum deflection.

$$f_{applied} = 1 \frac{\text{kip}}{\text{in}} * L = 1800 \text{ kip}$$

The applied force from the uniform load.

$$k_{effective} = \frac{f_{applied}}{\Delta_{max}} = 1525 \text{ kip/in}$$

The bridge's effective stiffness.

Now the transverse period can be calculated using the effective stiffness, the weight of the bridge, and the acceleration of gravity.

$$T = 2\pi \sqrt{\frac{W_{bridge}}{g * k_{effective}}} = 0.315 \text{ seconds}$$

The period of the temporary bridge in the transverse direction.
(AASHTO Eqn. C4.7.4.3.2c-2)

6.5 Longitudinal Period of the Temporary Bridge

The stiffness of the piles will be calculated assuming the superstructure acts as a rigid body transferring the uniform longitudinal load to the intermediate and end bents with piles that behave like cantilevered columns. The longitudinal stiffness of the intermediate bent is calculated as follows.

$$h_{cap} = 2.5 \text{ ft}$$

The height of the cap.

$$h_{BentPile} = 12 \text{ ft} + h_{cap} = 14.5 \text{ ft}$$

Now, including the height of the cap.

$$k_{BentUncracked} = \frac{3E_{pile}I_{uncracked}}{h_{BentPile}^3} * n = 89 \frac{\text{kip}}{\text{in}}$$

The stiffness of each intermediate bent before cracking.

$$k_{BentEffective} = \frac{3E_{pile}I_{effective}}{h_{BentPile}^3} * n = 53 \frac{\text{kip}}{\text{in}}$$

The effective stiffness of each intermediate bent.

Applying a unit load to the piles at each intermediate bent to calculate the deflection from the piles. Additionally, calculating the deflection of the cap from the rotation at the top of the piles (IDOT 2008).

$$P = 1 \text{ kip}$$

The unit load of 1 kip.

$$\Delta_{BentPiles} = \frac{P}{k_{BentEffective}} = 0.019 \text{ in}$$

Calculating the deflection of the intermediate bents from the unit load.

$$\theta_{cap} = \frac{P * h_{BentPile}^2}{2E_{pile}I_{effective}} = 0.001 \text{ radians}$$

The rotation at the top of the piles.

$$\Delta_{cap} = h_{cap} \theta_{cap} = 0.039 \text{ in}$$

The deflection from the rigid body rotation of the cap beam.

Now the stiffness of each intermediate bent can be calculated.

$$\Delta_{Total} = \Delta_{cap} + \Delta_{BentPiles} = 0.058 \text{ in}$$

Total deflection from the unit load.

$$k_{pier} = \frac{P}{\Delta_{Total}} = 17.37 \text{ kip/in}$$

The longitudinal stiffness at each intermediate bent.

Now the same procedure is used to calculate the longitudinal stiffness at each end bent.

$$h_{cap} = 2.5 \text{ ft}$$

The height of the cap.

$$h_{EndBentPile} = 8 \text{ ft} + h_{cap} = 10.5 \text{ ft}$$

Now, including the height of the cap.

$$k_{EndBentUncracked} = \frac{3E_{pile}I_{uncracked}}{h_{EndBentPile}^3} * n = 234 \frac{\text{kip}}{\text{in}}$$

The stiffness of each end bent before cracking.

$$k_{EndBentEffective} = \frac{3E_{pile}I_{effective}}{h_{EndBentPile}^3} * n = 140 \frac{\text{kip}}{\text{in}}$$

The effective stiffness of each end bent.

$$P = 1 \text{ kip}$$

The unit load of 1 kip.

$$\Delta_{EndBentPiles} = \frac{P}{k_{EndBentEffective}} = 0.007 \text{ in}$$

Calculating the deflection of the end bents from the unit load.

$$\theta_{cap} = \frac{P * h_{EndBentPile}^2}{2E_{pile}I_{effective}} = 0.000678 \text{ radians}$$

The rotation at the top of the piles.

$$\Delta_{cap} = h_{cap} \theta_{cap} = 0.02 \text{ in}$$

The deflection from the rigid body rotation of the cap beam.

$$\Delta_{Total} = \Delta_{cap} + \Delta_{EndBentPiles} = 0.027 \text{ in}$$

Total deflection from the unit load.

$$k_{abutment} = \frac{P}{\Delta_{Total}} = 36.40 \text{ kip/in}$$

The longitudinal stiffness at each end bent.

The total stiffness of the bridge can now be obtained by adding the stiffness values from the two end bents and the two intermediate bents.

$$k_{bridge} = 2 * k_{abutment} + 2 * k_{pier}$$

The total effective stiffness of the temporary bridge in the longitudinal direction.

$$k_{bridge} = 107.54 \text{ kip/in}$$

Now the period for the longitudinal direction can be obtained, using the AASHTO LRFD-BDS Equation C4.7.4.3.2c-3.

$$T = 2\pi \sqrt{\frac{W_{bridge}}{g * k_{bridge}}} = 1.188 \text{ seconds}$$

The period of the temporary bridge in the longitudinal direction.
(AASHTO Eqn. C4.7.4.3.2c-2)

6.6 Design Earthquake Load

With the period of the bridge known for both the transverse and longitudinal directions, the Elastic Seismic Response Coefficient defined in Article 3.10.4.2 of the LRFD-BDS, C_{sm} , can now be obtained. Note that the transverse period and the longitudinal period exceed the reference period T_S , and thus C_{sm} will be obtained using AASHTO LRFD-BDS Equation 3.10.4.2-6.

$$C_{smTransverse} = \frac{T_{transverse}}{S_{D1}} = 7.683$$

The Elastic Seismic Response Coefficient in the transverse direction.

$$C_{smLongitudinal} = \frac{T_{longitudinal}}{S_{D1}} = 28.976$$

The Elastic Seismic Response Coefficient in the longitudinal direction.

Now the design earthquake load in the transverse direction is calculated below using AASHTO LRFD-BDS Equation C4.7.4.3.2c-4.

$$p_e = \frac{C_{smTransverse} W_{bridge}}{L} = 76.04 \text{ kip/ft}$$

The design earthquake load in the transverse direction.

And now the same procedure will be used to calculate the design earthquake load in the longitudinal direction.

$$p_e = \frac{C_{smLongitudinal} W_{bridge}}{L} = 286.79 \text{ kip/ft}$$

The design earthquake load in the transverse direction.

Finally, with the earthquake load obtained the temporary bridge can be designed to resist the specified earthquake forces.

SECTION 7

CONCLUSION

Using the procedure outlined in Section 3 for obtaining spectral reduction factors, the site locations when categorized by geographic location demonstrated stronger correlation between spectral ratio values than when the site locations were arranged by the AASHTO defined Seismic Performance Zones, particularly for low to moderate response accelerations, or for site locations corresponding to Seismic Performance Zone 1 or 2 (as most of the locations considered here fell within those Seismic Performance Zones – as is the case for most locations in the USA).

The spectral reduction limit of 2.5 specified by the American Association of State Highway and Transportation Officials in Article 3.6 of the *Guide Specifications for LRFD Seismic Bridge Design* corresponds closely with spectral reduction factors obtained using the procedure outlined in Section 3 from site locations on the west coast. Therefore, the authors recommend a spectral reduction factor of 2.5 for the west coast of the United States, consistent with the current spectral reduction limit specified by the *Guide Specifications for LRFD Seismic Bridge Design*.

It was observed that site locations in the central and eastern United States generally have higher spectral ratios, and that spectral ratio generally increased from west to east across the continental United States (where spectral ratio is defined as the ratio between the seismic response coefficients corresponding to a 1000 year return period, and the seismic response coefficients corresponding to a 100 year return period). Considering the higher spectral ratios in the central and eastern United States, the authors propose a spectral reduction of 3.75 to reduce all three spectral response coefficients from values corresponding to permanent bridge design, to values corresponding to temporary bridge design. This proposed spectral reduction factor of 3.75 was found to be conservative, in that it resulted in a response spectrum with greater response accelerations than a spectrum obtained directly from the USGS website, for every site location in the central and eastern United States examined in this study, with the exception of Atlanta and the 2014 USGS seismic hazard data which was found to approximately be 10% unconservative.

SECTION 8

REFERENCES

- AASHTO (2015). "AASHTO Guide Specifications for LRFD Seismic Bridge Design (2nd Edition) with 2012, 2014 and 2015 Interim Revisions." American Association of State Highway and Transportation Officials (AASHTO).
- AASHTO (2016). "AASHTO LRFD Bridge Design Specifications, U.S. Customary Units with 2015 and 2016 Interim Revisions (7th Edition)." American Association of State Highway and Transportation Officials (AASHTO).
- ADOT (2001). *Bridge Design Guidelines*, Arizona Department of Transportation, (March 20, 2017).
- ALDOT (2016). *Structural Design Manual*, Alabama Department of Transportation, Bridge Bureau, (March 20, 2017).
- Algermissen, S. T. (1969, January 14, 1969). *Seismic Risk Studies in the United States*. Paper presented at the Fourth World Conference on Earthquake Engineering, Santiago, Chile.
- ATC/MCEER (2003). "Design Examples, Recommended LRFD Guidelines for the Seismic Design of Highway Bridges." a partnership of the Applied Technology Council and the Multidisciplinary Center for Earthquake Engineering.
- Benz, H. M., Frankel, A., and Boore, D. M. (1997). "Regional Lg Attenuation for the Continental United States." *Bulletin of the Seismological Society of America*, Vol. 87, No. 3, 606-619.
- Blume, J. A. (1965). "Earthquake Ground-Motion and Engineering Procedures for Important Installations Near Active Faults." *Proc. Third World Conf. on Eq. Engr.*, IV, 53-71.
- Bollinger, G. A. (1973). "Seismicity of the Southeastern United States." *Bulletin of the Seismological Society of America*, Vol 63, No. 5, 1785-1808.
- Bruneau, M., Uang, C. M., and Sabelli, R. (2011). *Ductile Design of Steel Structures*, McGraw Hill.
- Burland, J., Chapman, T., Skinner, H., and Brown, M. (2012). *ICE Manual of Geotechnical Engineering, Volume 1 - Geotechnical Engineering Principles, Problematic Soils and Site Investigation*, ICE Publishing.
- Caltrans (2011). "20-2 Site Seismicity for Temporary Bridges and Stage Construction." California Department of Transportation.
- Campbell, K. W. (1997). "Empirical Near-Source Attenuation Relationships for Horizontal and Vertical Components of Peak Ground Acceleration, Peak Ground Velocity, and Pseudo-Absolute Acceleration Response Spectra." *Seismological Research Letters*, 68, 154-179.
- Campbell, K. W., and Bozorgnia, Y. (2006, September 3-8, 2006). *Next Generation Attenuation (NGA) Empirical Ground Motion Models: Can they be used in Europe?* Paper presented at the First European Conference on Earthquake Engineering and Seismology, Geneva, Switzerland.
- CDOT (2012). *Bridge Design Manual*, Colorado Department of Transportation, Staff Bridge, (March 20, 2017).
- Chopra, A. K. (2012). *Dynamics of Structures Theory and Applications to Earthquake Engineering*, Prentice Hall, Upper Saddle River, NJ.

- Chung, D. H., and Bernreuter, D. L. (1981). "The Effect of Regional Variation of Seismic Wave Attenuation on the Strong Ground Motion from Earthquakes." Lawrence Livermore Laboratory, Washington, DC, 28-32.
- ConnDOT (2003). *Bridge Design Manual*, Revised 2/11, Connecticut Department of Transportation, Newton, Connecticut, (March 20, 2017).
- Cornell, C. A. (1968). "Engineering Seismic Risk Analysis." *Bulletin of the Seismological Society of America*, Vol. 58, No. 5,(5), 1583-1606.
- DelDOT (2016). *Bridge Design Manual*, Delaware Department of Transportation, (March 20, 2017).
- DOT&PF (2013). *Alaska Highway Preconstruction Manual*, Alaska Department of Transportation & Public Facilities, (March 20, 2017).
- Ellsworth, W. L. (2013). "Injection-Induced Earthquakes." *Science*, Vol 341.
- FDOT (2017). "Structures Design Guidelines." *Structures Manual*, Volume 1, Florida Department of Transportation, Structures Design Office, (March 20, 2017).
- Frankel, A. D., Petersen, M. D., Mueller, C. S., Haller, K. M., Wheeler, R. L., Leyendecker, E. V., Wesson, R. L., Harmsen, S. C., Cramer, C. H., Perkins, D. M., and Rukstales, K. S. (2002). "Documentation for the 2002 Update of the National Seismic Hazard Maps." U.S. Department of the Interior, ed.
- GDOT (2016). *Bridge and Structures Design Manual*, Rev. 2.2, State of Georgia Department of Transportation, Atlanta, Georgia, (March 20, 2017).
- Gregersen, S. (1984). "Lg-Wave Propagation and Crustal Structure Differences near Denmark and the North Sea." *Geophys. J. R. ast. Soc.*, Vo. 79, Issue 1, 217-234.
- IDOT (2008). "Bridge Design Guidelines." 3.15 - *Seismic Design*, Illinois Department of Transportation, Illinois.
- IDOT (2012). *Bridge Manual*, Illinois Department of Transportation, Bureau of Bridges and Structures, Division of Highways, Springfield, Illinois, (March 20, 2017).
- IDT (2002). *Load Resistance Factor Design (LRFD) Bridge Manual*, Revised April 2008, Idaho Transportation Department, (March 20, 2017).
- INDOT (2013). "Structural, Part 4." *Design Manual*, Revised March 2017, Indiana Department of Transportation, (March 20, 2017).
- IOWA DOT (2016). *LRFD Bridge Design Manual*, Iowa Department of Transportation, Methods Section of the Office of Bridges and Structures, (March 20, 2017).
- Judd, J. P., and Charney, F. A. (2014). "Performance-Based Design in the Central and Eastern United States." *Structures Congress 2014*.
- KDOT (2016). "Volume III - Bridge Section." *Design Manual*, Version 1/16, Kansas Department of Transportation, (March 20, 2017).
- LaDOTD (2014). *Bridge Design and Evaluation Manual*, Revised 12/14/2016, Louisiana Department of Transportation & Development, (March 20, 2017).
- Luco, N., Ellingwood, B. R., Hamburger, R. O., Hooper, J. D., Kimball, J. K., and Kircher, C. A. (2007). *Risk-Targeted versus Current Seismic Design Maps for the Conterminous United States*. Paper presented at the SEAOC.
- MaineDOT (2003). *Bridge Design Guide*, Revised 2014, Maine Department of Transportation, Prepared by Guertin Elkerton & Associates, (March 20, 2017).
- MassDOT (2013). "Part I - Design Guidelines." *LRFD Bridge Manual*, Massachusetts Department of Transportation, (March 20, 2017).

- McGarr, A. (2014). "Maximum Magnitude Earthquakes Induced by Fluid Injection." *J. Geophys. Res. Solid Earth*, Vol 119, 1008-1019.
- MDOT (2009). *Michigan Design Manual*, Michigan Department of Transportation, (March 20, 2017).
- MDT (2002). "Structural Design, Volume II." *Structures Manual*, Montana Department of Transportation, MDT Bridge Design Section, assistance from Roy Jorgensen Associates Inc. and its subcontractor SRD Engineering, (March 20, 2017).
- Mikami, N., and Hirahara, K. (1981). "Global Distribution of Long-Period P-Wave Attenuation and its Tectonic Implications." *J. Phys. Earth*, 29, 97-117.
- Mississippi DOT (2010). *Bridge Design Manual*, Version 6.1, Revised 3/5/2010, Mississippi Department of Transportation, Bridge Design Division, Jackson, Mississippi.
- Mitchell, B. J. (1975). "Regional Rayleigh Wave Attenuation in North America." *Journal of Geophysical Research*, 80, 4904-4916.
- MnDOT (2016). *LRFD Bridge Design Manual*, Revised March 2017, Minnesota Department of Transportation, Bridge Office, Oakdale, Minnesota, (March 20, 2017).
- MoDOT (2010). "751 LRFD Bridge Design Guidelines." Missouri Department of Transportation, <http://epg.modot.org/index.php?title=Category%3A751_LRFD_Bridge_Design_Guidelines>. (March 20, 2017).
- Mohammadi, J., and Heydari, A. Z. (2008). "Seismic and Wind Load Considerations for Temporary Structures." *Practice Periodical on Structural Design and Construction*, 13(3), 128-134.
- Mueller, C. S. (2010). "Colorado Earthquakes and Seismic Hazard." *GeoTrends: The Progress of Geological and Geotechnical Engineering in Colorado at the Cusp of a New Decade*, C. M. Goss, J. B. Kerrigan, J. C. Malama, W. O. McCarron, and R. L. Wiltshire, eds., Paper presented at the Biennial Geotechnical Seminar 2010, Denver, Colorado.
- NCDOT (2015). "2015 Highway Letting Dare B-2500AB C203756." <https://xfer.services.ncdot.gov/dsplan/2015%20Highway%20Letting/10-20-15/Plans%20and%20Proposals/Dare%20B-2500AB%20C203756/Standard%20PDF%20Plans/>>. (February 17, 2017).
- NCDOT (2016). *Structures Management Unit Manual*, State of North Carolina Department of Transportation, (March 20, 2017).
- NDDOT (2017). *Design Manual*, Revised 4/5/2017, North Dakota Department of Transportation, (March 20, 2017).
- NDOR (2016). *Bridge Office Policies and Procedures* Last updated December 2016, Nebraska Department of Roads, Bridge Division, (March 20, 2017).
- NDOT (2008). *Structures Manual*, Nevada Department of Transportation, Structures Division, Carson City, Nevada, (March 20, 2017).
- Newmark, N. M., and Hall, W. J. (1982). *Earthquake Design Spectra and Design*, Earthquake Engineering Research Institute.
- NHDOT (2015). *Bridge Design Manual*, January 2015 - v2.0, Revised April 2016, New Hampshire Department of Transportation, Bureau of Bridge Design, (March 20, 2017).
- NHI (2014). "LRFD Seismic Analysis and Design of Bridges Reference Manual." National Highway Institute, Parsons Brinckerhoff, Inc., National Highway Institute, Principal Investigators Marsh, L.M., Buckle, I.G., and Kavazanjian Jr., E., 1-10.
- NJDOT (2016). *Design Manual for Bridges and Structures*, New Jersey Department of Transportation, (March 20, 2017).

- NMDOT (2013). *Bridge Procedures and Design Guide*, New Mexico Department of Transportation, (March 20, 2017).
- NYSDOT (2006). *Bridge Manual*, 4th Edition, Revised April 2014, New York State Department of Transportation, Office of Structures, (March 20, 2017).
- Obermeier, S. F., Gohn, G. S., Weems, R. E., Gelinias, R. L., and Rubin, M. (1985). "Geologic Evidence for Recurrent Moderate to Large Earthquakes near Charleston, South Carolina." *Science*, Volume 227, 408-411.
- ODOT (2007). *Bridge Design Manual*, Revised 1/20/2017, Ohio Department of Transportation's Office of Structural Engineering, Office of Structural Engineering, Columbus, Ohio, (March 20, 2017).
- Oregon DOT (2016). *Bridge Design and Drafting Manual*, Oregon Department of Transportation, (March 20, 2017).
- PennDOT (2015). *Design Manual, Part 4*, Pennsylvania Department of Transportation, Bureau of Project Delivery, Bridge Design and Technology Division, (March 20, 2017).
- Petersen, M. D., Frankel, A. D., Harmsen, S. C., Mueller, C. S., Haller, K. M., Wheeler, R. L., Wesson, R. L., Zeng, Y., Boyd, O. S., Perkins, D. M., Luco, N., Field, E. H., Wills, C. J., and Rukstales, K. S. (2008). *Documentation for the 2008 Update of the United States National Seismic Hazard Maps*, U.S. Department of the Interior.
- Petersen, M. D., Moschetti, M. P., Powers, P. M., Mueller, C. S., Haller, K. M., Frankel, A. D., Zeng, Y., Rezaeian, S., Harmsen, S. C., Boyd, O. S., Field, N., Chen, R., Rukstales, K. S., Luco, N., Wheeler, R. L., Williams, R. A., and Olsen, A. H. (2014). "Documentation for the 2014 Update of the United States National Seismic Hazard Maps." U.S. Department of Interior, ed. Reston, Virginia.
- Petersen, M. D., Moschetti, M. P., Powers, P. M., Mueller, C. S., Haller, K. M., Frankel, A. D., Zeng, Y., Rezaeian, S., Harmsen, S. C., Boyd, O. S., Field, N., Chen, R., Rukstales, K. S., Luco, N., Wheeler, R. L., Williams, R. A., and Olsen, A. H. (2015). "The 2014 United States National Seismic Hazard Model." *The Professional Journal of the Earthquake Engineering Research Institute*, 31.
- RIDOT (2007). *Rhode Island LRFD Bridge Design Manual*, State of Rhode Island Department of Transportation, Providence, Rhode Island, (March 20, 2017).
- SCDOT (2008). *Seismic Design Specifications for Highway Bridges*, Version 2.0, South Carolina Department of Transportation, assistance from STV/Ralph Whitehead Associates, Inc., Carolina Stalite Company, Fugro, and PBS&J, (March 20, 2017).
- Solomon, S. C., and Toksöz, M. N. (1970). "Lateral Variation of Attenuation of P and S Waves Beneath the United States." *Bulletin of the Seismological Society of America*, Vol. 60, No. 3, 819-838.
- Steer, M. B. (2010). "Microwave and RF Design - A Systems Approach." SciTech Publishing.
- Trifunac, M. D. (2003). "70th Anniversary of Biot Spectrum." *ISET Journal of Earthquake Technology*, Paper No. 431, Vol. 40, No. 1, 19-50.
- TxDOT (2015). *Bridge Design Manual - LRFD*, Revised October 2015, Texas Department of Transportation, (March 20, 2017).
- UDOT (2015). *Structures Design and Detailing Manual*, Utah Department of Transportation, Structures Design Division, (March 20, 2017).
- USGS (2002). "2002 U.S. Hazard Data." United States Geological Survey, <<https://earthquake.usgs.gov/hazards/hazmaps/conterminous/2002/data.php>>. (December 28, 2016).

- USGS (2014). "2014 U.S. Hazard Data." United States Geological Survey, <<ftp://hazards.cr.usgs.gov/web/nshm/conterminous/2014/data/>>. (December 28, 2016).
- VDOT (2015). *VDOT Modifications to the AASHTO LRFD Bridge Design Specifications*, 7th Edition, Revised August 25, 2015, Virginia Department of Transportation, (March 20, 2017).
- VTrans (2010). *VTrans Structures Design Manual*, Fifth Edition, Vermont Agency of Transportation, VTrans Structures Section, Montpelier, Vermont.
- Walker, D. J. (2016). "Computational Physics - An Introduction." Mercury Learning and Information.
- WisDOT (2017). *WisDOT Bridge Manual*, Wisconsin Department of Transportation, (March 20, 2017).
- WSDOT (2016). *Bridge Design Manual (LRFD)*, Washington State Department of Transportation, Bridge and Structures Office, Olympia, Washington, (March 20, 2017).
- WVDOH (2004). *Bridge Design Manual*, Revised March 1, 2004, West Virginia Division of Highways, West Virginia Department of Transportation, Charleston, West Virginia, (March 20, 2017).
- WYDOT (2013). *Bridge Design Manual*, Wyoming Department of Transportation, Bridge Program, (March 20, 2017).

APPENDIX A

A.1 MATLAB Function for Spatial Interpolation

Given below is a MATLAB function provided by Nicolas Luco for two-dimensional interpolation. The function requires a latitude and longitude input, the output is a seismic hazard curve specific to the input latitude and longitude.

```
function [ siteVals ] = spatial_interp2_NL101026( gridLons, gridLats, gridVals, siteLons, siteLats )

%
% function [ siteVals ] = spatial_interp2_NL101026( gridLons, gridLats, gridVals, siteLons, siteLats )
%
% Author: Nicolas Luco (nluco@usgs.gov)
% Last Revised: 2010 October 26
%
% Input
% -----
% gridLons = ( # grid points x 1 ) vector of longitudes
% gridLats = ( # grid points x 1 ) vector of latitudes
% gridVals = ( # grid points x # values ) matrix of values
% siteLons = ( # sites x 1 ) vector of longitudes
% siteLats = ( # sites x 1 ) vector of latitudes
%
% Output
% -----
% siteVals = ( # sites x # values ) matrix of values
%

X = unique( gridLons )';
nLons = length( X );

Y = flipud( unique( gridLats ) );
nLats = length( Y );

nSites = length( siteLons );
nVals = size( gridVals, 2 ); % # values (e.g., 1 for Vs30, 20 for hazard curves)
for i = 1:nSites

    if rem(i,1000)==0, i, end

    XI = siteLons(i);
    YI = siteLats(i);

    for j = 1:nVals

        Z = reshape( gridVals(:,j), nLons, nLats )';
        siteVals(i,j) = interp2( X, Y, Z, XI, YI, '*linear', 0 )';

    end

end

end
```

A.2 MATLAB Function for Hazard Curve Interpolation

Given below is a MATLAB function provided by Nicolas Luco for interpolation between seismic hazard curve values at a specified location. The USGS seismic hazard data is provided in a gridded format using latitude and longitude. Each intersection of latitude and longitude has 19 to 20 (depending on the data set and seismic response coefficient) mean annual frequency of exceedance values corresponding to 19 to 20 spectral acceleration values. Use of this function along with the USGS seismic hazard data, allows for an input of a specified return period, in the form of mean annual frequency of exceedance, and the function outputs a spectral response acceleration specific to the input return period.

```
function [ SAI ] = interp1_HazCurve( MAFE, SA, MAFEI )

%clear;
%load( 'v070306.1hz.2007.mat' )
%MAFE = HazCurves.MAFE(end,:);
%SA = HazCurves.SA;
%MAFEI = - log( 1 - 0.02 ) / 50;

if MAFEI < min(MAFE)
    SAI = NaN;
    return
elseif MAFEI > max(MAFE)
    SAI = NaN;
    return
end

[ tmp1, ii, tmp2 ] = unique( MAFE );
if length(ii) == 1
    SAI = NaN;
    return
elseif length(ii) ~= length(MAFE)
    sortedii = sort( ii );
    MAFE = MAFE( sortedii );
    SA = SA( sortedii );
end

SAI = exp( interp1( log(MAFE), log(SA), log(MAFEI) ) );
```

A.3 2002 USGS Seismic Hazard Data

In the table below is the 2002 USGS seismic hazard data obtained from the USGS website, with use of the MATLAB functions provided by Nicolas Luco, for this report (USGS 2002).

Table A-1: The 100 site locations and the corresponding seismic hazard data from the 2002 USGS data set

State	City	Latitude	Longitude	PGA ₇₅	S _{S-75}	S _{I-75}	PGA ₁₀	S _{S-10}	S _{I-10}
Arizona	Phoenix	33.4478	-112.0750	0.0514	0.1166	0.0391	0.0172	0.0358	0.0098
Arizona	Tucson	32.2189	-110.9299	0.0740	0.1706	0.0487	0.0191	0.0398	0.0104
New Mexico	Albuquerque	35.0812	-106.5939	0.1479	0.3514	0.1010	0.0363	0.0799	0.0205
Colorado	Denver	39.7391	-104.9903	0.0589	0.1258	0.0338	0.0097	0.0234	0.0062
Washington	Seattle	47.6055	-122.3330	0.4515	1.0050	0.3358	0.1467	0.3169	0.0996
Oregon	Gresham	45.5000	-122.4303	0.2591	0.6105	0.2106	0.0676	0.1498	0.0464
Oregon	Eugene	44.0519	-123.0873	0.1859	0.4473	0.2132	0.0315	0.0663	0.0247
Oregon	Portland	45.5227	-122.6762	0.2727	0.6459	0.2247	0.0711	0.1578	0.0481
Idaho	Boise	43.6182	-116.2146	0.0855	0.2012	0.0700	0.0307	0.0663	0.0209
Utah	St. George	37.0886	-113.5719	0.1332	0.3175	0.1005	0.0381	0.0844	0.0256
Montana	Billings	45.7808	-108.5005	0.0420	0.0946	0.0350	0.0153	0.0327	0.0095
Wyoming	Casper	42.8639	-106.3138	0.1102	0.2112	0.0444	0.0175	0.0393	0.0075
Washington	Spokane	47.6397	-117.4230	0.1060	0.2406	0.0724	0.0289	0.0596	0.0186
Louisiana	Baton Rouge	30.4581	-91.1402	0.0301	0.0669	0.0307	NaN	0.0086	0.0039
Texas	Austin	30.2670	-97.7431	0.0195	0.0443	0.0193	NaN	0.0059	NaN
Texas	Houston	29.7602	-95.3711	0.0208	0.0465	0.0212	NaN	0.0059	0.0026
Texas	Dallas	32.7757	-96.7949	0.0291	0.0673	0.0299	NaN	0.0114	0.0041
Texas	San Antonio	29.4218	-98.4957	0.0235	0.0508	0.0158	NaN	NaN	NaN
Arkansas	Little Rock	34.7463	-92.2899	0.1330	0.2947	0.0909	0.0129	0.0309	0.0084
Minnesota	Minneapolis	44.9760	-93.2605	0.0145	0.0332	0.0162	NaN	0.0051	NaN
Nebraska	Lincoln	40.8255	-96.6850	0.0433	0.0890	0.0271	NaN	0.0111	0.0047
South Dakota	Sioux Falls	43.5444	-96.7314	0.0269	0.0609	0.0202	NaN	0.0085	0.0035
Kansas	Wichita	37.6592	-97.3690	0.0342	0.0776	0.0313	0.0058	0.0138	0.0052
Kansas	Dodge City	37.7481	-100.0198	0.0260	0.0614	0.0250	NaN	0.0114	0.0047
Oklahoma	Oklahoma City	35.4531	-97.5144	0.0944	0.1772	0.0421	0.0087	0.0195	0.0058
Oklahoma	Tulsa	36.0699	-95.9592	0.0439	0.1001	0.0405	0.0074	0.0178	0.0059
Missouri	Springfield	37.1986	-93.2981	0.0560	0.1356	0.0565	0.0092	0.0232	0.0076
Iowa	Des Moines	41.5938	-93.6109	0.0201	0.0465	0.0267	NaN	0.0094	0.0044
Minnesota	Ely	47.9021	-91.8680	0.0108	0.0259	0.0082	NaN	NaN	NaN
North Dakota	Fargo	46.8739	-96.7922	0.0168	0.0393	0.0117	NaN	NaN	NaN
North Dakota	Casselton	46.9004	-97.2111	0.0160	0.0380	0.0118	NaN	NaN	NaN

State	City	Latitude	Longitude	PGA ₇₅	S _{S-75}	S _{I-75}	PGA ₁₀	S _{S-10}	S _{I-10}
North Carolina	Asheville	35.5949	-82.5518	0.1120	0.2243	0.0647	0.0195	0.0437	0.0110
Florida	Miami	25.7615	-80.1919	0.0097	0.0207	0.0102	NaN	NaN	NaN
Georgia	Atlanta	33.7486	-84.3884	0.0611	0.1396	0.0538	0.0136	0.0318	0.0095
Florida	Jacksonville	30.3329	-81.6560	0.0345	0.0824	0.0347	NaN	0.0100	0.0039
North Carolina	Charlotte	35.2186	-80.8402	0.0842	0.1934	0.0637	0.0137	0.0324	0.0089
Virginia	Virginia Beach	36.8525	-75.9795	0.0263	0.0618	0.0275	NaN	0.0100	0.0041
Alabama	Mobile	30.6929	-88.0428	0.0297	0.0661	0.0322	NaN	0.0104	0.0050
New York	Amherst	42.9996	-78.7850	0.0759	0.1431	0.0340	0.0076	0.0185	0.0064
Massachusetts	Boston	42.3598	-71.0590	0.0748	0.1514	0.0386	0.0103	0.0242	0.0068
Maine	Portland	43.6597	-70.2519	0.0858	0.1720	0.0446	0.0126	0.0296	0.0080
Vermont	Burlington	44.4757	-73.2124	0.1092	0.2213	0.0566	0.0202	0.0460	0.0104
New York	Manhattan	40.7827	-73.9716	0.1005	0.1841	0.0379	0.0091	0.0212	0.0064
Pennsylvania	Philadelphia	39.9532	-75.1644	0.0705	0.1395	0.0332	0.0077	0.0178	0.0060
Washington DC	Washington DC	38.9054	-77.0352	0.0385	0.0877	0.0302	0.0065	0.0155	0.0055
Maryland	Baltimore	39.2901	-76.6121	0.0424	0.0942	0.0302	0.0066	0.0157	0.0056
Illinois	Chicago	41.8777	-87.6299	0.0414	0.0898	0.0356	0.0060	0.0145	0.0057
Ohio	Columbus	39.9608	-82.9990	0.0397	0.0895	0.0374	0.0078	0.0185	0.0075
Indiana	Indianapolis	39.7678	-86.1565	0.0513	0.1218	0.0510	0.0101	0.0249	0.0084
Kentucky	Louisville	38.2465	-85.7555	0.0648	0.1546	0.0628	0.0125	0.0309	0.0100
Michigan	Detroit	42.3310	-83.0477	0.0308	0.0695	0.0281	0.0054	0.0126	0.0057
California	San Francisco	37.7524	-122.4229	0.6937	1.6033	0.7841	0.2415	0.5583	0.2125
Nevada	Las Vegas	36.1694	-115.1375	0.1522	0.3629	0.1174	0.0464	0.1035	0.0368
California	San Diego	32.7155	-117.1617	0.4024	0.9342	0.3456	0.1015	0.2337	0.0995
California	San Jose	37.3371	-121.8881	0.6375	1.5538	0.6105	0.2863	0.6697	0.2289
California	Sacramento	38.5813	-121.4944	0.1805	0.4299	0.1878	0.0809	0.1837	0.0827
California	Oakland	37.8034	-122.2712	0.7950	1.8904	0.7462	0.2966	0.6906	0.2573
California	Bakersfield	35.3732	-119.0190	0.3570	0.8482	0.3148	0.1342	0.3073	0.1181
California	Costa Mesa	33.6397	-117.9197	0.5207	1.2139	0.4440	0.1622	0.3806	0.1513
California	Corona	33.8753	-117.5665	0.6743	1.6066	0.5924	0.2373	0.5639	0.2234
California	Modesto	37.6387	-120.9975	0.2577	0.6205	0.2275	0.0979	0.2243	0.0939
Nevada	Reno	39.5289	-119.8150	0.4716	1.1344	0.4106	0.1443	0.3451	0.1101
California	Los Angeles	34.0520	-118.2437	0.6863	1.6218	0.5485	0.2299	0.5441	0.2007
Utah	Salt Lake City	40.7598	-111.8929	0.4774	1.0999	0.4186	0.0714	0.1664	0.0524
Wyoming	Jackson	43.4794	-110.7637	0.3143	0.7399	0.2396	0.0846	0.1967	0.0574
Utah	Provo	40.2339	-111.6589	0.2953	0.6860	0.2474	0.0574	0.1321	0.0422

State	City	Latitude	Longitude	PGA ₇₅	S _{S-75}	S _{I-75}	PGA ₁₀	S _{S-10}	S _{I-10}
Idaho	Twin Falls	42.5504	-114.4622	0.0731	0.1698	0.0610	0.0270	0.0582	0.0192
Utah	Trout Creek	39.6890	-113.8285	0.0755	0.1757	0.0664	0.0279	0.0607	0.0208
Wyoming	Rock Springs	41.5863	-109.2027	0.1071	0.2082	0.0605	0.0249	0.0550	0.0159
Nevada	Elko	40.8293	-115.7638	0.1356	0.3259	0.1083	0.0390	0.0867	0.0266
Utah	Delta	39.3507	-112.5783	0.1305	0.3122	0.1041	0.0447	0.1008	0.0317
Idaho	Idaho Falls	43.4874	-112.0343	0.1430	0.3431	0.1153	0.0520	0.1186	0.0409
Nevada	Jarbridge	41.8732	-115.4306	0.0946	0.2219	0.0699	0.0282	0.0609	0.0183
Tennessee	Memphis	35.1463	-90.0491	0.3984	0.7416	0.1899	0.0271	0.0590	0.0124
Arkansas	Jonesboro	35.8261	-90.7199	0.6095	1.1025	0.2789	0.0326	0.0689	0.0131
Arkansas	Paragould	36.0513	-90.5046	0.5533	1.0043	0.2510	0.0364	0.0757	0.0139
Missouri	St. Louis	38.6122	-90.2283	0.1732	0.3498	0.0984	0.0240	0.0539	0.0114
Illinois	Salem	38.6001	-88.9704	0.2208	0.4361	0.1145	0.0311	0.0663	0.0129
Indiana	Evansville	37.9701	-87.5720	0.1937	0.3965	0.1106	0.0268	0.0591	0.0130
Arkansas	Searcy	35.2446	-91.7347	0.2091	0.4375	0.1214	0.0180	0.0415	0.0098
Arkansas	Jefferson	34.2268	-91.9099	0.1168	0.2657	0.0859	0.0117	0.0282	0.0080
Alabama	Florence	34.7932	-87.6804	0.0889	0.2123	0.0780	0.0147	0.0360	0.0107
Tennessee	Jackson	35.6112	-88.8133	0.2581	0.5161	0.1414	0.0279	0.0614	0.0133
South Carolina	Charleston	32.7761	-79.9308	0.3891	0.6844	0.1525	0.0146	0.0313	0.0073
Georgia	Savannah	32.0726	-81.1047	0.1014	0.2232	0.0668	0.0097	0.0225	0.0064
South Carolina	Columbia	33.9495	-81.1126	0.1593	0.3213	0.0831	0.0175	0.0390	0.0093
South Carolina	Greenville	34.7636	-82.4799	0.0993	0.2099	0.0648	0.0178	0.0409	0.0105
South Carolina	Myrtle Beach	33.6658	-78.9018	0.1441	0.3040	0.0830	0.0094	0.0219	0.0058
Georgia	Jesup	31.5941	-81.8835	0.0559	0.1337	0.0490	0.0071	0.0172	0.0058
Georgia	Baxley	31.7718	-82.3560	0.0520	0.1244	0.0478	0.0074	0.0179	0.0062
Georgia	Augusta	33.4706	-82.0172	0.1023	0.2222	0.0675	0.0148	0.0340	0.0089
North Carolina	Wilmington	34.2180	-77.9387	0.0695	0.1600	0.0523	0.0058	0.0145	0.0045
North Carolina	Lumberton	34.6106	-79.0118	0.0953	0.2152	0.0671	0.0089	0.0214	0.0065
Wyoming	Missoula	46.8325	-113.9941	0.1389	0.3323	0.1018	0.0447	0.0997	0.0296
California	Redding	40.5789	-122.3932	0.2221	0.5146	0.2036	0.0773	0.1703	0.0766
Oregon	Medford	42.3133	-122.8711	0.1598	0.3795	0.1726	0.0474	0.1035	0.0442
Washington	Kennewick	46.1670	-119.1138	0.1184	0.2723	0.0888	0.0346	0.0724	0.0231
Washington	Yakima	46.6123	-120.5255	0.1506	0.3473	0.1224	0.0509	0.1094	0.0381
Montana	Miles City	46.3645	-105.8862	0.0254	0.0614	0.0208	0.0050	0.0125	0.0038
Tennessee	Chattanooga	35.0335	-85.3130	0.1354	0.2518	0.0693	0.0194	0.0436	0.0117

A.4 2014 USGS Seismic Hazard Data

In the table below is the 2014 USGS seismic hazard data obtained from the USGS website, with use of the MATLAB functions provided by Nicolas Luco, for this report (USGS 2014).

Table A-2: The 100 site locations and the corresponding seismic hazard data from the 2014 USGS data set

State	City	Latitude	Longitude	PGA ₇₅	S _{S-75}	S ₁₋₇₅	PGA ₁₀	S _{S-10}	S ₁₋₁₀
Arizona	Phoenix	33.4478	-112.0750	0.0455	0.1004	0.0334	0.0091	0.0194	0.0083
Arizona	Tucson	32.2189	-110.9299	0.0660	0.1461	0.0403	0.0102	0.0216	0.0089
New Mexico	Albuquerque	35.0812	-106.5939	0.1038	0.2305	0.0628	0.0168	0.0365	0.0114
Colorado	Denver	39.7391	-104.9903	0.0631	0.1191	0.0301	0.0127	0.0272	0.0069
Washington	Seattle	47.6055	-122.3330	0.4132	0.9668	0.2777	0.1181	0.2676	0.0652
Oregon	Gresham	45.5000	-122.4303	0.2506	0.5608	0.2035	0.0467	0.1014	0.0293
Oregon	Eugene	44.0519	-123.0873	0.2023	0.4392	0.2093	0.0201	0.0426	0.0192
Oregon	Portland	45.5227	-122.6762	0.2541	0.5702	0.2141	0.0474	0.1031	0.0294
Idaho	Boise	43.6182	-116.2146	0.0841	0.1888	0.0599	0.0201	0.0429	0.0162
Utah	St. George	37.0886	-113.5719	0.1340	0.3023	0.0829	0.0272	0.0592	0.0199
Montana	Billings	45.7808	-108.5005	0.0396	0.0816	0.0322	0.0113	0.0241	0.0106
Wyoming	Casper	42.8639	-106.3138	0.0997	0.1747	0.0357	0.0195	0.0397	0.0078
Washington	Spokane	47.6397	-117.4230	0.0797	0.1751	0.0585	0.0158	0.0327	0.0134
Louisiana	Baton Rouge	30.4581	-91.1402	0.0263	0.0532	0.0321	NaN	0.0107	0.0046
Texas	Austin	30.2670	-97.7431	0.0149	0.0307	0.0170	NaN	0.0063	0.0026
Texas	Houston	29.7602	-95.3711	0.0189	0.0376	0.0221	NaN	0.0072	0.0031
Texas	Dallas	32.7757	-96.7949	0.0285	0.0593	0.0303	0.0061	0.0133	0.0046
Texas	San Antonio	29.4218	-98.4957	0.0132	0.0278	0.0119	NaN	NaN	NaN
Arkansas	Little Rock	34.7463	-92.2899	0.1277	0.2423	0.0801	0.0174	0.0365	0.0091
Minnesota	Minneapolis	44.9760	-93.2605	0.0136	0.0277	0.0167	NaN	0.0058	0.0025
Nebraska	Lincoln	40.8255	-96.6850	0.0223	0.0448	0.0256	NaN	0.0102	0.0047
South Dakota	Sioux Falls	43.5444	-96.7314	0.0248	0.0507	0.0195	NaN	0.0095	0.0038
Kansas	Wichita	37.6592	-97.3690	0.0274	0.0565	0.0313	0.0062	0.0137	0.0053
Kansas	Dodge City	37.7481	-100.0198	0.0232	0.0492	0.0241	0.0055	0.0120	0.0050
Oklahoma	Oklahoma City	35.4531	-97.5144	0.0978	0.1678	0.0418	0.0124	0.0244	0.0065
Oklahoma	Tulsa	36.0699	-95.9592	0.0404	0.0834	0.0408	0.0091	0.0196	0.0062
Missouri	Springfield	37.1986	-93.2981	0.0577	0.1234	0.0575	0.0105	0.0238	0.0076
Iowa	Des Moines	41.5938	-93.6109	0.0199	0.0400	0.0296	NaN	0.0093	0.0044
Minnesota	Ely	47.9021	-91.8680	0.0094	0.0207	0.0070	NaN	NaN	NaN

State	City	Latitude	Longitude	PGA ₇₅	S _{S-75}	S ₁₋₇₅	PGA ₁₀	S _{S-10}	S ₁₋₁₀
North Dakota	Fargo	46.8739	-96.7922	0.0146	0.0310	0.0095	NaN	NaN	NaN
North Dakota	Casselton	46.9004	-97.2111	0.0143	0.0306	0.0097	NaN	0.0052	NaN
North Carolina	Asheville	35.5949	-82.5518	0.0959	0.1734	0.0518	0.0218	0.0442	0.0114
Florida	Miami	25.7615	-80.1919	0.0093	0.0184	0.0103	NaN	NaN	NaN
Georgia	Atlanta	33.7486	-84.3884	0.0576	0.1163	0.0488	0.0165	0.0351	0.0101
Florida	Jacksonville	30.3329	-81.6560	0.0297	0.0632	0.0297	0.0050	0.0110	0.0046
North Carolina	Charlotte	35.2186	-80.8402	0.0626	0.1266	0.0455	0.0141	0.0299	0.0090
Virginia	Virginia Beach	36.8525	-75.9795	0.0222	0.0474	0.0209	NaN	0.0107	0.0041
Alabama	Mobile	30.6929	-88.0428	0.0281	0.0570	0.0340	0.0060	0.0130	0.0058
New York	Amherst	42.9996	-78.7850	0.0441	0.0824	0.0233	0.0068	0.0153	0.0057
Massachusetts	Boston	42.3598	-71.0590	0.0825	0.1454	0.0327	0.0134	0.0278	0.0071
Maine	Portland	43.6597	-70.2519	0.0873	0.1552	0.0366	0.0159	0.0328	0.0079
Vermont	Burlington	44.4757	-73.2124	0.1147	0.1981	0.0444	0.0223	0.0451	0.0097
New York	Manhattan	40.7827	-73.9716	0.0855	0.1447	0.0285	0.0097	0.0207	0.0061
Pennsylvania	Philadelphia	39.9532	-75.1644	0.0509	0.0952	0.0240	0.0079	0.0168	0.0058
Washington DC	Washington DC	38.9054	-77.0352	0.0379	0.0751	0.0229	0.0072	0.0153	0.0053
Maryland	Baltimore	39.2901	-76.6121	0.0390	0.0765	0.0226	0.0070	0.0151	0.0053
Illinois	Chicago	41.8777	-87.6299	0.0331	0.0665	0.0352	0.0064	0.0142	0.0055
Ohio	Columbus	39.9608	-82.9990	0.0353	0.0713	0.0342	0.0085	0.0184	0.0074
Indiana	Indianapolis	39.7678	-86.1565	0.0542	0.1091	0.0472	0.0112	0.0246	0.0082
Kentucky	Louisville	38.2465	-85.7555	0.0614	0.1282	0.0561	0.0137	0.0303	0.0097
Michigan	Detroit	42.3310	-83.0477	0.0288	0.0581	0.0261	0.0060	0.0129	0.0055
California	San Francisco	37.7524	-122.4229	0.5851	1.3242	0.4382	0.1831	0.4057	0.1173
Nevada	Las Vegas	36.1694	-115.1375	0.1422	0.3211	0.0967	0.0309	0.0660	0.0267
California	San Diego	32.7155	-117.1617	0.4229	0.9631	0.2627	0.0753	0.1635	0.0554
California	San Jose	37.3371	-121.8881	0.6751	1.5906	0.4938	0.2644	0.5929	0.1625
California	Sacramento	38.5813	-121.4944	0.1720	0.3863	0.1487	0.0659	0.1413	0.0536
California	Oakland	37.8034	-122.2712	0.6632	1.5430	0.4875	0.2196	0.4863	0.1387
California	Bakersfield	35.3732	-119.0190	0.2870	0.6418	0.1966	0.0948	0.2040	0.0617
California	Costa Mesa	33.6397	-117.9197	0.3897	0.8847	0.2620	0.1223	0.2701	0.0786
California	Corona	33.8753	-117.5665	0.6875	1.6034	0.4708	0.2029	0.4474	0.1236
California	Modesto	37.6387	-120.9975	0.2098	0.4744	0.1608	0.0811	0.1773	0.0612
Nevada	Reno	39.5289	-119.8150	0.4737	1.1077	0.3242	0.1318	0.2974	0.0797

State	City	Latitude	Longitude	PGA ₇₅	S _{S-75}	S ₁₋₇₅	PGA ₁₀	S _{S-10}	S ₁₋₁₀
California	Los Angeles	34.0520	-118.2437	0.5917	1.3706	0.4013	0.1698	0.3751	0.1036
Utah	Salt Lake City	40.7598	-111.8929	0.4112	0.9393	0.2732	0.0459	0.1001	0.0316
Wyoming	Jackson	43.4794	-110.7637	0.2951	0.6679	0.1765	0.0723	0.1590	0.0417
Utah	Provo	40.2339	-111.6589	0.3528	0.7959	0.2347	0.0426	0.0922	0.0285
Idaho	Twin Falls	42.5504	-114.4622	0.0531	0.1172	0.0463	0.0147	0.0310	0.0157
Utah	Trout Creek	39.6890	-113.8285	0.0719	0.1592	0.0541	0.0175	0.0373	0.0171
Wyoming	Rock Springs	41.5863	-109.2027	0.1038	0.1811	0.0452	0.0216	0.0442	0.0143
Nevada	Elko	40.8293	-115.7638	0.1350	0.3059	0.0859	0.0272	0.0587	0.0200
Utah	Delta	39.3507	-112.5783	0.1192	0.2682	0.0796	0.0319	0.0692	0.0227
Idaho	Idaho Falls	43.4874	-112.0343	0.1130	0.2545	0.0802	0.0346	0.0756	0.0274
Nevada	Jarbridge	41.8732	-115.4306	0.0794	0.1768	0.0547	0.0166	0.0351	0.0150
Tennessee	Memphis	35.1463	-90.0491	0.3586	0.6247	0.1694	0.0351	0.0680	0.0135
Arkansas	Jonesboro	35.8261	-90.7199	0.3965	0.6833	0.1875	0.0397	0.0756	0.0139
Arkansas	Paragould	36.0513	-90.5046	0.4046	0.6992	0.1922	0.0441	0.0823	0.0147
Missouri	St. Louis	38.6122	-90.2283	0.1525	0.2835	0.0886	0.0236	0.0484	0.0108
Illinois	Salem	38.6001	-88.9704	0.1918	0.3399	0.0983	0.0292	0.0578	0.0120
Indiana	Evansville	37.9701	-87.5720	0.1833	0.3297	0.0984	0.0283	0.0563	0.0125
Arkansas	Searcy	35.2446	-91.7347	0.1945	0.3539	0.1060	0.0249	0.0502	0.0109
Arkansas	Jefferson	34.2268	-91.9099	0.0953	0.1945	0.0740	0.0142	0.0306	0.0084
Alabama	Florence	34.7932	-87.6804	0.1009	0.2055	0.0793	0.0176	0.0386	0.0110
Tennessee	Jackson	35.6112	-88.8133	0.2568	0.4740	0.1443	0.0327	0.0648	0.0136
South Carolina	Charleston	32.7761	-79.9308	0.4588	0.7301	0.1484	0.0236	0.0430	0.0095
Georgia	Savannah	32.0726	-81.1047	0.0911	0.1771	0.0532	0.0115	0.0235	0.0070
South Carolina	Columbia	33.9495	-81.1126	0.1137	0.2107	0.0584	0.0172	0.0351	0.0094
South Carolina	Greenville	34.7636	-82.4799	0.1035	0.1836	0.0530	0.0207	0.0425	0.0112
South Carolina	Myrtle Beach	33.6658	-78.9018	0.0877	0.1717	0.0509	0.0101	0.0210	0.0060
Georgia	Jesup	31.5941	-81.8835	0.0509	0.1052	0.0409	0.0084	0.0181	0.0064
Georgia	Baxley	31.7718	-82.3560	0.0473	0.0983	0.0402	0.0087	0.0188	0.0068
Georgia	Augusta	33.4706	-82.0172	0.0850	0.1635	0.0518	0.0161	0.0333	0.0093
North Carolina	Wilmington	34.2180	-77.9387	0.0443	0.0929	0.0338	0.0060	0.0138	0.0044
North Carolina	Lumberton	34.6106	-79.0118	0.0587	0.1206	0.0430	0.0092	0.0200	0.0067
Wyoming	Missoula	46.8325	-113.9941	0.1141	0.2567	0.0741	0.0279	0.0608	0.0204
California	Redding	40.5789	-122.3932	0.3178	0.7125	0.2403	0.0848	0.1844	0.0561
Oregon	Medford	42.3133	-122.8711	0.1812	0.3943	0.1878	0.0299	0.0636	0.0293

State	City	Latitude	Longitude	PGA₇₅	S_{S-75}	S₁₋₇₅	PGA₁₀	S_{S-10}	S₁₋₁₀
Washington	Kennewick	46.1670	-119.1138	0.1068	0.2356	0.0798	0.0221	0.0460	0.0169
Washington	Yakima	46.6123	-120.5255	0.1367	0.3050	0.1079	0.0367	0.0793	0.0255
Montana	Miles City	46.3645	-105.8862	0.0250	0.0535	0.0173	0.0057	0.0131	0.0040
Tennessee	Chattanooga	35.0335	-85.3130	0.1606	0.2622	0.0658	0.0275	0.0538	0.0129

A.5 Weight of Example Temporary Bridge

Given below in Tables A-3, A-4, and A-5 are the weights of the structural components used in the example spectral reduction in Section 6.

Table A-3: Weight of each span for temporary bridge example

Bridge Span Element	Unit Weight	Total Weight
(12) Hollow Core Slab 3' x 1'9"	0.47 kip/ft	5.46 kip/ft
(2) Barrier Rail	0.45 kip/ft	0.90 kip/ft
2.75" Asphalt Wearing Surface	0.14 kip/ft ³	1.09 kip/ft
0.75" OGFC	0.14 kip/ft ³	0.30 kip/ft
Epoxy Coated Reinforcing Steel	-	0.084 kip/ft
Reinforcing Steel	-	0.13 kip/ft
Total Distributed Weight		7.96 kip/ft
Total Weight		398 kip

Table A-4: Weight of each intermediate bent for temporary bridge example

Bent Element	Unit Weight	Total Weight
40'10" x 3' x 2'6" Cap Beam	0.145 kip/ft ³	44.41 kip
(8) 12' x 16"φ Prestressed Piles	1.59 tons	25.44 kip
Pile Blockout Grout 1 CY	0.145 kip/ft ³	3.92 kip
Additional Steel	-	1.06 kip
Total Weight		74.83 kip

Table A-5: Weight of each end bent for temporary bridge example

Bent Element	Unit Weight	Total Weight
42' x 3' x 2'6" Cap Beam	0.145 kip/ft ³	45.68 kip
(8) 8' x 16"φ Prestressed Piles	1.59 tons	16.96 kip
Pile Blockout Grout 1 CY	0.145 kip/ft ³	3.92 kip
Additional Steel	-	1.20 kip
Concrete for Wings 0.7 CY	0.145 kip/ft ³	2.74 kip
Total Weight		70.50 kip

MCEER Technical Reports

MCEER publishes technical reports on a variety of subjects written by authors funded through MCEER. These reports can be downloaded from the MCEER website at <http://www.buffalo.edu/mceer>. They can also be requested through NTIS, P.O. Box 1425, Springfield, Virginia 22151. NTIS accession numbers are shown in parenthesis, if available.

- NCEER-87-0001 "First-Year Program in Research, Education and Technology Transfer," 3/5/87, (PB88-134275, A04, MF-A01).
- NCEER-87-0002 "Experimental Evaluation of Instantaneous Optimal Algorithms for Structural Control," by R.C. Lin, T.T. Soong and A.M. Reinhorn, 4/20/87, (PB88-134341, A04, MF-A01).
- NCEER-87-0003 "Experimentation Using the Earthquake Simulation Facilities at University at Buffalo," by A.M. Reinhorn and R.L. Ketter, not available.
- NCEER-87-0004 "The System Characteristics and Performance of a Shaking Table," by J.S. Hwang, K.C. Chang and G.C. Lee, 6/1/87, (PB88-134259, A03, MF-A01). This report is available only through NTIS (see address given above).
- NCEER-87-0005 "A Finite Element Formulation for Nonlinear Viscoplastic Material Using a Q Model," by O. Gyebi and G. Dasgupta, 11/2/87, (PB88-213764, A08, MF-A01).
- NCEER-87-0006 "Symbolic Manipulation Program (SMP) - Algebraic Codes for Two and Three Dimensional Finite Element Formulations," by X. Lee and G. Dasgupta, 11/9/87, (PB88-218522, A05, MF-A01).
- NCEER-87-0007 "Instantaneous Optimal Control Laws for Tall Buildings Under Seismic Excitations," by J.N. Yang, A. Akbarpour and P. Ghaemmaghami, 6/10/87, (PB88-134333, A06, MF-A01). This report is only available through NTIS (see address given above).
- NCEER-87-0008 "IDARC: Inelastic Damage Analysis of Reinforced Concrete Frame - Shear-Wall Structures," by Y.J. Park, A.M. Reinhorn and S.K. Kunnath, 7/20/87, (PB88-134325, A09, MF-A01). This report is only available through NTIS (see address given above).
- NCEER-87-0009 "Liquefaction Potential for New York State: A Preliminary Report on Sites in Manhattan and Buffalo," by M. Budhu, V. Vijayakumar, R.F. Giese and L. Baumgras, 8/31/87, (PB88-163704, A03, MF-A01). This report is available only through NTIS (see address given above).
- NCEER-87-0010 "Vertical and Torsional Vibration of Foundations in Inhomogeneous Media," by A.S. Veletsos and K.W. Dotson, 6/1/87, (PB88-134291, A03, MF-A01). This report is only available through NTIS (see address given above).
- NCEER-87-0011 "Seismic Probabilistic Risk Assessment and Seismic Margins Studies for Nuclear Power Plants," by Howard H.M. Hwang, 6/15/87, (PB88-134267, A03, MF-A01). This report is only available through NTIS (see address given above).
- NCEER-87-0012 "Parametric Studies of Frequency Response of Secondary Systems Under Ground-Acceleration Excitations," by Y. Yong and Y.K. Lin, 6/10/87, (PB88-134309, A03, MF-A01). This report is only available through NTIS (see address given above).
- NCEER-87-0013 "Frequency Response of Secondary Systems Under Seismic Excitation," by J.A. HoLung, J. Cai and Y.K. Lin, 7/31/87, (PB88-134317, A05, MF-A01). This report is only available through NTIS (see address given above).
- NCEER-87-0014 "Modelling Earthquake Ground Motions in Seismically Active Regions Using Parametric Time Series Methods," by G.W. Ellis and A.S. Cakmak, 8/25/87, (PB88-134283, A08, MF-A01). This report is only available through NTIS (see address given above).
- NCEER-87-0015 "Detection and Assessment of Seismic Structural Damage," by E. DiPasquale and A.S. Cakmak, 8/25/87, (PB88-163712, A05, MF-A01). This report is only available through NTIS (see address given above).

- NCEER-87-0016 "Pipeline Experiment at Parkfield, California," by J. Isenberg and E. Richardson, 9/15/87, (PB88-163720, A03, MF-A01). This report is available only through NTIS (see address given above).
- NCEER-87-0017 "Digital Simulation of Seismic Ground Motion," by M. Shinozuka, G. Deodatis and T. Harada, 8/31/87, (PB88-155197, A04, MF-A01). This report is available only through NTIS (see address given above).
- NCEER-87-0018 "Practical Considerations for Structural Control: System Uncertainty, System Time Delay and Truncation of Small Control Forces," J.N. Yang and A. Akbarpour, 8/10/87, (PB88-163738, A08, MF-A01). This report is only available through NTIS (see address given above).
- NCEER-87-0019 "Modal Analysis of Nonclassically Damped Structural Systems Using Canonical Transformation," by J.N. Yang, S. Sarkani and F.X. Long, 9/27/87, (PB88-187851, A04, MF-A01).
- NCEER-87-0020 "A Nonstationary Solution in Random Vibration Theory," by J.R. Red-Horse and P.D. Spanos, 11/3/87, (PB88-163746, A03, MF-A01).
- NCEER-87-0021 "Horizontal Impedances for Radially Inhomogeneous Viscoelastic Soil Layers," by A.S. Veletsos and K.W. Dotson, 10/15/87, (PB88-150859, A04, MF-A01).
- NCEER-87-0022 "Seismic Damage Assessment of Reinforced Concrete Members," by Y.S. Chung, C. Meyer and M. Shinozuka, 10/9/87, (PB88-150867, A05, MF-A01). This report is available only through NTIS (see address given above).
- NCEER-87-0023 "Active Structural Control in Civil Engineering," by T.T. Soong, 11/11/87, (PB88-187778, A03, MF-A01).
- NCEER-87-0024 "Vertical and Torsional Impedances for Radially Inhomogeneous Viscoelastic Soil Layers," by K.W. Dotson and A.S. Veletsos, 12/87, (PB88-187786, A03, MF-A01).
- NCEER-87-0025 "Proceedings from the Symposium on Seismic Hazards, Ground Motions, Soil-Liquefaction and Engineering Practice in Eastern North America," October 20-22, 1987, edited by K.H. Jacob, 12/87, (PB88-188115, A23, MF-A01). This report is available only through NTIS (see address given above).
- NCEER-87-0026 "Report on the Whittier-Narrows, California, Earthquake of October 1, 1987," by J. Pantelic and A. Reinhorn, 11/87, (PB88-187752, A03, MF-A01). This report is available only through NTIS (see address given above).
- NCEER-87-0027 "Design of a Modular Program for Transient Nonlinear Analysis of Large 3-D Building Structures," by S. Srivastav and J.F. Abel, 12/30/87, (PB88-187950, A05, MF-A01). This report is only available through NTIS (see address given above).
- NCEER-87-0028 "Second-Year Program in Research, Education and Technology Transfer," 3/8/88, (PB88-219480, A04, MF-A01).
- NCEER-88-0001 "Workshop on Seismic Computer Analysis and Design of Buildings With Interactive Graphics," by W. McGuire, J.F. Abel and C.H. Conley, 1/18/88, (PB88-187760, A03, MF-A01). This report is only available through NTIS (see address given above).
- NCEER-88-0002 "Optimal Control of Nonlinear Flexible Structures," by J.N. Yang, F.X. Long and D. Wong, 1/22/88, (PB88-213772, A06, MF-A01).
- NCEER-88-0003 "Substructuring Techniques in the Time Domain for Primary-Secondary Structural Systems," by G.D. Manolis and G. Juhn, 2/10/88, (PB88-213780, A04, MF-A01).
- NCEER-88-0004 "Iterative Seismic Analysis of Primary-Secondary Systems," by A. Singhal, L.D. Lutes and P.D. Spanos, 2/23/88, (PB88-213798, A04, MF-A01).
- NCEER-88-0005 "Stochastic Finite Element Expansion for Random Media," by P.D. Spanos and R. Ghanem, 3/14/88, (PB88-213806, A03, MF-A01).
- NCEER-88-0006 "Combining Structural Optimization and Structural Control," by F.Y. Cheng and C.P. Pantelides, 1/10/88, (PB88-213814, A05, MF-A01).

- NCEER-88-0007 "Seismic Performance Assessment of Code-Designed Structures," by H.H-M. Hwang, J-W. Jaw and H-J. Shau, 3/20/88, (PB88-219423, A04, MF-A01). This report is only available through NTIS (see address given above).
- NCEER-88-0008 "Reliability Analysis of Code-Designed Structures Under Natural Hazards," by H.H-M. Hwang, H. Ushiba and M. Shinozuka, 2/29/88, (PB88-229471, A07, MF-A01). This report is only available through NTIS (see address given above).
- NCEER-88-0009 "Seismic Fragility Analysis of Shear Wall Structures," by J-W Jaw and H.H-M. Hwang, 4/30/88, (PB89-102867, A04, MF-A01).
- NCEER-88-0010 "Base Isolation of a Multi-Story Building Under a Harmonic Ground Motion - A Comparison of Performances of Various Systems," by F-G Fan, G. Ahmadi and I.G. Tadjbakhsh, 5/18/88, (PB89-122238, A06, MF-A01). This report is only available through NTIS (see address given above).
- NCEER-88-0011 "Seismic Floor Response Spectra for a Combined System by Green's Functions," by F.M. Lavelle, L.A. Bergman and P.D. Spanos, 5/1/88, (PB89-102875, A03, MF-A01).
- NCEER-88-0012 "A New Solution Technique for Randomly Excited Hysteretic Structures," by G.Q. Cai and Y.K. Lin, 5/16/88, (PB89-102883, A03, MF-A01).
- NCEER-88-0013 "A Study of Radiation Damping and Soil-Structure Interaction Effects in the Centrifuge," by K. Weissman, supervised by J.H. Prevost, 5/24/88, (PB89-144703, A06, MF-A01).
- NCEER-88-0014 "Parameter Identification and Implementation of a Kinematic Plasticity Model for Frictional Soils," by J.H. Prevost and D.V. Griffiths, not available.
- NCEER-88-0015 "Two- and Three- Dimensional Dynamic Finite Element Analyses of the Long Valley Dam," by D.V. Griffiths and J.H. Prevost, 6/17/88, (PB89-144711, A04, MF-A01).
- NCEER-88-0016 "Damage Assessment of Reinforced Concrete Structures in Eastern United States," by A.M. Reinhorn, M.J. Seidel, S.K. Kunnath and Y.J. Park, 6/15/88, (PB89-122220, A04, MF-A01). This report is only available through NTIS (see address given above).
- NCEER-88-0017 "Dynamic Compliance of Vertically Loaded Strip Foundations in Multilayered Viscoelastic Soils," by S. Ahmad and A.S.M. Israil, 6/17/88, (PB89-102891, A04, MF-A01).
- NCEER-88-0018 "An Experimental Study of Seismic Structural Response With Added Viscoelastic Dampers," by R.C. Lin, Z. Liang, T.T. Soong and R.H. Zhang, 6/30/88, (PB89-122212, A05, MF-A01). This report is available only through NTIS (see address given above).
- NCEER-88-0019 "Experimental Investigation of Primary - Secondary System Interaction," by G.D. Manolis, G. Juhn and A.M. Reinhorn, 5/27/88, (PB89-122204, A04, MF-A01).
- NCEER-88-0020 "A Response Spectrum Approach For Analysis of Nonclassically Damped Structures," by J.N. Yang, S. Sarkani and F.X. Long, 4/22/88, (PB89-102909, A04, MF-A01).
- NCEER-88-0021 "Seismic Interaction of Structures and Soils: Stochastic Approach," by A.S. Veletsos and A.M. Prasad, 7/21/88, (PB89-122196, A04, MF-A01). This report is only available through NTIS (see address given above).
- NCEER-88-0022 "Identification of the Serviceability Limit State and Detection of Seismic Structural Damage," by E. DiPasquale and A.S. Cakmak, 6/15/88, (PB89-122188, A05, MF-A01). This report is available only through NTIS (see address given above).
- NCEER-88-0023 "Multi-Hazard Risk Analysis: Case of a Simple Offshore Structure," by B.K. Bhartia and E.H. Vanmarcke, 7/21/88, (PB89-145213, A05, MF-A01).

- NCEER-88-0024 "Automated Seismic Design of Reinforced Concrete Buildings," by Y.S. Chung, C. Meyer and M. Shinozuka, 7/5/88, (PB89-122170, A06, MF-A01). This report is available only through NTIS (see address given above).
- NCEER-88-0025 "Experimental Study of Active Control of MDOF Structures Under Seismic Excitations," by L.L. Chung, R.C. Lin, T.T. Soong and A.M. Reinhorn, 7/10/88, (PB89-122600, A04, MF-A01).
- NCEER-88-0026 "Earthquake Simulation Tests of a Low-Rise Metal Structure," by J.S. Hwang, K.C. Chang, G.C. Lee and R.L. Ketter, 8/1/88, (PB89-102917, A04, MF-A01).
- NCEER-88-0027 "Systems Study of Urban Response and Reconstruction Due to Catastrophic Earthquakes," by F. Kozin and H.K. Zhou, 9/22/88, (PB90-162348, A04, MF-A01).
- NCEER-88-0028 "Seismic Fragility Analysis of Plane Frame Structures," by H.H-M. Hwang and Y.K. Low, 7/31/88, (PB89-131445, A06, MF-A01).
- NCEER-88-0029 "Response Analysis of Stochastic Structures," by A. Kardara, C. Bucher and M. Shinozuka, 9/22/88, (PB89-174429, A04, MF-A01).
- NCEER-88-0030 "Nonnormal Accelerations Due to Yielding in a Primary Structure," by D.C.K. Chen and L.D. Lutes, 9/19/88, (PB89-131437, A04, MF-A01).
- NCEER-88-0031 "Design Approaches for Soil-Structure Interaction," by A.S. Veletsos, A.M. Prasad and Y. Tang, 12/30/88, (PB89-174437, A03, MF-A01). This report is available only through NTIS (see address given above).
- NCEER-88-0032 "A Re-evaluation of Design Spectra for Seismic Damage Control," by C.J. Turkstra and A.G. Tallin, 11/7/88, (PB89-145221, A05, MF-A01).
- NCEER-88-0033 "The Behavior and Design of Noncontact Lap Splices Subjected to Repeated Inelastic Tensile Loading," by V.E. Sagan, P. Gergely and R.N. White, 12/8/88, (PB89-163737, A08, MF-A01).
- NCEER-88-0034 "Seismic Response of Pile Foundations," by S.M. Mamoon, P.K. Banerjee and S. Ahmad, 11/1/88, (PB89-145239, A04, MF-A01).
- NCEER-88-0035 "Modeling of R/C Building Structures With Flexible Floor Diaphragms (IDARC2)," by A.M. Reinhorn, S.K. Kunnath and N. Panahshahi, 9/7/88, (PB89-207153, A07, MF-A01).
- NCEER-88-0036 "Solution of the Dam-Reservoir Interaction Problem Using a Combination of FEM, BEM with Particular Integrals, Modal Analysis, and Substructuring," by C-S. Tsai, G.C. Lee and R.L. Ketter, 12/31/88, (PB89-207146, A04, MF-A01).
- NCEER-88-0037 "Optimal Placement of Actuators for Structural Control," by F.Y. Cheng and C.P. Pantelides, 8/15/88, (PB89-162846, A05, MF-A01).
- NCEER-88-0038 "Teflon Bearings in Aseismic Base Isolation: Experimental Studies and Mathematical Modeling," by A. Mokha, M.C. Constantinou and A.M. Reinhorn, 12/5/88, (PB89-218457, A10, MF-A01). This report is available only through NTIS (see address given above).
- NCEER-88-0039 "Seismic Behavior of Flat Slab High-Rise Buildings in the New York City Area," by P. Weidlinger and M. Ettouney, 10/15/88, (PB90-145681, A04, MF-A01).
- NCEER-88-0040 "Evaluation of the Earthquake Resistance of Existing Buildings in New York City," by P. Weidlinger and M. Ettouney, 10/15/88, not available.
- NCEER-88-0041 "Small-Scale Modeling Techniques for Reinforced Concrete Structures Subjected to Seismic Loads," by W. Kim, A. El-Attar and R.N. White, 11/22/88, (PB89-189625, A05, MF-A01).
- NCEER-88-0042 "Modeling Strong Ground Motion from Multiple Event Earthquakes," by G.W. Ellis and A.S. Cakmak, 10/15/88, (PB89-174445, A03, MF-A01).

- NCEER-88-0043 "Nonstationary Models of Seismic Ground Acceleration," by M. Grigoriu, S.E. Ruiz and E. Rosenblueth, 7/15/88, (PB89-189617, A04, MF-A01).
- NCEER-88-0044 "SARCF User's Guide: Seismic Analysis of Reinforced Concrete Frames," by Y.S. Chung, C. Meyer and M. Shinozuka, 11/9/88, (PB89-174452, A08, MF-A01).
- NCEER-88-0045 "First Expert Panel Meeting on Disaster Research and Planning," edited by J. Pantelic and J. Stoyke, 9/15/88, (PB89-174460, A05, MF-A01).
- NCEER-88-0046 "Preliminary Studies of the Effect of Degrading Infill Walls on the Nonlinear Seismic Response of Steel Frames," by C.Z. Chrysostomou, P. Gergely and J.F. Abel, 12/19/88, (PB89-208383, A05, MF-A01).
- NCEER-88-0047 "Reinforced Concrete Frame Component Testing Facility - Design, Construction, Instrumentation and Operation," by S.P. Pessiki, C. Conley, T. Bond, P. Gergely and R.N. White, 12/16/88, (PB89-174478, A04, MF-A01).
- NCEER-89-0001 "Effects of Protective Cushion and Soil Compliancy on the Response of Equipment Within a Seismically Excited Building," by J.A. HoLung, 2/16/89, (PB89-207179, A04, MF-A01).
- NCEER-89-0002 "Statistical Evaluation of Response Modification Factors for Reinforced Concrete Structures," by H.H-M. Hwang and J-W. Jaw, 2/17/89, (PB89-207187, A05, MF-A01).
- NCEER-89-0003 "Hysteretic Columns Under Random Excitation," by G-Q. Cai and Y.K. Lin, 1/9/89, (PB89-196513, A03, MF-A01).
- NCEER-89-0004 "Experimental Study of 'Elephant Foot Bulge' Instability of Thin-Walled Metal Tanks," by Z-H. Jia and R.L. Ketter, 2/22/89, (PB89-207195, A03, MF-A01).
- NCEER-89-0005 "Experiment on Performance of Buried Pipelines Across San Andreas Fault," by J. Isenberg, E. Richardson and T.D. O'Rourke, 3/10/89, (PB89-218440, A04, MF-A01). This report is available only through NTIS (see address given above).
- NCEER-89-0006 "A Knowledge-Based Approach to Structural Design of Earthquake-Resistant Buildings," by M. Subramani, P. Gergely, C.H. Conley, J.F. Abel and A.H. Zaghaw, 1/15/89, (PB89-218465, A06, MF-A01).
- NCEER-89-0007 "Liquefaction Hazards and Their Effects on Buried Pipelines," by T.D. O'Rourke and P.A. Lane, 2/1/89, (PB89-218481, A09, MF-A01).
- NCEER-89-0008 "Fundamentals of System Identification in Structural Dynamics," by H. Imai, C-B. Yun, O. Maruyama and M. Shinozuka, 1/26/89, (PB89-207211, A04, MF-A01).
- NCEER-89-0009 "Effects of the 1985 Michoacan Earthquake on Water Systems and Other Buried Lifelines in Mexico," by A.G. Ayala and M.J. O'Rourke, 3/8/89, (PB89-207229, A06, MF-A01).
- NCEER-89-R010 "NCEER Bibliography of Earthquake Education Materials," by K.E.K. Ross, Second Revision, 9/1/89, (PB90-125352, A05, MF-A01). This report is replaced by NCEER-92-0018.
- NCEER-89-0011 "Inelastic Three-Dimensional Response Analysis of Reinforced Concrete Building Structures (IDARC-3D), Part I - Modeling," by S.K. Kunnath and A.M. Reinhorn, 4/17/89, (PB90-114612, A07, MF-A01). This report is available only through NTIS (see address given above).
- NCEER-89-0012 "Recommended Modifications to ATC-14," by C.D. Poland and J.O. Malley, 4/12/89, (PB90-108648, A15, MF-A01).
- NCEER-89-0013 "Repair and Strengthening of Beam-to-Column Connections Subjected to Earthquake Loading," by M. Corazao and A.J. Durrani, 2/28/89, (PB90-109885, A06, MF-A01).
- NCEER-89-0014 "Program EXKAL2 for Identification of Structural Dynamic Systems," by O. Maruyama, C-B. Yun, M. Hoshiya and M. Shinozuka, 5/19/89, (PB90-109877, A09, MF-A01).

- NCEER-89-0015 "Response of Frames With Bolted Semi-Rigid Connections, Part I - Experimental Study and Analytical Predictions," by P.J. DiCorso, A.M. Reinhorn, J.R. Dickerson, J.B. Radzimirski and W.L. Harper, 6/1/89, not available.
- NCEER-89-0016 "ARMA Monte Carlo Simulation in Probabilistic Structural Analysis," by P.D. Spanos and M.P. Mignolet, 7/10/89, (PB90-109893, A03, MF-A01).
- NCEER-89-P017 "Preliminary Proceedings from the Conference on Disaster Preparedness - The Place of Earthquake Education in Our Schools," Edited by K.E.K. Ross, 6/23/89, (PB90-108606, A03, MF-A01).
- NCEER-89-0017 "Proceedings from the Conference on Disaster Preparedness - The Place of Earthquake Education in Our Schools," Edited by K.E.K. Ross, 12/31/89, (PB90-207895, A012, MF-A02). This report is available only through NTIS (see address given above).
- NCEER-89-0018 "Multidimensional Models of Hysteretic Material Behavior for Vibration Analysis of Shape Memory Energy Absorbing Devices, by E.J. Graesser and F.A. Cozzarelli, 6/7/89, (PB90-164146, A04, MF-A01).
- NCEER-89-0019 "Nonlinear Dynamic Analysis of Three-Dimensional Base Isolated Structures (3D-BASIS)," by S. Nagarajaiah, A.M. Reinhorn and M.C. Constantinou, 8/3/89, (PB90-161936, A06, MF-A01). This report has been replaced by NCEER-93-0011.
- NCEER-89-0020 "Structural Control Considering Time-Rate of Control Forces and Control Rate Constraints," by F.Y. Cheng and C.P. Pantelides, 8/3/89, (PB90-120445, A04, MF-A01).
- NCEER-89-0021 "Subsurface Conditions of Memphis and Shelby County," by K.W. Ng, T-S. Chang and H-H.M. Hwang, 7/26/89, (PB90-120437, A03, MF-A01).
- NCEER-89-0022 "Seismic Wave Propagation Effects on Straight Jointed Buried Pipelines," by K. Elhmadi and M.J. O'Rourke, 8/24/89, (PB90-162322, A10, MF-A02).
- NCEER-89-0023 "Workshop on Serviceability Analysis of Water Delivery Systems," edited by M. Grigoriu, 3/6/89, (PB90-127424, A03, MF-A01).
- NCEER-89-0024 "Shaking Table Study of a 1/5 Scale Steel Frame Composed of Tapered Members," by K.C. Chang, J.S. Hwang and G.C. Lee, 9/18/89, (PB90-160169, A04, MF-A01).
- NCEER-89-0025 "DYNA1D: A Computer Program for Nonlinear Seismic Site Response Analysis - Technical Documentation," by Jean H. Prevost, 9/14/89, (PB90-161944, A07, MF-A01). This report is available only through NTIS (see address given above).
- NCEER-89-0026 "1:4 Scale Model Studies of Active Tendon Systems and Active Mass Dampers for Aseismic Protection," by A.M. Reinhorn, T.T. Soong, R.C. Lin, Y.P. Yang, Y. Fukao, H. Abe and M. Nakai, 9/15/89, (PB90-173246, A10, MF-A02). This report is available only through NTIS (see address given above).
- NCEER-89-0027 "Scattering of Waves by Inclusions in a Nonhomogeneous Elastic Half Space Solved by Boundary Element Methods," by P.K. Hadley, A. Askar and A.S. Cakmak, 6/15/89, (PB90-145699, A07, MF-A01).
- NCEER-89-0028 "Statistical Evaluation of Deflection Amplification Factors for Reinforced Concrete Structures," by H.H.M. Hwang, J-W. Jaw and A.L. Ch'ng, 8/31/89, (PB90-164633, A05, MF-A01).
- NCEER-89-0029 "Bedrock Accelerations in Memphis Area Due to Large New Madrid Earthquakes," by H.H.M. Hwang, C.H.S. Chen and G. Yu, 11/7/89, (PB90-162330, A04, MF-A01).
- NCEER-89-0030 "Seismic Behavior and Response Sensitivity of Secondary Structural Systems," by Y.Q. Chen and T.T. Soong, 10/23/89, (PB90-164658, A08, MF-A01).
- NCEER-89-0031 "Random Vibration and Reliability Analysis of Primary-Secondary Structural Systems," by Y. Ibrahim, M. Grigoriu and T.T. Soong, 11/10/89, (PB90-161951, A04, MF-A01).

- NCEER-89-0032 "Proceedings from the Second U.S. - Japan Workshop on Liquefaction, Large Ground Deformation and Their Effects on Lifelines, September 26-29, 1989," Edited by T.D. O'Rourke and M. Hamada, 12/1/89, (PB90-209388, A22, MF-A03).
- NCEER-89-0033 "Deterministic Model for Seismic Damage Evaluation of Reinforced Concrete Structures," by J.M. Bracci, A.M. Reinhorn, J.B. Mander and S.K. Kunnath, 9/27/89, (PB91-108803, A06, MF-A01).
- NCEER-89-0034 "On the Relation Between Local and Global Damage Indices," by E. DiPasquale and A.S. Cakmak, 8/15/89, (PB90-173865, A05, MF-A01).
- NCEER-89-0035 "Cyclic Undrained Behavior of Nonplastic and Low Plasticity Silts," by A.J. Walker and H.E. Stewart, 7/26/89, (PB90-183518, A10, MF-A01).
- NCEER-89-0036 "Liquefaction Potential of Surficial Deposits in the City of Buffalo, New York," by M. Budhu, R. Giese and L. Baumgrass, 1/17/89, (PB90-208455, A04, MF-A01).
- NCEER-89-0037 "A Deterministic Assessment of Effects of Ground Motion Incoherence," by A.S. Veletsos and Y. Tang, 7/15/89, (PB90-164294, A03, MF-A01).
- NCEER-89-0038 "Workshop on Ground Motion Parameters for Seismic Hazard Mapping," July 17-18, 1989, edited by R.V. Whitman, 12/1/89, (PB90-173923, A04, MF-A01).
- NCEER-89-0039 "Seismic Effects on Elevated Transit Lines of the New York City Transit Authority," by C.J. Costantino, C.A. Miller and E. Heymsfield, 12/26/89, (PB90-207887, A06, MF-A01).
- NCEER-89-0040 "Centrifugal Modeling of Dynamic Soil-Structure Interaction," by K. Weissman, Supervised by J.H. Prevost, 5/10/89, (PB90-207879, A07, MF-A01).
- NCEER-89-0041 "Linearized Identification of Buildings With Cores for Seismic Vulnerability Assessment," by I-K. Ho and A.E. Aktan, 11/1/89, (PB90-251943, A07, MF-A01).
- NCEER-90-0001 "Geotechnical and Lifeline Aspects of the October 17, 1989 Loma Prieta Earthquake in San Francisco," by T.D. O'Rourke, H.E. Stewart, F.T. Blackburn and T.S. Dickerman, 1/90, (PB90-208596, A05, MF-A01).
- NCEER-90-0002 "Nonnormal Secondary Response Due to Yielding in a Primary Structure," by D.C.K. Chen and L.D. Lutes, 2/28/90, (PB90-251976, A07, MF-A01).
- NCEER-90-0003 "Earthquake Education Materials for Grades K-12," by K.E.K. Ross, 4/16/90, (PB91-251984, A05, MF-A05). This report has been replaced by NCEER-92-0018.
- NCEER-90-0004 "Catalog of Strong Motion Stations in Eastern North America," by R.W. Busby, 4/3/90, (PB90-251984, A05, MF-A01).
- NCEER-90-0005 "NCEER Strong-Motion Data Base: A User Manual for the GeoBase Release (Version 1.0 for the Sun3)," by P. Friberg and K. Jacob, 3/31/90 (PB90-258062, A04, MF-A01).
- NCEER-90-0006 "Seismic Hazard Along a Crude Oil Pipeline in the Event of an 1811-1812 Type New Madrid Earthquake," by H.H.M. Hwang and C-H.S. Chen, 4/16/90, (PB90-258054, A04, MF-A01).
- NCEER-90-0007 "Site-Specific Response Spectra for Memphis Sheahan Pumping Station," by H.H.M. Hwang and C.S. Lee, 5/15/90, (PB91-108811, A05, MF-A01).
- NCEER-90-0008 "Pilot Study on Seismic Vulnerability of Crude Oil Transmission Systems," by T. Ariman, R. Dobry, M. Grigoriu, F. Kozin, M. O'Rourke, T. O'Rourke and M. Shinozuka, 5/25/90, (PB91-108837, A06, MF-A01).
- NCEER-90-0009 "A Program to Generate Site Dependent Time Histories: EQGEN," by G.W. Ellis, M. Srinivasan and A.S. Cakmak, 1/30/90, (PB91-108829, A04, MF-A01).
- NCEER-90-0010 "Active Isolation for Seismic Protection of Operating Rooms," by M.E. Talbott, Supervised by M. Shinozuka, 6/8/9, (PB91-110205, A05, MF-A01).

- NCEER-90-0011 "Program LINEARID for Identification of Linear Structural Dynamic Systems," by C-B. Yun and M. Shinozuka, 6/25/90, (PB91-110312, A08, MF-A01).
- NCEER-90-0012 "Two-Dimensional Two-Phase Elasto-Plastic Seismic Response of Earth Dams," by A.N. Yiagos, Supervised by J.H. Prevost, 6/20/90, (PB91-110197, A13, MF-A02).
- NCEER-90-0013 "Secondary Systems in Base-Isolated Structures: Experimental Investigation, Stochastic Response and Stochastic Sensitivity," by G.D. Manolis, G. Juhn, M.C. Constantinou and A.M. Reinhorn, 7/1/90, (PB91-110320, A08, MF-A01).
- NCEER-90-0014 "Seismic Behavior of Lightly-Reinforced Concrete Column and Beam-Column Joint Details," by S.P. Pessiki, C.H. Conley, P. Gergely and R.N. White, 8/22/90, (PB91-108795, A11, MF-A02).
- NCEER-90-0015 "Two Hybrid Control Systems for Building Structures Under Strong Earthquakes," by J.N. Yang and A. Daniellians, 6/29/90, (PB91-125393, A04, MF-A01).
- NCEER-90-0016 "Instantaneous Optimal Control with Acceleration and Velocity Feedback," by J.N. Yang and Z. Li, 6/29/90, (PB91-125401, A03, MF-A01).
- NCEER-90-0017 "Reconnaissance Report on the Northern Iran Earthquake of June 21, 1990," by M. Mehrain, 10/4/90, (PB91-125377, A03, MF-A01).
- NCEER-90-0018 "Evaluation of Liquefaction Potential in Memphis and Shelby County," by T.S. Chang, P.S. Tang, C.S. Lee and H. Hwang, 8/10/90, (PB91-125427, A09, MF-A01).
- NCEER-90-0019 "Experimental and Analytical Study of a Combined Sliding Disc Bearing and Helical Steel Spring Isolation System," by M.C. Constantinou, A.S. Mokha and A.M. Reinhorn, 10/4/90, (PB91-125385, A06, MF-A01). This report is available only through NTIS (see address given above).
- NCEER-90-0020 "Experimental Study and Analytical Prediction of Earthquake Response of a Sliding Isolation System with a Spherical Surface," by A.S. Mokha, M.C. Constantinou and A.M. Reinhorn, 10/11/90, (PB91-125419, A05, MF-A01).
- NCEER-90-0021 "Dynamic Interaction Factors for Floating Pile Groups," by G. Gazetas, K. Fan, A. Kaynia and E. Kausel, 9/10/90, (PB91-170381, A05, MF-A01).
- NCEER-90-0022 "Evaluation of Seismic Damage Indices for Reinforced Concrete Structures," by S. Rodriguez-Gomez and A.S. Cakmak, 9/30/90, PB91-171322, A06, MF-A01).
- NCEER-90-0023 "Study of Site Response at a Selected Memphis Site," by H. Desai, S. Ahmad, E.S. Gazetas and M.R. Oh, 10/11/90, (PB91-196857, A03, MF-A01).
- NCEER-90-0024 "A User's Guide to Strongmo: Version 1.0 of NCEER's Strong-Motion Data Access Tool for PCs and Terminals," by P.A. Friberg and C.A.T. Susch, 11/15/90, (PB91-171272, A03, MF-A01).
- NCEER-90-0025 "A Three-Dimensional Analytical Study of Spatial Variability of Seismic Ground Motions," by L-L. Hong and A.H.-S. Ang, 10/30/90, (PB91-170399, A09, MF-A01).
- NCEER-90-0026 "MUMOID User's Guide - A Program for the Identification of Modal Parameters," by S. Rodriguez-Gomez and E. DiPasquale, 9/30/90, (PB91-171298, A04, MF-A01).
- NCEER-90-0027 "SARCF-II User's Guide - Seismic Analysis of Reinforced Concrete Frames," by S. Rodriguez-Gomez, Y.S. Chung and C. Meyer, 9/30/90, (PB91-171280, A05, MF-A01).
- NCEER-90-0028 "Viscous Dampers: Testing, Modeling and Application in Vibration and Seismic Isolation," by N. Makris and M.C. Constantinou, 12/20/90 (PB91-190561, A06, MF-A01).
- NCEER-90-0029 "Soil Effects on Earthquake Ground Motions in the Memphis Area," by H. Hwang, C.S. Lee, K.W. Ng and T.S. Chang, 8/2/90, (PB91-190751, A05, MF-A01).

- NCEER-91-0001 "Proceedings from the Third Japan-U.S. Workshop on Earthquake Resistant Design of Lifeline Facilities and Countermeasures for Soil Liquefaction, December 17-19, 1990," edited by T.D. O'Rourke and M. Hamada, 2/1/91, (PB91-179259, A99, MF-A04).
- NCEER-91-0002 "Physical Space Solutions of Non-Proportionally Damped Systems," by M. Tong, Z. Liang and G.C. Lee, 1/15/91, (PB91-179242, A04, MF-A01).
- NCEER-91-0003 "Seismic Response of Single Piles and Pile Groups," by K. Fan and G. Gazetas, 1/10/91, (PB92-174994, A04, MF-A01).
- NCEER-91-0004 "Damping of Structures: Part 1 - Theory of Complex Damping," by Z. Liang and G. Lee, 10/10/91, (PB92-197235, A12, MF-A03).
- NCEER-91-0005 "3D-BASIS - Nonlinear Dynamic Analysis of Three Dimensional Base Isolated Structures: Part II," by S. Nagarajaiah, A.M. Reinhorn and M.C. Constantinou, 2/28/91, (PB91-190553, A07, MF-A01). This report has been replaced by NCEER-93-0011.
- NCEER-91-0006 "A Multidimensional Hysteretic Model for Plasticity Deforming Metals in Energy Absorbing Devices," by E.J. Graesser and F.A. Cozzarelli, 4/9/91, (PB92-108364, A04, MF-A01).
- NCEER-91-0007 "A Framework for Customizable Knowledge-Based Expert Systems with an Application to a KBES for Evaluating the Seismic Resistance of Existing Buildings," by E.G. Ibarra-Anaya and S.J. Fennes, 4/9/91, (PB91-210930, A08, MF-A01).
- NCEER-91-0008 "Nonlinear Analysis of Steel Frames with Semi-Rigid Connections Using the Capacity Spectrum Method," by G.G. Deierlein, S-H. Hsieh, Y-J. Shen and J.F. Abel, 7/2/91, (PB92-113828, A05, MF-A01).
- NCEER-91-0009 "Earthquake Education Materials for Grades K-12," by K.E.K. Ross, 4/30/91, (PB91-212142, A06, MF-A01). This report has been replaced by NCEER-92-0018.
- NCEER-91-0010 "Phase Wave Velocities and Displacement Phase Differences in a Harmonically Oscillating Pile," by N. Makris and G. Gazetas, 7/8/91, (PB92-108356, A04, MF-A01).
- NCEER-91-0011 "Dynamic Characteristics of a Full-Size Five-Story Steel Structure and a 2/5 Scale Model," by K.C. Chang, G.C. Yao, G.C. Lee, D.S. Hao and Y.C. Yeh, 7/2/91, (PB93-116648, A06, MF-A02).
- NCEER-91-0012 "Seismic Response of a 2/5 Scale Steel Structure with Added Viscoelastic Dampers," by K.C. Chang, T.T. Soong, S-T. Oh and M.L. Lai, 5/17/91, (PB92-110816, A05, MF-A01).
- NCEER-91-0013 "Earthquake Response of Retaining Walls; Full-Scale Testing and Computational Modeling," by S. Alampalli and A-W.M. Elgamal, 6/20/91, not available.
- NCEER-91-0014 "3D-BASIS-M: Nonlinear Dynamic Analysis of Multiple Building Base Isolated Structures," by P.C. Tsopelas, S. Nagarajaiah, M.C. Constantinou and A.M. Reinhorn, 5/28/91, (PB92-113885, A09, MF-A02).
- NCEER-91-0015 "Evaluation of SEAOC Design Requirements for Sliding Isolated Structures," by D. Theodossiou and M.C. Constantinou, 6/10/91, (PB92-114602, A11, MF-A03).
- NCEER-91-0016 "Closed-Loop Modal Testing of a 27-Story Reinforced Concrete Flat Plate-Core Building," by H.R. Somaprasad, T. Toksoy, H. Yoshiyuki and A.E. Aktan, 7/15/91, (PB92-129980, A07, MF-A02).
- NCEER-91-0017 "Shake Table Test of a 1/6 Scale Two-Story Lightly Reinforced Concrete Building," by A.G. El-Attar, R.N. White and P. Gergely, 2/28/91, (PB92-222447, A06, MF-A02).
- NCEER-91-0018 "Shake Table Test of a 1/8 Scale Three-Story Lightly Reinforced Concrete Building," by A.G. El-Attar, R.N. White and P. Gergely, 2/28/91, (PB93-116630, A08, MF-A02).
- NCEER-91-0019 "Transfer Functions for Rigid Rectangular Foundations," by A.S. Veletsos, A.M. Prasad and W.H. Wu, 7/31/91, not available.

- NCEER-91-0020 "Hybrid Control of Seismic-Excited Nonlinear and Inelastic Structural Systems," by J.N. Yang, Z. Li and A. Daniellians, 8/1/91, (PB92-143171, A06, MF-A02).
- NCEER-91-0021 "The NCEER-91 Earthquake Catalog: Improved Intensity-Based Magnitudes and Recurrence Relations for U.S. Earthquakes East of New Madrid," by L. Seeber and J.G. Armbruster, 8/28/91, (PB92-176742, A06, MF-A02).
- NCEER-91-0022 "Proceedings from the Implementation of Earthquake Planning and Education in Schools: The Need for Change - The Roles of the Changemakers," by K.E.K. Ross and F. Winslow, 7/23/91, (PB92-129998, A12, MF-A03).
- NCEER-91-0023 "A Study of Reliability-Based Criteria for Seismic Design of Reinforced Concrete Frame Buildings," by H.H.M. Hwang and H-M. Hsu, 8/10/91, (PB92-140235, A09, MF-A02).
- NCEER-91-0024 "Experimental Verification of a Number of Structural System Identification Algorithms," by R.G. Ghanem, H. Gavin and M. Shinozuka, 9/18/91, (PB92-176577, A18, MF-A04).
- NCEER-91-0025 "Probabilistic Evaluation of Liquefaction Potential," by H.H.M. Hwang and C.S. Lee," 11/25/91, (PB92-143429, A05, MF-A01).
- NCEER-91-0026 "Instantaneous Optimal Control for Linear, Nonlinear and Hysteretic Structures - Stable Controllers," by J.N. Yang and Z. Li, 11/15/91, (PB92-163807, A04, MF-A01).
- NCEER-91-0027 "Experimental and Theoretical Study of a Sliding Isolation System for Bridges," by M.C. Constantinou, A. Kartoum, A.M. Reinhorn and P. Bradford, 11/15/91, (PB92-176973, A10, MF-A03).
- NCEER-92-0001 "Case Studies of Liquefaction and Lifeline Performance During Past Earthquakes, Volume 1: Japanese Case Studies," Edited by M. Hamada and T. O'Rourke, 2/17/92, (PB92-197243, A18, MF-A04).
- NCEER-92-0002 "Case Studies of Liquefaction and Lifeline Performance During Past Earthquakes, Volume 2: United States Case Studies," Edited by T. O'Rourke and M. Hamada, 2/17/92, (PB92-197250, A20, MF-A04).
- NCEER-92-0003 "Issues in Earthquake Education," Edited by K. Ross, 2/3/92, (PB92-222389, A07, MF-A02).
- NCEER-92-0004 "Proceedings from the First U.S. - Japan Workshop on Earthquake Protective Systems for Bridges," Edited by I.G. Buckle, 2/4/92, (PB94-142239, A99, MF-A06).
- NCEER-92-0005 "Seismic Ground Motion from a Haskell-Type Source in a Multiple-Layered Half-Space," A.P. Theoharis, G. Deodatis and M. Shinozuka, 1/2/92, not available.
- NCEER-92-0006 "Proceedings from the Site Effects Workshop," Edited by R. Whitman, 2/29/92, (PB92-197201, A04, MF-A01).
- NCEER-92-0007 "Engineering Evaluation of Permanent Ground Deformations Due to Seismically-Induced Liquefaction," by M.H. Baziar, R. Dobry and A-W.M. Elgamal, 3/24/92, (PB92-222421, A13, MF-A03).
- NCEER-92-0008 "A Procedure for the Seismic Evaluation of Buildings in the Central and Eastern United States," by C.D. Poland and J.O. Malley, 4/2/92, (PB92-222439, A20, MF-A04).
- NCEER-92-0009 "Experimental and Analytical Study of a Hybrid Isolation System Using Friction Controllable Sliding Bearings," by M.Q. Feng, S. Fujii and M. Shinozuka, 5/15/92, (PB93-150282, A06, MF-A02).
- NCEER-92-0010 "Seismic Resistance of Slab-Column Connections in Existing Non-Ductile Flat-Plate Buildings," by A.J. Durrani and Y. Du, 5/18/92, (PB93-116812, A06, MF-A02).
- NCEER-92-0011 "The Hysteretic and Dynamic Behavior of Brick Masonry Walls Upgraded by Ferrocement Coatings Under Cyclic Loading and Strong Simulated Ground Motion," by H. Lee and S.P. Prawel, 5/11/92, not available.
- NCEER-92-0012 "Study of Wire Rope Systems for Seismic Protection of Equipment in Buildings," by G.F. Demetriades, M.C. Constantinou and A.M. Reinhorn, 5/20/92, (PB93-116655, A08, MF-A02).

- NCEER-92-0013 "Shape Memory Structural Dampers: Material Properties, Design and Seismic Testing," by P.R. Witting and F.A. Cozzarelli, 5/26/92, (PB93-116663, A05, MF-A01).
- NCEER-92-0014 "Longitudinal Permanent Ground Deformation Effects on Buried Continuous Pipelines," by M.J. O'Rourke, and C. Nordberg, 6/15/92, (PB93-116671, A08, MF-A02).
- NCEER-92-0015 "A Simulation Method for Stationary Gaussian Random Functions Based on the Sampling Theorem," by M. Grigoriu and S. Balopoulou, 6/11/92, (PB93-127496, A05, MF-A01).
- NCEER-92-0016 "Gravity-Load-Designed Reinforced Concrete Buildings: Seismic Evaluation of Existing Construction and Detailing Strategies for Improved Seismic Resistance," by G.W. Hoffmann, S.K. Kunnath, A.M. Reinhorn and J.B. Mander, 7/15/92, (PB94-142007, A08, MF-A02).
- NCEER-92-0017 "Observations on Water System and Pipeline Performance in the Limón Area of Costa Rica Due to the April 22, 1991 Earthquake," by M. O'Rourke and D. Ballantyne, 6/30/92, (PB93-126811, A06, MF-A02).
- NCEER-92-0018 "Fourth Edition of Earthquake Education Materials for Grades K-12," Edited by K.E.K. Ross, 8/10/92, (PB93-114023, A07, MF-A02).
- NCEER-92-0019 "Proceedings from the Fourth Japan-U.S. Workshop on Earthquake Resistant Design of Lifeline Facilities and Countermeasures for Soil Liquefaction," Edited by M. Hamada and T.D. O'Rourke, 8/12/92, (PB93-163939, A99, MF-E11).
- NCEER-92-0020 "Active Bracing System: A Full Scale Implementation of Active Control," by A.M. Reinhorn, T.T. Soong, R.C. Lin, M.A. Riley, Y.P. Wang, S. Aizawa and M. Higashino, 8/14/92, (PB93-127512, A06, MF-A02).
- NCEER-92-0021 "Empirical Analysis of Horizontal Ground Displacement Generated by Liquefaction-Induced Lateral Spreads," by S.F. Bartlett and T.L. Youd, 8/17/92, (PB93-188241, A06, MF-A02).
- NCEER-92-0022 "IDARC Version 3.0: Inelastic Damage Analysis of Reinforced Concrete Structures," by S.K. Kunnath, A.M. Reinhorn and R.F. Lobo, 8/31/92, (PB93-227502, A07, MF-A02).
- NCEER-92-0023 "A Semi-Empirical Analysis of Strong-Motion Peaks in Terms of Seismic Source, Propagation Path and Local Site Conditions, by M. Kamiyama, M.J. O'Rourke and R. Flores-Berrones, 9/9/92, (PB93-150266, A08, MF-A02).
- NCEER-92-0024 "Seismic Behavior of Reinforced Concrete Frame Structures with Nonductile Details, Part I: Summary of Experimental Findings of Full Scale Beam-Column Joint Tests," by A. Beres, R.N. White and P. Gergely, 9/30/92, (PB93-227783, A05, MF-A01).
- NCEER-92-0025 "Experimental Results of Repaired and Retrofitted Beam-Column Joint Tests in Lightly Reinforced Concrete Frame Buildings," by A. Beres, S. El-Borgi, R.N. White and P. Gergely, 10/29/92, (PB93-227791, A05, MF-A01).
- NCEER-92-0026 "A Generalization of Optimal Control Theory: Linear and Nonlinear Structures," by J.N. Yang, Z. Li and S. Vongchavalitkul, 11/2/92, (PB93-188621, A05, MF-A01).
- NCEER-92-0027 "Seismic Resistance of Reinforced Concrete Frame Structures Designed Only for Gravity Loads: Part I - Design and Properties of a One-Third Scale Model Structure," by J.M. Bracci, A.M. Reinhorn and J.B. Mander, 12/1/92, (PB94-104502, A08, MF-A02).
- NCEER-92-0028 "Seismic Resistance of Reinforced Concrete Frame Structures Designed Only for Gravity Loads: Part II - Experimental Performance of Subassemblages," by L.E. Aycaardi, J.B. Mander and A.M. Reinhorn, 12/1/92, (PB94-104510, A08, MF-A02).
- NCEER-92-0029 "Seismic Resistance of Reinforced Concrete Frame Structures Designed Only for Gravity Loads: Part III - Experimental Performance and Analytical Study of a Structural Model," by J.M. Bracci, A.M. Reinhorn and J.B. Mander, 12/1/92, (PB93-227528, A09, MF-A01).

- NCEER-92-0030 "Evaluation of Seismic Retrofit of Reinforced Concrete Frame Structures: Part I - Experimental Performance of Retrofitted Subassemblages," by D. Choudhuri, J.B. Mander and A.M. Reinhorn, 12/8/92, (PB93-198307, A07, MF-A02).
- NCEER-92-0031 "Evaluation of Seismic Retrofit of Reinforced Concrete Frame Structures: Part II - Experimental Performance and Analytical Study of a Retrofitted Structural Model," by J.M. Bracci, A.M. Reinhorn and J.B. Mander, 12/8/92, (PB93-198315, A09, MF-A03).
- NCEER-92-0032 "Experimental and Analytical Investigation of Seismic Response of Structures with Supplemental Fluid Viscous Dampers," by M.C. Constantinou and M.D. Symans, 12/21/92, (PB93-191435, A10, MF-A03). This report is available only through NTIS (see address given above).
- NCEER-92-0033 "Reconnaissance Report on the Cairo, Egypt Earthquake of October 12, 1992," by M. Khater, 12/23/92, (PB93-188621, A03, MF-A01).
- NCEER-92-0034 "Low-Level Dynamic Characteristics of Four Tall Flat-Plate Buildings in New York City," by H. Gavin, S. Yuan, J. Grossman, E. Pekelis and K. Jacob, 12/28/92, (PB93-188217, A07, MF-A02).
- NCEER-93-0001 "An Experimental Study on the Seismic Performance of Brick-Infilled Steel Frames With and Without Retrofit," by J.B. Mander, B. Nair, K. Wojtkowski and J. Ma, 1/29/93, (PB93-227510, A07, MF-A02).
- NCEER-93-0002 "Social Accounting for Disaster Preparedness and Recovery Planning," by S. Cole, E. Pantoja and V. Razak, 2/22/93, (PB94-142114, A12, MF-A03).
- NCEER-93-0003 "Assessment of 1991 NEHRP Provisions for Nonstructural Components and Recommended Revisions," by T.T. Soong, G. Chen, Z. Wu, R-H. Zhang and M. Grigoriu, 3/1/93, (PB93-188639, A06, MF-A02).
- NCEER-93-0004 "Evaluation of Static and Response Spectrum Analysis Procedures of SEAOC/UBC for Seismic Isolated Structures," by C.W. Winters and M.C. Constantinou, 3/23/93, (PB93-198299, A10, MF-A03).
- NCEER-93-0005 "Earthquakes in the Northeast - Are We Ignoring the Hazard? A Workshop on Earthquake Science and Safety for Educators," edited by K.E.K. Ross, 4/2/93, (PB94-103066, A09, MF-A02).
- NCEER-93-0006 "Inelastic Response of Reinforced Concrete Structures with Viscoelastic Braces," by R.F. Lobo, J.M. Bracci, K.L. Shen, A.M. Reinhorn and T.T. Soong, 4/5/93, (PB93-227486, A05, MF-A02).
- NCEER-93-0007 "Seismic Testing of Installation Methods for Computers and Data Processing Equipment," by K. Kosar, T.T. Soong, K.L. Shen, J.A. HoLung and Y.K. Lin, 4/12/93, (PB93-198299, A07, MF-A02).
- NCEER-93-0008 "Retrofit of Reinforced Concrete Frames Using Added Dampers," by A. Reinhorn, M. Constantinou and C. Li, not available.
- NCEER-93-0009 "Seismic Behavior and Design Guidelines for Steel Frame Structures with Added Viscoelastic Dampers," by K.C. Chang, M.L. Lai, T.T. Soong, D.S. Hao and Y.C. Yeh, 5/1/93, (PB94-141959, A07, MF-A02).
- NCEER-93-0010 "Seismic Performance of Shear-Critical Reinforced Concrete Bridge Piers," by J.B. Mander, S.M. Waheed, M.T.A. Chaudhary and S.S. Chen, 5/12/93, (PB93-227494, A08, MF-A02).
- NCEER-93-0011 "3D-BASIS-TABS: Computer Program for Nonlinear Dynamic Analysis of Three Dimensional Base Isolated Structures," by S. Nagarajaiah, C. Li, A.M. Reinhorn and M.C. Constantinou, 8/2/93, (PB94-141819, A09, MF-A02).
- NCEER-93-0012 "Effects of Hydrocarbon Spills from an Oil Pipeline Break on Ground Water," by O.J. Helweg and H.H.M. Hwang, 8/3/93, (PB94-141942, A06, MF-A02).
- NCEER-93-0013 "Simplified Procedures for Seismic Design of Nonstructural Components and Assessment of Current Code Provisions," by M.P. Singh, L.E. Suarez, E.E. Matheu and G.O. Maldonado, 8/4/93, (PB94-141827, A09, MF-A02).
- NCEER-93-0014 "An Energy Approach to Seismic Analysis and Design of Secondary Systems," by G. Chen and T.T. Soong, 8/6/93, (PB94-142767, A11, MF-A03).

- NCEER-93-0015 "Proceedings from School Sites: Becoming Prepared for Earthquakes - Commemorating the Third Anniversary of the Loma Prieta Earthquake," Edited by F.E. Winslow and K.E.K. Ross, 8/16/93, (PB94-154275, A16, MF-A02).
- NCEER-93-0016 "Reconnaissance Report of Damage to Historic Monuments in Cairo, Egypt Following the October 12, 1992 Dahshur Earthquake," by D. Sykora, D. Look, G. Croci, E. Karaesmen and E. Karaesmen, 8/19/93, (PB94-142221, A08, MF-A02).
- NCEER-93-0017 "The Island of Guam Earthquake of August 8, 1993," by S.W. Swan and S.K. Harris, 9/30/93, (PB94-141843, A04, MF-A01).
- NCEER-93-0018 "Engineering Aspects of the October 12, 1992 Egyptian Earthquake," by A.W. Elgamal, M. Amer, K. Adalier and A. Abul-Fadl, 10/7/93, (PB94-141983, A05, MF-A01).
- NCEER-93-0019 "Development of an Earthquake Motion Simulator and its Application in Dynamic Centrifuge Testing," by I. Krstelj, Supervised by J.H. Prevost, 10/23/93, (PB94-181773, A-10, MF-A03).
- NCEER-93-0020 "NCEER-Taisei Corporation Research Program on Sliding Seismic Isolation Systems for Bridges: Experimental and Analytical Study of a Friction Pendulum System (FPS)," by M.C. Constantinou, P. Tsopelas, Y-S. Kim and S. Okamoto, 11/1/93, (PB94-142775, A08, MF-A02).
- NCEER-93-0021 "Finite Element Modeling of Elastomeric Seismic Isolation Bearings," by L.J. Billings, Supervised by R. Shepherd, 11/8/93, not available.
- NCEER-93-0022 "Seismic Vulnerability of Equipment in Critical Facilities: Life-Safety and Operational Consequences," by K. Porter, G.S. Johnson, M.M. Zadeh, C. Scawthorn and S. Eder, 11/24/93, (PB94-181765, A16, MF-A03).
- NCEER-93-0023 "Hokkaido Nansei-oki, Japan Earthquake of July 12, 1993, by P.I. Yanev and C.R. Scawthorn, 12/23/93, (PB94-181500, A07, MF-A01).
- NCEER-94-0001 "An Evaluation of Seismic Serviceability of Water Supply Networks with Application to the San Francisco Auxiliary Water Supply System," by I. Markov, Supervised by M. Grigoriu and T. O'Rourke, 1/21/94, (PB94-204013, A07, MF-A02).
- NCEER-94-0002 "NCEER-Taisei Corporation Research Program on Sliding Seismic Isolation Systems for Bridges: Experimental and Analytical Study of Systems Consisting of Sliding Bearings, Rubber Restoring Force Devices and Fluid Dampers," Volumes I and II, by P. Tsopelas, S. Okamoto, M.C. Constantinou, D. Ozaki and S. Fujii, 2/4/94, (PB94-181740, A09, MF-A02 and PB94-181757, A12, MF-A03).
- NCEER-94-0003 "A Markov Model for Local and Global Damage Indices in Seismic Analysis," by S. Rahman and M. Grigoriu, 2/18/94, (PB94-206000, A12, MF-A03).
- NCEER-94-0004 "Proceedings from the NCEER Workshop on Seismic Response of Masonry Infills," edited by D.P. Abrams, 3/1/94, (PB94-180783, A07, MF-A02).
- NCEER-94-0005 "The Northridge, California Earthquake of January 17, 1994: General Reconnaissance Report," edited by J.D. Goltz, 3/11/94, (PB94-193943, A10, MF-A03).
- NCEER-94-0006 "Seismic Energy Based Fatigue Damage Analysis of Bridge Columns: Part I - Evaluation of Seismic Capacity," by G.A. Chang and J.B. Mander, 3/14/94, (PB94-219185, A11, MF-A03).
- NCEER-94-0007 "Seismic Isolation of Multi-Story Frame Structures Using Spherical Sliding Isolation Systems," by T.M. Al-Hussaini, V.A. Zayas and M.C. Constantinou, 3/17/94, (PB94-193745, A09, MF-A02).
- NCEER-94-0008 "The Northridge, California Earthquake of January 17, 1994: Performance of Highway Bridges," edited by I.G. Buckle, 3/24/94, (PB94-193851, A06, MF-A02).
- NCEER-94-0009 "Proceedings of the Third U.S.-Japan Workshop on Earthquake Protective Systems for Bridges," edited by I.G. Buckle and I. Friedland, 3/31/94, (PB94-195815, A99, MF-A06).

- NCEER-94-0010 "3D-BASIS-ME: Computer Program for Nonlinear Dynamic Analysis of Seismically Isolated Single and Multiple Structures and Liquid Storage Tanks," by P.C. Tsopelas, M.C. Constantinou and A.M. Reinhorn, 4/12/94, (PB94-204922, A09, MF-A02).
- NCEER-94-0011 "The Northridge, California Earthquake of January 17, 1994: Performance of Gas Transmission Pipelines," by T.D. O'Rourke and M.C. Palmer, 5/16/94, (PB94-204989, A05, MF-A01).
- NCEER-94-0012 "Feasibility Study of Replacement Procedures and Earthquake Performance Related to Gas Transmission Pipelines," by T.D. O'Rourke and M.C. Palmer, 5/25/94, (PB94-206638, A09, MF-A02).
- NCEER-94-0013 "Seismic Energy Based Fatigue Damage Analysis of Bridge Columns: Part II - Evaluation of Seismic Demand," by G.A. Chang and J.B. Mander, 6/1/94, (PB95-18106, A08, MF-A02).
- NCEER-94-0014 "NCEER-Taisei Corporation Research Program on Sliding Seismic Isolation Systems for Bridges: Experimental and Analytical Study of a System Consisting of Sliding Bearings and Fluid Restoring Force/Damping Devices," by P. Tsopelas and M.C. Constantinou, 6/13/94, (PB94-219144, A10, MF-A03).
- NCEER-94-0015 "Generation of Hazard-Consistent Fragility Curves for Seismic Loss Estimation Studies," by H. Hwang and J-R. Huo, 6/14/94, (PB95-181996, A09, MF-A02).
- NCEER-94-0016 "Seismic Study of Building Frames with Added Energy-Absorbing Devices," by W.S. Pong, C.S. Tsai and G.C. Lee, 6/20/94, (PB94-219136, A10, A03).
- NCEER-94-0017 "Sliding Mode Control for Seismic-Excited Linear and Nonlinear Civil Engineering Structures," by J. Yang, J. Wu, A. Agrawal and Z. Li, 6/21/94, (PB95-138483, A06, MF-A02).
- NCEER-94-0018 "3D-BASIS-TABS Version 2.0: Computer Program for Nonlinear Dynamic Analysis of Three Dimensional Base Isolated Structures," by A.M. Reinhorn, S. Nagarajaiah, M.C. Constantinou, P. Tsopelas and R. Li, 6/22/94, (PB95-182176, A08, MF-A02).
- NCEER-94-0019 "Proceedings of the International Workshop on Civil Infrastructure Systems: Application of Intelligent Systems and Advanced Materials on Bridge Systems," Edited by G.C. Lee and K.C. Chang, 7/18/94, (PB95-252474, A20, MF-A04).
- NCEER-94-0020 "Study of Seismic Isolation Systems for Computer Floors," by V. Lambrou and M.C. Constantinou, 7/19/94, (PB95-138533, A10, MF-A03).
- NCEER-94-0021 "Proceedings of the U.S.-Italian Workshop on Guidelines for Seismic Evaluation and Rehabilitation of Unreinforced Masonry Buildings," Edited by D.P. Abrams and G.M. Calvi, 7/20/94, (PB95-138749, A13, MF-A03).
- NCEER-94-0022 "NCEER-Taisei Corporation Research Program on Sliding Seismic Isolation Systems for Bridges: Experimental and Analytical Study of a System Consisting of Lubricated PTFE Sliding Bearings and Mild Steel Dampers," by P. Tsopelas and M.C. Constantinou, 7/22/94, (PB95-182184, A08, MF-A02).
- NCEER-94-0023 "Development of Reliability-Based Design Criteria for Buildings Under Seismic Load," by Y.K. Wen, H. Hwang and M. Shinozuka, 8/1/94, (PB95-211934, A08, MF-A02).
- NCEER-94-0024 "Experimental Verification of Acceleration Feedback Control Strategies for an Active Tendon System," by S.J. Dyke, B.F. Spencer, Jr., P. Quast, M.K. Sain, D.C. Kaspari, Jr. and T.T. Soong, 8/29/94, (PB95-212320, A05, MF-A01).
- NCEER-94-0025 "Seismic Retrofitting Manual for Highway Bridges," Edited by I.G. Buckle and I.F. Friedland, published by the Federal Highway Administration (PB95-212676, A15, MF-A03).
- NCEER-94-0026 "Proceedings from the Fifth U.S.-Japan Workshop on Earthquake Resistant Design of Lifeline Facilities and Countermeasures Against Soil Liquefaction," Edited by T.D. O'Rourke and M. Hamada, 11/7/94, (PB95-220802, A99, MF-E08).

- NCEER-95-0001 “Experimental and Analytical Investigation of Seismic Retrofit of Structures with Supplemental Damping: Part 1 - Fluid Viscous Damping Devices,” by A.M. Reinhorn, C. Li and M.C. Constantinou, 1/3/95, (PB95-266599, A09, MF-A02).
- NCEER-95-0002 “Experimental and Analytical Study of Low-Cycle Fatigue Behavior of Semi-Rigid Top-And-Seat Angle Connections,” by G. Pekcan, J.B. Mander and S.S. Chen, 1/5/95, (PB95-220042, A07, MF-A02).
- NCEER-95-0003 “NCEER-ATC Joint Study on Fragility of Buildings,” by T. Anagnos, C. Rojahn and A.S. Kiremidjian, 1/20/95, (PB95-220026, A06, MF-A02).
- NCEER-95-0004 “Nonlinear Control Algorithms for Peak Response Reduction,” by Z. Wu, T.T. Soong, V. Gattulli and R.C. Lin, 2/16/95, (PB95-220349, A05, MF-A01).
- NCEER-95-0005 “Pipeline Replacement Feasibility Study: A Methodology for Minimizing Seismic and Corrosion Risks to Underground Natural Gas Pipelines,” by R.T. Eguchi, H.A. Seligson and D.G. Honegger, 3/2/95, (PB95-252326, A06, MF-A02).
- NCEER-95-0006 “Evaluation of Seismic Performance of an 11-Story Frame Building During the 1994 Northridge Earthquake,” by F. Naeim, R. DiSulio, K. Benuska, A. Reinhorn and C. Li, not available.
- NCEER-95-0007 “Prioritization of Bridges for Seismic Retrofitting,” by N. Basöz and A.S. Kiremidjian, 4/24/95, (PB95-252300, A08, MF-A02).
- NCEER-95-0008 “Method for Developing Motion Damage Relationships for Reinforced Concrete Frames,” by A. Singhal and A.S. Kiremidjian, 5/11/95, (PB95-266607, A06, MF-A02).
- NCEER-95-0009 “Experimental and Analytical Investigation of Seismic Retrofit of Structures with Supplemental Damping: Part II - Friction Devices,” by C. Li and A.M. Reinhorn, 7/6/95, (PB96-128087, A11, MF-A03).
- NCEER-95-0010 “Experimental Performance and Analytical Study of a Non-Ductile Reinforced Concrete Frame Structure Retrofitted with Elastomeric Spring Dampers,” by G. Pekcan, J.B. Mander and S.S. Chen, 7/14/95, (PB96-137161, A08, MF-A02).
- NCEER-95-0011 “Development and Experimental Study of Semi-Active Fluid Damping Devices for Seismic Protection of Structures,” by M.D. Symans and M.C. Constantinou, 8/3/95, (PB96-136940, A23, MF-A04).
- NCEER-95-0012 “Real-Time Structural Parameter Modification (RSPM): Development of Innervated Structures,” by Z. Liang, M. Tong and G.C. Lee, 4/11/95, (PB96-137153, A06, MF-A01).
- NCEER-95-0013 “Experimental and Analytical Investigation of Seismic Retrofit of Structures with Supplemental Damping: Part III - Viscous Damping Walls,” by A.M. Reinhorn and C. Li, 10/1/95, (PB96-176409, A11, MF-A03).
- NCEER-95-0014 “Seismic Fragility Analysis of Equipment and Structures in a Memphis Electric Substation,” by J-R. Huo and H.H.M. Hwang, 8/10/95, (PB96-128087, A09, MF-A02).
- NCEER-95-0015 “The Hanshin-Awaji Earthquake of January 17, 1995: Performance of Lifelines,” Edited by M. Shinozuka, 11/3/95, (PB96-176383, A15, MF-A03).
- NCEER-95-0016 “Highway Culvert Performance During Earthquakes,” by T.L. Youd and C.J. Beckman, available as NCEER-96-0015.
- NCEER-95-0017 “The Hanshin-Awaji Earthquake of January 17, 1995: Performance of Highway Bridges,” Edited by I.G. Buckle, 12/1/95, not available.
- NCEER-95-0018 “Modeling of Masonry Infill Panels for Structural Analysis,” by A.M. Reinhorn, A. Madan, R.E. Valles, Y. Reichmann and J.B. Mander, 12/8/95, (PB97-110886, MF-A01, A06).
- NCEER-95-0019 “Optimal Polynomial Control for Linear and Nonlinear Structures,” by A.K. Agrawal and J.N. Yang, 12/11/95, (PB96-168737, A07, MF-A02).

- NCEER-95-0020 "Retrofit of Non-Ductile Reinforced Concrete Frames Using Friction Dampers," by R.S. Rao, P. Gergely and R.N. White, 12/22/95, (PB97-133508, A10, MF-A02).
- NCEER-95-0021 "Parametric Results for Seismic Response of Pile-Supported Bridge Bents," by G. Mylonakis, A. Nikolaou and G. Gazetas, 12/22/95, (PB97-100242, A12, MF-A03).
- NCEER-95-0022 "Kinematic Bending Moments in Seismically Stressed Piles," by A. Nikolaou, G. Mylonakis and G. Gazetas, 12/23/95, (PB97-113914, MF-A03, A13).
- NCEER-96-0001 "Dynamic Response of Unreinforced Masonry Buildings with Flexible Diaphragms," by A.C. Costley and D.P. Abrams, 10/10/96, (PB97-133573, MF-A03, A15).
- NCEER-96-0002 "State of the Art Review: Foundations and Retaining Structures," by I. Po Lam, not available.
- NCEER-96-0003 "Ductility of Rectangular Reinforced Concrete Bridge Columns with Moderate Confinement," by N. Wehbe, M. Saiidi, D. Sanders and B. Douglas, 11/7/96, (PB97-133557, A06, MF-A02).
- NCEER-96-0004 "Proceedings of the Long-Span Bridge Seismic Research Workshop," edited by I.G. Buckle and I.M. Friedland, not available.
- NCEER-96-0005 "Establish Representative Pier Types for Comprehensive Study: Eastern United States," by J. Kulicki and Z. Prucz, 5/28/96, (PB98-119217, A07, MF-A02).
- NCEER-96-0006 "Establish Representative Pier Types for Comprehensive Study: Western United States," by R. Imbsen, R.A. Schamber and T.A. Osterkamp, 5/28/96, (PB98-118607, A07, MF-A02).
- NCEER-96-0007 "Nonlinear Control Techniques for Dynamical Systems with Uncertain Parameters," by R.G. Ghanem and M.I. Bujakov, 5/27/96, (PB97-100259, A17, MF-A03).
- NCEER-96-0008 "Seismic Evaluation of a 30-Year Old Non-Ductile Highway Bridge Pier and Its Retrofit," by J.B. Mander, B. Mahmoodzadegan, S. Bhadra and S.S. Chen, 5/31/96, (PB97-110902, MF-A03, A10).
- NCEER-96-0009 "Seismic Performance of a Model Reinforced Concrete Bridge Pier Before and After Retrofit," by J.B. Mander, J.H. Kim and C.A. Ligozio, 5/31/96, (PB97-110910, MF-A02, A10).
- NCEER-96-0010 "IDARC2D Version 4.0: A Computer Program for the Inelastic Damage Analysis of Buildings," by R.E. Valles, A.M. Reinhorn, S.K. Kunnath, C. Li and A. Madan, 6/3/96, (PB97-100234, A17, MF-A03).
- NCEER-96-0011 "Estimation of the Economic Impact of Multiple Lifeline Disruption: Memphis Light, Gas and Water Division Case Study," by S.E. Chang, H.A. Seligson and R.T. Eguchi, 8/16/96, (PB97-133490, A11, MF-A03).
- NCEER-96-0012 "Proceedings from the Sixth Japan-U.S. Workshop on Earthquake Resistant Design of Lifeline Facilities and Countermeasures Against Soil Liquefaction, Edited by M. Hamada and T. O'Rourke, 9/11/96, (PB97-133581, A99, MF-A06).
- NCEER-96-0013 "Chemical Hazards, Mitigation and Preparedness in Areas of High Seismic Risk: A Methodology for Estimating the Risk of Post-Earthquake Hazardous Materials Release," by H.A. Seligson, R.T. Eguchi, K.J. Tierney and K. Richmond, 11/7/96, (PB97-133565, MF-A02, A08).
- NCEER-96-0014 "Response of Steel Bridge Bearings to Reversed Cyclic Loading," by J.B. Mander, D-K. Kim, S.S. Chen and G.J. Premus, 11/13/96, (PB97-140735, A12, MF-A03).
- NCEER-96-0015 "Highway Culvert Performance During Past Earthquakes," by T.L. Youd and C.J. Beckman, 11/25/96, (PB97-133532, A06, MF-A01).
- NCEER-97-0001 "Evaluation, Prevention and Mitigation of Pounding Effects in Building Structures," by R.E. Valles and A.M. Reinhorn, 2/20/97, (PB97-159552, A14, MF-A03).
- NCEER-97-0002 "Seismic Design Criteria for Bridges and Other Highway Structures," by C. Rojahn, R. Mayes, D.G. Anderson, J. Clark, J.H. Hom, R.V. Nutt and M.J. O'Rourke, 4/30/97, (PB97-194658, A06, MF-A03).

- NCEER-97-0003 "Proceedings of the U.S.-Italian Workshop on Seismic Evaluation and Retrofit," Edited by D.P. Abrams and G.M. Calvi, 3/19/97, (PB97-194666, A13, MF-A03).
- NCEER-97-0004 "Investigation of Seismic Response of Buildings with Linear and Nonlinear Fluid Viscous Dampers," by A.A. Seleemah and M.C. Constantinou, 5/21/97, (PB98-109002, A15, MF-A03).
- NCEER-97-0005 "Proceedings of the Workshop on Earthquake Engineering Frontiers in Transportation Facilities," edited by G.C. Lee and I.M. Friedland, 8/29/97, (PB98-128911, A25, MR-A04).
- NCEER-97-0006 "Cumulative Seismic Damage of Reinforced Concrete Bridge Piers," by S.K. Kunnath, A. El-Bahy, A. Taylor and W. Stone, 9/2/97, (PB98-108814, A11, MF-A03).
- NCEER-97-0007 "Structural Details to Accommodate Seismic Movements of Highway Bridges and Retaining Walls," by R.A. Imbsen, R.A. Schamber, E. Thorkildsen, A. Kartoum, B.T. Martin, T.N. Rosser and J.M. Kulicki, 9/3/97, (PB98-108996, A09, MF-A02).
- NCEER-97-0008 "A Method for Earthquake Motion-Damage Relationships with Application to Reinforced Concrete Frames," by A. Singhal and A.S. Kiremidjian, 9/10/97, (PB98-108988, A13, MF-A03).
- NCEER-97-0009 "Seismic Analysis and Design of Bridge Abutments Considering Sliding and Rotation," by K. Fishman and R. Richards, Jr., 9/15/97, (PB98-108897, A06, MF-A02).
- NCEER-97-0010 "Proceedings of the FHWA/NCEER Workshop on the National Representation of Seismic Ground Motion for New and Existing Highway Facilities," edited by I.M. Friedland, M.S. Power and R.L. Mayes, 9/22/97, (PB98-128903, A21, MF-A04).
- NCEER-97-0011 "Seismic Analysis for Design or Retrofit of Gravity Bridge Abutments," by K.L. Fishman, R. Richards, Jr. and R.C. Divito, 10/2/97, (PB98-128937, A08, MF-A02).
- NCEER-97-0012 "Evaluation of Simplified Methods of Analysis for Yielding Structures," by P. Tsopelas, M.C. Constantinou, C.A. Kircher and A.S. Whittaker, 10/31/97, (PB98-128929, A10, MF-A03).
- NCEER-97-0013 "Seismic Design of Bridge Columns Based on Control and Repairability of Damage," by C-T. Cheng and J.B. Mander, 12/8/97, (PB98-144249, A11, MF-A03).
- NCEER-97-0014 "Seismic Resistance of Bridge Piers Based on Damage Avoidance Design," by J.B. Mander and C-T. Cheng, 12/10/97, (PB98-144223, A09, MF-A02).
- NCEER-97-0015 "Seismic Response of Nominally Symmetric Systems with Strength Uncertainty," by S. Balopoulou and M. Grigoriu, 12/23/97, (PB98-153422, A11, MF-A03).
- NCEER-97-0016 "Evaluation of Seismic Retrofit Methods for Reinforced Concrete Bridge Columns," by T.J. Wipf, F.W. Klaiber and F.M. Russo, 12/28/97, (PB98-144215, A12, MF-A03).
- NCEER-97-0017 "Seismic Fragility of Existing Conventional Reinforced Concrete Highway Bridges," by C.L. Mullen and A.S. Cakmak, 12/30/97, (PB98-153406, A08, MF-A02).
- NCEER-97-0018 "Loss Assessment of Memphis Buildings," edited by D.P. Abrams and M. Shinozuka, 12/31/97, (PB98-144231, A13, MF-A03).
- NCEER-97-0019 "Seismic Evaluation of Frames with Infill Walls Using Quasi-static Experiments," by K.M. Mosalam, R.N. White and P. Gergely, 12/31/97, (PB98-153455, A07, MF-A02).
- NCEER-97-0020 "Seismic Evaluation of Frames with Infill Walls Using Pseudo-dynamic Experiments," by K.M. Mosalam, R.N. White and P. Gergely, 12/31/97, (PB98-153430, A07, MF-A02).
- NCEER-97-0021 "Computational Strategies for Frames with Infill Walls: Discrete and Smeared Crack Analyses and Seismic Fragility," by K.M. Mosalam, R.N. White and P. Gergely, 12/31/97, (PB98-153414, A10, MF-A02).

- NCEER-97-0022 "Proceedings of the NCEER Workshop on Evaluation of Liquefaction Resistance of Soils," edited by T.L. Youd and I.M. Idriss, 12/31/97, (PB98-155617, A15, MF-A03).
- MCEER-98-0001 "Extraction of Nonlinear Hysteretic Properties of Seismically Isolated Bridges from Quick-Release Field Tests," by Q. Chen, B.M. Douglas, E.M. Maragakis and I.G. Buckle, 5/26/98, (PB99-118838, A06, MF-A01).
- MCEER-98-0002 "Methodologies for Evaluating the Importance of Highway Bridges," by A. Thomas, S. Eshenaur and J. Kulicki, 5/29/98, (PB99-118846, A10, MF-A02).
- MCEER-98-0003 "Capacity Design of Bridge Piers and the Analysis of Overstrength," by J.B. Mander, A. Dutta and P. Goel, 6/1/98, (PB99-118853, A09, MF-A02).
- MCEER-98-0004 "Evaluation of Bridge Damage Data from the Loma Prieta and Northridge, California Earthquakes," by N. Basoz and A. Kiremidjian, 6/2/98, (PB99-118861, A15, MF-A03).
- MCEER-98-0005 "Screening Guide for Rapid Assessment of Liquefaction Hazard at Highway Bridge Sites," by T. L. Youd, 6/16/98, (PB99-118879, A06, not available on microfiche).
- MCEER-98-0006 "Structural Steel and Steel/Concrete Interface Details for Bridges," by P. Ritchie, N. Kauh and J. Kulicki, 7/13/98, (PB99-118945, A06, MF-A01).
- MCEER-98-0007 "Capacity Design and Fatigue Analysis of Confined Concrete Columns," by A. Dutta and J.B. Mander, 7/14/98, (PB99-118960, A14, MF-A03).
- MCEER-98-0008 "Proceedings of the Workshop on Performance Criteria for Telecommunication Services Under Earthquake Conditions," edited by A.J. Schiff, 7/15/98, (PB99-118952, A08, MF-A02).
- MCEER-98-0009 "Fatigue Analysis of Unconfined Concrete Columns," by J.B. Mander, A. Dutta and J.H. Kim, 9/12/98, (PB99-123655, A10, MF-A02).
- MCEER-98-0010 "Centrifuge Modeling of Cyclic Lateral Response of Pile-Cap Systems and Seat-Type Abutments in Dry Sands," by A.D. Gadre and R. Dobry, 10/2/98, (PB99-123606, A13, MF-A03).
- MCEER-98-0011 "IDARC-BRIDGE: A Computational Platform for Seismic Damage Assessment of Bridge Structures," by A.M. Reinhorn, V. Simeonov, G. Mylonakis and Y. Reichman, 10/2/98, (PB99-162919, A15, MF-A03).
- MCEER-98-0012 "Experimental Investigation of the Dynamic Response of Two Bridges Before and After Retrofitting with Elastomeric Bearings," by D.A. Wendichansky, S.S. Chen and J.B. Mander, 10/2/98, (PB99-162927, A15, MF-A03).
- MCEER-98-0013 "Design Procedures for Hinge Restrainers and Hinge Sear Width for Multiple-Frame Bridges," by R. Des Roches and G.L. Fenves, 11/3/98, (PB99-140477, A13, MF-A03).
- MCEER-98-0014 "Response Modification Factors for Seismically Isolated Bridges," by M.C. Constantinou and J.K. Quarshie, 11/3/98, (PB99-140485, A14, MF-A03).
- MCEER-98-0015 "Proceedings of the U.S.-Italy Workshop on Seismic Protective Systems for Bridges," edited by I.M. Friedland and M.C. Constantinou, 11/3/98, (PB2000-101711, A22, MF-A04).
- MCEER-98-0016 "Appropriate Seismic Reliability for Critical Equipment Systems: Recommendations Based on Regional Analysis of Financial and Life Loss," by K. Porter, C. Scawthorn, C. Taylor and N. Blais, 11/10/98, (PB99-157265, A08, MF-A02).
- MCEER-98-0017 "Proceedings of the U.S. Japan Joint Seminar on Civil Infrastructure Systems Research," edited by M. Shinozuka and A. Rose, 11/12/98, (PB99-156713, A16, MF-A03).
- MCEER-98-0018 "Modeling of Pile Footings and Drilled Shafts for Seismic Design," by I. PoLam, M. Kapuskar and D. Chaudhuri, 12/21/98, (PB99-157257, A09, MF-A02).

- MCEER-99-0001 "Seismic Evaluation of a Masonry Infilled Reinforced Concrete Frame by Pseudodynamic Testing," by S.G. Buonopane and R.N. White, 2/16/99, (PB99-162851, A09, MF-A02).
- MCEER-99-0002 "Response History Analysis of Structures with Seismic Isolation and Energy Dissipation Systems: Verification Examples for Program SAP2000," by J. Scheller and M.C. Constantinou, 2/22/99, (PB99-162869, A08, MF-A02).
- MCEER-99-0003 "Experimental Study on the Seismic Design and Retrofit of Bridge Columns Including Axial Load Effects," by A. Dutta, T. Kokorina and J.B. Mander, 2/22/99, (PB99-162877, A09, MF-A02).
- MCEER-99-0004 "Experimental Study of Bridge Elastomeric and Other Isolation and Energy Dissipation Systems with Emphasis on Uplift Prevention and High Velocity Near-source Seismic Excitation," by A. Kasalanati and M. C. Constantinou, 2/26/99, (PB99-162885, A12, MF-A03).
- MCEER-99-0005 "Truss Modeling of Reinforced Concrete Shear-flexure Behavior," by J.H. Kim and J.B. Mander, 3/8/99, (PB99-163693, A12, MF-A03).
- MCEER-99-0006 "Experimental Investigation and Computational Modeling of Seismic Response of a 1:4 Scale Model Steel Structure with a Load Balancing Supplemental Damping System," by G. Pekcan, J.B. Mander and S.S. Chen, 4/2/99, (PB99-162893, A11, MF-A03).
- MCEER-99-0007 "Effect of Vertical Ground Motions on the Structural Response of Highway Bridges," by M.R. Button, C.J. Cronin and R.L. Mayes, 4/10/99, (PB2000-101411, A10, MF-A03).
- MCEER-99-0008 "Seismic Reliability Assessment of Critical Facilities: A Handbook, Supporting Documentation, and Model Code Provisions," by G.S. Johnson, R.E. Sheppard, M.D. Quilici, S.J. Eder and C.R. Scawthorn, 4/12/99, (PB2000-101701, A18, MF-A04).
- MCEER-99-0009 "Impact Assessment of Selected MCEER Highway Project Research on the Seismic Design of Highway Structures," by C. Rojahn, R. Mayes, D.G. Anderson, J.H. Clark, D'Appolonia Engineering, S. Gloyd and R.V. Nutt, 4/14/99, (PB99-162901, A10, MF-A02).
- MCEER-99-0010 "Site Factors and Site Categories in Seismic Codes," by R. Dobry, R. Ramos and M.S. Power, 7/19/99, (PB2000-101705, A08, MF-A02).
- MCEER-99-0011 "Restraint Design Procedures for Multi-Span Simply-Supported Bridges," by M.J. Randall, M. Saiidi, E. Maragakis and T. Isakovic, 7/20/99, (PB2000-101702, A10, MF-A02).
- MCEER-99-0012 "Property Modification Factors for Seismic Isolation Bearings," by M.C. Constantinou, P. Tsopelas, A. Kasalanati and E. Wolff, 7/20/99, (PB2000-103387, A11, MF-A03).
- MCEER-99-0013 "Critical Seismic Issues for Existing Steel Bridges," by P. Ritchie, N. Kauh and J. Kulicki, 7/20/99, (PB2000-101697, A09, MF-A02).
- MCEER-99-0014 "Nonstructural Damage Database," by A. Kao, T.T. Soong and A. Vender, 7/24/99, (PB2000-101407, A06, MF-A01).
- MCEER-99-0015 "Guide to Remedial Measures for Liquefaction Mitigation at Existing Highway Bridge Sites," by H.G. Cooke and J. K. Mitchell, 7/26/99, (PB2000-101703, A11, MF-A03).
- MCEER-99-0016 "Proceedings of the MCEER Workshop on Ground Motion Methodologies for the Eastern United States," edited by N. Abrahamson and A. Becker, 8/11/99, (PB2000-103385, A07, MF-A02).
- MCEER-99-0017 "Quindío, Colombia Earthquake of January 25, 1999: Reconnaissance Report," by A.P. Asfura and P.J. Flores, 10/4/99, (PB2000-106893, A06, MF-A01).
- MCEER-99-0018 "Hysteretic Models for Cyclic Behavior of Deteriorating Inelastic Structures," by M.V. Sivaselvan and A.M. Reinhorn, 11/5/99, (PB2000-103386, A08, MF-A02).

- MCEER-99-0019 "Proceedings of the 7th U.S.- Japan Workshop on Earthquake Resistant Design of Lifeline Facilities and Countermeasures Against Soil Liquefaction," edited by T.D. O'Rourke, J.P. Bardet and M. Hamada, 11/19/99, (PB2000-103354, A99, MF-A06).
- MCEER-99-0020 "Development of Measurement Capability for Micro-Vibration Evaluations with Application to Chip Fabrication Facilities," by G.C. Lee, Z. Liang, J.W. Song, J.D. Shen and W.C. Liu, 12/1/99, (PB2000-105993, A08, MF-A02).
- MCEER-99-0021 "Design and Retrofit Methodology for Building Structures with Supplemental Energy Dissipating Systems," by G. Pekcan, J.B. Mander and S.S. Chen, 12/31/99, (PB2000-105994, A11, MF-A03).
- MCEER-00-0001 "The Marmara, Turkey Earthquake of August 17, 1999: Reconnaissance Report," edited by C. Scawthorn; with major contributions by M. Bruneau, R. Eguchi, T. Holzer, G. Johnson, J. Mander, J. Mitchell, W. Mitchell, A. Papageorgiou, C. Scaethorn, and G. Webb, 3/23/00, (PB2000-106200, A11, MF-A03).
- MCEER-00-0002 "Proceedings of the MCEER Workshop for Seismic Hazard Mitigation of Health Care Facilities," edited by G.C. Lee, M. Ettouney, M. Grigoriu, J. Hauer and J. Nigg, 3/29/00, (PB2000-106892, A08, MF-A02).
- MCEER-00-0003 "The Chi-Chi, Taiwan Earthquake of September 21, 1999: Reconnaissance Report," edited by G.C. Lee and C.H. Loh, with major contributions by G.C. Lee, M. Bruneau, I.G. Buckle, S.E. Chang, P.J. Flores, T.D. O'Rourke, M. Shinozuka, T.T. Soong, C-H. Loh, K-C. Chang, Z-J. Chen, J-S. Hwang, M-L. Lin, G-Y. Liu, K-C. Tsai, G.C. Yao and C-L. Yen, 4/30/00, (PB2001-100980, A10, MF-A02).
- MCEER-00-0004 "Seismic Retrofit of End-Sway Frames of Steel Deck-Truss Bridges with a Supplemental Tendon System: Experimental and Analytical Investigation," by G. Pekcan, J.B. Mander and S.S. Chen, 7/1/00, (PB2001-100982, A10, MF-A02).
- MCEER-00-0005 "Sliding Fragility of Unrestrained Equipment in Critical Facilities," by W.H. Chong and T.T. Soong, 7/5/00, (PB2001-100983, A08, MF-A02).
- MCEER-00-0006 "Seismic Response of Reinforced Concrete Bridge Pier Walls in the Weak Direction," by N. Abo-Shadi, M. Saiidi and D. Sanders, 7/17/00, (PB2001-100981, A17, MF-A03).
- MCEER-00-0007 "Low-Cycle Fatigue Behavior of Longitudinal Reinforcement in Reinforced Concrete Bridge Columns," by J. Brown and S.K. Kunnath, 7/23/00, (PB2001-104392, A08, MF-A02).
- MCEER-00-0008 "Soil Structure Interaction of Bridges for Seismic Analysis," I. PoLam and H. Law, 9/25/00, (PB2001-105397, A08, MF-A02).
- MCEER-00-0009 "Proceedings of the First MCEER Workshop on Mitigation of Earthquake Disaster by Advanced Technologies (MEDAT-1), edited by M. Shinozuka, D.J. Inman and T.D. O'Rourke, 11/10/00, (PB2001-105399, A14, MF-A03).
- MCEER-00-0010 "Development and Evaluation of Simplified Procedures for Analysis and Design of Buildings with Passive Energy Dissipation Systems, Revision 01," by O.M. Ramirez, M.C. Constantinou, C.A. Kircher, A.S. Whittaker, M.W. Johnson, J.D. Gomez and C. Chrysostomou, 11/16/01, (PB2001-105523, A23, MF-A04).
- MCEER-00-0011 "Dynamic Soil-Foundation-Structure Interaction Analyses of Large Caissons," by C-Y. Chang, C-M. Mok, Z-L. Wang, R. Settgast, F. Waggoner, M.A. Ketchum, H.M. Gonnermann and C-C. Chin, 12/30/00, (PB2001-104373, A07, MF-A02).
- MCEER-00-0012 "Experimental Evaluation of Seismic Performance of Bridge Restrainers," by A.G. Vlassis, E.M. Maragakis and M. Saiid Saiidi, 12/30/00, (PB2001-104354, A09, MF-A02).
- MCEER-00-0013 "Effect of Spatial Variation of Ground Motion on Highway Structures," by M. Shinozuka, V. Saxena and G. Deodatis, 12/31/00, (PB2001-108755, A13, MF-A03).
- MCEER-00-0014 "A Risk-Based Methodology for Assessing the Seismic Performance of Highway Systems," by S.D. Werner, C.E. Taylor, J.E. Moore, II, J.S. Walton and S. Cho, 12/31/00, (PB2001-108756, A14, MF-A03).

- MCEER-01-0001 "Experimental Investigation of P-Delta Effects to Collapse During Earthquakes," by D. Vian and M. Bruneau, 6/25/01, (PB2002-100534, A17, MF-A03).
- MCEER-01-0002 "Proceedings of the Second MCEER Workshop on Mitigation of Earthquake Disaster by Advanced Technologies (MEDAT-2)," edited by M. Bruneau and D.J. Inman, 7/23/01, (PB2002-100434, A16, MF-A03).
- MCEER-01-0003 "Sensitivity Analysis of Dynamic Systems Subjected to Seismic Loads," by C. Roth and M. Grigoriu, 9/18/01, (PB2003-100884, A12, MF-A03).
- MCEER-01-0004 "Overcoming Obstacles to Implementing Earthquake Hazard Mitigation Policies: Stage 1 Report," by D.J. Alesch and W.J. Petak, 12/17/01, (PB2002-107949, A07, MF-A02).
- MCEER-01-0005 "Updating Real-Time Earthquake Loss Estimates: Methods, Problems and Insights," by C.E. Taylor, S.E. Chang and R.T. Eguchi, 12/17/01, (PB2002-107948, A05, MF-A01).
- MCEER-01-0006 "Experimental Investigation and Retrofit of Steel Pile Foundations and Pile Bents Under Cyclic Lateral Loadings," by A. Shama, J. Mander, B. Blabac and S. Chen, 12/31/01, (PB2002-107950, A13, MF-A03).
- MCEER-02-0001 "Assessment of Performance of Bolu Viaduct in the 1999 Duzce Earthquake in Turkey" by P.C. Roussis, M.C. Constantinou, M. Erdik, E. Durukal and M. Dicleli, 5/8/02, (PB2003-100883, A08, MF-A02).
- MCEER-02-0002 "Seismic Behavior of Rail Counterweight Systems of Elevators in Buildings," by M.P. Singh, Rildova and L.E. Suarez, 5/27/02. (PB2003-100882, A11, MF-A03).
- MCEER-02-0003 "Development of Analysis and Design Procedures for Spread Footings," by G. Mylonakis, G. Gazetas, S. Nikolaou and A. Chauncey, 10/02/02, (PB2004-101636, A13, MF-A03, CD-A13).
- MCEER-02-0004 "Bare-Earth Algorithms for Use with SAR and LIDAR Digital Elevation Models," by C.K. Huyck, R.T. Eguchi and B. Houshmand, 10/16/02, (PB2004-101637, A07, CD-A07).
- MCEER-02-0005 "Review of Energy Dissipation of Compression Members in Concentrically Braced Frames," by K.Lee and M. Bruneau, 10/18/02, (PB2004-101638, A10, CD-A10).
- MCEER-03-0001 "Experimental Investigation of Light-Gauge Steel Plate Shear Walls for the Seismic Retrofit of Buildings" by J. Berman and M. Bruneau, 5/2/03, (PB2004-101622, A10, MF-A03, CD-A10).
- MCEER-03-0002 "Statistical Analysis of Fragility Curves," by M. Shinozuka, M.Q. Feng, H. Kim, T. Uzawa and T. Ueda, 6/16/03, (PB2004-101849, A09, CD-A09).
- MCEER-03-0003 "Proceedings of the Eighth U.S.-Japan Workshop on Earthquake Resistant Design of Lifeline Facilities and Countermeasures Against Liquefaction," edited by M. Hamada, J.P. Bardet and T.D. O'Rourke, 6/30/03, (PB2004-104386, A99, CD-A99).
- MCEER-03-0004 "Proceedings of the PRC-US Workshop on Seismic Analysis and Design of Special Bridges," edited by L.C. Fan and G.C. Lee, 7/15/03, (PB2004-104387, A14, CD-A14).
- MCEER-03-0005 "Urban Disaster Recovery: A Framework and Simulation Model," by S.B. Miles and S.E. Chang, 7/25/03, (PB2004-104388, A07, CD-A07).
- MCEER-03-0006 "Behavior of Underground Piping Joints Due to Static and Dynamic Loading," by R.D. Meis, M. Maragakis and R. Siddharthan, 11/17/03, (PB2005-102194, A13, MF-A03, CD-A00).
- MCEER-04-0001 "Experimental Study of Seismic Isolation Systems with Emphasis on Secondary System Response and Verification of Accuracy of Dynamic Response History Analysis Methods," by E. Wolff and M. Constantinou, 1/16/04 (PB2005-102195, A99, MF-E08, CD-A00).
- MCEER-04-0002 "Tension, Compression and Cyclic Testing of Engineered Cementitious Composite Materials," by K. Kesner and S.L. Billington, 3/1/04, (PB2005-102196, A08, CD-A08).

- MCEER-04-0003 "Cyclic Testing of Braces Laterally Restrained by Steel Studs to Enhance Performance During Earthquakes," by O.C. Celik, J.W. Berman and M. Bruneau, 3/16/04, (PB2005-102197, A13, MF-A03, CD-A00).
- MCEER-04-0004 "Methodologies for Post Earthquake Building Damage Detection Using SAR and Optical Remote Sensing: Application to the August 17, 1999 Marmara, Turkey Earthquake," by C.K. Huyck, B.J. Adams, S. Cho, R.T. Eguchi, B. Mansouri and B. Houshmand, 6/15/04, (PB2005-104888, A10, CD-A00).
- MCEER-04-0005 "Nonlinear Structural Analysis Towards Collapse Simulation: A Dynamical Systems Approach," by M.V. Sivaselvan and A.M. Reinhorn, 6/16/04, (PB2005-104889, A11, MF-A03, CD-A00).
- MCEER-04-0006 "Proceedings of the Second PRC-US Workshop on Seismic Analysis and Design of Special Bridges," edited by G.C. Lee and L.C. Fan, 6/25/04, (PB2005-104890, A16, CD-A00).
- MCEER-04-0007 "Seismic Vulnerability Evaluation of Axially Loaded Steel Built-up Laced Members," by K. Lee and M. Bruneau, 6/30/04, (PB2005-104891, A16, CD-A00).
- MCEER-04-0008 "Evaluation of Accuracy of Simplified Methods of Analysis and Design of Buildings with Damping Systems for Near-Fault and for Soft-Soil Seismic Motions," by E.A. Pavlou and M.C. Constantinou, 8/16/04, (PB2005-104892, A08, MF-A02, CD-A00).
- MCEER-04-0009 "Assessment of Geotechnical Issues in Acute Care Facilities in California," by M. Lew, T.D. O'Rourke, R. Dobry and M. Koch, 9/15/04, (PB2005-104893, A08, CD-A00).
- MCEER-04-0010 "Scissor-Jack-Damper Energy Dissipation System," by A.N. Sigaher-Boyle and M.C. Constantinou, 12/1/04 (PB2005-108221).
- MCEER-04-0011 "Seismic Retrofit of Bridge Steel Truss Piers Using a Controlled Rocking Approach," by M. Pollino and M. Bruneau, 12/20/04 (PB2006-105795).
- MCEER-05-0001 "Experimental and Analytical Studies of Structures Seismically Isolated with an Uplift-Restraint Isolation System," by P.C. Roussis and M.C. Constantinou, 1/10/05 (PB2005-108222).
- MCEER-05-0002 "A Versatile Experimentation Model for Study of Structures Near Collapse Applied to Seismic Evaluation of Irregular Structures," by D. Kusumastuti, A.M. Reinhorn and A. Rutenberg, 3/31/05 (PB2006-101523).
- MCEER-05-0003 "Proceedings of the Third PRC-US Workshop on Seismic Analysis and Design of Special Bridges," edited by L.C. Fan and G.C. Lee, 4/20/05, (PB2006-105796).
- MCEER-05-0004 "Approaches for the Seismic Retrofit of Braced Steel Bridge Piers and Proof-of-Concept Testing of an Eccentrically Braced Frame with Tubular Link," by J.W. Berman and M. Bruneau, 4/21/05 (PB2006-101524).
- MCEER-05-0005 "Simulation of Strong Ground Motions for Seismic Fragility Evaluation of Nonstructural Components in Hospitals," by A. Wanitkorkul and A. Filiatrault, 5/26/05 (PB2006-500027).
- MCEER-05-0006 "Seismic Safety in California Hospitals: Assessing an Attempt to Accelerate the Replacement or Seismic Retrofit of Older Hospital Facilities," by D.J. Alesch, L.A. Arendt and W.J. Petak, 6/6/05 (PB2006-105794).
- MCEER-05-0007 "Development of Seismic Strengthening and Retrofit Strategies for Critical Facilities Using Engineered Cementitious Composite Materials," by K. Kesner and S.L. Billington, 8/29/05 (PB2006-111701).
- MCEER-05-0008 "Experimental and Analytical Studies of Base Isolation Systems for Seismic Protection of Power Transformers," by N. Murota, M.Q. Feng and G-Y. Liu, 9/30/05 (PB2006-111702).
- MCEER-05-0009 "3D-BASIS-ME-MB: Computer Program for Nonlinear Dynamic Analysis of Seismically Isolated Structures," by P.C. Tsopelas, P.C. Roussis, M.C. Constantinou, R. Buchanan and A.M. Reinhorn, 10/3/05 (PB2006-111703).
- MCEER-05-0010 "Steel Plate Shear Walls for Seismic Design and Retrofit of Building Structures," by D. Vian and M. Bruneau, 12/15/05 (PB2006-111704).

- MCEER-05-0011 "The Performance-Based Design Paradigm," by M.J. Astrella and A. Whittaker, 12/15/05 (PB2006-111705).
- MCEER-06-0001 "Seismic Fragility of Suspended Ceiling Systems," H. Badillo-Almaraz, A.S. Whittaker, A.M. Reinhorn and G.P. Cimellaro, 2/4/06 (PB2006-111706).
- MCEER-06-0002 "Multi-Dimensional Fragility of Structures," by G.P. Cimellaro, A.M. Reinhorn and M. Bruneau, 3/1/06 (PB2007-106974, A09, MF-A02, CD A00).
- MCEER-06-0003 "Built-Up Shear Links as Energy Dissipators for Seismic Protection of Bridges," by P. Dusicka, A.M. Itani and I.G. Buckle, 3/15/06 (PB2006-111708).
- MCEER-06-0004 "Analytical Investigation of the Structural Fuse Concept," by R.E. Vargas and M. Bruneau, 3/16/06 (PB2006-111709).
- MCEER-06-0005 "Experimental Investigation of the Structural Fuse Concept," by R.E. Vargas and M. Bruneau, 3/17/06 (PB2006-111710).
- MCEER-06-0006 "Further Development of Tubular Eccentrically Braced Frame Links for the Seismic Retrofit of Braced Steel Truss Bridge Piers," by J.W. Berman and M. Bruneau, 3/27/06 (PB2007-105147).
- MCEER-06-0007 "REDARS Validation Report," by S. Cho, C.K. Huyck, S. Ghosh and R.T. Eguchi, 8/8/06 (PB2007-106983).
- MCEER-06-0008 "Review of Current NDE Technologies for Post-Earthquake Assessment of Retrofitted Bridge Columns," by J.W. Song, Z. Liang and G.C. Lee, 8/21/06 (PB2007-106984).
- MCEER-06-0009 "Liquefaction Remediation in Silty Soils Using Dynamic Compaction and Stone Columns," by S. Thevanayagam, G.R. Martin, R. Nashed, T. Shenthan, T. Kanagalingam and N. Ecemis, 8/28/06 (PB2007-106985).
- MCEER-06-0010 "Conceptual Design and Experimental Investigation of Polymer Matrix Composite Infill Panels for Seismic Retrofitting," by W. Jung, M. Chiewanichakorn and A.J. Aref, 9/21/06 (PB2007-106986).
- MCEER-06-0011 "A Study of the Coupled Horizontal-Vertical Behavior of Elastomeric and Lead-Rubber Seismic Isolation Bearings," by G.P. Warn and A.S. Whittaker, 9/22/06 (PB2007-108679).
- MCEER-06-0012 "Proceedings of the Fourth PRC-US Workshop on Seismic Analysis and Design of Special Bridges: Advancing Bridge Technologies in Research, Design, Construction and Preservation," Edited by L.C. Fan, G.C. Lee and L. Ziang, 10/12/06 (PB2007-109042).
- MCEER-06-0013 "Cyclic Response and Low Cycle Fatigue Characteristics of Plate Steels," by P. Dusicka, A.M. Itani and I.G. Buckle, 11/1/06 06 (PB2007-106987).
- MCEER-06-0014 "Proceedings of the Second US-Taiwan Bridge Engineering Workshop," edited by W.P. Yen, J. Shen, J-Y. Chen and M. Wang, 11/15/06 (PB2008-500041).
- MCEER-06-0015 "User Manual and Technical Documentation for the REDARSTM Import Wizard," by S. Cho, S. Ghosh, C.K. Huyck and S.D. Werner, 11/30/06 (PB2007-114766).
- MCEER-06-0016 "Hazard Mitigation Strategy and Monitoring Technologies for Urban and Infrastructure Public Buildings: Proceedings of the China-US Workshops," edited by X.Y. Zhou, A.L. Zhang, G.C. Lee and M. Tong, 12/12/06 (PB2008-500018).
- MCEER-07-0001 "Static and Kinetic Coefficients of Friction for Rigid Blocks," by C. Kafali, S. Fathali, M. Grigoriu and A.S. Whittaker, 3/20/07 (PB2007-114767).
- MCEER-07-0002 "Hazard Mitigation Investment Decision Making: Organizational Response to Legislative Mandate," by L.A. Arendt, D.J. Alesch and W.J. Petak, 4/9/07 (PB2007-114768).
- MCEER-07-0003 "Seismic Behavior of Bidirectional-Resistant Ductile End Diaphragms with Unbonded Braces in Straight or Skewed Steel Bridges," by O. Celik and M. Bruneau, 4/11/07 (PB2008-105141).

- MCEER-07-0004 “Modeling Pile Behavior in Large Pile Groups Under Lateral Loading,” by A.M. Dodds and G.R. Martin, 4/16/07(PB2008-105142).
- MCEER-07-0005 “Experimental Investigation of Blast Performance of Seismically Resistant Concrete-Filled Steel Tube Bridge Piers,” by S. Fujikura, M. Bruneau and D. Lopez-Garcia, 4/20/07 (PB2008-105143).
- MCEER-07-0006 “Seismic Analysis of Conventional and Isolated Liquefied Natural Gas Tanks Using Mechanical Analogs,” by I.P. Christovasilis and A.S. Whittaker, 5/1/07, not available.
- MCEER-07-0007 “Experimental Seismic Performance Evaluation of Isolation/Restraint Systems for Mechanical Equipment – Part 1: Heavy Equipment Study,” by S. Fathali and A. Filiatrault, 6/6/07 (PB2008-105144).
- MCEER-07-0008 “Seismic Vulnerability of Timber Bridges and Timber Substructures,” by A.A. Sharma, J.B. Mander, I.M. Friedland and D.R. Allicock, 6/7/07 (PB2008-105145).
- MCEER-07-0009 “Experimental and Analytical Study of the XY-Friction Pendulum (XY-FP) Bearing for Bridge Applications,” by C.C. Marin-Artieda, A.S. Whittaker and M.C. Constantinou, 6/7/07 (PB2008-105191).
- MCEER-07-0010 “Proceedings of the PRC-US Earthquake Engineering Forum for Young Researchers,” Edited by G.C. Lee and X.Z. Qi, 6/8/07 (PB2008-500058).
- MCEER-07-0011 “Design Recommendations for Perforated Steel Plate Shear Walls,” by R. Purba and M. Bruneau, 6/18/07, (PB2008-105192).
- MCEER-07-0012 “Performance of Seismic Isolation Hardware Under Service and Seismic Loading,” by M.C. Constantinou, A.S. Whittaker, Y. Kalpakidis, D.M. Fenz and G.P. Warn, 8/27/07, (PB2008-105193).
- MCEER-07-0013 “Experimental Evaluation of the Seismic Performance of Hospital Piping Subassemblies,” by E.R. Goodwin, E. Maragakis and A.M. Itani, 9/4/07, (PB2008-105194).
- MCEER-07-0014 “A Simulation Model of Urban Disaster Recovery and Resilience: Implementation for the 1994 Northridge Earthquake,” by S. Miles and S.E. Chang, 9/7/07, (PB2008-106426).
- MCEER-07-0015 “Statistical and Mechanistic Fragility Analysis of Concrete Bridges,” by M. Shinozuka, S. Banerjee and S-H. Kim, 9/10/07, (PB2008-106427).
- MCEER-07-0016 “Three-Dimensional Modeling of Inelastic Buckling in Frame Structures,” by M. Schachter and AM. Reinhorn, 9/13/07, (PB2008-108125).
- MCEER-07-0017 “Modeling of Seismic Wave Scattering on Pile Groups and Caissons,” by I. Po Lam, H. Law and C.T. Yang, 9/17/07 (PB2008-108150).
- MCEER-07-0018 “Bridge Foundations: Modeling Large Pile Groups and Caissons for Seismic Design,” by I. Po Lam, H. Law and G.R. Martin (Coordinating Author), 12/1/07 (PB2008-111190).
- MCEER-07-0019 “Principles and Performance of Roller Seismic Isolation Bearings for Highway Bridges,” by G.C. Lee, Y.C. Ou, Z. Liang, T.C. Niu and J. Song, 12/10/07 (PB2009-110466).
- MCEER-07-0020 “Centrifuge Modeling of Permeability and Pinning Reinforcement Effects on Pile Response to Lateral Spreading,” by L.L Gonzalez-Lagos, T. Abdoun and R. Dobry, 12/10/07 (PB2008-111191).
- MCEER-07-0021 “Damage to the Highway System from the Pisco, Perú Earthquake of August 15, 2007,” by J.S. O’Connor, L. Mesa and M. Nykamp, 12/10/07, (PB2008-108126).
- MCEER-07-0022 “Experimental Seismic Performance Evaluation of Isolation/Restraint Systems for Mechanical Equipment – Part 2: Light Equipment Study,” by S. Fathali and A. Filiatrault, 12/13/07 (PB2008-111192).
- MCEER-07-0023 “Fragility Considerations in Highway Bridge Design,” by M. Shinozuka, S. Banerjee and S.H. Kim, 12/14/07 (PB2008-111193).

- MCEER-07-0024 "Performance Estimates for Seismically Isolated Bridges," by G.P. Warn and A.S. Whittaker, 12/30/07 (PB2008-112230).
- MCEER-08-0001 "Seismic Performance of Steel Girder Bridge Superstructures with Conventional Cross Frames," by L.P. Carden, A.M. Itani and I.G. Buckle, 1/7/08, (PB2008-112231).
- MCEER-08-0002 "Seismic Performance of Steel Girder Bridge Superstructures with Ductile End Cross Frames with Seismic Isolators," by L.P. Carden, A.M. Itani and I.G. Buckle, 1/7/08 (PB2008-112232).
- MCEER-08-0003 "Analytical and Experimental Investigation of a Controlled Rocking Approach for Seismic Protection of Bridge Steel Truss Piers," by M. Pollino and M. Bruneau, 1/21/08 (PB2008-112233).
- MCEER-08-0004 "Linking Lifeline Infrastructure Performance and Community Disaster Resilience: Models and Multi-Stakeholder Processes," by S.E. Chang, C. Pasion, K. Tatebe and R. Ahmad, 3/3/08 (PB2008-112234).
- MCEER-08-0005 "Modal Analysis of Generally Damped Linear Structures Subjected to Seismic Excitations," by J. Song, Y-L. Chu, Z. Liang and G.C. Lee, 3/4/08 (PB2009-102311).
- MCEER-08-0006 "System Performance Under Multi-Hazard Environments," by C. Kafali and M. Grigoriu, 3/4/08 (PB2008-112235).
- MCEER-08-0007 "Mechanical Behavior of Multi-Spherical Sliding Bearings," by D.M. Fenz and M.C. Constantinou, 3/6/08 (PB2008-112236).
- MCEER-08-0008 "Post-Earthquake Restoration of the Los Angeles Water Supply System," by T.H.P. Tabucchi and R.A. Davidson, 3/7/08 (PB2008-112237).
- MCEER-08-0009 "Fragility Analysis of Water Supply Systems," by A. Jacobson and M. Grigoriu, 3/10/08 (PB2009-105545).
- MCEER-08-0010 "Experimental Investigation of Full-Scale Two-Story Steel Plate Shear Walls with Reduced Beam Section Connections," by B. Qu, M. Bruneau, C-H. Lin and K-C. Tsai, 3/17/08 (PB2009-106368).
- MCEER-08-0011 "Seismic Evaluation and Rehabilitation of Critical Components of Electrical Power Systems," S. Ersoy, B. Feizi, A. Ashrafi and M. Ala Saadeghvaziri, 3/17/08 (PB2009-105546).
- MCEER-08-0012 "Seismic Behavior and Design of Boundary Frame Members of Steel Plate Shear Walls," by B. Qu and M. Bruneau, 4/26/08 . (PB2009-106744).
- MCEER-08-0013 "Development and Appraisal of a Numerical Cyclic Loading Protocol for Quantifying Building System Performance," by A. Filiatrault, A. Wanitkorkul and M. Constantinou, 4/27/08 (PB2009-107906).
- MCEER-08-0014 "Structural and Nonstructural Earthquake Design: The Challenge of Integrating Specialty Areas in Designing Complex, Critical Facilities," by W.J. Petak and D.J. Alesch, 4/30/08 (PB2009-107907).
- MCEER-08-0015 "Seismic Performance Evaluation of Water Systems," by Y. Wang and T.D. O'Rourke, 5/5/08 (PB2009-107908).
- MCEER-08-0016 "Seismic Response Modeling of Water Supply Systems," by P. Shi and T.D. O'Rourke, 5/5/08 (PB2009-107910).
- MCEER-08-0017 "Numerical and Experimental Studies of Self-Centering Post-Tensioned Steel Frames," by D. Wang and A. Filiatrault, 5/12/08 (PB2009-110479).
- MCEER-08-0018 "Development, Implementation and Verification of Dynamic Analysis Models for Multi-Spherical Sliding Bearings," by D.M. Fenz and M.C. Constantinou, 8/15/08 (PB2009-107911).
- MCEER-08-0019 "Performance Assessment of Conventional and Base Isolated Nuclear Power Plants for Earthquake Blast Loadings," by Y.N. Huang, A.S. Whittaker and N. Luco, 10/28/08 (PB2009-107912).

- MCEER-08-0020 “Remote Sensing for Resilient Multi-Hazard Disaster Response – Volume I: Introduction to Damage Assessment Methodologies,” by B.J. Adams and R.T. Eguchi, 11/17/08 (PB2010-102695).
- MCEER-08-0021 “Remote Sensing for Resilient Multi-Hazard Disaster Response – Volume II: Counting the Number of Collapsed Buildings Using an Object-Oriented Analysis: Case Study of the 2003 Bam Earthquake,” by L. Gusella, C.K. Huyck and B.J. Adams, 11/17/08 (PB2010-100925).
- MCEER-08-0022 “Remote Sensing for Resilient Multi-Hazard Disaster Response – Volume III: Multi-Sensor Image Fusion Techniques for Robust Neighborhood-Scale Urban Damage Assessment,” by B.J. Adams and A. McMillan, 11/17/08 (PB2010-100926).
- MCEER-08-0023 “Remote Sensing for Resilient Multi-Hazard Disaster Response – Volume IV: A Study of Multi-Temporal and Multi-Resolution SAR Imagery for Post-Katrina Flood Monitoring in New Orleans,” by A. McMillan, J.G. Morley, B.J. Adams and S. Chesworth, 11/17/08 (PB2010-100927).
- MCEER-08-0024 “Remote Sensing for Resilient Multi-Hazard Disaster Response – Volume V: Integration of Remote Sensing Imagery and VIEWS™ Field Data for Post-Hurricane Charley Building Damage Assessment,” by J.A. Womble, K. Mehta and B.J. Adams, 11/17/08 (PB2009-115532).
- MCEER-08-0025 “Building Inventory Compilation for Disaster Management: Application of Remote Sensing and Statistical Modeling,” by P. Sarabandi, A.S. Kiremidjian, R.T. Eguchi and B. J. Adams, 11/20/08 (PB2009-110484).
- MCEER-08-0026 “New Experimental Capabilities and Loading Protocols for Seismic Qualification and Fragility Assessment of Nonstructural Systems,” by R. Retamales, G. Mosqueda, A. Filiatrault and A. Reinhorn, 11/24/08 (PB2009-110485).
- MCEER-08-0027 “Effects of Heating and Load History on the Behavior of Lead-Rubber Bearings,” by I.V. Kalpakidis and M.C. Constantinou, 12/1/08 (PB2009-115533).
- MCEER-08-0028 “Experimental and Analytical Investigation of Blast Performance of Seismically Resistant Bridge Piers,” by S.Fujikura and M. Bruneau, 12/8/08 (PB2009-115534).
- MCEER-08-0029 “Evolutionary Methodology for Aseismic Decision Support,” by Y. Hu and G. Dargush, 12/15/08.
- MCEER-08-0030 “Development of a Steel Plate Shear Wall Bridge Pier System Conceived from a Multi-Hazard Perspective,” by D. Keller and M. Bruneau, 12/19/08 (PB2010-102696).
- MCEER-09-0001 “Modal Analysis of Arbitrarily Damped Three-Dimensional Linear Structures Subjected to Seismic Excitations,” by Y.L. Chu, J. Song and G.C. Lee, 1/31/09 (PB2010-100922).
- MCEER-09-0002 “Air-Blast Effects on Structural Shapes,” by G. Ballantyne, A.S. Whittaker, A.J. Aref and G.F. Dargush, 2/2/09 (PB2010-102697).
- MCEER-09-0003 “Water Supply Performance During Earthquakes and Extreme Events,” by A.L. Bonneau and T.D. O’Rourke, 2/16/09 (PB2010-100923).
- MCEER-09-0004 “Generalized Linear (Mixed) Models of Post-Earthquake Ignitions,” by R.A. Davidson, 7/20/09 (PB2010-102698).
- MCEER-09-0005 “Seismic Testing of a Full-Scale Two-Story Light-Frame Wood Building: NEESWood Benchmark Test,” by I.P. Christovasilis, A. Filiatrault and A. Wanitkorkul, 7/22/09 (PB2012-102401).
- MCEER-09-0006 “IDARC2D Version 7.0: A Program for the Inelastic Damage Analysis of Structures,” by A.M. Reinhorn, H. Roh, M. Sivaselvan, S.K. Kunnath, R.E. Valles, A. Madan, C. Li, R. Lobo and Y.J. Park, 7/28/09 (PB2010-103199).
- MCEER-09-0007 “Enhancements to Hospital Resiliency: Improving Emergency Planning for and Response to Hurricanes,” by D.B. Hess and L.A. Arendt, 7/30/09 (PB2010-100924).

- MCEER-09-0008 “Assessment of Base-Isolated Nuclear Structures for Design and Beyond-Design Basis Earthquake Shaking,” by Y.N. Huang, A.S. Whittaker, R.P. Kennedy and R.L. Mayes, 8/20/09 (PB2010-102699).
- MCEER-09-0009 “Quantification of Disaster Resilience of Health Care Facilities,” by G.P. Cimellaro, C. Fumo, A.M. Reinhorn and M. Bruneau, 9/14/09 (PB2010-105384).
- MCEER-09-0010 “Performance-Based Assessment and Design of Squat Reinforced Concrete Shear Walls,” by C.K. Gulec and A.S. Whittaker, 9/15/09 (PB2010-102700).
- MCEER-09-0011 “Proceedings of the Fourth US-Taiwan Bridge Engineering Workshop,” edited by W.P. Yen, J.J. Shen, T.M. Lee and R.B. Zheng, 10/27/09 (PB2010-500009).
- MCEER-09-0012 “Proceedings of the Special International Workshop on Seismic Connection Details for Segmental Bridge Construction,” edited by W. Phillip Yen and George C. Lee, 12/21/09 (PB2012-102402).
- MCEER-10-0001 “Direct Displacement Procedure for Performance-Based Seismic Design of Multistory Woodframe Structures,” by W. Pang and D. Rosowsky, 4/26/10 (PB2012-102403).
- MCEER-10-0002 “Simplified Direct Displacement Design of Six-Story NEESWood Capstone Building and Pre-Test Seismic Performance Assessment,” by W. Pang, D. Rosowsky, J. van de Lindt and S. Pei, 5/28/10 (PB2012-102404).
- MCEER-10-0003 “Integration of Seismic Protection Systems in Performance-Based Seismic Design of Woodframed Structures,” by J.K. Shinde and M.D. Symans, 6/18/10 (PB2012-102405).
- MCEER-10-0004 “Modeling and Seismic Evaluation of Nonstructural Components: Testing Frame for Experimental Evaluation of Suspended Ceiling Systems,” by A.M. Reinhorn, K.P. Ryu and G. Maddaloni, 6/30/10 (PB2012-102406).
- MCEER-10-0005 “Analytical Development and Experimental Validation of a Structural-Fuse Bridge Pier Concept,” by S. El-Bahey and M. Bruneau, 10/1/10 (PB2012-102407).
- MCEER-10-0006 “A Framework for Defining and Measuring Resilience at the Community Scale: The PEOPLES Resilience Framework,” by C.S. Renschler, A.E. Frazier, L.A. Arendt, G.P. Cimellaro, A.M. Reinhorn and M. Bruneau, 10/8/10 (PB2012-102408).
- MCEER-10-0007 “Impact of Horizontal Boundary Elements Design on Seismic Behavior of Steel Plate Shear Walls,” by R. Purba and M. Bruneau, 11/14/10 (PB2012-102409).
- MCEER-10-0008 “Seismic Testing of a Full-Scale Mid-Rise Building: The NEESWood Capstone Test,” by S. Pei, J.W. van de Lindt, S.E. Pryor, H. Shimizu, H. Isoda and D.R. Rammer, 12/1/10 (PB2012-102410).
- MCEER-10-0009 “Modeling the Effects of Detonations of High Explosives to Inform Blast-Resistant Design,” by P. Sherkar, A.S. Whittaker and A.J. Aref, 12/1/10 (PB2012-102411).
- MCEER-10-0010 “L’Aquila Earthquake of April 6, 2009 in Italy: Rebuilding a Resilient City to Withstand Multiple Hazards,” by G.P. Cimellaro, I.P. Christovasilis, A.M. Reinhorn, A. De Stefano and T. Kirova, 12/29/10.
- MCEER-11-0001 “Numerical and Experimental Investigation of the Seismic Response of Light-Frame Wood Structures,” by I.P. Christovasilis and A. Filiatrault, 8/8/11 (PB2012-102412).
- MCEER-11-0002 “Seismic Design and Analysis of a Precast Segmental Concrete Bridge Model,” by M. Anagnostopoulou, A. Filiatrault and A. Aref, 9/15/11.
- MCEER-11-0003 “Proceedings of the Workshop on Improving Earthquake Response of Substation Equipment,” Edited by A.M. Reinhorn, 9/19/11 (PB2012-102413).
- MCEER-11-0004 “LRFD-Based Analysis and Design Procedures for Bridge Bearings and Seismic Isolators,” by M.C. Constantinou, I. Kalpakidis, A. Filiatrault and R.A. Ecker Lay, 9/26/11.

- MCEER-11-0005 “Experimental Seismic Evaluation, Model Parameterization, and Effects of Cold-Formed Steel-Framed Gypsum Partition Walls on the Seismic Performance of an Essential Facility,” by R. Davies, R. Retamales, G. Mosqueda and A. Filiatrault, 10/12/11.
- MCEER-11-0006 “Modeling and Seismic Performance Evaluation of High Voltage Transformers and Bushings,” by A.M. Reinhorn, K. Oikonomou, H. Roh, A. Schiff and L. Kempner, Jr., 10/3/11.
- MCEER-11-0007 “Extreme Load Combinations: A Survey of State Bridge Engineers,” by G.C. Lee, Z. Liang, J.J. Shen and J.S. O’Connor, 10/14/11.
- MCEER-12-0001 “Simplified Analysis Procedures in Support of Performance Based Seismic Design,” by Y.N. Huang and A.S. Whittaker.
- MCEER-12-0002 “Seismic Protection of Electrical Transformer Bushing Systems by Stiffening Techniques,” by M. Koliou, A. Filiatrault, A.M. Reinhorn and N. Oliveto, 6/1/12.
- MCEER-12-0003 “Post-Earthquake Bridge Inspection Guidelines,” by J.S. O’Connor and S. Alampalli, 6/8/12.
- MCEER-12-0004 “Integrated Design Methodology for Isolated Floor Systems in Single-Degree-of-Freedom Structural Fuse Systems,” by S. Cui, M. Bruneau and M.C. Constantinou, 6/13/12.
- MCEER-12-0005 “Characterizing the Rotational Components of Earthquake Ground Motion,” by D. Basu, A.S. Whittaker and M.C. Constantinou, 6/15/12.
- MCEER-12-0006 “Bayesian Fragility for Nonstructural Systems,” by C.H. Lee and M.D. Grigoriu, 9/12/12.
- MCEER-12-0007 “A Numerical Model for Capturing the In-Plane Seismic Response of Interior Metal Stud Partition Walls,” by R.L. Wood and T.C. Hutchinson, 9/12/12.
- MCEER-12-0008 “Assessment of Floor Accelerations in Yielding Buildings,” by J.D. Wieser, G. Pekcan, A.E. Zaghi, A.M. Itani and E. Maragakis, 10/5/12.
- MCEER-13-0001 “Experimental Seismic Study of Pressurized Fire Sprinkler Piping Systems,” by Y. Tian, A. Filiatrault and G. Mosqueda, 4/8/13.
- MCEER-13-0002 “Enhancing Resource Coordination for Multi-Modal Evacuation Planning,” by D.B. Hess, B.W. Conley and C.M. Farrell, 2/8/13.
- MCEER-13-0003 “Seismic Response of Base Isolated Buildings Considering Pounding to Moat Walls,” by A. Masroor and G. Mosqueda, 2/26/13.
- MCEER-13-0004 “Seismic Response Control of Structures Using a Novel Adaptive Passive Negative Stiffness Device,” by D.T.R. Pasala, A.A. Sarlis, S. Nagarajaiah, A.M. Reinhorn, M.C. Constantinou and D.P. Taylor, 6/10/13.
- MCEER-13-0005 “Negative Stiffness Device for Seismic Protection of Structures,” by A.A. Sarlis, D.T.R. Pasala, M.C. Constantinou, A.M. Reinhorn, S. Nagarajaiah and D.P. Taylor, 6/12/13.
- MCEER-13-0006 “Emilia Earthquake of May 20, 2012 in Northern Italy: Rebuilding a Resilient Community to Withstand Multiple Hazards,” by G.P. Cimellaro, M. Chiriatti, A.M. Reinhorn and L. Tirca, June 30, 2013.
- MCEER-13-0007 “Precast Concrete Segmental Components and Systems for Accelerated Bridge Construction in Seismic Regions,” by A.J. Aref, G.C. Lee, Y.C. Ou and P. Sideris, with contributions from K.C. Chang, S. Chen, A. Filiatrault and Y. Zhou, June 13, 2013.
- MCEER-13-0008 “A Study of U.S. Bridge Failures (1980-2012),” by G.C. Lee, S.B. Mohan, C. Huang and B.N. Fard, June 15, 2013.
- MCEER-13-0009 “Development of a Database Framework for Modeling Damaged Bridges,” by G.C. Lee, J.C. Qi and C. Huang, June 16, 2013.

- MCEER-13-0010 “Model of Triple Friction Pendulum Bearing for General Geometric and Frictional Parameters and for Uplift Conditions,” by A.A. Sarlis and M.C. Constantinou, July 1, 2013.
- MCEER-13-0011 “Shake Table Testing of Triple Friction Pendulum Isolators under Extreme Conditions,” by A.A. Sarlis, M.C. Constantinou and A.M. Reinhorn, July 2, 2013.
- MCEER-13-0012 “Theoretical Framework for the Development of MH-LRFD,” by G.C. Lee (coordinating author), H.A. Capers, Jr., C. Huang, J.M. Kulicki, Z. Liang, T. Murphy, J.J.D. Shen, M. Shinozuka and P.W.H. Yen, July 31, 2013.
- MCEER-13-0013 “Seismic Protection of Highway Bridges with Negative Stiffness Devices,” by N.K.A. Attary, M.D. Symans, S. Nagarajaiah, A.M. Reinhorn, M.C. Constantinou, A.A. Sarlis, D.T.R. Pasala, and D.P. Taylor, September 3, 2014.
- MCEER-14-0001 “Simplified Seismic Collapse Capacity-Based Evaluation and Design of Frame Buildings with and without Supplemental Damping Systems,” by M. Hamidia, A. Filiatrault, and A. Aref, May 19, 2014.
- MCEER-14-0002 “Comprehensive Analytical Seismic Fragility of Fire Sprinkler Piping Systems,” by Siavash Soroushian, Emmanuel “Manos” Maragakis, Arash E. Zaghi, Alicia Echevarria, Yuan Tian and Andre Filiatrault, August 26, 2014.
- MCEER-14-0003 “Hybrid Simulation of the Seismic Response of a Steel Moment Frame Building Structure through Collapse,” by M. Del Carpio Ramos, G. Mosqueda and D.G. Lignos, October 30, 2014.
- MCEER-14-0004 “Blast and Seismic Resistant Concrete-Filled Double Skin Tubes and Modified Steel Jacketed Bridge Columns,” by P.P. Fouche and M. Bruneau, June 30, 2015.
- MCEER-14-0005 “Seismic Performance of Steel Plate Shear Walls Considering Various Design Approaches,” by R. Purba and M. Bruneau, October 31, 2014.
- MCEER-14-0006 “Air-Blast Effects on Civil Structures,” by Jinwon Shin, Andrew S. Whittaker, Amjad J. Aref and David Cormie, October 30, 2014.
- MCEER-14-0007 “Seismic Performance Evaluation of Precast Girders with Field-Cast Ultra High Performance Concrete (UHPC) Connections,” by G.C. Lee, C. Huang, J. Song, and J. S. O’Connor, July 31, 2014.
- MCEER-14-0008 “Post-Earthquake Fire Resistance of Ductile Concrete-Filled Double-Skin Tube Columns,” by Reza Imani, Gilberto Mosqueda and Michel Bruneau, December 1, 2014.
- MCEER-14-0009 “Cyclic Inelastic Behavior of Concrete Filled Sandwich Panel Walls Subjected to In-Plane Flexure,” by Y. Alzeni and M. Bruneau, December 19, 2014.
- MCEER-14-0010 “Analytical and Experimental Investigation of Self-Centering Steel Plate Shear Walls,” by D.M. Dowden and M. Bruneau, December 19, 2014.
- MCEER-15-0001 “Seismic Analysis of Multi-story Unreinforced Masonry Buildings with Flexible Diaphragms,” by J. Aleman, G. Mosqueda and A.S. Whittaker, June 12, 2015.
- MCEER-15-0002 “Site Response, Soil-Structure Interaction and Structure-Soil-Structure Interaction for Performance Assessment of Buildings and Nuclear Structures,” by C. Bolisetti and A.S. Whittaker, June 15, 2015.
- MCEER-15-0003 “Stress Wave Attenuation in Solids for Mitigating Impulsive Loadings,” by R. Rafiee-Dehkharghani, A.J. Aref and G. Dargush, August 15, 2015.
- MCEER-15-0004 “Computational, Analytical, and Experimental Modeling of Masonry Structures,” by K.M. Dolatshahi and A.J. Aref, November 16, 2015.
- MCEER-15-0005 “Property Modification Factors for Seismic Isolators: Design Guidance for Buildings,” by W.J. McVitty and M.C. Constantinou, June 30, 2015.

- MCEER-15-0006 “Seismic Isolation of Nuclear Power Plants using Sliding Bearings,” by Manish Kumar, Andrew S. Whittaker and Michael C. Constantinou, December 27, 2015.
- MCEER-15-0007 “Quintuple Friction Pendulum Isolator Behavior, Modeling and Validation,” by Donghun Lee and Michael C. Constantinou, December 28, 2015.
- MCEER-15-0008 “Seismic Isolation of Nuclear Power Plants using Elastomeric Bearings,” by Manish Kumar, Andrew S. Whittaker and Michael C. Constantinou, December 29, 2015.
- MCEER-16-0001 “Experimental, Numerical and Analytical Studies on the Seismic Response of Steel-Plate Concrete (SC) Composite Shear Walls,” by Siamak Epackachi and Andrew S. Whittaker, June 15, 2016.
- MCEER-16-0002 “Seismic Demand in Columns of Steel Frames,” by Lisa Shrestha and Michel Bruneau, June 17, 2016.
- MCEER-16-0003 “Development and Evaluation of Procedures for Analysis and Design of Buildings with Fluidic Self-Centering Systems” by Shoma Kitayama and Michael C. Constantinou, July 21, 2016.
- MCEER-16-0004 “Real Time Control of Shake Tables for Nonlinear Hysteretic Systems,” by Ki Pung Ryu and Andrei M. Reinhorn, October 22, 2016.
- MCEER-16-0006 “Seismic Isolation of High Voltage Electrical Power Transformers,” by Kostis Oikonomou, Michael C. Constantinou, Andrei M. Reinhorn and Leon Kemper, Jr., November 2, 2016.
- MCEER-16-0007 “Open Space Damping System Theory and Experimental Validation,” by Erkan Polat and Michael C. Constantinou, December 13, 2016.
- MCEER-16-0008 “Seismic Response of Low Aspect Ratio Reinforced Concrete Walls for Buildings and Safety-Related Nuclear Applications,” by Bismarck N. Luna and Andrew S. Whittaker.
- MCEER-16-0009 “Buckling Restrained Braces Applications for Superstructure and Substructure Protection in Bridges,” by Xiaone Wei and Michel Bruneau, December 28, 2016.
- MCEER-16-0010 “Procedures and Results of Assessment of Seismic Performance of Seismically Isolated Electrical Transformers with Due Consideration for Vertical Isolation and Vertical Ground Motion Effects,” by Shoma Kitayama, Michael C. Constantinou and Donghun Lee, December 31, 2016.
- MCEER-17-0001 “Diagonal Tension Field Inclination Angle in Steel Plate Shear Walls,” by Yushan Fu, Fangbo Wang and Michel Bruneau, February 10, 2017.
- MCEER-17-0002 “Behavior of Steel Plate Shear Walls Subjected to Long Duration Earthquakes,” by Ramla Qureshi and Michel Bruneau, September 1, 2017.
- MCEER-17-0003 “Response of Steel-plate Concrete (SC) Wall Piers to Combined In-plane and Out-of-plane Seismic Loadings,” by Brian Terranova, Andrew S. Whittaker, Siamak Epackachi and Nebojsa Orbovic, July 17, 2017.
- MCEER-17-0004 “Design of Reinforced Concrete Panels for Wind-borne Missile Impact,” by Brian Terranova, Andrew S. Whittaker and Len Schwer, July 18, 2017.
- MCEER-17-0005 “A Simple Strategy for Dynamic Substructuring and its Application to Soil-Foundation-Structure Interaction,” by Aikaterini Stefanaki and Mettupalayam V. Sivaselvan, December 15, 2017.
- MCEER-17-0006 “Dynamics of Cable Structures: Modeling and Applications,” by Nicholas D. Oliveto and Mettupalayam V. Sivaselvan, December 1, 2017.
- MCEER-17-0007 “Development and Validation of a Combined Horizontal-Vertical Seismic Isolation System for High-Voltage-Power Transformers,” by Donghun Lee and Michael C. Constantinou, November 3, 2017.

MCEER-18-0001 “Reduction of Seismic Acceleration Parameters for Temporary Bridge Design,” by Conor Stucki and Michel Bruneau, March 22, 2018.

